Investigating brain metabolism in multiple sclerosis to examine mechanisms of injury and disability using magnetic resonance spectroscopy

Nevin Alex John

University College London

Thesis submitted to University College London for the degree of Doctor of Philosophy

Declaration

I, Nevin Alex John confirm that the work presented in this thesis is my own. Where information has been derived from other sources, I confirm that this has been indicated in the thesis.

The following pertains to the Multiple Sclerosis – Secondary Progressive Multi-Arm Randomisation Trial (MS-SMART) UCL magnetic resonance imaging (MRI) substudy:

Patient recruitment, screening and baseline visits were completed by my co-fellows Dr Floriana De Angelis, Dr Anisha Doshi and Dr Domenico Platone. MRI quality assurance for brain segmentation, SIENA, magnetisation transfer imaging, T2 lesion volume and mean upper cervical cord area were completed by Dr. Floriana De Angelis. Manual lesion segmentation for calculation of T2 lesion volume was completed by Dr Floriana De Angelis, Dr Alberto Calvi and Almu Gomez Garcia. Patient assessment and paper data collation was shared between myself and my co-fellows. MRI analysis pipelines were generated and implemented by Dr. Ferran Prados and Mr. Jon Stutters.

The research nurses Tiggy Beyene, Vanessa Bassan, Nicola Stuart, Laura Brockway and Alvin Zapata were responsible for maintenance of the case record forms. Almudena Garcia Gomez and the admin staff from the Queen Square MS Centre performed the clinical data entry for the UCL site.

The MS-SMART trial was designed by the UK Multiple Sclerosis Society Clinical Trials Network and led by Professor Jeremy Chataway as the Chief investigator of the study. All the applications for ethics, Medicine Health and Research Authority, and research & development approval were carried out by Ms Moira Ross from the Edinburgh Clinical Trials Unit (ECTU).

The MRI sub-study activated at UCL was designed by the Queen Square MS Team led by Professor David Miller, Professor Claudia Gandini Wheeler-Kingshott and Professor Jeremy Chataway. Dr. Bhavana Solankly generated the acquisition protocol for the chemical shift imaging sequence and set up the LCModel program to enable metabolite quantification. Jon Stutters and

Dr Torben Schneider completed the registration process for the chemical shift imaging slice to enable tissue type segmentation. Jon Stutters collated the LCModel outputs to generate the per voxel metabolite levels.

The following declarations refer to the work completed as part of the clinically isolated syndrome (CIS) 15 year follow up cohort:

Prof David Miller, Dr. M.A MacLean, Dr. P Brex, Dr C.M Dalton, Dr. K.A Miszkiel, Dr. Declan Chard, Dr K. Fernando and Prof A.J Thompson were involved in original study design, MRI acquisition protocol, analysis pipelines, patient recruitment and data collection at the baseline and 3-month visits. Follow up data at the 15-year visit was captured and collated by Dr. W J Brownlee.

Abstract

The work presented in this thesis investigates the use of proton magnetic resonance spectroscopy (^{1}H-MRS) to examine metabolic markers of brain injury in clinically isolated syndrome (CIS) and secondary progressive multiple sclerosis (SPMS); and their relationship to both cross-sectional and longitudinal measures of physical and cognitive disability. Metabolic markers of brain injury were measured to examine: (1) the cross-sectional and longitudinal relationships with clinical disability in SPMS; (2) the natural history of metabolites over 96-weeks in SPMS; (3) drug-specific mechanisms of action in a phase 2b multi-arm trial in SPMS; (4) associations with MRI markers of axonal, myelin injury and regional atrophy; and (5) the association between early metabolic changes and long-term disability in a 15-year follow-up cohort with CIS.

CIS represents the first clinical attack in relapse onset multiple sclerosis (MS) and in a significant proportion of patients leads to moderate-severe long term disability including progression to the secondary progressive form of the disease. Whilst CIS and early MS are driven by focal inflammatory demyelination, SPMS encompasses several candidate mechanisms that ultimately lead to neurodegeneration. Whilst there has been much work done on understanding the pathology in these two subtypes of MS, there is an ongoing need to further understand *in vivo* pathology and their relationship to long-term disability.

I firstly examined a large cross-sectional cohort from the Multiple Sclerosis – Secondary progressive Multi-Arm Randomisation Trial (MS-SMART, NCT01910259). I demonstrated that total N-acetyl aspartate (tNAA) levels in normal appearing white matter was associated with upper limb function. Associations between metabolic markers of neuroaxonal integrity, astrogliosis, membrane turnover and information processing speed were also found.

Using ^{1}H-MRS to longitudinally explore the largest ever reported cohort with SPMS, I confirmed that tNAA is associated with upper limb function at baseline and 96-weeks. I also identified changes in membrane turnover and cellularity

(reflected by total choline) in grey and white matter; and identified riluzole as reaching its therapeutic target, but failing to have an impact on decreasing brain atrophy.

I then examined which MRI measures are associated with clinical disability over 96-weeks in SPMS. Incorporating MR measures of axonal injury, myelin damage, regional atrophy and lesion load, I demonstrated that cortical grey matter and spinal cord atrophy; and decreased normal appearing white matter tNAA were the MRI measures associated with decreased upper limb function at 96-weeks. Furthermore, spinal cord atrophy was also the only MRI measure associated with a change in upper limb and ambulatory function over 96-weeks. White matter lesion load and tNAA in normal appearing white matter were the markers associated with longitudinal performance on measures of information processing speed in SPMS.

Examining long term outcomes from a cohort with CIS, I demonstrated that early changes in neuroaxonal integrity and mitochondrial function (as reflected by tNAA) in normal appearing white matter were associated with moderate-severe disability at 15-years.

Impact Statement

Multiple sclerosis is an autoimmune disease that causes inflammation and degeneration in the brain and spinal cord. It affects over 140,000 in the United Kingdom alone and is a major cause of morbidity and disability in adults. There is a need for further therapies in the secondary progressive phase of MS (SPMS), reflective of the need to better understand the factors in disease progression.

The work in this thesis makes important contributions to understanding metabolic changes as a marker of brain injury in the SPMS. Using proton magnetic resonance spectroscopy, I also investigated the relationship of brain metabolism and clinical disability in both the early and late stages of MS.

The results provide insight into the *in vivo* metabolic and pathological processes that drive disability progression in early and late forms of the disease. I have shown for the first time that neuroaxonal and mitochondrial injury in early MS is associated with long term disability. This may stimulate further research to validate this finding.

I demonstrated a role for measuring brain metabolites to determine if therapies used in clinical trials reached and engaged with their proposed target. This may help inform the design of future phase II clinical trials.

The importance of spinal cord pathology in upper limb and walking disability in later phases of MS is again demonstrated. It highlights the need for further mechanistic studies to better understand the underlying causes of spinal cord pathology. It also underscores the need to consider using spinal cord atrophy (both cross-sectional and changes in spinal cord volume) to monitor both upper limb and ambulatory function in progressive MS clinical trials.

Sections of this research have been published in scholarly journals with further publications being submitted and planned. This work will also be further presented at conferences and disseminated via various media organisations.

Acknowledgements

I would firstly like to thank Prof. Jeremy Chataway. His ongoing support, help and oversight have been truly amazing. He has been a wonderful mentor, supervisor, colleague and friend. I will be forever grateful for the opportunities he provided me, his calm and encouraging presence and his ability to always make me feel valued.

I would also like to thank my other supervisors. First, Dr Bhavana Solanky who took me on several years ago. She showed enormous patience in helping me understand MR physics and was a tremendous sounding board and support in all aspects of my PhD and student life. Second, Prof. Claudia Wheeler-Kingshott who provided me with sound advice about PhD content and direction.

I would like to thank my co-fellows – Dr Floriana De Angelis, Dr Anisha Doshi, Dr. Thomas Williams and Dr Alberto Calvi; all of whom have been a wonderful support. Our friendship and camaraderie made QSMSC a great place to work and study.

I would like to acknowledge the contribution by Dr Richard Parker and Prof Chris J Weir. They were incredibly patient and helpful when it came to the statistical issues I encountered.

Wallace J Brownlee has been a great friend and colleague from the time I arrived in the UK. He has supported me along all aspects of my UK journey.

Jon Stutters provided key guidance during times when I had issues writing statistical code for the software. His timely assistance got me through many difficult moments.

I would like to thank the wider QSMSC team including Marie Braisher, Tiggy Beyene, Vanessa Basan, Alvin Zapata, Laura Cecconi, Sarah MacLaughlin, Mariana Agiu and Staci Conway - they were a wonderful group that always made QSMSC a fun and friendly place to be.

I would sincerely like to thank all the study participants who volunteered to be involved in the studies.

I would also like to thank my parents, Vijay & Sally John, who provided with endless opportunities and support since the day I was born. They have always believed in me, provided constant encouragement and have always taken an incredible interest in my work – no matter how complex the subject matter. Finally, I would like to thank my wife, Sarah Alexander. She moved to London with me and has been incredibly supportive throughout my PhD, always there to provide words of encouragement or listen to me during difficult moments.

Table of Contents

Abbreviations

^{1}H-MRS – proton magnetic resonance spectroscopy

T25FW – timed 25-foot walk

9HPT – nine-hole peg test

BET – Brain Extraction Tool

CDMS – clinically definite multiple sclerosis

CGM – cortical grey matter

Cho – choline

CI – confidence interval

CIS – clinically isolated syndrome

CNS – central nervous system

CSI – chemical shift imaging

CSF – cerebrospinal fluid

DMT – disease modifying therapy

DSS – disability status scale

DTI – diffusion tensor imaging

EBV – Epstein Barr Virus

EDSS – expanded disability status scale

FLAIR – fluid attenuated inversion recovery

FOV – field of view

FS – functional system

Glx – glutamate and glutamine

GM - grey matter

HC – healthy controls

IPS – information processing speed

IU – institutional units

mIns - myoinositol

MRI – magnetic resonance imaging

MRS – magnetic resonance spectroscopy

MS – multiple sclerosis

MSFC – multiple sclerosis functional composite

MS-SMART – Multiple Sclerosis, Secondary Progressive Multi-Arm Randomisation Trial

MTR – magnetisation transfer ratio

MUCCA – mean upper cervical cord area

NAA – N-acetyl aspartate

NAAG - N-acetyl aspartyl glutamate

NAWM – normal appearing white matter

OR – odds ratio

PASAT3 – paced auditory serial addition test (3-second)

PMS – progressive multiple sclerosis

PPMS – primary progressive multiple sclerosis

PRESS – point resolved spectroscopy

RF – radiofrequency

RRMS – relapsing remitting multiple sclerosis

SCA – spinal cord atrophy

SD – standard deviation

SDMT - symbol digit modalities test

SNR – signal to noise ratio

SPMS – secondary progressive multiple sclerosis

STEAM – stimulated echo acquisition mode

tCho – total choline

tCr – total creatine

TE – time to echo

TI – inversion time

tNAA – total N-acetyl aspartate

TR – time to repetition

VOI – volume of interest

WM – white matter

WML – white matter lesion

List of tables

List of figures

Publications and abstracts associated with this thesis

Bhavana S Solanky*, Nevin A John*, Floriana De Angelis *et al.* (2020) 'NAA is a Marker of Disability in Secondary-Progressive MS: A Proton MR Spectroscopic Imaging Study', *American Journal of Neuroradiology*. American Journal of Neuroradiology. doi: 10.3174/ajnr.A6809.

*Dr Bhavana Solanky and Dr N A John were co-first authors

Floriana De Angelis, Nevin A John, Wallace J Brownlee, *Therapeutics for multiple sclerosis.* BMJ. 2018 Nov 27;363:k4674.

N John, B Solanky, F De Angelis et al. The effects of amiloride, fluoxetine and riluzole over 96-weeks on metabolic markers of brain injury in secondary progressive multiple sclerosis. Multiple Sclerosis Journal. 26 (3_ SUPPL), 428-428 (Presented at ECTRIMS 2020)

N John, B Solanky, F De Angelis et al. Baseline neuroaxonal integrity is associated with upper limb function at 96-weeks in secondary progressive multiple sclerosis. Multiple Sclerosis Journal 26 (3_ SUPPL), 379-380 (Presented at ECTRIMS 2020)

NA John, B Solanky, F De Angelis et al. A Neurometabolic Profile of Secondary Progressive Multiple Sclerosis: The Relationship between Brain Metabolites and Clinical Disability. (Presented at ACTRIMS Forum 2019)

Chapter 1. Multiple sclerosis

Multiple sclerosis (MS) is an immune disease that combines neuroinflammation and neurodegeneration that affects more than 2.5 million people worldwide (Browne *et al.*, 2014; Mackenzie *et al.*, 2014; Wallin *et al.*, 2019). The condition takes a relapsing remitting course in 85% of patients with 50-66% of untreated patients developing a more progressive course over 15-30 years (Weinshenker *et al.*, 1989; Scalfari *et al.*, 2014; Brown *et al.*, 2019). SPMS is characterised by clinical disability progression that may or may not be interspersed with radiological or clinical evidence of disease activity (new or enhancing lesions on MRI and/or clinical relapses) (Lublin *et al.*, 2014).

1.1 Epidemiology

MS shows a higher incidence in females, with a sex ratio of 3:1 in most developed countries (Orton *et al.*, 2006; Wallin *et al.*, 2012). The incidence and prevalence of MS increases with increasing latitude from the equator. This could potentially be linked to UV-B exposure which stimulates vitamin D production, with vitamin D and genetic susceptibility being implicated in the aetiology of MS (Sintzel, Rametta and Reder, 2018).

1.2 Aetiology

The aetiology for MS is presently unknown. There are, however, a number of established risk factors for the disease. These are detailed below:

1.2.1 Genetic risk

Studies have demonstrated that there is a genetic predisposition for the development of MS. One in eight MS patients have a positive family history and there is 25-30% concordance between mono-zygotic twins demonstrated in various studies (Sadovnick *et al.*, 1993; Mumford *et al.*, 1994; Chataway *et al.*, 2001; Harirchian *et al.*, 2018). Genome-wide association studies have identified more than 150 genomic loci that are associated with an increased risk of MS (Beecham *et al.*, 2013), with the highest risk associated with HLA-DRB1*15 (odds ratio 3.2) (Cotsapas and Mitrovic, 2018).

1.2.2 **Epstein Barr Virus**

Epstein-Barr virus (EBV) is an established risk factor for the development of MS. 90% of the normal population show evidence of EBV infection compared to 99% of people with MS (Bagert, 2009; Guan *et al.*, 2019).

1.2.3 **Vitamin D**

The role of vitamin D in MS has been studied extensively. Higher dietary intake of vitamin D (≥ 400IU/day) decreases MS risk (OR 0.59), whilst higher circulating vitamin D levels independent of dietary intake (>100 nmol/L) have also been shown to decrease MS risk (OR 0.38) (Sintzel, Rametta and Reder, 2018).

When examining the role of vitamin D in MS disease activity, several studies have shown that lower vitamin D levels were associated with an increased risk of MS relapse, MRI activity, disease progression and development of clinically definite multiple sclerosis (CDMS) in patients with CIS (Smolders *et al.*, 2008; Mowry *et al.*, 2010; Simpson *et al.*, 2010; Runia *et al.*, 2012; Ascherio *et al.*, 2014).

1.2.4 **Obesity**

Observational studies have demonstrated an association between increasing body-mass index and MS risk (Munger, Chitnis and Ascherio, 2009; Hedström, Olsson and Alfredsson, 2012; Munger *et al.*, 2013; Mokry *et al.*, 2016). This finding also supports the increasing recognition that comorbidities have a significant impact on MS risk, morbidity and mortality (Marrie *et al.*, 2010; Marrie, Cohen, *et al.*, 2015; Marrie, Elliott, *et al.*, 2015; Magyari and Sorensen, 2020).

1.2.5 **Smoking**

Smoking has been identified as increasing the risk of developing MS. There is also some evidence to support it increasing the risk of conversion from CIS to CDMS (Manouchehrinia *et al.*, 2013; Degelman and Herman, 2017; van der Vuurst de Vries *et al.*, 2018).

1.3 Pathology and immunology

MS is driven by immune mediated inflammation in the central nervous system (CNS) resulting in primary demyelination that is followed by variable degrees of remyelination. Throughout this inflammatory process axonal loss also occurs (Trapp *et al.*, 1998). Whilst inflammation occurs in all phases of MS from early relapsing MS to late-stage progressive MS, the main driver of disability in progressive forms of multiple sclerosis (PMS) (i.e. primary progressive MS (PPMS) and SPMS) is thought to be neurodegeneration.

1.3.1 Immune-mediated inflammation

The pathological hallmark of MS is perivenular inflammation mediated by microglia, B and T lymphocytes resulting in demyelination, axonal loss and damage to oligodendrocytes. This perivenular inflammation can extend into the normal appearing white matter (NAWM). Astrocytes are active in the inflammatory process and lead to fibrillary astrogliosis in inactive lesions. Remyelination, mediated via oligodendrocyte progenitor cells is seen in variable degrees in MS lesions (Lassmann, 2018, 2019).

The trigger(s) for the generation of the autoimmune and neuroinflammatory response remain(s) unknown but it leads to the activation and infiltration of T and B-lymphocytes across the blood brain barrier. Subsequent activation and release of cytokines and chemokines leads to macrophage and microglial activation, which in turn leads to myelin damage. CD8+ T-cell and CD-20+ B cells dominate this CNS infiltration particularly in early relapsing MS with myelin damage often leading to the formation of a focal white matter lesion (WML). Active lesions see the presence of tissue injury and demyelination that are dominated by macrophages and microglia. The macrophages are seen centrally, whilst the activated microglia are seen predominantly around the lesion edges and can be seen to extend further into the periplaque region and NAWM (Lassmann, 2018). In the later stages of PMS, a greater proportion (~30%) of WML are slowly expanding lesions. Slowly expanding lesions contain an inactive centre with a rim of activated microglia. WML can also become inactive, demonstrating primary demyelination, partial axonal preservation and reactive gliosis (Lassmann, 2018, 2019).

1.3.2 **Grey matter pathology**

It is now recognised that grey matter (GM) pathology occurs early in MS and is seen throughout all stages. GM is affected by primary demyelination leading to severe axon and myelin damage (Lassmann, 2018). Cortical lesions are also identified and are classed into four types of based on their location within the cortex and adjacent structures: I – cortical-subcortical border, II – intracortical, III – subpial and IV – entire cortex, non-white matter cortex (Kidd *et al.*, 1999). Cortical inflammation, particularly subpial lesions are thought to be mediated by meningeal inflammation and these subpial cortical lesions are specific to MS. The prominent leukocyte infiltration by T-, B- and plasma cells seen in active WM lesions is not prominent here and these lesions appear to be driven by active microglia (Lassmann and Lucchinetti, 2008; Moll *et al.*, 2008; Gh Popescu and Lucchinetti, 2012; Lassmann, 2018).

Diffuse GM changes are also seen in MS and appear to be more prevalent in PMS compared to RRMS. Diffuse pathological changes include perivascular inflammatory infiltrates, microglial activation, diffuse axonal injury and astrocytic gliosis (Kutzelnigg *et al.*, 2005; Lassmann, 2018). It is also mediated by GM and WM lesions leading to Wallerian degeneration. Pathology studies have demonstrated that cortical demyelination is profound leading to severe axonal, myelin and neuronal loss (Lassmann, 2018, 2019).

GM pathology in MS affects both cortical and deep GM structures. Areas that appear to be most affected include the thalamus, cortex, hippocampus, cerebellar cortex, hypothalamus and basal ganglia (Geurts and Barkhof, 2008; Geurts *et al.*, 2012).

1.3.3 **Meningeal inflammation**

It has been shown in PMS, that neuroinflammation can be mediated by meningeal inflammation characterised by the presence of meningeal lymphoid follicles (Magliozzi *et al.*, 2007; James *et al.*, 2020). These follicles contain lymphocytes, plasma cells and plasmablasts which then release chemokines and cytokines that mediate cortical damage (Magliozzi *et al.*, 2007; James *et al.*, 2020). Given these follicles are separated from the parenchyma by the

meninges it is thought that they may mediate tissue damage via a soluble factor – however this soluble factor has yet to be identified. Similarly, neuroinflammation is seen to originate from large perivascular spaces (Lassmann, 2018, 2019).

1.3.4 **Normal appearing white matter**

NAWM is defined pathologically as “macroscopically normal white matter that is microscopically normally myelinated and at least 1 cm away from a plaque’s edge” (Allen and McKeown, 1979). In a study of multiple biopsy specimens, the major histopathological abnormalities seen in NAWM were focal and diffuse infiltrates containing $CD8^+$ T-cells, reactive astrocytic scarring and activated microglia (Allen and McKeown, 1979). The extensive cortical damage seen more in PMS can extend into the normal cortex and subsequent Wallerian degeneration can slowly lead to axonal loss in NAWM. Axonal density is decreased in NAWM depending on the region studied (Bjartmar, Wujek and Trapp, 2003). NAWM damage does occur independently of the Wallerian degeneration and can additionally be mediated via the meningeal inflammatory processes outlined above, particularly in the spinal cord (Bjartmar *et al.*, 2001; Aboul-Enein *et al.*, 2010; West *et al.*, 2014). Lastly, in studies of PMS examining truly NAWM [normal T1, T2 intensities and normal magnetisation transfer ratio (MTR)], activated microglia were a prominent feature compared to axon and myelin loss (Moll *et al.*, 2011).

1.3.5 **Spinal cord pathology**

The presence of spinal cord pathology in multiple sclerosis has been demonstrated in post-mortem studies (Gass *et al.*, 2015; Lassmann, 2018). Focal cord lesions are seen in the spinal cord and most commonly affect the postero-lateral white matter. The cervical cord is the most common site of MS lesion formation (Gass *et al.*, 2015) and GM seems to be more homogenously involved through the cord. There is significant axonal loss seen within all areas of the cord including focal lesions and NAWM (Petrova *et al.*, 2018), with motor neurons and interneurons seen to more affected in demyelinated GM, particularly in higher spinal levels (Gilmore *et al.*, 2009).

Spinal cord atrophy (SCA) is due to axonal loss that can be due to tissue damage seen within focal lesions, degeneration of tracts and gliosis (Moccia *et al.*, 2019). It is likely that several processes lead to SCA with evidence that significant axonal loss can occur independently of focal lesions and that myelin density does not correlate with axonal loss (Bergers *et al.*, 2002; Bot *et al.*, 2004; Evangelou *et al.*, 2005). SCA also tends to occur more extensively in the cervical than in the thoracic or lumbar spinal cord (Evangelou *et al.*, 2005; Gilmore *et al.*, 2009).

1.3.6 **Neurodegeneration**

Demyelination and neurodegeneration occur throughout all stages of MS with the degenerative component thought to be a key driver of disease progression. Based on animal models and post-mortem studies, neuronal degeneration has several inter-linked candidate mechanisms. These include inflammation, oxidative microglial burst, mitochondrial damage and dysfunction leading to energy failure, histotoxic hypoxia and age-dependent iron accumulation. These lead to a final pathway of calcium influx that cascades to neuronal cell death (Trapp and Stys, 2009; Mahad, Trapp and Lassmann, 2015).

The trigger for these processes is unknown but studies have identified genes e.g. NADPH oxidase that are associated with this oxidative burst (Fischer *et al.*, 2012). Microglia generate reactive oxygen species that can result in direct degeneration of neurons and oligodendrocytes, and may also result in mitochondrial damage (Mahad, Trapp and Lassmann, 2015).

Mitochondrial damage is one of the key components of this neurodegenerative pathway and is caused by cortical damage and reactive oxygen species. Furthermore, mitochondrial damage results in a release of electrons which interact to form reactive oxygen species creating a vicious positive cycle. Under conditions of mitochondrial dysfunction in active lesions, there is reduced sodium clearance which leads to reversal of the Ca^{2+}/Na^{+} exchanger leading to Ca^{2+} influx into the axolemma leading to calpain activation cascading to neuronal cell death (Trapp and Stys, 2009; Criste, Trapp and Dutta, 2014; Mahad, Trapp and Lassmann, 2015).

At-risk axons and neurons can develop histotoxic hypoxia where energy failure occurs in the presence of normal blood and oxygen supply. Additionally, factors that reduce local oxygen tensions or blood flow can further worsen this histotoxic hypoxia that leads to energy failure (Trapp and Stys, 2009; Lassmann, 2017).

Release of iron by inflammatory cells can enhance chronic oxidative damage that can also lead to neurodegeneration. Iron is also detected in increasing levels in the basal ganglia and slowly expanding lesions. Slowly expanding lesions are characterised by a hypointense iron rim due to the ingestion of iron by microglia and macrophages located at the edges of these lesions (Hametner *et al.*, 2013; Mahad, Trapp and Lassmann, 2015; Absinta, Lassmann and Trapp, 2020). Further pathological correlation is needed to identify the role of iron in the pathophysiology of PMS.

Glutamatergic excitotoxicity has been demonstrated in experimental animal studies and is thought to occur via release by inflammatory cells, excessive presynaptic release in GM, altered re-uptake due to decreased expression of glial glutamate transport channels by oligodendrocytes induced by active lesions and potentially glutaminase over-expression (Macrez *et al.*, 2016).

Acute and chronic oxidative damage; and mitochondrial dysfunction when severe enough, ultimately lead to calcium influx which cascades to a final pathway of irreversible cell death (Mahad, Trapp and Lassmann, 2015; Correale *et al.*, 2017; Lassmann, 2018, 2019).

1.3.7 Pathological mechanisms in progressive forms of multiple sclerosis

Large pathological studies have demonstrated that there are no qualitative differences between PPMS and SPMS. There are some quantitative changes with a greater degree of classic active inflammation in SPMS compared to PPMS (Mahad, Trapp and Lassmann, 2015; Correale *et al.*, 2017; Lassmann, 2018, 2019).

Summarising many of the points above, the pathological hallmarks of PMS are thought to be characterised by several key features that distinguish it from early relapsing MS. Firstly, neuroinflammation continues in PMS and lesions are either chronic active or slowly expanding. There is evidence now to support compartmentalised inflammation in perivascular spaces and meninges where T and B lymphocytes form aggregates that secrete local pro-inflammatory factors that likely lead to subpial cortical lesions that are driven by activated microglia. There is extensive GM damage likely due to a combination of primary demyelination, neuroaxonal loss and Wallerian degeneration (Mahad, Trapp and Lassmann, 2015; Lassmann, 2018, 2019; Absinta, Lassmann and Trapp, 2020).

It is recognised that a series of processes are involved in the pathophysiology of neuroaxonal dysfunction and neurodegeneration in PMS including: oxidative microglial burst, reactive oxygen species, mitochondrial dysfunction (outlined above) and decreased repair potential due to age and exhaustion of oligodendrocyte progenitor cells in a lifelong toxic environment that ultimately overwhelms reserve capacity.

Additional processes that are also involved include iron pathology and glutamatergic excitotoxicity (Mahad, Trapp and Lassmann, 2015; Macrez *et al.*, 2016; Filippi *et al.*, 2019).

1.4 Multiple sclerosis classification and phenotypes

MS was originally recognised to be a chronic neurological disease characterised clinically by relapses and progression. Relapsing forms of MS begin with a first clinical attack termed “clinically isolated syndrome” (CIS).

CIS

CIS by definition, is monophasic and specific to the affected CNS region. The term is typically used in adult patients where there is acute-subacute onset of the neurological deficit that lasts continuously for at least 24 hours in the absence of fever or infection (Miller, Chard and Ciccarelli, 2012). There are a number of typical CIS syndromes including unilateral optic neuritis, brainstem

syndromes such as internuclear ophthalmoplegia, incomplete transverse myelitis and hemispheric syndromes (Miller, Chard and Ciccarelli, 2012).

CIS is now recognised as being part of the MS spectrum as it confers an increased risk of developing MS (Miller, Chard and Ciccarelli, 2012; Thompson *et al.*, 2018). Using natural history studies, it has been demonstrated that the presence of typical demyelinating lesions on baseline MRI strongly predicts future MS risk. The risk of developing MS in adults with CIS with asymptomatic WML on MRI is approximately 60-80% over 7-20 years compared to 20% in those a normal MRI scan (Swanton *et al.*, 2006; Brodsky *et al.*, 2008; L. K. Fisniku *et al.*, 2008; Allen *et al.*, 2020). The diagnosis of MS requires evidence of dissemination in time and space and the criteria to demonstrate this are summarised in the McDonald criteria (Table 1-2).

MS Phenotypes

Relapses are defined as “episodes of acute worsening of neurological function followed by a variable degree of recovery” (Lublin and Reingold, 1996). Progression is defined as “gradually nearly continuously worsening baseline with minor fluctuation but no distinct relapses” (Lublin and Reingold, 1996).

Initial phenotypes were described as RRMS, PPMS, SPMS and progressive relapsing MS (Lublin and Reingold, 1996). Additionally, benign MS was defined as “disease in which the patient remains fully functional in all neurologic systems 15 years after disease onset.” Malignant MS was defined as “disease with a rapid progressive course, leading to significant disability in multiple neurologic systems or death in a relatively short time after disease onset” (Lublin and Reingold, 1996).

MS phenotypes were revised in 2013 by the International Advisory Committee on Clinical Trials in MS. Some of the key recommendations included the following (Lublin *et al.*, 2014):

- The removal of progressive relapsing MS as it overlapped with other phenotypes.
- Using benign and malignant MS definitions with caution.

- Clinically isolated syndrome should be included in the MS spectrum.
- Radiologically isolated syndrome should no longer be considered as an MS phenotype due to the absence of a clinical correlate.

The committee also recommended the introduction of regular assessments of disease activity and progression. Active disease was defined as clinical relapses and/or MRI activity (contrast enhancing lesions and/or new or enlarging T2 lesions) assessed at least annually (Lublin *et al.*, 2014). It was also recommended that patients be assessed to determine if there was progression, independent of relapses in patients with PPMS or SPMS (Lublin *et al.*, 2014). These new definitions are shown in Table 1-1.

Table 1-1: Updated definitions of disease activity and progression
(Lublin *et al.*, 2014)

Active disease
Clinical: relapses, acute or subacute episodes of new or increasing neurological dysfunction followed by full or partial recovery, in the absence of fever or infection
And/or
Imaging (MRI): Occurrence of contrast enhancing T1 hyperintense or new or unequivocally enlarging T2 hyperintense lesions
Progressive disease

Clinical: steadily increasing objectively documented neurological dysfunction/disability without unequivocal recovery (fluctuations and phases of stability may occur)
Imaging (MRI): imaging measures of progression are not established or standardised and not yet useful as phenotype descriptors for individual patients.

The concepts of disease activity and progression and their link to the existing MS phenotypes – (RRMS, PPMS, SPMS) are illustrated below in Figure 1-1.

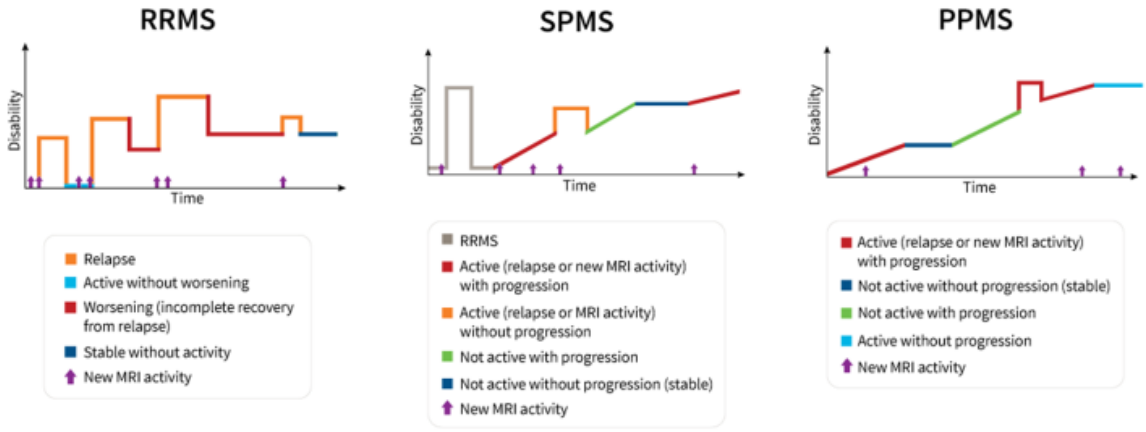

Figure 1-1: Multiple sclerosis phenotypes

Figure provided courtesy of National Multiple Sclerosis Society

1.5 Diagnosis of multiple sclerosis

Following CIS, the diagnosis of MS has been predicated on the demonstration of dissemination in time and space. Dissemination in time can be demonstrated by a second relapse (clinical attack) and/or para-clinical evidence. Para-clinical evidence can be from MRI – simultaneous presence of enhancing and non-enhancing lesions on a single scan or the development of a new lesion typical of MS at subsequent MRI regardless of timing of the follow-

up MRI; or the presence of unmatched CSF oligoclonal bands (2017 McDonald criteria). Dissemination in space can be demonstrated clinically by the occurrence of a second clinical attack/relapse or para-clinical evidence. MRI can provide para-clinical evidence of dissemination in space by demonstrating the presence of one typical MRI lesion in any two of four specific locations: periventricular, juxta- or intracortical or infratentorial (McDonald *et al.*, 2001; Polman *et al.*, 2005, 2011; Thompson *et al.*, 2018).

The first MS diagnostic criteria – the Poser criteria – were published in 1983 (Poser *et al.*, 1983). This was then revised leading to the publication of updated diagnostic criteria in 2001 which later became known as the McDonald Criteria (McDonald *et al.*, 2001). The McDonald criteria have subsequently been revised and updated in 2005 and 2011, with the most recent iteration being published in 2017 (Table 1-2) (Polman *et al.*, 2005, 2011; Thompson *et al.*, 2018).

Table 1-2: 2017 McDonald criteria for diagnosis of MS with CIS onset
(Thompson *et al.*, 2018)

Number of clinical attacks	Lesions with objective clinical evidence	Additional requirements
≥2	≥2	None
≥2	1	Must be evidence on history of a lesion involving another distinct area
≥2	1	Demonstrate DIS with another clinical attack of a different site OR ≥1 lesion based on MRI criteria
1	≥2	Demonstrate DIT with another clinical attack OR ≥1 lesion based on MRI criteria OR CSF-specific oligoclonal bands

1	1	Demonstrate DIS with another clinical attack of a different site OR ≥1 lesion based on MRI criteria AND DIT by another clinical attack OR CSF oligoclonal bands

The 2017 revisions of the McDonald's diagnostic criteria. DIS=dissemination in space, DIT=dissemination in time, MRI criteria are described in the main text.

Diagnostic criteria for PPMS have also been published by the same working group (see Table 1-3) (Thompson *et al.*, 2018).

Table 1-3: McDonald criteria for diagnosis of multiple sclerosis in patient with disease course characterised by progression from onset (primary progressive multiple sclerosis)

Primary progressive multiple sclerosis can be diagnosed in patients with: • 1 year of disability progression (retrospectively or prospectively determined independent of clinical relapse
Plus, two of the following criteria • One or more T2-hyperintense lesions characteristic of multiple sclerosis in one or more of the following brain regions: periventricular, cortical or juxtacortical, or infratentorial • Two or more T2-hyperintense lesions in the spinal cord • Presence of CSF-specific oligoclonal bands

There is a lack of consensus on diagnostic criteria for SPMS with heterogeneity in reporting in both research studies and clinical practice (Lublin *et al.*, 2014). Recent advances in the development of SPMS diagnostic criteria are covered in 1.10.3.

1.6 Clinical features

MS can result in a variety of clinical symptoms depending on the site of CNS injury. CIS and current MS phenotypes, including the contributions of relapses and progression are now discussed.

Typical CIS include optic neuritis, brainstem or cerebellar features such as internuclear ophthalmoplegia, ataxia, gaze evoked nystagmus or cranial nerve VI palsies. The spinal cord can often be affected resulting in incomplete transverse myelitis, sphincter symptoms and asymmetrical limb weakness (Miller, Chard and Ciccarelli, 2012; Tintore *et al.*, 2019).

MS symptoms:

Depending on the site of CNS injury, MS can result in diplopia, dysarthria, limb weakness, ataxia, sphincter disturbance and sensory abnormalities. Mobility is also commonly affected, resulting in problems with balance, walking distance and speed. Fatigue is the most common symptom in MS and mood disorders such as depression are also seen with increased incidence and prevalence (Kister *et al.*, 2013).

Cognitive impairment:

Cognitive impairment is now recognised as a significant cause of disability (Fischer *et al.*, 2014; Rocca *et al.*, 2015; Sumowski *et al.*, 2018). The most commonly and earliest affected cognitive domains include learning memory, information processing speed (IPS) and executive function (Charcot, 1885; Rao *et al.*, 1991; Chiaravalloti and DeLuca, 2008).

1.7 Measures of clinical disability

There are a number of clinical outcome measures that are used to assess both physical and cognitive impairment in MS.

Expanded disability status scale

The Expanded Disability Status Scale (EDSS) is an ordinal non-linear scale from 0.0 – 10.0 with higher scores reflecting higher levels of disability (Table 1-4: Expanded Disability Status Scale)) (Kurtzke, 1983).

Table 1-4: Expanded Disability Status Scale

Score	Description
0.0	Normal neurological function
1.0	No disability, minimal signs in one functional system (FS)
1.5	No disability, minimal signs in more than one FS
2.0	Minimal disability in one FS
2.5	Mild disability in one FS or minimal disability in two FS
3.0	Moderate disability in one FS, or mild disability in three or four FS. No impairment to walking
3.5	Moderate disability in one FS and more than minimal disability in several others. No impairment to walking
4.0	Significant disability but self-sufficient and up and about some 12 hours a day. Able to walk without aid or rest for 500m
4.5	Significant disability but up and about much of the day, able to work a full day, may otherwise have some limitation of full activity or require minimal assistance. Able to walk without aid or rest for 300m
5.0	Disability severe enough to impair full daily activities and ability to work a full day without special provisions. Able to walk without aid or rest for 200m
5.5	Disability severe enough to preclude full daily activities. Able to walk without aid or rest for 100m

6.0	Requires a walking aid – cane, crutch, etc. – to walk about 100m with or without resting
6.5	Requires two walking aids – pair of canes, crutches, etc. – to walk about 20m without resting
7.0	Unable to walk beyond approximately 5m even with aid. Essentially restricted to wheelchair; though wheels self in standard wheelchair and transfers alone. Up and about in wheelchair some 12 hours a day
7.5	Unable to take more than a few steps. Restricted to wheelchair and may need aid in transferring. Can wheel self but cannot carry on in standard wheelchair for a full day and may require a motorised wheelchair
8.0	Essentially restricted to bed or chair or pushed in wheelchair. May be out of bed itself much of the day. Retains many self-care functions. Generally has effective use of arms
8.5	Essentially restricted to bed much of day. Has some effective use of arms retains some self-care functions
9.0	Confined to bed. Can still communicate and eat
9.5	Confined to bed and totally dependent. Unable to communicate effectively or eat/swallow
10.0	Death due to MS

EDSS remains one of the most widely used clinical endpoints of disability progression in clinical trials. It does however have several limitations. It is non-linear, heavily weighted towards ambulation once EDSS > 4.0, insensitive to changes in upper limb function and cognition; and suffers from inter- and intra-rater variability (Noseworthy *et al.*, 1990; Tur *et al.*, 2018).

The multiple sclerosis functional composite (MSFC)

The MSFC combines the 9-hole peg test (9HPT), timed 25-foot walk (T25FW) and the paced auditory serial addition test (PASAT3) to calculate a composite z-score (Cutter *et al.*, 1999; Kalkers *et al.*, 2000). A composite score encompassing different aspects of MS related clinical disability. It is used to measure disability progression in clinical trials (Tur *et al.*, 2018)

Nine-hole peg test

The 9HPT is a test of upper limb function whereby participants use one hand to move pegs into holes and the time taken to complete this task is recorded. With a high prevalence of upper limb dysfunction in MS, this outcome measure is commonly used both in the clinical and research spheres being a reliable, validated outcome measure that is sensitive to change (Goodkin, Hertsguard and Seminary, 1988; Rudick *et al.*, 1997; Kister *et al.*, 2013; Feys *et al.*, 2017).

Timed 25 Foot Walk

The T25FW measures the time taken to walk 25 feet. Two trials are completed with the average time calculated. It has been accepted as a reliable and validated measure of walking in MS with a 20% change representing a significant change (Motl *et al.*, 2017).

Paced auditory serial addition test

The PASAT3 is a measure of IPS and requires participants to serially add up digits for three minutes. Digits can be read by the instructor every 2 or 3 seconds. It is a component of the MSFC and limitations include patient dissatisfaction and practice effects (Gronwall, 1977; Barkercollo, 2005).

Symbol digit modalities test (SDMT)

The SDMT is another measure of IPS. It requires patients to match numbers to symbols for ninety seconds and can be completed in a verbal or written format. It has been validated and is a sensitive measure of cognitive change with a shift in four points thought to be the minimal change required for clinical significance (Benedict *et al.*, 2017; Strober *et al.*, 2019).

1.8 Prognosis

The prognosis from MS remains variable at an individual level with no clear genetic, environmental, clinical or para-clinical factors that can predict individual trajectories.

Time to disability progression

Depending on definitions, natural history studies have shown some variability in the median times to reach disability levels – Disability status scale (DSS) score 3, 6 or 8. In 2009, the median time to DSS 3 and DSS 6 for all people with MS was 8-12 years and 14-28 years respectively (Degenhardt *et al.*, 2009).

Survival

Analysing natural history studies that captured adequate data to analyse survival, the overall time to death from MS onset was 35 years (Swanton *et al.*, 2006). The median time to death was 6-15 years earlier in people with MS compared to the general population (Degenhardt *et al.*, 2009). More recently, a 60-year population based study of 1388 MS patients demonstrated that patients with MS had a 7-year shorter life expectancy and three-fold higher mortality compared to the general population.(Lunde *et al.*, 2017)

Prognostic factors

Results from natural history studies using univariate and multivariate analysis were varied but the main negative prognostic factors that were consistent across all studies and MS phenotypes were having PPMS or SPMS and shorter time to progression (defined as time to DSS 5). In active or relapsing MS, incomplete recovery from MS relapses and having multi-system involvement were also negative prognostic factors (Degenhardt *et al.*, 2009).

1.9 Clinically isolated syndrome

Relapse onset MS most commonly begins with focal neurological symptoms known as CIS. The demographics of people with CIS are similar to those

outlined previously in 1.1. The definition of CIS is provided in 1.4 (Brownlee and Miller, 2014). Disease activity can be defined based on the occurrence of a clinical relapse or MRI activity, with active CIS diagnosed as MS if 2017 McDonald criteria are met (Lublin *et al.*, 2014; Thompson *et al.*, 2018). There are a number of recognised CIS syndromes which are outlined in 1.6 (Miller, Chard and Ciccarelli, 2012; Brownlee and Miller, 2014).

1.9.1 Clinical course

Following initial diagnosis and evaluation, CIS can broadly take one of two trajectories. First, some CIS patients never experience any further clinical attacks or MRI activity and therefore remain diagnosed as CIS. Second, a proportion of CIS patients will develop clinical relapses and/or MRI activity and therefore be diagnosed with MS.

Besides conversion from CIS to MS, the other consideration is the development of long-term disability in those with CIS. A number of studies have examined the risk factors and biomarkers for the development of long-term disability following CIS. These are summarised below.

1.9.2 Risk factors for the development of long-term disability

Demographic factors

Several studies have identified older age at onset as being associated with shorter times to disability (Eriksson, Andersen and Runmarker, 2003; Scalfari *et al.*, 2011, 2014). However, prospective CIS studies did not demonstrate this association (Swanton *et al.*, 2009).

Environmental factors

Lower Vitamin D levels may be associated with the development of disability at 5 years. In a clinical trial of patients with high risk CIS, a vitamin D level of < 50 IU was associated with an increased risk of disability at 5 years (Ascherio *et al.*, 2014).

Clinical features

Incomplete recovery from CIS may be a negative prognostic marker and associated with a shorter time to SPMS (Eriksson, Andersen and Runmarker, 2003).

MRI abnormalities

Over the last 3 decades, numerous studies have consistently shown lesion load, change in lesion load and lesion location to be associated with long term disability following CIS.

Several follow up studies of CIS cohorts have demonstrated that T2 lesion volume when measured during CIS is moderately associated with long-term EDSS outcomes (defined as EDSS $\geq$ 3.0) (Filippi *et al.*, 1994; O'Riordan *et al.*, 1998; Sailer *et al.*, 1999; Brex *et al.*, 2002; L. K. Fisniku *et al.*, 2008; Rahn *et al.*, 2019).

Multiple studies have also shown that the number of T2 lesions in CIS are moderately correlated with long term disability defined by EDSS scores $\geq$ 3.0 in CIS cohorts that were followed up for 5-19 years (Morrissey *et al.*, 1993; O'Riordan *et al.*, 1998; Brex *et al.*, 2002; Tintoré *et al.*, 2006; L. K. Fisniku *et al.*, 2008; Tintore *et al.*, 2015, 2019; Rahn *et al.*, 2019).

In optic neuritis and CIS cohorts followed up for periods ranging 5-30 years, the presence of infratentorial and/or spinal cord lesions at CIS exhibits a strong relationship with long term disability and development of SPMS (Swanton *et al.*, 2009; Tintore *et al.*, 2010; Brownlee *et al.*, 2019; Chung *et al.*, 2020).

Decreased mean upper cervical cord area (MUCCA) and GM fraction were associated with disability at 5 and 15 years (defined as increased risk of reaching EDSS 3.0) post CIS respectively (Brownlee *et al.*, 2017; Vidal-Jordana *et al.*, 2018).

More recently, there has been an increasing body of work examining the role of advanced MRI measures e.g. MTR and proton magnetic resonance spectroscopy (^{1}H-MRS) in CIS. MRI measures of myelin and axonal density (MTR, peak histogram height and location) were measured in a CIS cohort followed up for 20 years. Abnormalities in magnetisation transfer histogram

metrics were found in both GM and NAWM relative to controls. GM peak histogram levels were associated with both EDSS and MSFC scores (Fisniku *et al.*, 2009).

1.10 Secondary progressive multiple sclerosis

According to the recent MS phenotype definition by Lublin et al, "SPMS is diagnosed retrospectively by a history of gradual worsening after an initial relapsing disease course, with or without acute exacerbations during the progressive course" (Lublin *et al.*, 2014). Our understanding of SPMS is increasing but translating this into effective treatments to stabilise or decrease disability progression presents an ongoing challenge.

1.10.1 Risk factors for the development of secondary progressive multiple sclerosis

There have been numerous studies using natural history cohorts that have examined risk factors for the development of SPMS. There is heterogeneity within these studies that needs to be taken into account including a lack of consensus diagnostic criteria for SPMS, changes and updates to McDonald criteria, commencement and then changes in the use of disease-modifying therapy (DMT), variability in MRI techniques used and the interpretation of results using uni- or multivariate analysis.

Time to conversion

Multiple natural history studies have examined time from CIS to SPMS diagnosis. A 20 year follow up of a London cohort found that 42% converted to SPMS when followed up at 20 years (L. K. Fisniku *et al.*, 2008). In a cohort of untreated patients, it was found that 80% of untreated patients could transition from RRMS to SPMS over 20 years (Thompson and Baneke, 2013). Further studies of untreated cohorts suggest that development of SPMS occurs in 33% within 8 years, 50% after 15 years and 66% after 30 years (Scalfari *et al.*, 2014; Coret *et al.*, 2018). More recent studies have suggested that this rate of SPMS development may be lower in patients treated with DMT (Cree *et al.*, 2016; Brown *et al.*, 2019); although several studies have also

published results that did not show this (Ebers *et al.*, 2010; Tedeholm *et al.*, 2013; Zhang *et al.*, 2015; Bergamaschi *et al.*, 2016; Signori *et al.*, 2016).

Demographic and clinical factors:

A review of natural history studies published from 1950-2007 found that there was mixed evidence to male sex being a negative prognostic factor for SPMS development (Degenhardt *et al.*, 2009; Alroughani *et al.*, 2015). The weight of studies seems to suggest that higher age of MS onset is associated with shorter time to SPMS but there are also several studies that have not reported this association (Koch *et al.*, 2008; Degenhardt *et al.*, 2009). The total number of relapses was not significant whilst the number of relapses in the early years is important (Scalfari *et al.*, 2014). A finding that was consistent across studies was that a faster rate of disability progression (variable definitions) was associated with earlier development of SPMS (Degenhardt *et al.*, 2009).

A recent study using diagnostic criteria published by Lorscheider et al (Lorscheider *et al.*, 2016), used repeated observations in a clustered survival model to estimate “averaged” hazard ratios to identify factors that predict development of SPMS. They demonstrated that older age of onset, longer disease duration, greater disability and a greater number of relapses in the previous year were associated with an increased risk of developing SPMS (Fambiatos *et al.*, 2019). Using this definition of SPMS, Brown JW et al recently demonstrated that early DMT use was associated with later development of SPMS (Brown *et al.*, 2019).

MRI measures:

Earlier studies examining MRI metrics that predict development of SPMS and time to certain disability states (usually based on EDSS scores e.g. time to EDSS score 7) suggest that T2 lesion load has a modest relationship with long term disability outcomes (Leonora K. Fisniku *et al.*, 2008). Recent studies suggest that the following factors can predict SPMS development (when compared to remaining RRMS) – baseline higher number of median spinal cord lesions, higher number of supratentorial, infratentorial and spinal cord

lesions at 1 year post CIS; higher median number of new infratentorial, spinal cord and gadolinium-enhancing lesions at 3 years (Brownlee *et al.*, 2019).

1.10.2 **Clinical course**

Using the more recent changes in MS phenotype classification, adults with SPMS can have:

1) Active disease as reflected by the presence of relapses and/or MRI activity
2) Disease progression (Lublin *et al.*, 2014).

SPMS phenotypes can therefore take on combinations of active disease progression. These combinations include active with progression, active but without progression, not active with progression and active with progression (Lublin *et al.*, 2014).

Transition from predominantly relapsing course to progressive course

There is always a transition period from RRMS to SPMS. One natural history study of 120 patients found the transitional period of uncertainty from RRMS to a definitive diagnosis of SPMS was 2.9 $\pm$ 0.8 years and 70% (14/20) patients had reached EDSS $\geq$ 6.0 by this time (Katz Sand *et al.*, 2014).

Disability progression

The hallmark of SPMS is disease progression that is independent of relapses. The new guidance regarding MS phenotypes does allow for active disease in SPMS. Natural history studies have demonstrated that median times to DSS 3 is 8 years for SPMS and 3 years for PPMS; time to DSS 6 in SPMS demonstrated significant variability amongst the available studies and there was an absence of formal diagnostic criteria for SPMS (Degenhardt *et al.*, 2009). Data regarding the impact of relapses during SPMS on disability is mixed, with relapses during SPMS carrying either a favourable prognosis or having no effect at all (Degenhardt *et al.*, 2009).

Cognitive impairment

Cohorts with PMS demonstrate a higher degree of cognitive impairment in all cognitive domains with overall prevalence rates of up to 80%. It is suggested that there are differences in the cognitive deficits seen in SPMS when compared to other MS phenotypes. Adults with SPMS have a decreased ability to complete tasks that involve higher order working memory compared to other MS phenotypes and healthy controls (Huijbregts *et al.*, 2004; Connick, Chandran and Bak, 2013; Rocca *et al.*, 2015; Johnen *et al.*, 2017; Nicholas *et al.*, 2017). SPMS patients also show additional deficits in executive function, attention and IPS efficiency (Connick, Chandran and Bak, 2013; Nicholas *et al.*, 2017). Intelligence quotient (IQ), simple attention, naming and comprehension abilities are relatively preserved in MS (Rocca *et al.*, 2015; Sumowski *et al.*, 2018). There is also a need for biomarkers to predict and monitor progress of cognitive impairment in PMS – this is further expanded upon in 1.10.4.

1.10.3 Diagnosis of secondary progressive multiple sclerosis

Diagnosis of SPMS was addressed by Lorscheider et al who analysed 576 data derived SPMS onset definitions for SPMS and identified a set of criteria that would inform consistent, accurate and timely SPMS diagnosis when compared to best consensus diagnosis (Lorscheider *et al.*, 2016).There is still however, a lack of consensus about SPMS diagnosis, where, unlike its RRMS and PPMS counterparts, there is a continued absence of clear accepted diagnostic criteria.

1.10.4 Biomarkers of progression in secondary progressive multiple sclerosis

Spinal cord cross-sectional area, whole brain and regional GM atrophy appearing promising markers of disease progression in SPMS (Moccia, de Stefano and Barkhof, 2017). The imaging markers used in PMS are summarised in 2.2.

With increasing recognition of the impact of cognitive impairment in all forms of MS, studies have examined the role of MR imaging to better understand the

pathobiology of cognitive impairment and identify biomarkers. In mostly RRMS cohorts, lesional measures were initially shown to be associated with neuropsychological measures but further studies only demonstrated a modest correlation between lesional metrics and cognition suggesting other pathological processes are involved (Rao *et al.*, 1989; Filippi and Rocca, 2010; Yildiz *et al.*, 2014; van Geest *et al.*, 2018). Regional lesion measures were associated with specific neuropsychological measures e.g. tests of executive function were associated with lesion load in the frontal lobe (Swirsky-Sacchetti *et al.*, 1992; Arnett *et al.*, 1994). Cortical lesions in RRMS cohorts were moderately associated with cognitive measures and predictive of longer term disability, including cognitive disability (Calabrese *et al.*, 2009; Deloire *et al.*, 2011). In PPMS, Penny et al showed that from amongst a group of MR metrics, T2 lesion volume (T2LV) was the strongest predictor of verbal memory and IPS at 5 years (Penny *et al.*, 2010). Whole brain atrophy is greatest in PMS and cross sectional measures of brain volume have been shown relationships with tests of cognition but these associations would be enhanced by examining brain atrophy over time (van Geest *et al.*, 2018).

GM atrophy is now well established in all stages of MS and is associated with cognitive performance. Deep GM volume changes show a strong correlation with IPS and memory in RRMS cohorts (Batista *et al.*, 2012; Debernard *et al.*, 2015). Furthermore, thalamic atrophy shows a strong correlation with various tests of cognition including IPS, verbal and visuospatial memory and executive function (van Geest *et al.*, 2018). These associations however, do not completely explain the variation in cognitive impairment. With the majority of findings from RRMS cohorts, further research is needed to better understand the pathobiology of cognitive impairment in PMS.

1.11 Rationale for thesis

Relapse onset MS spans across a spectrum from CIS to SPMS. There is significant variability in disease course following CIS.

Conventional MRI is crucial in making the diagnosis of MS and identifying areas of focal inflammation (on T2 sequences). However, it is not specific for

concurrent pathological processes such as axonal loss, demyelination, remyelination, glutamatergic excitotoxicity and fibrillary gliosis. A large proportion of untreated patients with relapse onset MS will develop SPMS. SPMS causes progressive disability and the relative paucity of DMT reflects our incomplete understanding of the pathobiology. There is also the need for improved prognostic markers that can better define the long-term trajectory (> 5 years) in those with CIS and SPMS.

The measurement of metabolic markers of brain injury using ^{1}H-MRS has the potential to improve our understanding of the pathobiology of disease progression in SPMS, determine the ability of therapeutic interventions to reach their target and predict long term disability outcomes.

In this thesis, I will aim to address the following research objectives:

i) To improve the understanding of the underlying natural history of metabolic markers of brain injury in adults with SPMS
ii) To determine the ability of several potential neuroprotective agents to reach their purported mechanistic target in a phase 2b trial in SPMS
iii) To understand the association between brain metabolites and physical and cognitive disability measures in SPMS
iv) To explore the relationship of metabolic markers of neuroaxonal integrity, MRI measures of axonal and myelin injury; and regional atrophy with clinical disability outcomes in SPMS
v) To examine the relationship between brain metabolites measured during CIS and long-term disability and development of SPMS at 15 years

To complete these objectives, I have conducted a cross-sectional and longitudinal analyses of ^{1}H-MRS and clinical data to interrogate a large SPMS cohort from a phase 2b clinical trial in SPMS; and an analysis of 15-year outcomes in a CIS follow-up cohort.

This first chapter provides an introduction to the disease and highlights the issues in predicting long-term disability in MS and our understanding of pathophysiology in SPMS.

Chapter 2 presents the MRI techniques used in this thesis that provide information on underlying pathology in MS with a focus on the ^{1}H-MRS technique and its role in CIS and SPMS.

Chapter 3 introduces the study design for MS-SMART; and the SPMS cohort that is analysed for the ^{1}H-MRS and advanced MRI sub-studies. The design for the prospective CIS cohort study is then outlined.

Chapter 4 presents the results of the cross-sectional analysis of the SPMS cohort from the MS-SMART advanced MRI substudy to demonstrate metabolite values in a typical SPMS population and identify associations with clinical disability measures.

Chapter 5 focuses on the longitudinal analysis of the SPMS cohort from the MS-SMART advanced MRI substudy - investigating the natural history of brain metabolites over 96-weeks, examining the mechanistic action of three potential neuroprotective agents and building on the cross-sectional analysis from Chapter 4.

Using data from the MS-SMART MRI substudy, chapter 6 investigates which MRI measure/s of neuro-axonal injury, lesion load, myelin damage and regional atrophy are most closely associated with disability at and over 96-weeks in SPMS.

Chapter 7 examines the 15-year CIS follow up cohort to determine whether brain metabolites measured during CIS are associated with disability at 15 years.

Chapter 2. Methodologies used in this thesis

Magnetic resonance imaging (MRI) is introduced, followed by the different MRI techniques used in this thesis. There is a focus on the major MRI technique employed in this thesis – ^{1}H-MRS. The methods explained in this section are used in chapters 4-7.

2.1 Basic principles of MRI

2.1.1 Introduction to MRI

Nuclear magnetic resonance is based upon the physics of atoms placed in a magnetic field. An atom of a given element contains neutrons and protons within a nucleus and this nucleus is surrounded by electrons in orbit. The mass number is the number of protons and neutrons (nucleons) added together and atoms that have an odd number have a "magnetic moment", i.e. it can interact with an external magnetic field. As a result, hydrogen (referred to as a proton because hydrogen atoms have only 1 proton) is the most commonly studied atom in MRI as it has both an odd mass number and is found in abundance in the human body. Protons have both a positive charge and motion, known as spin, and thus generate a magnetic field. When you place protons in an external magnetic field (B_0), the nuclear spins of these will align parallel or anti-parallel to the direction of this magnetic field, splitting the spins into high and low energy states. These protons will then rotate or move around the external magnetic field in a process known as precession (Westbrook and Kaut, 1998; Dale, Brown and Semelka, 2015). The frequency of precession is specific to each atom and is specified by the Larmor equation:

Equation 2-1

$$\omega_0 = \gamma B_0$$

where ω_0 is the precession frequency, γ is the gyromagnetic ratio and B_0 is the strength of the external magnetic field (in Tesla). Due to the slight difference between the nuclear spins of the protons aligned parallel and anti-parallel to B_0, there is a net magnetisation vector (M). M_0 is the net magnetisation at equilibrium, and we are now considering this magnetisation in classical terms,

as it is an ensemble representation of the spin system. If we apply a radiofrequency (RF) pulse B1(t) i.e. an oscillating magnetic field delivered at the exact Larmor frequency, M_0 interacts with B1(t) exchanging energy. The net magnetisation M(t) will change from its alignment with B_0 by a flip angle that depends on the duration and amplitude of B1(t). Signal that is produced from the net magnetisation vector can only be acquired by the receiver coil when the nuclear spins are in phase in the transverse (xy) plane, due to the very small net magnetisation vector in the longitudinal (z) plane compared to the size of the main static magnetic field (B_0) (Dale, Brown and Semelka, 2015)(Westbrook and Kaut, 1998).

For example, if a 90^0 pulse is applied, the net magnetisation is flipped 90^0 into the transverse plane, and when the RF pulse is turned off the process of returning to equilibrium starts. This happens through two relaxation processes: the nuclear spins of the protons lose energy to the surrounding "lattice" (environment) and also lose energy due to interactions between nuclei ("spin-spin" interactions) and return to their previous low energy state and realign with B_0.

2.1.2 **Relaxation theory**

This leads to the concepts of T1 relaxation (longitudinal signal recovery), T2 relaxation (transverse signal) decay, and the T2* effect. T1 (longitudinal) relaxation occurs when the nuclear spins of the protons lose energy to the surrounding lattice to return to equilibrium, once again aligning with the external magnetic field B_0 (generally known as the 'longitudinal' or z-direction). T1 relaxation is the recovery of the magnetisation along the longitudinal (z) direction (longitudinal relaxation). Within a given tissue, the time taken for full recovery of magnetisation in the longitudinal plane varies between 300-2000ms for biological tissues. It is difficult to measure the exact time at which T1 longitudinal recovery is complete and thus T1 is defined as the time for 63% of the original longitudinal magnetisation to be reached. It is defined by the equation below and longitudinal relaxation takes on a slow exponential curve (see Figure 2-1):

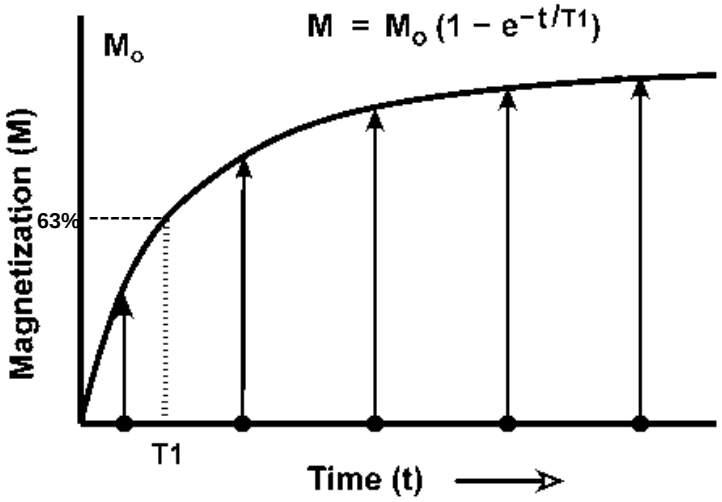

Figure 2-1: T1 relaxation curve and equation governing exponential T1 recovery

T2 relaxation, also known as spin-spin relaxation, refers to the loss or transfer of energy due to interactions between spins. This T2 decay is seen as transverse relaxation in the XY plane. The T2 decay follows an exponential process and T2 is defined as the time for transverse magnetisation to decrease to 37% of its original value and for biological tissues this is approximately between 30-150ms. Again, different substances (e.g. fat, water) within tissue exhibit different T2 times. The T2 equation and relaxation curve (Bloch, 1946) are shown in Figure 2-2:

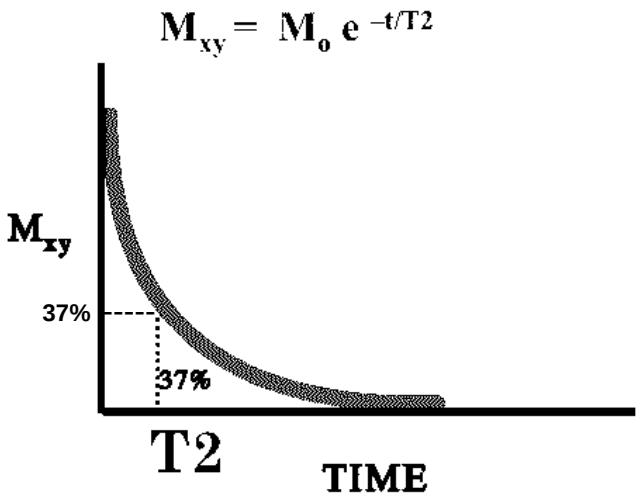

Figure 2-2: T2 relaxation curve and equation governing T2 signal decay

T2* describes the transverse relaxation or decay that occurs at a faster rate than T2 decay due to macroscopic and microscopic magnetic field inhomogeneities and is always shorter than (or at most equal to) T2 relaxation times.

2.1.3 **Spatial encoding and image reconstruction**

Slice selection:

The central frequency of the slice is the Larmor frequency. The first step of spatial encoding is slice selection. Using a magnetic gradient field, the frequency of the precessing protons is altered slightly, dependant on position, and using a RF pulse with a specific frequency bandwidth, a given slice can be selected, the resonant frequencies of which match the bandwidth (Westbrook and Kaut, 1998; Dale, Brown and Semelka, 2015).

Spatial encoding along other axes:

Following slice selection, we need to determine the specific location of the signal in each axis. This involves two steps – frequency and phase encoding. In frequency encoding, magnetic gradient field is used to alter the precessional frequencies of the protons along that axis, imposing a frequency encoding of positions along that direction.

In phase encoding, a separate gradient is applied in the perpendicular axis again shifting the frequency of the precessing nuclear spins slightly out of phase. During the phase encoding gradient, spins at different positions along the direction of application of that gradient are characterised by different phases. Using mathematical calculations i.e the Fourier Transform, this phase shift can then be used together with frequency encoding to assign a certain signal component to a specific position in the selected slice (Westbrook and Kaut, 1998; Dale, Brown and Semelka, 2015).

K-space encoding and image reconstruction:

K-space is the space used to store digitised MR signals during data acquisition over time. K-space therefore is the signal containing the frequency and phase

information from the selected slice. This includes information about the real space e.g. matrix size in k-space also controls matrix size of the final image. Every digitised sample point has its own unique location in k-space but image space pixels do not correspond directly to k-space. Image reconstruction occurs via Fourier transformation.

2.1.4 Introduction to MR pulse sequences

The proton density, T1 and T2 properties of different tissues can be exploited to generate contrast. MRI parameters are adjusted to be sensitive to different pathologies. This is then ultimately used to generate an MR image used in research or clinical practice.

Proton density:

This relies on the density of protons in different tissue to generate contrast and is done by minimising T2 and T1 relaxation effects by keeping short echo time (TE) 10-25ms and long repetition time (TR) 2000+ms.

T1 weighting:

The T1 weighted image uses a short TR to maximise the difference between fat and water as fat has a much shorter TR time than water. To minimise the effect of T2, the TE is short. Typical times for T1 weighted imaging are TR 250-700ms and TE 14ms.

T2 weighting:

T2 weighted images adjust the TE to be close to the T2 values of the tissues that require imaging but with enough signal to noise ratio to be measurable. It is also important to keep TR long to minimise T1 effects and complete T1 recovery. If the TE is too long, then proton nuclear spins within the tissues will have all dephased and there will be no signal to acquire but if TE is too short then there will be insufficient time for tissue contrast to be created based on differing tissues being imaged. Typical TE times for a T2 weighted image are 60+ms and TR 2000+ms (Westbrook and Kaut, 1998; Dale, Brown and Semelka, 2015).

Introduction to sequences:

The application of repeated RF pulses and the adjusting parameters governing T1 and T2 relaxation times can be used to acquire MRI sequences. During the application of a single RF pulse, the net magnetisation vector is flipped to the transverse plane, and signal is acquired through the receiver coil (when the RF pulse is turned off). The TR is the time from application of one RF pulse to the next and determines the time allowed for T1 relaxation before the next pulse is delivered. The TE timing is the time from RF pulse to measuring signal. When you insert a receiver coil within B_0, it will detect a signal which is then sent for processing. Signal is acquired from in-phase nuclear spins in the transverse plane. After the RF pulse ends, nuclei are losing or transferring energy immediately and the signal is acquired from the free induction delay.

To acquire a sequence, repeated RF pulses need to be administered. Pulse sequences are generated by adjusting TR, TE and RF parameters.

Following the RF pulse and flip of net magnetisation into the transverse plane, there is longitudinal (T1) relaxation. Ideally, there should be complete relaxation of the excited nuclear spins before the next RF pulse is applied. If there is incomplete longitudinal relaxation, then the number of available nuclear spins to absorb energy from the next RF pulse will be less and there will be resultant decrease in signal. When there is complete saturation, no signal can be acquired, reflecting a state of non-equilibrium with no net magnetisation.

Spin echo sequence:

With application of the RF pulse, the net magnetisation vector is flipped 90^0 into the transverse plane. When the RF is turned off, these nuclear spins will then fall out of phase at certain speeds. A second RF pulse is then applied to flip the nuclear spins 180^0 to bring them back in phase where the “faster” precessing spins will “catch up” to the slower spins to bring them both back in-phase and then re-acquire this spin echo signal. The time from first 90^0 RF pulse to the maximum signal acquired from spin echo is TE. This second RF pulse decreases the effect of magnetic inhomogeneity to thereby maximise the

free induction decay signal. The TR time is time from the first 90^0 RF pulse to the next 90^0 RF pulse.

Gradient echo sequence:

Magnetic gradient fields can be used to alter the magnetic fields experienced by nuclear spins within the external magnetic field B_0. Gradients are coils of wire within the magnetic bores. When current is run through with coils, a magnetic field is generated which is known as a magnetic gradient field. When applied, magnetic gradient fields can alter the precession frequency of all the nuclear spins that experience this magnetic gradient field. The application of magnetic gradient fields can achieve a similar result to the second 180^0 refocusing pulse used in spin echo sequences in that they can bring nuclear spins back into phase (or alternatively dephase) but this sequence can be affected to a greater degree by magnetic field inhomogeneities.

Inversion recovery sequence

Inversion recovery sequences initially apply a RF pulse to flip the net magnetisation vector 180^0. After a period of time known as the inversion time (TI), a 90^0 RF pulse is applied. The inverted longitudinal magnetisation recovers according to the T1 of the tissue, thus it is heavily T1 weighted.

Several commonly utilised sequences employ this method including fluid attenuated inversion recovery (FLAIR) and short TI inversion recovery (STIR). In FLAIR, a long TI is used to suppress CSF and long TE results in a T2 weighting effect thereby creating an image whereby CSF is nulled with no signal but keeping the T2 effect which can be analysed to identify pathology. This is of use in MS where FLAIR enables improved detection of periventricular lesions.

2.1.5 **Image quality and fast imaging sequences**

Parameters that govern image quality and time:

The quality of each image is governed by four inter-related factors: signal to noise ratio (SNR), contrast to noise ratio, spatial resolution and scan time. SNR

is proportional to voxel volume, number of signal averages (NEX) and inversely proportional to the square root of sampling bandwidth, and the number of frequency and phase encoding steps.

Spatial resolution is the ability to distinguish between two tissue types next to each other and is related to voxel size (whose dimensions are given by the pixel size and slice thickness).

Scan time is governed by three parameters: TR, number of phase encodings (or matrix size) and number of averages. An alteration in one parameter may create a trade-off in the other. Increasing the number of phase encodings may increase matrix size and resolution but comes at the cost of increased scan time. Likewise increasing the number of averages improves SNR but takes more time. There are several methods to decrease scan time such as the use of gradient echo (see 2.1.4) and faster sampling approaches where multiple echoes are acquired per TR which enables faster encoding of K-space. Fast spin echo and echo-planar imaging are examples of this where multiple echoes, known as echo trains are acquired per TR thus enhancing the speed of acquisition (Westbrook and Kaut, 1998; Dale, Brown and Semelka, 2015).

2.2 Structural MRI

2.2.1 Introduction

MRI imaging has become essential for the diagnosis and monitoring of MS (Kaunzner and Gauthier, 2017). MRI and various quantitative metrics also provide valuable information on *in vivo* pathology occurring in MS. This section provides an overview of the outcome measures using conventional MRI that are used in PMS with a focus on techniques and metrics that are used in this thesis.

2.2.2 White matter lesions

White matter lesions (WML) are seen in MS and are identified using MRI where they appear hyperintense on T2 and FLAIR sequences. They are typically ovoid lesions, ranging from a few millimetres to more than one centimetre in diameter and often perivenular (Fazekas *et al.*, 1999). Brain lesions are

typically found in the periventricular, juxtacortical and infratentorial regions (Fazekas *et al.*, 1999).

10-30% of WML are T1-hypointense and in the acute stages represent oedema and demyelination which can disappear following abatement of acute inflammation; whilst T1-hypointensity in chronic lesions represent areas of axonal loss and pathologically confirmed tissue destruction (also termed “black holes”) (Fazekas *et al.*, 1999; Filippi *et al.*, 2012).

Conventional MRI is able to differentiate between acute active lesions and chronic inactive lesions on the basis of gadolinium enhancement (Filippi *et al.*, 2012). Gadolinium is a contrast agent that crosses the blood brain barrier and can highlight areas of active inflammation (Fazekas *et al.*, 1999; Filippi *et al.*, 2012; Saade *et al.*, 2018). Enhancement patterns are typically nodular and less commonly ring enhancing. Gadolinium enhancement is also dependent on the dose given, acquisition timings and potential use of corticosteroids. Enhancement typically persists for 2-6 weeks but less commonly can persist for 3-6 months (Filippi *et al.*, 2012; Saade *et al.*, 2018). WML do evolve over time due to varying degrees of demyelination, axonal loss, fibrillary gliosis and remyelination; and hyperintense lesions seen on T2 or FLAIR sequences are unable to differentiate between these processes to better understand lesion evolution (Filippi *et al.*, 2012).

Lesion evolution between the active, chronic active and chronic inactive stages (1.3) may be better represented by smouldering or slowly expanding lesions that are seen in pathological studies (Filippi *et al.*, 2012). Early active relapsing forms of MS are dominated by active lesions whilst slowly expanding lesions and chronic inactive lesions are the predominant lesion type in PMS; and may contribute to disease progression reflecting ongoing inflammation in later stages disease (Filippi *et al.*, 2012, 2019). There has been a recent interest in the development of MRI techniques that identify slowly expanding lesions (Elliott, Belachew, *et al.*, 2019; Elliott, Wolinsky, *et al.*, 2019; Calvi *et al.*, 2020).

2.2.3 **Grey matter lesions**

The presence of GM inflammation has been demonstrated in pathological studies (1.3), and are seen to occur in all layers of the cortex. However focal GM lesions are poorly visualised using conventional MRI (Filippi *et al.*, 2019). Sequences such as double inversion recovery, phase-sensitive inversion recovery and 3D magnetisation-prepared rapid acquisition echo have increased detection rates of GM lesions but still have limited sensitivity (Filippi *et al.*, 2019). Histopathological studies have demonstrated improved detection of cortical GM (CGM) lesions at ultra-high field strengths compared to 3.0 Tesla. However our ability to detect GM lesions is still incomplete and further techniques are required to improve sensitivity (Kilsdonk *et al.*, 2016).

2.2.4 **Brain atrophy**

The pathological mechanisms underpinning both whole brain and regional atrophy have been described previously (1.3). In SPMS, the main MRI metric for investigating neurodegeneration – the substrate of progressive and irreversible disability – is the change (reduction) in brain volume (atrophy) (Barkhof *et al.*, 2009; Rocca *et al.*, 2017). On average there is 0.5-1% loss of brain volume/year in SPMS, as opposed to 0.1-0.2%/year in age-matched controls. Amongst all types of MS, SPMS shows the fastest rate of brain atrophy per year, which in large, multi-centre settings has been estimated to be 0.64%/year (De Stefano *et al.*, 2010). There are several methods to calculate brain atrophy with accurate calculation relies on image normalisation, segmentation and registration. Raw brain volumes need to be rescaled to adjust for confounding factors like differences in head size; and this is achieved either using a ratio method like brain parenchymal fraction (ratio of brain parenchymal volume to total intracranial volume) or rescaled via registration to an atlas (Rocca *et al.*, 2017). Current methods primarily use T1 high resolution 3D volumetric acquisition and involve lesion filling and tissue segmentation using *a priori* information from atlases. Longitudinal whole brain atrophy measurements involve co-registration of pairs of scans from the same patient rather than cross-sectional registration to atlases. Brain atrophy can also be measured using segmentation techniques e.g.

brain parenchymal fraction with studies suggesting that registration techniques show better reproducibility and accuracy (Rudick *et al.*, 1999; Smith *et al.*, 2002, 2007; Moccia, de Stefano and Barkhof, 2017). There are several freely available software programs that can be used to generate and run MR analysis pipelines with examples including ANTs (https://github.com/ANTsX/ANTs), FSL - https://fsl.fmrib.ox.ac.uk/fsl/fslwiki) and FreeSurfer (http://surfer.nmr.mhg.harvard.edu/) (Rocca *et al.*, 2017).

Structural Image Evaluation, using Normalisation, of Atrophy X (SIENAX) and Structural Image Evaluation, using Normalisation, of Atrophy (SIENA) are two methods used to calculate cross-sectional normalised brain volume (NBV) and longitudinal percentage brain volume change (PBVC) respectively (Smith *et al.*, 2002). SIENAX uses the Brain Extraction Tool (BET), to segment brain from non-brain head tissue and the outer surface of the skull is estimated (Smith, 2002). It is then registered to a standard space, a probabilistic tissue mask created to ensure non-brain tissue e.g. eyes/optic nerves are absent and tissue segmentation completed to calculate NBV (Smith *et al.*, 2002). In SIENA, brain is once again extracted using BET, images are aligned, registered and normalised. Local atrophy is measured based on changes of image edges and expressed as percentage brain volume change (Smith, 2002; Smith *et al.*, 2002). These analysis pipelines are used throughout the thesis and are expanded upon in 3.2.9.

There are several factors that need to considered when measuring brain atrophy to minimise measurement bias and optimise precision. It is important to maintain high-quality and consistent MR acquisition, optimise patient positioning and avoiding imaging artefacts. There are also patient based confounding factors that need to be considered such as lifestyle factors, ageing, the presence of ageing alongside comorbidities, hydration and use of DMT (Rocca *et al.*, 2017).

2.2.5 **Grey matter atrophy and regional atrophy**

GM atrophy is seen through all stages of MS (Geurts and Barkhof, 2008). Furthermore, regional GM atrophy may have stronger correlations with clinical disability measures than whole brain atrophy (Leonora K. Fisniku *et al.*, 2008;

Eshaghi, Marinescu, *et al.*, 2018; Eshaghi, Prados, *et al.*, 2018). GM atrophy can discriminate between different MS phenotypes and shows an association with clinical disability outcome measures, physical and cognitive (Rocca *et al.*, 2017). Furthermore, in a 4 year longitudinal study, compared to controls, GM atrophy was greatest in SPMS, followed by those converting to SPMS from RRMS and those with RRMS; WM atrophy however was constant amongst these groups over the 4 years (Fisher *et al.*, 2008). GM atrophy appears to affect different GM regions at different disease stages with the thalamus effected in early MS followed by regions in the CGM (Eshaghi, Marinescu, *et al.*, 2018).

2.2.6 **Spinal cord atrophy**

The pathological changes seen in MS are described in 1.3.5. Spinal cord MRI can detect the presence of focal spinal cord lesions and measure spinal cord area. Post-mortem studies correlating MRI findings with histopathological analysis have shown that high field MRI has a high sensitivity in detecting spinal cord WM and GM lesions (Gilmore *et al.*, 2009). Higher signal intensities reflect complete or partial demyelination (Nijeholt *et al.*, 2001), and axonal density seen in these are similar to those in normal appearing cord tissue (Bergers *et al.*, 2002). Decreased cord area and MTR are best associated with myelin content but not axonal density (Mottershead *et al.*, 2003; Bot *et al.*, 2004).

Spinal cord imaging has been limited by the accuracy required to scan and re-scan a small structure like the cord. However, upgrades in hardware and the development of analysis techniques have improved our ability to image the spinal cord and obtain quantitative measures. Cord atrophy is generally measured as cervical cord area and most commonly acquired from the upper cervical spinal levels (Moccia *et al.*, 2019). Techniques used to measure SCA can be separated into intensity based, active surface models and imaging based. Following earlier intensity-based methods (Losseff *et al.*, 1996), semi-automated active surface models using software such as Jim or NeuroQ were developed (Lukas *et al.*, 2004; ‘Xinapse. Cord finder – Introduction, http:// www.xinapse.com/Manual/ (2018, accessed 28 December 2018)’, 2018).

Details of the analysis pipeline using the active surface model in Jim is outlined in more detail in 3.2.9. Currently, SCA is calculated by subtracting cross-sectional area measurements from two or more timepoints. There has now been a move towards fully automated pipelines using *PropSeg* from the spinal cord toolbox and volumetric brain imaging to measure cervical cord area with techniques such as the boundary shift integral (Yiannakas *et al.*, 2016; De Leener *et al.*, 2017; Moccia *et al.*, 2019).

Various studies have shown that cervical cord area is decreased in MS. In a recent meta-analysis, pooled mean cervical spinal cross-sectional area was decreased in MS compared to healthy control; with PMS (PPMS and SPMS) having the lowest values (Casserly *et al.*, 2018). Pooled estimates of SCA showed that the rate in all MS was -1.78%/year with PMS showing the greatest atrophy rate at -2.08%/year (Casserly *et al.*, 2018). Several studies have shown that the rate of atrophy in the spinal cord may be greater than that seen in the brain (Moccia *et al.*, 2019).

Many studies have demonstrated associations between the extent of SCA at a single timepoint (measured as spinal cord area) and clinical disability or clinical disability progression (Gass *et al.*, 2015; Kearney, Miller and Ciccarelli, 2015; Casserly *et al.*, 2018; Moccia *et al.*, 2019). The rate of SCA over time has also shown associations with clinical disability progression (Kidd *et al.*, 1996; Gass *et al.*, 2015; Kearney, Miller and Ciccarelli, 2015; Casserly *et al.*, 2018; Moccia *et al.*, 2019).

2.2.7 **Magnetisation transfer imaging**

Magnetisation transfer imaging uses off resonance RF pulses to saturate protons bound to macromolecules. There is then an energy exchange between the spins of the protons bound to macromolecules (e.g. myelin, axonal membranes) and freely moving (unbound) protons. In regions of higher macromolecular content e.g. brain, this magnetisation transfer effect can be used in quantitative measurements e.g. MTR (Tofts, Steens and van Buchem, 2003). Post-mortem studies correlating histo-pathology with MRI have demonstrated that MTR is associated with decreased myelin content (demyelination) Barkhof *et al.*, 2003; Schmierer *et al.*, 2004, 2007). MTR is

also associated with axonal density which may have been reflected by the more heterogenous sampling of post mortem tissue in these studies (JH *et al.*, 1999; Barkhof *et al.*, 2003; Schmierer *et al.*, 2004, 2007).

Multiple studies have demonstrated an association between MTR measured in WML, GM and NAWM and clinical disability; and disease progression (Gass *et al.*, 1994; Filippi *et al.*, 2000; Ramió-Torrentà *et al.*, 2006; Khaleeli, Cercignani, *et al.*, 2007; Khaleeli, Sastre-Garriga, *et al.*, 2007; Rovaris *et al.*, 2008; Hayton *et al.*, 2009, 2012; Tur, Penny, *et al.*, 2011; Tur, Khaleeli, *et al.*, 2011; Amann *et al.*, 2015).

2.3 Proton magnetic resonance spectroscopy

2.3.1 Introduction to proton magnetic resonance spectroscopy

Proton magnetic resonance spectroscopy (^{1}H-MRS) can be used to detect and measure the concentration of proton containing brain metabolites *in vivo*. Building on the concepts described in 2.1.1, protons that precess in the B_0 magnetic field are also affected by orbiting electrons that create an additional "shielding" effect on the local magnetic field experienced by these protons. Each proton containing molecule with differing molecular structures therefore has a slightly differing resonance frequency – a property known as chemical shift. The chemical shift experienced by proton containing nuclei in the external magnetic field can be acquired as a spectrum where we can identify peaks that represent different proton-containing metabolites (Figure 2-3) (Salibi and Brown, 1997). The resonance frequencies of the spectral peaks are expressed in Hz or in ppm where ppm is a ratio to magnetic field strength and thus is not affected by changes in the strength of the external magnetic field (Salibi and Brown, 1997).

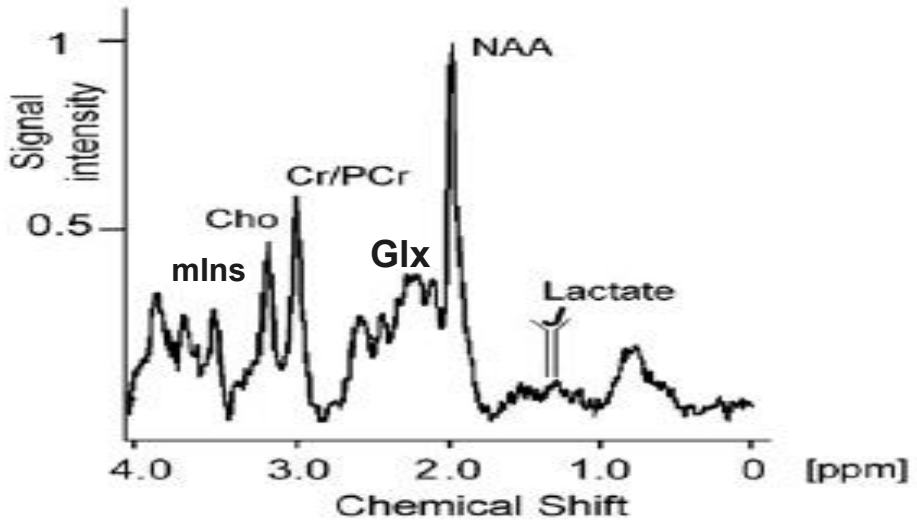

mIns = myo-inositol, Cho = choline, Cr/PCr = total creatine, Glx = glutamate + glutamine, NAA = N-acetyl aspartate

Figure 2-3. Example spectrum

Spectra can be acquired from a single voxel (single voxel spectroscopy (SVS)) or multiple voxels using a technique called chemical shift imaging (CSI). In SVS, spatial localisation techniques such as Point Resolved Spectroscopy (PRESS) or stimulated echo acquisition mode (STEAM) (see below) are used to define the voxel and obtain spectrum from a single volume of interest. The positioning in the brain depends on the analysis requirements and may include WML, NAWM, GM or a combination of the three (Frahm *et al.*, 1989; Longo and Vidimari, 1994). Typical voxel size ranges from 2-27cm^3 depending on the tissue pathology being analysed.

CSI uses phase encoding in one, two or three dimensions thereby acquiring spectra from multiple voxels during a single acquisition which provides more metabolite data than could be obtained from SVS (Brown, Kincaid and Ugurbil, 1982). Voxel dimensions in the phase encoded direction are determined by the field of view divided by the number of phase encoding steps (Salibi and Brown, 1997). The advantages of CSI include superior spatial resolution and the fact that this technique can be particularly useful when pathology is heterogeneous or multifocal. However, CSI generally requires longer scan times.

CSI is a form of proton magnetic resonance spectroscopic imaging. For consistency through this thesis, I will refer to CSI rather than proton magnetic resonance spectroscopic imaging whilst the single voxel spectroscopy technique will be referred to as SVS. ^{1}H-MRS will therefore be referred to when commenting on proton magnetic resonance spectroscopy as an advanced MRI technique encompassing both SVS and CSI.

The following sections concern the acquisition of both SVS and CSI.

Water suppression

When acquiring spectra, the proton containing metabolites are at a much lower concentration than the main proton containing molecule – water. With the spectral peak being proportional to the number of nuclear spins, water needs to be suppressed in order to better visualise the other proton containing metabolites in the spectrum. There are number of techniques for water suppression including the method used in this thesis: chemical shift selective saturation (CHESS) pulse. CHESS uses a frequency selective RF followed by a spoiler gradient to achieve water suppression. Other commonly used options for water suppression include (but not limited to) water suppression enhanced through T1 effects (WET) that uses four frequency selective RF pulses with different flip angles (Ogg, Kingsley and Taylor, 1994); and Water Elimination Fourier Transform (WEFT) that uses inversion recovery to null water signal (Patt and Sykes, 1972).

B_0 shimming

Magnetic inhomogeneities due to magnetic field distortions can have a significant effect on the quality of spectral acquisition, water suppression and accurate metabolite quantification. Shimming across the volume of interest is essential to ensure quality spectral acquisition. Shimming is of greater importance in CSI due to the larger volume of interest (VOI).

Repetition times and TE considerations

We need to use long TR to minimise the effects of T1 saturation, and short TE to decrease the impact of T2 relaxation. Short TE (~20-35ms) may improve

the spectral resolution of metabolites with complex *J*-coupled patterns e.g. myoinositol (mIns), glutamate and glutamine (Glx) (Wilson *et al.*, 2019). The TE can impact the metabolite peaks that can be measured in the spectra. Early MS studies used long TE of 272ms which enabled the accurate quantification of metabolites with longer T2 relaxation rates such as N-acetyl aspartate and lactate (Arnold *et al.*, 1990). It also produced a more stable baseline as metabolites with shorter T2 times have lost signal and macromolecules/lipids are less likely to cause baseline distortion. Later studies have used shorter TE values, e.g. 20-40ms, which enabled the measurement of metabolites with shorter T2 relaxation rates such as mIns and glutamate but at the expense of greater baseline distortion. For the experiments used in this thesis, short TE times were employed to facilitate the measurement of mIns and Glx peaks, both of which are of interest in MS.

Spatial localisation

Spatial localisation of signal from ^{1}H-MRS can be achieved using several methods. PRESS and STEAM are the two most commonly employed techniques and use slice-selective gradients on each axis and three RF pulses to obtain signal from excited spins at the intersection of the three orthogonal planes. PRESS sequences use 90^{o}-180^{o}-180^{o} pulses whilst STEAM sequences use three 90^{o} pulses (Bottomley and Park, 1982; Moonen *et al.*, 1989; Longo and Vidimari, 1994). PRESS provides higher SNR at longer TE values, whilst the STEAM sequence can to detect metabolites with a very short TE and use of 90^{o} RF pulses enables sharper slice profiles. However, PRESS provides greater SNR than STEAM at same TR and TE; and given we had additional focus on metabolites with T2 30-35ms (mIns), it was chosen as the spatial localisation technique for the studies used in this thesis (Salibi and Brown, 1997).

All localisation techniques exhibit a localisation error called the chemical shift displacement error (Wilson *et al.*, 2019). Chemical shift displacement error is the difference in parts per million between metabolites as a percentage of slice pre-localisation width. The absolute chemical shift displacement increases with the width of the slice (Wilson *et al.*, 2011).

There can be contamination of a voxel from signal arising outside of it. This is more of an issue in CSI where a grid of voxels is being imaged. The point spread function is a measurement of the amount of signal contribution from outside the displayed grid boundaries. For phase encoded CSI, it is represented by a complex sinc function and therefore signal arising from within the voxel decreases as you venture away from the centre (Wilson *et al.*, 2019).

Outer volume suppression

Lipid artefact at the periphery of the skull can contaminate and interfere with the signal obtained from adjacent tissues. This effect can be minimised by the use of outer volume suppression bands that use saturation pulses to dephase lipid spins (Salibi and Brown, 1997).

Metabolite quantification

Quantification of metabolites acquired at short echo times is challenging for several reasons - overlapping spectral peaks, signal background mainly comprising macromolecules overlaps with metabolite peaks, low SNR and correct fitting of line-shapes at higher field strengths (Graveron-Demilly, 2014).

Metabolite peaks can be quantified from either the time-domain or frequency domain signal (Mierisová and Ala-Korpela, 2001; Vanhamme *et al.*, 2001; Poullet, Sima and Van Huffel, 2008; Graveron-Demilly, 2014). Advantages of the time domain signal include avoiding the need to convert to frequency domain using Fourier Transformation and missing data points in signal can be ignored. An advantage of frequency domain is that the residual water peak does not need to be removed prior to the quantification step (Graveron-Demilly, 2014).

Following this step, metabolite concentrations need to be modelled using mathematical functions. This model function needs to estimate a) the metabolite concentration (potentially using a basis set) b) background signal, c) gaussian distributed noise and d) decay function which is the lineshape (Mierisová and Ala-Korpela, 2001; Vanhamme *et al.*, 2001; Poullet, Sima and Van Huffel, 2008; Graveron-Demilly, 2014).

There are a number of software programs used in metabolite quantification. The most commonly used programs are summarised in Table 2-1.

Table 2-1 . Commonly used software programs used in metabolite quantification

Program	Metabolite basis-set	Domain	Model function
AMARES	No	Time	Any
LCModel	Yes	Frequency	Any
SiToolsFITT	Yes	Frequency	Any
QUEST	Yes	Time	Any
AQSES	Yes	Time	Any
TARQIUN	Yes	Time	Any

AMARES = advanced method for accurate, robust, and efficient spectral fitting (Vanhamme, Van Den Boogaart and Van Huffel, 1997), LCModel = linear combination of model spectra (Provencher, 1993), SiToolsFITT (Young, Soher and Maudsley, 1998), QUEST = quantitation based on semi-parametric quantum estimation (Ratiney *et al.*, 2005), AQSES = Automated Quantitation of Short Echo time MRS spectra (Poullet *et al.*, 2007),TARQUIN = totally automatic robust quantitation in NMR (Reynolds *et al.*, 2006)

LCModel® uses smoothly varying spline functions to fit a basis set of spectra to the patient *in vivo* data (Provencher, 1993). An example of a spectrum obtained from LCModel® is shown in The fitted spectrum is shown in red which overlays the original data. The spline baseline is seen at the bottom. The residual difference between the observed and fitted spectrum is seen in the box at the top.

Figure 2-4.

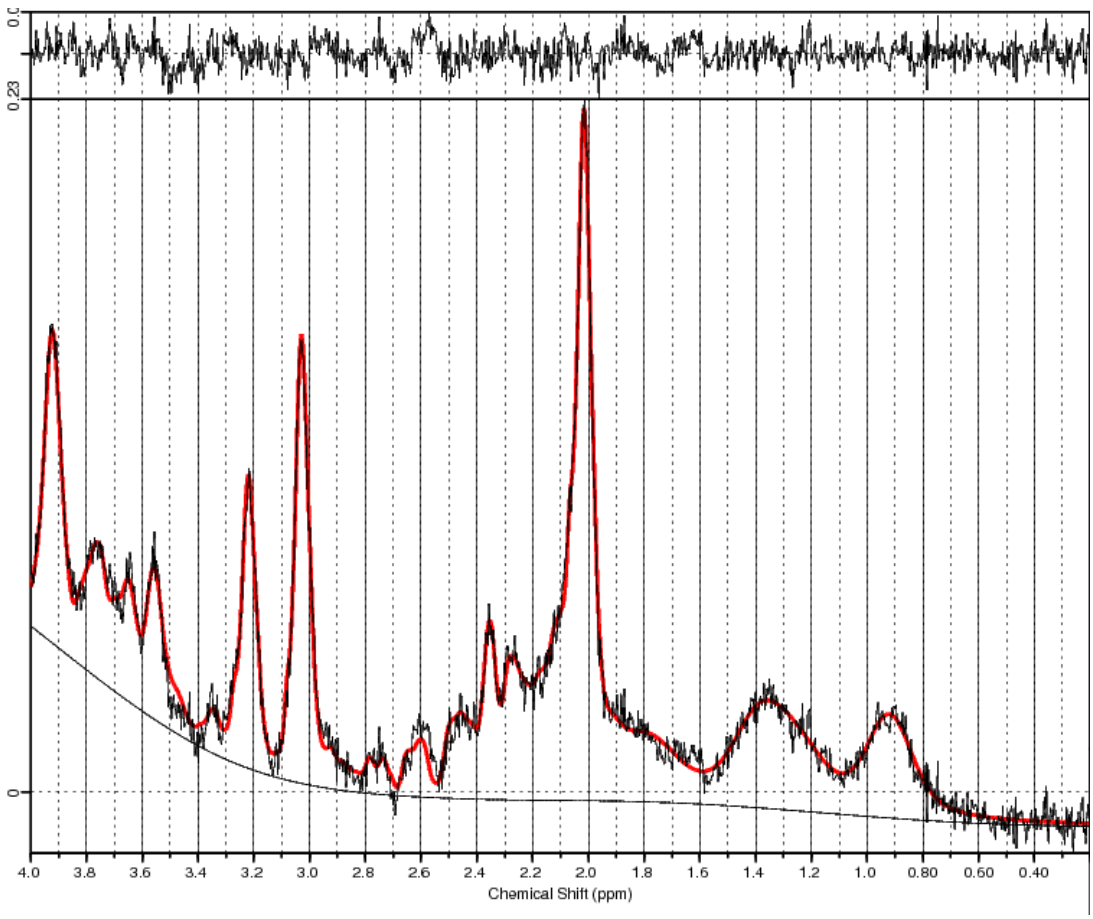

The fitted spectrum is shown in red which overlays the original data. The spline baseline is seen at the bottom. The residual difference between the observed and fitted spectrum is seen in the box at the top.

Figure 2-4: Example spectrum from LCModel output from a healthy subject.

The fact we do not know the numerous factors that influence MR spectra mean that the spectral peaks need to be normalised to enable accurate metabolite quantification and comparison within and between subjects. The factors that vary include T1 and T2 relaxation times, partial volume effect and head coil sensitivity. Factors such as T1 and T2 relaxation times and coil sensitivity can be corrected for or minimised by the use of stable acquisition parameters and consistent VOI placement for all subjects within a given study.

Normalised peak areas can be quantified using two main methods:

i) Ratios to a stable “normal” reference

ii) Absolute quantification

Peak area ratios express the metabolite as a ratio to a stable internal reference and results are expressed in institutional units (IU). The most

commonly used stable internal reference is total creatine (tCr) (see below for outline). However, there is evidence from several studies that tCr may not be a stable denominator in MS (Suhy *et al.*, 2000; Vrenken *et al.*, 2005). Another issue is that changes can be masked when the numerator and denominator change in the same direction. The advantages of this method are that no correction for T1 or T2 relaxation effects is required, they are simple to use and require minimal post-processing compared to absolute metabolite quantification.

Absolute metabolite concentrations are expressed in millimolar units or institutional units (IU) and are referenced using an internal stable metabolite (most commonly water) or an external phantom (Ernst, Kreis and Ross, 1993; Kreis, Ernst and Ross, 1993; Michaelis *et al.*, 1993). Questions remain as to the suitability of intravoxel water content as an internal reference given the possibility that water distribution is heterogenous and non-constant in pathology states such as MS. Multiple adjustments and corrections also need to be made to account for differences in relaxation and coil loading. Coil loading can be corrected for by acquiring subject metabolite and reference data under the same coil loading conditions; coil loading is also the same for an internal reference.

2.3.2 Metabolites of interest in multiple sclerosis

N-acetyl aspartate:

N-acetyl aspartate (NAA) is an amino acid synthesised by mitochondria found in high concentrations in the mammalian brain (Tallan, Moore and Stein, 1956; Tallan, 1957; Benuck and D'Adamo, 1968; Goldstein, 1969; Patel and Clark, 1979). The NAA peak also consists of contributions from N-acetyl aspartate glutamate (NAAG) (~15-20% of total NAA signal) (Pouwels and Frahm, 1997; Clark *et al.*, 2006). Studies over several decades have established that NAA is located in neuronal cell populations (Moffett *et al.*, 1991; Urenjak *et al.*, 1992; Moffett and Namboodiri, 1995; Bjartmar *et al.*, 2002). Subsequent studies also identified the presence of NAA in oligodendrocyte progenitor cells but there is minimal contribution to the *in vivo* human NAA signal (Bhakoo and Pearce, 2001; Bjartmar *et al.*, 2002; Moffett *et al.*, 2006). The peak containing total

methyl resonance of N-acetyl containing compounds resonates at 2.01ppm. This peak primarily reflects NAA and to a lesser extent N-acetyl aspartyl glutamate (NAAG) (Pouwels and Frahm, 1997). Due to overlapping resonances, NAA and NAAG are not separately resolved in the majority of papers, and are referred to as “NAA” or total NAA (tNAA).

Using histopathological studies to examine NAA in PMS, NAA has been demonstrated to be a marker of neuro-axonal integrity with NAA decreased in WML and deep GM structures in MS (Davies *et al.*, 1995; Bjartmar *et al.*, 2002; Cifelli *et al.*, 2002). Further work using in vivo imaging modelling techniques showed that NAA (synthesised in mitochondria) is a potential marker of mitochondrial dysfunction (Ciccarelli *et al.*, 2010).

For the remainder of this thesis, I will refer to total NAA (tNAA) = N-acetyl aspartate (NAA) + N-acetyl aspartyl glutamate (NAAG); and unless specified is synonymous with NAA. NAA and NAAG is only referred to in studies that specifically resolve and report them separately.

Creatine:

Creatine is a nitrogenous organic acid that can be synthesised endogenously in the brain (Wallimann *et al.*, 1992; Braissant *et al.*, 2001, 2010; Wallimann, Tokarska-Schlattner and Schlattner, 2011). It is found in high concentrations in the human brain and exhibits functions in ATP regeneration, as an osmolyte and potentially as a neurotransmitter (Wyss and Kaddurah-Daouk, 2000; Bothwell *et al.*, 2001; Bothwell, Styles and Bhakoo, 2002; Neu *et al.*, 2002; Koga *et al.*, 2005; Almeida *et al.*, 2006; Béard and Braissant, 2010; Peral, Vázquez-Carretero and Ilundain, 2010). It is reliably detected using MRS as a singlet peak resonating at 3.0ppm (Pfeuffer *et al.*, 1999; Govindaraju, Young and Maudsley, 2000; Rackayova, Pouwels and Braissant, 2017). The total creatine peak consists of creatine and phosphocreatine. Whilst it has been proposed that tCr is glial-specific and thus a putative marker of gliosis, this is not supported by animal studies where tCr is found in both neurons and glial cells (Schmidt, 2004; Tachikawa *et al.*, 2004; Braissant *et al.*, 2010).

The majority of studies do not resolve creatine and phosphocreatine and report total creatine resonances as either “total creatine” or “creatine”. From here on unless specified otherwise, total creatine (tCr = creatine + phosphocreatine) is used and is synonymous with creatine (Cr).

Myoinositol:

Myo-inositol (mIns) is a precursor molecule of inositol phospholipids and is synthesised de novo from glucose by the kidneys, brain and testis (Hauser and Finelli, 1963; Clements and Diethelm, 1979). Its distribution in the brain is thought be either exclusively or predominantly in glial cells (Glanville *et al.*, 1989; Brand, Richter-Landsberg and Leibfritz, 1993). A study correlating histopathology with *in vivo* ^{1}H-MRS of biopsies taken from acute lesions showed increases of mIns and mIns/tCr in WML, with mIns higher in WML showing fibrillary gliosis suggesting that mIns is a marker of astrogliosis (Bitsch *et al.*, 1999).

Choline:

Choline (Cho) is the precursor for acetylcholine and phosphatidylcholine. Acetylcholine is a neurotransmitter synthesised by cholinergic neurons whilst phosphatidylcholine is a major constituent of cell membranes. Cho is phosphorylated to phosphocholine with phosphocholine then being used in the formation of phosphatidylcholine. Phosphatidylcholine is then catabolised into fatty acid and glycerophosphocholine (Miller, 1991).

The Cho peak resonates at 3.2 ppm and likely consists of several Cho-containing compounds including free choline, phosphocholine, glycerophosphocholine and phosphatidylcholine (Miller, 1991). Total choline (tCho) has been shown to be increased in active MS lesions and a marker of membrane turnover where membrane turnover in active enhancing lesions likely reflects the combined processes of inflammatory demyelination, axonal loss and remyelination; whilst studies from brain tumours suggest it is also a marker of cellularity (Brenner *et al.*, 1993; Davies *et al.*, 1995; De Stefano *et al.*, 1995; Miller *et al.*, 1996; Swanberg *et al.*, 2019).

Almost all MS studies exploring Cho are actually referring to tCho and do not separately resolve for each of the Cho containing compounds that make up the spectrum peak. Therefore, tCho is used for the remainder of this thesis and unless otherwise specified, is synonymous with Cho.

Glutamate and glutamine:

Glutamate is an excitatory neurotransmitter in the CNS and is synthesised from its pre-cursor molecule glutamine via the action of the enzyme glutaminase. In ^{1}H-MRS, at clinical field strengths it is often measured as a peak with glutamine (Glx) that resonates at approximately 2.30ppm. All three studies that have examined either cross-sectional or longitudinal changes in glutamate in PMS have found that glutamate or Glx concentrations are lower in PMS compared to healthy controls (HC) (in CGM) and that concentrations decrease over time (Sastre-Garriga *et al.*, 2005; Azevedo *et al.*, 2014; MacMillan *et al.*, 2016). Experimental animal work has shown extracellular glutaminergic excitotoxicity to be involved of MS pathophysiology (Macrez *et al.*, 2016), but as yet there are no studies that have examined the histopathological correlation between glutamate (or Glx) measured using ^{1}H-MRS techniques in humans. As a result, studies examining glutamate in PMS have found varying results and the significance of these remains unclear when explaining the underlying pathophysiology.

2.3.3 The role of proton magnetic resonance spectroscopy imaging in understanding pathology in progressive multiple sclerosis

Studies using ^{1}H-MRS in MS initially focused on WML but over time as the understanding of MS grew, the technique was used to also explore NAWM and GM. The following section summarises the key findings using ^{1}H-MRS for different tissue types (WML, NAWM, GM) in the brain in PMS. Studies that contained and reported results for PMS cohorts are summarised in Table 2-2.

White matter lesions:

Numerous studies have demonstrated that the tNAA/tCr is decreased in WML in all MS subtypes. The earliest studies using SVS to examine WML in PMS

showed that tNAA ratios to tCr and the tNAA ratio to tCho were lower in PMS cohorts compared to HC (Arnold *et al.*, 1990, 1994; Matthews *et al.*, 1991; Van Hecke *et al.*, 1991; Fu *et al.*, 1996; Davie *et al.*, 1997; van Walderveen *et al.*, 1998; Van Walderveen *et al.*, 1999; Brex *et al.*, 2000; Pelletier *et al.*, 2003; Rahimian *et al.*, 2013).

A single study by Simone et al reported contrasting results with no statistical differences in tCho, tNAA/tCr and tNAA/tCho in a mixed MS cohort (SPMS = 7). This may have been due to a lack of statistical power owing to the small number of lesions analysed in the study (Simone *et al.*, 2001).

The ratio of tNAA/tCr was initially postulated to be driven by changes in tNAA but Suhy et al suggested that tCr may not always be a stable denominator. They showed that tNAA/tCr was decreased in WML in PPMS compared to RRMS and using absolute metabolite quantification showed that the decrease in tNAA/tCr was due to increased tCr (Suhy *et al.*, 2000).

Numerous studies have demonstrated that the NAA/tCr and thereby neuro-axonal integrity/mitochondrial function is decreased when examining WML in all MS subtypes (Swanberg *et al.*, 2019) (Caramanos, Narayanan and Arnold, 2005).

Normal appearing white matter:

tNAA:

Histopathological analysis of NAWM in MS showed that there were significant changes including gliosis, unsuspected demyelination and axonal damage/loss (Allen and McKeown, 1979; Evangelou *et al.*, 2000). The earliest work looking at brain metabolites in NAWM in PMS subjects using ^{1}H-MRS showed that NAWM was metabolically different to HC with decreased tNAA/tCr or tNAA levels suggesting the presence of metabolic changes that were not reflected during more conventional structural white matter (WM) imaging, findings that were also supported by histopathological studies (Husted *et al.*, 1994; Davies *et al.*, 1995; Bjartmar *et al.*, 2000).

Subsequently, multiple studies have shown that tNAA/tCr and tNAA in NAWM; and central regions of interest in NAWM are lower in PMS compared to HC (Peters *et al.*, 1995; Fu *et al.*, 1996; A. Tourbah *et al.*, 1999; S M Leary *et al.*, 1999; Sarchielli *et al.*, 1999; Suhy *et al.*, 2000; De Stefano *et al.*, 2001; Pelletier *et al.*, 2002; Oh, 2004; Oh, Pelletier and Nelson, 2004; Aboul-Enein *et al.*, 2010; Swanberg *et al.*, 2019).

Myo-inositol:

Several studies have shown that mIns in NAWM is higher in PPMS and SPMS cohorts compared to HC (Sastre-Garriga *et al.*, 2005; Vrenken *et al.*, 2005).

Obert et al most recently used a SVS technique to undertake a longitudinal analysis of RRMS (n =21) and SPMS (n = 15). tNAA/tCr showed a statistically significant decrease over 2 years in the SPMS cohort ($p < 0.01$). They also showed that mIns and mIns/tCr were higher in WML of the combined RRMS/SPMS cohort compared to NAWM over 2 years ($p < 0.01$) (Obert *et al.*, 2016).

Grey matter

The measurement of GM metabolite concentrations provides technical challenges due to higher partial volume effects. These factors need to be considered and careful voxel placement or regression modelling is important when analysing CGM. In the few studies that examined GM, tNAA and its ratio to tCr were consistently shown to be decreased in PMS when compared to HC and/or RRMS (Sarchielli *et al.*, 2002; Adalsteinsson *et al.*, 2003; Sastre-Garriga *et al.*, 2005; Geurts *et al.*, 2006; Sijens, Mostert, *et al.*, 2006; Caramanos *et al.*, 2009).

2.3.4 Longitudinal studies of brain metabolites in progressive multiple sclerosis

There have been numerous cross-sectional studies of brain metabolites in PMS. However, there have been comparatively far fewer longitudinal studies exploring changes in brain metabolites. These have shown conflicting results with several studies showing no statistically significant reductions in tNAA or

tNAA/tCr over 24-30 months (De Stefano *et al.*, 1998; Fu *et al.*, 1998; MacMillan *et al.*, 2016), whilst a single study showed a decrease in tNAA/tCr in NAWM over 24 months (Obert *et al.*, 2016).

2.3.5 Proton magnetic resonance spectroscopy imaging and clinically isolated syndrome

Studies using ^{1}H-MRS in CIS have mainly examined metabolites from NAWM. Results seemed to suggest that there was no difference in metabolites e.g. tNAA in CIS compared to HC (P A Brex *et al.*, 1999; Kapeller *et al.*, 2002; Ranjeva *et al.*, 2003; Fernando *et al.*, 2004). Other studies however, found that tNAA and tNAA/tCr were decreased in NAWM of adults with CIS suggesting that there were changes in neuroaxonal integrity in early relapse onset MS (Rocca *et al.*, 2003; Wattjes *et al.*, 2007; M. P. Wattjes *et al.*, 2008; Mike P. Wattjes *et al.*, 2008). The conflicting results could be explained by the fact that early negative studies used 1.5T MR scanners and the VOI was placed in the corpus callosum as opposed to the positive studies that measured metabolites from parietal NAWM or tNAA from the whole brain. There were also mixed results in studies that measured mIns, with several studies showing no difference, and a single study showing an increase in NAWM mIns in CIS (P A Brex *et al.*, 1999; Kapeller *et al.*, 2002; Fernando *et al.*, 2004; M. P. Wattjes *et al.*, 2008; Mike P. Wattjes *et al.*, 2008). tNAA/tCr showed a moderate association with T2LV and a smaller association with normalised brain volume (NBV) (Sbardella *et al.*, 2011). Studies that have examined ^{1}H-MRS in CIS cohorts are summarised in Table 2-3.

Table 2-2. Summary of proton magnetic resonance spectroscopy studies containing progressive multiple sclerosis cohorts

Study	Cohorts		^{1}H-MRS acquisition						Spectral post-processing			Key findings
First Author	**MS type**	**HC**	**Metabolite**	**Tissue**	**Scanner**	**MRS type**	**Localis-ation**	**TR/TE (ms)**	**Reference**	**Quantific-ation type / program**	**Unit**	
Arnold (Arnold *et al.*, 1990)	MS- 7	2	tNAA, tCho, Lac	WML	1.5T Phillips	SVS	ns	2500 / 272, 136, 68	Ratio to tCr	Peak heights above baseline	IU	↓tNAA/tCr in 4/7 with MS
Van Hecke (Van Hecke *et al.*, 1991)	8 RRMS 10 SPMS	17	tNAA, tCho	WML	1.5T Siemens	SVS	STEAM	3000/ 270	Ratio to tCr and tCho	Measured peaks	IU	↓tNAA/tCr, ↓tNAA/tCho
Matthews (Matthew	8 severe MS	9	tNAA	WML	1.5T Philips	SVS	PRESS	2000-4000/	Ratio to tCr	Relative peak heights	IU	↓tNAA/tCr

Study	Cohorts		^{1}H-MRS acquisition						Spectral post-processing			Key findings
First Author	**MS type**	**HC**	**Metabolite**	**Tissue**	**Scanner**	**MRS type**	**Localis-ation**	**TR/TE (ms)**	**Reference**	**Quantific-ation type / program**	**Unit**	
s *et al.*, 1991)								136-272				
Arnold (Arnold *et al.*, 1994)	4 RRMS 3 SPMS	13	tNAA, tCr	WML	1.5T Philips	SVS	PRESS	2000/ 272	Ratio to tCr	Peak heights relative to baseline	IU	↓tNAA/tCr over 18 months
Davies (Davies *et al.*, 1995)	8 post mortem – 6 CDMS, 2 probable MS	6	NAA, NAAG, tCr, mIns, tCho, Lac, Glut	WML, NAWM	N/A	Ex vivo	N/A	N/A	$TSPd_3$	Absolute concentrations	mM	↓NAA in WM adjacent to WML, WML but not NAWM ↓tCr in WM adjacent to WML, WML but not NAWM ↑mIns/tCr in WM adjacent to WML and WML

Study	Cohorts		^{1}H-MRS acquisition						Spectral post-processing			Key findings
First Author	**MS type**	**HC**	**Metabolite**	**Tissue**	**Scanner**	**MRS type**	**Localis-ation**	**TR/TE (ms)**	**Reference**	**Quantific-ation type / program**	**Unit**	
Peters (Peters *et al.*, 1995)	4 RRMS 5 SPMS 2 PPMS	3	tNAA, tCho, tCr, lac	WML, NAWM	1.5T Philips	CSI	2D-PRESS	1200 / 272	Ratio to summed metabolite peaks	Sun Sparcstation IPX	IU	↓tNAA in MS group
Matthews (Matthews *et al.*, 1996)	11 RRMS 18 SPMS	19	tNAA, tCr	Mixed VOI	1.5T Philips	SVS	PRESS	2000 / 272	Ratio to tCr	Peak area	IU	↓tNAA/tCr
Fu (Fu *et al.*, 1996)	14 RRMS 21 SPMS	17	tNAA, tCr	Mixed VOI	1.5T Philips	2D CSI	PRESS	2000/ 272	Ratio to tCr	SUNSpec 1	IU	↓tNAA/tCr in NAWM and WML compared to HC tNAA/tCr associated with clinical disability

Study	Cohorts		^{1}H-MRS acquisition						Spectral post-processing			Key findings
First Author	**MS type**	**HC**	**Metabolite**	**Tissue**	**Scanner**	**MRS type**	**Localis-ation**	**TR/TE (ms)**	**Reference**	**Quantific-ation type / program**	**Unit**	
Narayanan (Narayanan *et al.*, 1997)	11 RRMS 17 PMS	13	tNAA, tCr	Heterogenous VOI	1.5T Philips	CSI	PRESS	2000 / 272	Ratio to tCr	Sun SPRAC station IPX	IU	tNAA/tCr lowest in PMS compared to RRMS and HC
Davie (Davie *et al.*, 1997)	9 RRMS 9 BMS SPMS 10 PPMS 8	9	tNAA, tCho, tCr	WML, NAWM	1.5 GE	SVS	STEAM	2000 / 135	Water	SA GE®	mM	↓tNAA in WML
De Stefano	11 RRMS 18 SPMS	20	tNAA, tCr	WML, NAWM	1.5T Philips	CSI	PRESS	2000/ 272	Ratio to tCr	XUNspec 1	IU	Nil significant % change in tNAA/tCr. No correlation with EDSS in SPMS

Study	Cohorts		^{1}H-MRS acquisition						Spectral post-processing			Key findings
First Author	**MS type**	**HC**	**Metabolite**	**Tissue**	**Scanner**	**MRS type**	**Localis-ation**	**TR/TE (ms)**	**Reference**	**Quantific-ation type / program**	**Unit**	
(De Stefano *et al.*, 1998)												
Fu (Fu *et al.*, 1998)	11 RRMS 17 SPMS	12	tNAA, tCr	NAWM, WML	1.5T Philips	CSI	PRESS	2000 / 272	Ratio to tCr	SUN/SPARC using XUNspec 1	IU	↓tNAA/tCr
Falini (Falini *et al.*, 1998)	16 BMS 14 SPMS	13	tNAA, tCr, tCho	WML, NAWM, frontal cortex	1.5T	SVS	STEAM	1500 / 20	Ratio to tCr	Standard software	IU	↓tNAA/tCr and ↓tNAA/tCho in WML WML tNAA/tCr in BMS > SPMS

Study	Cohorts		^{1}H-MRS acquisition						Spectral post-processing			Key findings
First Author	**MS type**	**HC**	**Metabolite**	**Tissue**	**Scanner**	**MRS type**	**Localis-ation**	**TR/TE (ms)**	**Reference**	**Quantific-ation type / program**	**Unit**	
Foong (Foong *et al.*, 1999)	16 SPMS 6 RRMS 3 PPMS	38	tNAA, tCr, tCho	Frontal VOI (WML, NAWM)	1.5T GE	SVS	STEAM	2000 / 135	Ratio to tCr	SA GE®	IU	↓tNAA/tCr No correlation with cognitive (executive) function or physical performance scores
Sarchielli (Sarchielli *et al.*, 1999)	27 RRMS 13 SPMS	12	tNAA, tCr, tCho	NAWM	1.5T GE	SVS	STEAM	4000/ 18, 100	External Water	External water	mM/ Kg WW	↓tNAA in NAWM in MS and SPMS cohorts Correlation (r=-0.79) between EDSS and tNAA in whole MS group
Pike (Pike *et al.*, 1999)	11 RRMS 5 PPMS 14 SPMS	12	tNAA/tCr	NAWM, WML	1.5T Philips	CSI	PRESS	2000/ 272	Ratio to tCr	SunSpec 1	IU	No correlation for MTR and tNAA/tCr in PMS groups

Study	Cohorts		^{1}H-MRS acquisition						Spectral post-processing			Key findings
First Author	**MS type**	**HC**	**Metabolite**	**Tissue**	**Scanner**	**MRS type**	**Localis-ation**	**TR/TE (ms)**	**Reference**	**Quantific-ation type / program**	**Unit**	
Tourbah (A. Tourbah *et al.*, 1999)	40 RRMS 15 SPMS	15	tNAA, tCho, tCr, mIns	WML, NAWM	1.5T GE	SVS	STEAM	1500 / 18 & 136	Ratio to tCr and tCho	SA GE®	IU	No differences at short TE. At long TE, ↓tNAA/tCr in MS group
Davie (Davie *et al.*, 1999)	3 RRMS 5 BMS 10 SPMS	1*	tNAA, tCr	WML	1.5T GE	SVS	STEAM	2135 / 135	Internal Water	SA GE®	mM	↓tNAA in chronic WML Correlation between tNAA and MTR in SPMS (r=0.83)
Walderveen (Van Walderveen *et al.*, 1999)	2 RRMS 12 SPMS	4	tNAA, tCho, tCr	WML, NAWM	1.5T Siemens	SVS	PRESS	2500 / 135	1. Ratio to tCr 2. Coil	LCModel	mM	↓tNAA and tNAA/tCr in NAWM WML: ↓tNAA and ↓tCr compared to NAWM

Study	Cohorts		^{1}H-MRS acquisition						Spectral post-processing			Key findings
First Author	**MS type**	**HC**	**Metabolite**	**Tissue**	**Scanner**	**MRS type**	**Localis-ation**	**TR/TE (ms)**	**Reference**	**Quantific-ation type / program**	**Unit**	
												↓tNAA in T1 hypointense lesions
Tourbah (A Tourbah *et al.*, 1999)	72 RRMS 32 SPMS	15	tNAA, tCho, tCr, mIns	WML, NAWM	1.5T GE	SVS	STEAM	1500 / 135, 18	Ratio tCr, tCho	SA GE®	IU	↓tNAA/tCr in WML. ↑tCho/tCr in WML No difference in tNAA/tCr in NAWM of SPMS
Leary (S. M. Leary *et al.*, 1999)	24 PPMS	16	tNAA, tCr	NAWM	1.5T GE	SVS	PRESS	3000/ 30	1. Ratio to tCr 2. External phantom	LCModel	IU/ mM	↓tNAA/tCr, ↓tNAA tCr stable

Study	Cohorts		^{1}H-MRS acquisition						Spectral post-processing			Key findings
First Author	**MS type**	**HC**	**Metabolite**	**Tissue**	**Scanner**	**MRS type**	**Localis-ation**	**TR/TE (ms)**	**Reference**	**Quantific-ation type / program**	**Unit**	
Bjartmar+ (Bjartmar *et al.*, 2000)	7 SPMS	6	NAA	SC WML, NAWM	N/A	N/A	N/A	N/A	N/A	Absolute	nmol /mg	↓NAA in demyelinated axons and normally appearing myelinated axons
Cifelli (Cifelli *et al.*, 2002)	14 SPMS 10 autopsies (6 SPMS, 3 PPMS)	13	tNAA, tCho, tCr	Deep GM	3T Varien	SVS	PRESS	5000 / 26	Water	LCModel	mM	↓tNAA

Study	Cohorts		^{1}H-MRS acquisition						Spectral post-processing			Key findings
First Author	**MS type**	**HC**	**Metabolite**	**Tissue**	**Scanner**	**MRS type**	**Localis-ation**	**TR/TE (ms)**	**Reference**	**Quantific-ation type / program**	**Unit**	
Cucurella (Cucurella *et al.*, 2000)	18 SPMS 17 PPMS	17	tNAA, tCho, tCr	WML, NAWM	1.5T Siemens	SVS	PRESS	1600 / 135	1. Ratio to tCr 2. CSF/ head coil loading	MRUI & VARPRO	IU	NAWM: ↓tNAA, ↓tNAA/tCho in whole group. ↓tNAA/tCr in PPMS only WML ↓tNAA, ↓tNAA/tCr.↑tCho/tCr in SPMS
Brex (Brex *et al.*, 2000)	11 SPMS	Nil	tNAA, tCho, tCr, mIns	WML	1.5T GE	SVS	PRESS	3000 / 30	External phantom	LCModel	mM	↓tNAA in T1 hypointense lesions ↑mIns in T1 hypointense lesions
Suhy (Suhy *et al.*, 2000)	13 RRMS 15 PPMS	20	tNAA, tCr	WML, NAWM	1.5T Siemens	CSI	PRESS	1800/ 135	1. CSF 2. Ratio to tCr	In house software	mM /IU	NAWM: tNAA/tCr in PPMS < RRMS < HC. tCr in PPMS > RRMS > HC. Correlation tNAA/tCr and EDSS (r=0.67)

Study	Cohorts		^{1}H-MRS acquisition						Spectral post-processing			Key findings
First Author	**MS type**	**HC**	**Metabolite**	**Tissue**	**Scanner**	**MRS type**	**Localis-ation**	**TR/TE (ms)**	**Reference**	**Quantific-ation type / program**	**Unit**	
												WML: ↓tNAA/tCr. No correlation with EDSS
Simone (Simone *et al.*, 2001)	47 RRMS 7 SPMS	22	tNAA, lac, tCho, tCr	WML	1.5T Siemens	SVS	ns	1500 / 135	Ratio to tCr	ns	IU	No changes in SPMS
De Stefano (De Stefano *et al.*, 2001)	55 RRMS 33 SPMS	17	tNAA, tCr	NAWM	1.5T Philips	CSI	PRESS	2000 / 272	Ratio to tCr	ns	IU	↓tNAA/tCr in SPMS and RRMS groups No correlation between tNAA/tCr and EDSS in higher EDSS subgroup

Study	Cohorts		^{1}H-MRS acquisition						Spectral post-processing			Key findings
First Author	**MS type**	**HC**	**Metabolite**	**Tissue**	**Scanner**	**MRS type**	**Localis-ation**	**TR/TE (ms)**	**Reference**	**Quantific-ation type / program**	**Unit**	
Pelletier (Pelletier *et al.*, 2002)	9 RRMS 21 SPMS 18 PPMS	10	tNAA, tCr	Corpus callosum, WML	1.5T GE	3 ROI	3D EPSI	2000 / 144	Ratio to tCr	Sun Microsystems®	IU	↓tNAA/tCr in supratentorial brain and central brain
Pan (Pan *et al.*, 2002)	8 RRMS 8 PPMS 8 SPMS	8	tCho, tNAA, tCr	Periventricular WM	4T	SVS	Refocusing slice selection	2000 / 50	Ratio to tNAA Internal water	ns	IU/ mM	↓tNAA in SPMS compared to PPMS
Sarchielli (Sarchielli *et al.*, 2002)	15 RRMS 15 SPMS	8	tNAA, tCho, tCr	CGM	1.5T GE	SVS	STEAM	4000/ 100, 18	External water	ns	mM	↓tNAA in SPMS ↓tCr in SPMS compared to RRMS, HC

Study	Cohorts		^{1}H-MRS acquisition						Spectral post-processing			Key findings
First Author	**MS type**	**HC**	**Metabolite**	**Tissue**	**Scanner**	**MRS type**	**Localis-ation**	**TR/TE (ms)**	**Reference**	**Quantific-ation type / program**	**Unit**	
Tartaglia (Tartaglia *et al.*, 2002)	7 RRMS 5 SPMS	29	tNAA, tCr	Periventricular WM	1.5T Philips	CSI	MRSI	2000 / 272	Ratio to tCr	XunSpec 1	IU	↑tCho/tCr in pre-lesional NAWM
Pelletier (Pelletier *et al.*, 2003)	18 PPMS	10	tNAA, tCr	Mixed VOI	1.5T GE	2D-CSI	3D EPSI	2000/ 144	Ratio to tCr	Sun Microsystems®	IU	No significant changes in tNAA/tCr No correlation between tNAA/tCr and T2LV or index brain atrophy
Adalsteinsso-n (Adalsteinsson *et al.*, 2003)	5 RRMS 5 SPMS	9	tNAA, tCho, tCr	NAGM, GM	1.5T GE	CSI	ns	2000 / 144	Water	In house software	mM	↓tNAA in NAGM in SPMS ↓tNAA in NAWM in SPMS & RRMS

Study	Cohorts		^{1}H-MRS acquisition						Spectral post-processing			Key findings
First Author	**MS type**	**HC**	**Metabolite**	**Tissue**	**Scanner**	**MRS type**	**Localis-ation**	**TR/TE (ms)**	**Reference**	**Quantific-ation type / program**	**Unit**	
												No correlation between tNAA and EDSS in GM
Brass (Brass *et al.*, 2004)	13 BMS 10 SPMS	15	tNAA, tCr	Mixed VOI of NAWM, GM	1.5T Philips	CSI	PRESS	2000 / 272	Ratio to tCr	ns	IU	↓tNAA/tCr in BMS and SPMS
Narayana (Narayana *et al.*, 2004)	53 PPMS	0	tNAA, tCr	NAWM, WML	1.5T GE	CSI	ns	1000 / 30	Ratio to tCr	Custom IDL environment	IU	↓tNAA/tCr No difference between tNAA in NAWM and lesion containing regions

Study	Cohorts		^{1}H-MRS acquisition						Spectral post-processing			Key findings
First Author	**MS type**	**HC**	**Metabolite**	**Tissue**	**Scanner**	**MRS type**	**Localis-ation**	**TR/TE (ms)**	**Reference**	**Quantific-ation type / program**	**Unit**	
Oh (Oh, Pelletier and Nelson, 2004)	12 RRMS 12 SPMS	15	tNAA, tCho, tCr	Normal Corpus callosum	1.5T GE	CSI	PRESS	1000 / 144	Ratio to tCr	Sun Ultra10	IU	↓tNAA/tCr in SPMS
Cox (Cox *et al.*, 2004)	19 SPMS	0	tNAA/tCr	WML, NAWM	1.5T GE	CSI	3D EPSI	2000 / 144	Ratio to tCr	Sun Microsystems®	IU	tNAA/tCr not associated with tests of cognitive performance

Study	Cohorts		^{1}H-MRS acquisition						Spectral post-processing			Key findings
First Author	**MS type**	**HC**	**Metabolite**	**Tissue**	**Scanner**	**MRS type**	**Localis-ation**	**TR/TE (ms)**	**Reference**	**Quantific-ation type / program**	**Unit**	
Vrenken (Vrenken *et al.*, 2005)	40 RRMS 12 PPMS 16 SPMS	25	tNAA, tCr, NAA, NAAG, tCho, mIns, Glu, Gln	NAWM	1.5T Siemens	SVS	STEAM	6000 / 20	Ratio to tCr Head coil loading	LCModel	mM	No difference in tNAA ↓NAA/tCr compared to HC in PPMS, RRMS and SPMS ↑tCr compared to HC in RRMS and SPMS groups ↑mIns in all MS groups No association with EDSS
Rovaris (Marco Rovaris *et al.*, 2005)	32 PPMS	16	tNAA	Whole brain	1.5T Siemens	Whole brain	180^{0} selective pulses	768 / 180	External phantom	Sun SPARCstation	mM	No difference in tNAA

Study	Cohorts		^{1}H-MRS acquisition						Spectral post-processing			Key findings
First Author	**MS type**	**HC**	**Metabolite**	**Tissue**	**Scanner**	**MRS type**	**Localis-ation**	**TR/TE (ms)**	**Reference**	**Quantific-ation type / program**	**Unit**	
Sijens (Sijens *et al.*, 2005)	4 PPMS	4	tNAA	WM	1.5T Siemens	SVS	PRESS	1500 / 135	Internal water	Numaris-3®	mM	↓Fractional anisotropy and ↓tNAA
Sastre-garriga (Sastre-Garriga *et al.*, 2005)	41 PPMS	44	tNAA, tCr, mIns, Glx	CGM, NAWM	1.5T GE	CSI	PRESS	3000 / 35		LCModel	mM	CGM: ↓tNAA and Glx NAWM: ↓tNAA, ↑mIns Associations with EDSS in CGM: tNAA (r=-0.44), mIns (r=0.41). Glx in NAWM associated with EDSS (r=0.41)
Sijens (Sijens, *et al.*, 2006)	4 RRMS 4 PPMS	6	tNAA, tCho, tCr	NAWM, GM	1.5T Siemens	CSI	PRESS	1500 / 135	Internal water	Numaris-3®	mM	NAWM: ↓tNAA GM: ↓tCho, ↓tCr, ↓tNAA

Study	Cohorts		^{1}H-MRS acquisition						Spectral post-processing			Key findings
First Author	**MS type**	**HC**	**Metabolite**	**Tissue**	**Scanner**	**MRS type**	**Localis-ation**	**TR/TE (ms)**	**Reference**	**Quantific-ation type / program**	**Unit**	
	4 SPMS 3 BMS											
Geurts (Geurts *et al.*, 2006)	11 RRMS 11 PPMS 11 SPMS	10	tNAA, tCr, tCho, Glx, mIns	Deep and CGM	1.5T Siemens	SVS	STEAM	6000 / 20	Transmitter amplitude	Absolute LCModel	mM	Thalamic ↓tNAA in PPMS Thalamic ↑mIns in all MS group
Pulizzi (Pulizzi *et al.*, 2007)	27 CIS 21 RRMS 29 SPMS	10	tNAA	Whole brain	1.5T Siemens	Whole brain	ns	10000 /		Offline methods ns	mM	SPMS - ↑T2LV, FA and MD. tNAA not different in SPMS

Study	Cohorts		^{1}H-MRS acquisition						Spectral post-processing			Key findings
First Author	**MS type**	**HC**	**Metabolite**	**Tissue**	**Scanner**	**MRS type**	**Localis-ation**	**TR/TE (ms)**	**Reference**	**Quantific-ation type / program**	**Unit**	
Gustafsson (Gustafsson *et al.*, 2007)	9 RRMS 5 SPMS	14	NAA, tNAA, mIns, tCr, tCho	NAWM	1.5T GE	SVS	PRESS	6000/ 35	Internal water	Absolute - LCModel	mM	↓tNAA, ↓NAA in SPMS < RRMS < HC Associations with EDSS: mIns, tNAA
Strasser-Fuchs (Strasser-Fuchs *et al.*, 2008)	13 BMS 15 SPMS	Nil	tNAA, tCr	Corpus callosum	1.5T Philips	SVS	PRESS	ns/ 30	Ratio to tCr	LCModel	IU	No metabolite differences between BMS and SPMS
Sajja (Sajja, Narayana and	58 PPMS	Nil	tNAA, tCho, tCr	WML, NAWM	1.5T GE	2D CSI	2D MRSI	1000 / 30	Ratio to tCr	In house-fitting	IU	No significant differences in any metabolite over 3 years

Study	Cohorts		^{1}H-MRS acquisition						Spectral post-processing			Key findings
First Author	**MS type**	**HC**	**Metabolite**	**Tissue**	**Scanner**	**MRS type**	**Localis-ation**	**TR/TE (ms)**	**Reference**	**Quantific-ation type / program**	**Unit**	
Wolinsky, 2008)												
Caramanos (Caramanos *et al.*, 2009)	10 RRMS 10 SPMS	18	tNAA, tCr	CGM	1.5T Philips	CSI	PRESS	2000 / 272	Ratio to tCr	AVIS	IU	↓tNAA/tCr in SPMS compared to HC No association between SPMS tNAA/tCr and EDSS
Aboul-Enein (Aboul-Enein *et al.*, 2010)	27 RRMS 10 SPMS	8	tNAA, tCho, tCr	NAWM	3T Siemens	CSI	PRESS	1500 / 135	1. Ratio to tCr 2. Internal Water	jMRUI, AMARES	IU / mM	↓tNAA/tCr, ↓tNAA/tCho compared to HC ↓tNAA compared to RRMS and HC ↓tCr in SPMS compared to RRMS

Study	Cohorts		^{1}H-MRS acquisition						Spectral post-processing			Key findings
First Author	**MS type**	**HC**	**Metabolite**	**Tissue**	**Scanner**	**MRS type**	**Localis-ation**	**TR/TE (ms)**	**Reference**	**Quantific-ation type / program**	**Unit**	
Steen (Steen *et al.*, 2010)	14 PMS 9 BMS	10	tNAA/tCr	NAWM	3T Philips	CSI	PRESS	2000 / 144	Ratio to tCr	Fitted to peaks	IU	↓tNAA/tCr in PMS
Penny (Penny *et al.*, 2010)	31 PPMS	31	tNAA, mIns, tCho, tCr, Glx	Mixed GM & WM	1.5T GE	SVS	PRESS	3000 / 30	ns	LCModel	mM	T2LV but not metabolites associated with cognitive performance at 5 years
Hannoun (Hannoun *et al.*, 2012)	27 RRMS 26 SPMS 18 PPMS	24	tNAA, tCho, tCr	Heterogenous VOI	1.5T Siemens	CSI	PRESS	1690 /135	1. Ratio to tCr 2. External phantom-om	QUEST	IU / mM	↓tNAA, ↓tNAA/tCr and ↓tNAA/tCho in PPMS and SPMS tNAA correlated with DTI metrics and T2LV
Bellenberg (Bellenber	9 RRMS 13 SPMS	17	tNAA, tCho, tCr, mIns	Spinal cord	1.5T Siemens	SVS	PRESS	1500 / 30	Phased array coils	ns	IU	In MS group: ↓tNAA, ↓tNAA/tCr, ↑mIns, ↑mIns/tCr

Study	Cohorts		^{1}H-MRS acquisition						Spectral post-processing			Key findings
First Author	**MS type**	**HC**	**Metabolite**	**Tissue**	**Scanner**	**MRS type**	**Localis-ation**	**TR/TE (ms)**	**Reference**	**Quantific-ation type / program**	**Unit**	
g *et al.*, 2013)									1. Ratio to tCr 2. Ratio to tCho			No correlation with clinical outcome measures Lower tNAA/tCr and tCho at baseline associated with progression
Choi (Choi *et al.*, 2011)	17 SPMS	17	GSH	Frontal, parietal mixed VOI	3T Siemens	CSI	3 scout gradient echo VOI	1500/ 115	Ratio to tCr	Home written software in IDL 6.3	IU	↓GSH in fronto-parietal area
Rahimian (Rahimian	15 RRMS 15 PPMS	na	tNAA, tCr, tCho	Perive ntricul	3T Siemens	CSI	PRESS	1000 / 135	1. Ratio to tCr	Subtract QUEST	IU	↓tNAA/tCr in PPMS compared to RRMS

Study	Cohorts		^{1}H-MRS acquisition						Spectral post-processing			Key findings
First Author	**MS type**	**HC**	**Metabolite**	**Tissue**	**Scanner**	**MRS type**	**Localis-ation**	**TR/TE (ms)**	**Reference**	**Quantific-ation type / program**	**Unit**	
et al., 2013)				ar WML					2. External phantom	NMR-SCOP of jMRUI		↓tCr in RRMS compared to RRMS
Llufrui (Llufriu *et al.*, 2014)	33 CIS 164 RRMS 17 SPMS 6 PPMS	43	tNAA, mIns	NAWM, GM	3T GE	CSI	PRESS	1000 / 40	TE average internal water	LCModel	mM	mIns/tNAA associated with 12 months change in brain volume, MSFC scores, EDSS change
Azevedo (Azevedo *et al.*, 2014)	CIS 49 RRMS 263	42	Glu, tNAA	NAWM, GM	3T GE	CSI	TE averaged PRESS	1000 / multi-short TE	Phantom basis set	LCModel	mM	Glutamate longitudinal association with decline in tNAA

Study	Cohorts		^{1}H-MRS acquisition						Spectral post-processing			Key findings
First Author	**MS type**	**HC**	**Metabolite**	**Tissue**	**Scanner**	**MRS type**	**Localis-ation**	**TR/TE (ms)**	**Reference**	**Quantific-ation type / program**	**Unit**	
	SPMS 20 PPMS 11											
Cawley (Cawley *et al.*, 2015)	30 SPMS	17	GABA, tNAA, Glx	CGM – 3 ROI	3T Philips	SVS	MEGA-PRESS	2000 / 68	Internal water	TARQUIN	mM	↓GABA in hippocampus ↓tNAA and GABA in sensorimotor cortex ↓motor function in right upper limb associated with ↓GABA
Sedel (Sedel *et al.*, 2015)	23 PMS (14 PPMS and 9 SPMS)	nil	tNAA, tCr, tCho	Heterogenous VOI	3T GE	SVS	PRESS	1500/ 135	Ratio to tCr	ns	IU	Single PMS patient had ↓Choline over 9 months

Study	Cohorts		^{1}H-MRS acquisition						Spectral post-processing			Key findings
First Author	**MS type**	**HC**	**Metabolite**	**Tissue**	**Scanner**	**MRS type**	**Localis-ation**	**TR/TE (ms)**	**Reference**	**Quantific-ation type / program**	**Unit**	
Abdel-Aziz (Abdel-Aziz *et al.*, 2015)	21 PPMS	24	tNAA, Glx	Cervical cord	3T Philips	SVS	PRESS	3000 / 30	Internal water	LCModel	mM	↓tNAA, ↓Glx compared to HC
Obert (Obert *et al.*, 2016)	21 RRMS 15 SPMS	12	tNAA, mIns, tCho, tCr, Glx	WM, NAWM	3T Siemens	SVS	STEAM	6000/ 20	1. Internal water, coil loading 2. Ratio to tCr	LCModel	mM	↓tNAA in SPMS over 24 months Association between tCho and EDSS (r=0.37) in SPMS
Macmillan (MacMillan *et al.*, 2016)	47 SPMS	nil	tNAA, Glu, Glx, tCho, tCr, mIns	NAWM	3T Philips	SVS	PRESS	5000 / 35	Internal water	LCModel	mM	↓Glutamate and ↓Glx over 2 years.

Study	Cohorts		^{1}H-MRS acquisition						Spectral post-processing			Key findings
First Author	**MS type**	**HC**	**Metabolite**	**Tissue**	**Scanner**	**MRS type**	**Localis-ation**	**TR/TE (ms)**	**Reference**	**Quantific-ation type / program**	**Unit**	
												No correlations with EDSS and MSFC.
Choi (Choi *et al.*, 2017)	13 SPMS	17	GSH	Regions of brain	3T Siemens	SVS	ns	1500/ 115	1. Ratio to tCr 2. Head coil	LCModel	IU / mM	No change in GSH over 3-5 year follow-up period Frontal GSH different between stable and progressive group
Nantes (Nantes *et al.*, 2017)	27 RRMS 14 SPMS 6 PPMS	21	Glu, GABA, tNAA	Mixed VOI – WM, GM	3T Siemens	SVS	MEGA-PRESS	3000/ 68	External phantom	LCModel	IU	GABA higher in MS compared to HC ↓GABA associated with disability performance measures

Study	Cohorts		^{1}H-MRS acquisition						Spectral post-processing			Key findings
First Author	**MS type**	**HC**	**Metabolite**	**Tissue**	**Scanner**	**MRS type**	**Localis-ation**	**TR/TE (ms)**	**Reference**	**Quantific-ation type / program**	**Unit**	
Ion-Marginea nu (Ion-Mărginea nu *et al.*, 2017)	12 CIS 30 RRMS 17 PPMS 28 SPMS	18	tNAA, tCho, tCr	Centra l mixed VOI	1.5T Siemens	CSI	PRESS	1690 / 135	Ratio to tCr	SPID in MATLAB 2015a, AQSES-MRSI	IU	Machine learning method to classify MS phenotypes
Marshall (Marshall *et al.*, 2018)	42 SPMS	nil	tNAA, tCho, tCr, Glx, mIns	WML, NAWM , GM	3T Siemens	CSI	Semi-LASER excitation	2000/ 43	Head coil loading factor	LCModel	IU	↑tCho, ↓tCr, ↓Glx in NAWM compared to GM ↑tCho, ↑tCr, ↑mIns in WML compared to NAWM and GM

+Histo-pathology study using HPLC analysis to measure NAA concentrations

*Pathological control from confirmed central pontine myelinolysis

na = not applicable, ns = not specified, MS = multiple sclerosis, CIS = clinically isolated syndrome, BMS = benign multiple sclerosis, RRMS = relapsing remitting multiple sclerosis, PMS = progressive multiple sclerosis, PPMS = primary progressive multiple sclerosis, SPMS = secondary progressive multiple sclerosis, NAA = N-acetyl aspartate, tNAA = total N-acetyl aspartate, tCr = creatine, tCho = choline, mIns = myoinositol, Glx = sum of glutamate and glutamine, GABA = Gamma aminobutyric acid, Glu = glutamate, GSH = Glutathione, WM = white matter, GM = grey matter, NAWM = normal appearing white matter, WML = white matter lesion, VOI = volume of interest, SVS = single voxel spectroscopy, CSI = chemical shift imaging, PRESS = Point resolved spectroscopy, STEAM = stimulated echo acquisition mode, EPSI = echoplanar spectroscopy imaging, TE = echo time, TR = repetition time, IU = institutional units, mM = millimolar, MTR = magnetisation transfer ratio

Table 2-3: Studies using proton magnetic resonance spectroscopy in clinically isolated syndrome

Study	Cohorts			MRS acquisition					Spectral post-processing		
First Author	**CIS (n)**	**HC (n)**	**Metabolite**	**Region**	**Scanner**	**SVS or CSI**	**Localisation**	**TR/TE (ms)**	**Reference**	**Quantification type**	**Key findings**
Brex et al (P A Brex *et al.*, 1999)	20	20	tNAA, tCr, tCho, mIns	NAWM	GE 1.5T	SVS	PRESS	3000/14 and 84	External	Absolute	No difference in metabolites in NAWM. ↓ tNAA in WML
Tourbah et al (A. Tourbah *et al.*, 1999)	42	15	tNAA, mIns, tCho	NAWM	1.5T	SVS	STEAM	1500/ 18 and 136	Internal	Ratio to tCr and tCho	No difference between CIS and HC
Kapeller et al (Kapeller *et al.*, 2002)	41	20	tNAA, tCr, tCho, mIns	NAWM, WML	GE 1.5T	CSI	PRESS	3000/30	External	Absolute	No difference between

											CIS and HC. ↓tNAA in MS in WML. ↑mIns in WML and NAWM in MS. ↑tCho in WML in MS.
Ranjeva et al (Ranjeva *et al.*, 2003)	46	24	tNAA, tCr, tCho	Corpus callosum	Siemens 1.5T	SVS	2D-SE	1500/136	Intravoxel tCr	Ratio to tCr and tCho	No difference in tNAA/tCr. ↑tCho/tCr
Rocca M et al (Rocca *et al.*, 2003)	16	15	tNAA	Whole brain	Siemens 1.5T	Whole brain		3300/16 and 98	External	Absolute	↓whole brain tNAA in CIS

Fernando K et al (Fernando *et al.*, 2004)	96	44	tNAA, tCr, tCho, Glx, mIns	NAWM	GE 1.5T		PRESS	3000/30	External	Absolute	↑mIns and ↑tCr. No difference in tNAA.
Rovaris M et al (M. Rovaris *et al.*, 2005)	35	12	tNAA	Whole brain	Siemens 1.5T	Whole brain	4 step 180^{o} inversion pulses		External	Absolute	↓Whole brain tNAA in CIS and at 1 year follow up
Audoin B et al (Audoin *et al.*, 2007) 2 year follow up	24	6	tNAA, tCr, tCho	Corpus callosum	1.5T	Corpus callosum		1500/136	Sum of signals of all metabolites	Ratio to sum of signals of all metabolites	↓tNAA/tCr compared to HC. tNAA recovers over 2 years
Wattjes et al (Wattjes *et al.*, 2007)	36	20	tNAA, mIns	NAWM	Philips 3T	SVS	PRESS	2000/38	External	Absolute	↓tNAA and tNAA/tCr in CIS.

											↓Glx/tCr in CIS
Wattjes et al (M. P. Wattjes *et al.*, 2008)	25	20	tNAA, mIns, tCho, tCr, Glx	NAWM	Philips 3T	SVS	PRESS	2000/38 and 140	External	Absolute and ratios	↓tNAA and tNAA/tCr in CIS
Wattjes et al (Mike P. Wattjes *et al.*, 2008)	31	20	tNAA, mIns, tCho, tCr	NAWM	Philips 3T	SVS	PRESS	2000/38 and 140	External	Absolute and ratios	↓tNAA and tNAA/tCr in CIS. No correlation with MR imaging criteria
Sbardella et al (Sbardella *et al.*, 2011)	49	25	tNAA, tCho, tCr	Corpus callosum	Philips 1.5T	CSI	PRESS	2000/272	Intravoxel tCr	Ratio to tCr	No difference in tNAA/tCr or tCho/tCr. tNAA/tCr correlated

											with T2LV (r=-0.49), NBV (r=0.3)

SVS = single voxel spectroscopy, CSI = chemical shift imaging, TR = time to repetition, TE = echo time, NAA = N-acetyl aspartate, tCr = creatine, tCho = choline, mIns = inositol, NAWM = normal appearing white matter, WML = white matter lesion, CIS = clinically isolated syndrome, HC = healthy control, Glx = glutamine and glutamine, mIns = myoinositol, T2LV, T2 lesion volume, NBV, normalised brain volume

2.3.6 Brain metabolites and their use a measure of treatment efficacy

Only a few studies have examined brain metabolites as an exploratory outcome measure in phase 2 and 3 treatment trials in PMS. Defining changes to generate a treatment outcome measure and minimising differences in multi-centre trials have been challenging (Narayana *et al.*, 2004; Sajja, Narayana and Wolinsky, 2008; Sedel *et al.*, 2015).

2.3.7 Brain metabolites as a biomarker in progressive multiple sclerosis

Many studies have examined the relationship between metabolites measured using ^{1}H-MRS techniques and clinical disability in PMS. The EDSS is the most common measure of physical disability used in MS and is the primary endpoint for most phase 3 clinical trials in MS.

EDSS and measures of physical disability:

Studies examining the correlation between metabolites and measures of physical disability e.g. EDSS have shown mixed results with several studies showing significant associations but others failing to find significant relationships (Fu *et al.*, 1996; Pike *et al.*, 1999; Sarchielli *et al.*, 1999; Narayana *et al.*, 2004; Marco Rovaris *et al.*, 2005; Sastre-Garriga *et al.*, 2005; Vrenken *et al.*, 2005; Geurts *et al.*, 2006; Bagory *et al.*, 2007; Hannoun *et al.*, 2012). Obert et al were one group to show a moderate association between tCho and EDSS (tau = 0.37, $p < 0.01$) (Obert *et al.*, 2016).

In studies of PMS cohorts that reported on other measures of physical disability – 9HPT, T25FW, a several cross-sectional studies showed a moderate correlation between CGM tNAA, mIns; and EDSS, MSFC and 9HPT (Sastre-Garriga *et al.*, 2005; Caramanos *et al.*, 2009).

Cognition:

There have been several studies that examined the association between metabolites and measures of cognitive function in PMS cohorts. Accounting for the different cognitive assessments used that examined different domains, all studies (cross-sectional and longitudinal) thus far have failed to show any

association between metabolite values/ratios and measures of cognitive performance in PMS (Foong *et al.*, 1999; Cox *et al.*, 2004; Geurts *et al.*, 2006; Penny *et al.*, 2010).

Chapter 3. Study design for secondary progressive multiple sclerosis and clinically isolated syndrome cohorts

3.1 Introduction

The remaining chapters in this thesis present analyses of a large SPMS cohort drawn from the Multiple Sclerosis – Secondary Progressive Multi-arm randomisation trial (MS-SMART) and a CIS cohort followed up at 15-years. This chapter introduces the study design for the MS-SMART study including patient recruitment, potential neuroprotective agents, outcome measures and details of MR acquisitions/analysis. Following this, the study design for the CIS cohort is outlined including patient recruitment, visit design, outcome measures and methods used in MRI analysis.

3.2 Multiple Sclerosis- Secondary Progressive Multi-Arm Randomisation Trial

With the relative paucity of neuroprotective agents in SPMS, the MS-SMART (NCT01910259) was undertaken to test the neuroprotective potential of three agents based on putative pathobiological mechanisms. Based on systematic literature searches of SPMS pathobiology and drug mechanisms, three potential neuroprotective agents were chosen for study in this Phase 2b trial: amiloride, fluoxetine and riluzole (Vesterinen *et al.*, 2015).

3.2.1 Study design

MS-SMART was a phase 2b double-blind, placebo-controlled, multi-arm, multi-centre study assessing the neuroprotective potential of amiloride, fluoxetine and riluzole in SPMS (Connick *et al.*, 2018).

3.2.2 Participants

Participants recruited into the main MS-SMART study were people with SPMS aged 25-65 years, with an EDSS score of 4.0-6.5, that showed evidence of progression independent of relapses over the last 2 years. Formal eligibility criteria are shown in Table 3-1.

Consent was obtained for all patients according to the Declaration of Helsinki and ethical approval for the study was provided by the Scotland A Research Ethics Committee.

Table 3-1: Multiple sclerosis - Secondary Progressive Multi-Arm Randomisation Trial eligibility criteria

INCLUSION CRITERIA	• Confirmed diagnosis of SPMS. Steady progression rather than relapse must be the major cause of increasing disability in the preceding 2 years. • EDSS 4.0-6.5 • Aged 25 to 65 inclusive • Participants must be willing and able to comply with the trial protocol and give written informed consent. • Women and men with partners of childbearing potential must be using an appropriate method of contraception from time of consent to 6 weeks post study drug. • Negative pregnancy test within 7 days prior to the baseline visit if childbearing potential.
EXCLUSION CRITERIA	• Primary progressive MS or Relapsing-remitting MS. • Pregnancy or breastfeeding patients. • Baseline MRI scan not of adequate quality for analysis (e.g., too much movement artefact). • Significant organ comorbidity (e.g., malignancy or renal or hepatic failure). • Relapse +/- treated with intravenous or oral steroids for an MS relapse/progression within 3 months of baseline visit. • Use of simvastatin at 80 mg dose within 3 months of baseline visit (lower doses of simvastatin and other statins are permissible). • Commencement of fampridine within 6 months of baseline visit. • Use of immunosuppressants (e.g., azathioprine, methotrexate, ciclosporin) or first-generation disease-

	modifying treatments (β-interferons, glatiramer) within 6 months of baseline visit. • Use of fingolimod, fumarate, teriflunomide, laquinimod, or other experimental disease-modifying treatment (including research of an investigational medicinal product), mitoxantrone, natalizumab, alemtuzumab, daclizumab within 12 months of baseline visit. • Known allergy or adverse reaction to the trial drugs. • Use of an SSRI, monoamine oxidase inhibitors, phenytoin, L-tryptophan and/or neuroleptic drugs, lithium, chlorpropamide, triamterene, or spironolactone within 6 months of the baseline visit. • Current use of tamoxifen, use of herbal treatments containing St. John's wort • Significant signs of depression or bipolar disorder. A Beck Depression Index score of 19 or higher. • Patients with a history of bleeding disorders or currently on anticoagulants, epilepsy/seizures, receiving or previously received electroconvulsive therapy, glaucoma. • Routine screening blood values: – LFTs (ALT/AST, bilirubin, GGT)>3x upper limit of normal of site reference ranges.– Potassium<2.8 mmol/L or >5.5 mmol/L. – Sodium<125 mmol/L. – Creatinine>130µmol/L. – WBCs<3×10^9/L. – Lymphocytes<0.8×10^9/L. – Neutrophil count<1.0×10^9/L. – Platelet count<90×10^9/L.

EDSS = Expanded disability status scale, SSRI = selective serotonin reuptake inhibitor, LFT = liver function test, ALT = alanine aminotransferase, AST = aspartate aminotransferase, WBC = white blood cell

3.2.3 **Intervention**

Participants were randomised 1:1:1:1 to amiloride, fluoxetine, riluzole or placebo. The minimisation variables used were: sex, age (<45 years; 45 years or more), baseline EDSS (4.0–5.5; 6.0–6.5) and trial site.

Participants are seen every three months for a total of nine visits. For the main study, brain imaging was acquired at baseline, week 24 and week 96; clinical efficacy parameters (3.2.6) were measured at baseline, week 48 and week 96.

3.2.4 Primary outcome measures

The primary outcome measure was the percentage brain volume change over 2 years measured using SIENA.

3.2.5 Secondary and exploratory outcome measures

The secondary outcome measure was the count of new and enlarging T2 lesions. Exploratory outcome measures included the proportion of new and enlarging T2 lesions at 24 weeks being persistently T1 hypointense at 96-weeks; and the change in brain GM volume from baseline to 96-weeks.

3.2.6 Clinical outcome measures

All participants underwent a series of clinical assessments including EDSS and the MSFC, which comprises the T25FW, 9HPT and the 3-second Paced Auditory Serial Addition Test (PASAT3) – measures of walking speed, upper limb function and information processing speed (IPS) respectively (Kurtzke, 1983; Cutter *et al.*, 1999). The Symbol Digit Modalities Tests (SDMT) – a cognitive test of IPS - was also completed (Benedict *et al.*, 2017). Sloane low contrast visual acuity was completed.

Participants also underwent a series of patient reported outcome measures including the multiple sclerosis impact scale (MSIS29 version 2) and multiple sclerosis walking scale (MSWS version 2) (Connick *et al.*, 2018).

3.2.7 The advanced MRI substudy

Participants involved in the MS-SMART study at our site (Queen Square MS Centre, University College London) were invited to take part in an optional "Advanced MRI sub-study" inclusive of ^{1}H-MRS scans. Patients who consented to this substudy underwent the following MRI acquisition:

- Proton magnetic resonance spectroscopy (chemical shift imaging)
- Magnetisation transfer ratio

- Spinal cord imaging

These participants in the advanced MRI study had the “advanced” MR scans at baseline and 96-weeks. They also underwent clinical assessments as per the main study. Flow through the advanced MR study is shown in Figure 3-1.

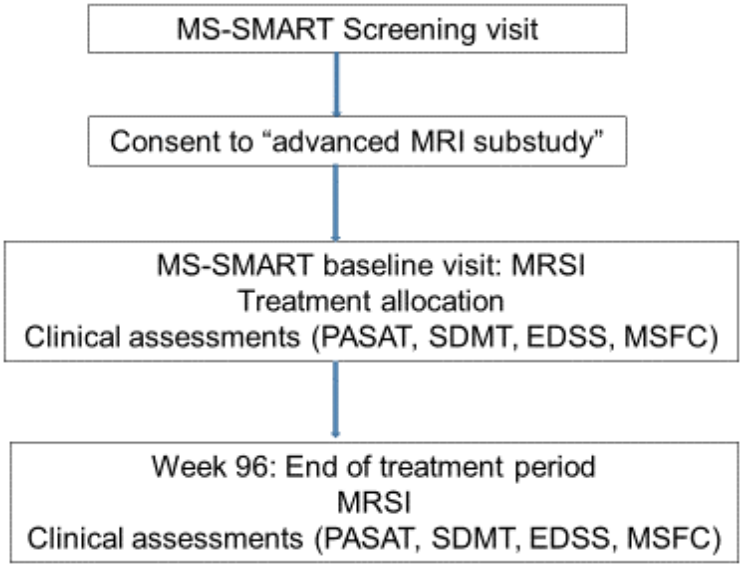

Figure 3-1: Study flow through advanced MRI substudy

3.2.8 **MRI acquisition**

Metabolite spectra were acquired from multiple voxels within one scan using chemical shift imaging (CSI) - as this was an efficient method of determining metabolite changes by obtaining average metabolite concentrations from a slice of neuronal tissue (Brink, Buschmann and Rosen, 1989). Imaging was acquired using a Philips Achieva 3T MRI scanner (Philips Healthcare, Best) using a 16 channel neurovascular coil. The acquisition protocol was designed by Dr Bhavana Solanky and images acquired by Dr Marios Yiannakis.

All participants underwent the following scans:

CSI: A 210x160mm^2 volume of interest (VOI) with 15mm slice thickness was selected for CSI, placed superior to the lateral ventricles (see The red band shows the slice that was selected. The outer blue bands demonstrate the outer volume suppression.

Figure 3-2). This location for slice placement was chosen as it aimed to minimise signal loss and partial volume effect from CSF; and also contained large regions of NAWM and GM (cortical). The CSI VOI was subdivided into a 21x16 grid giving a voxel size of 10x10x15mm^3. Spectra were acquired using a 2D PRESS sequence (short TE 35ms/ TR 2000ms). Outer volume suppression using fat saturation was applied to limit artefacts, and the VOI was shimmed using the pencil beam-auto technique (Shen *et al.*, 1999). CHESS pulses were used for water suppression. A reference scan with no water suppression was also collected with identical parameters during the same exam for quantification. Details of the acquisition are presented in Table 3-2.

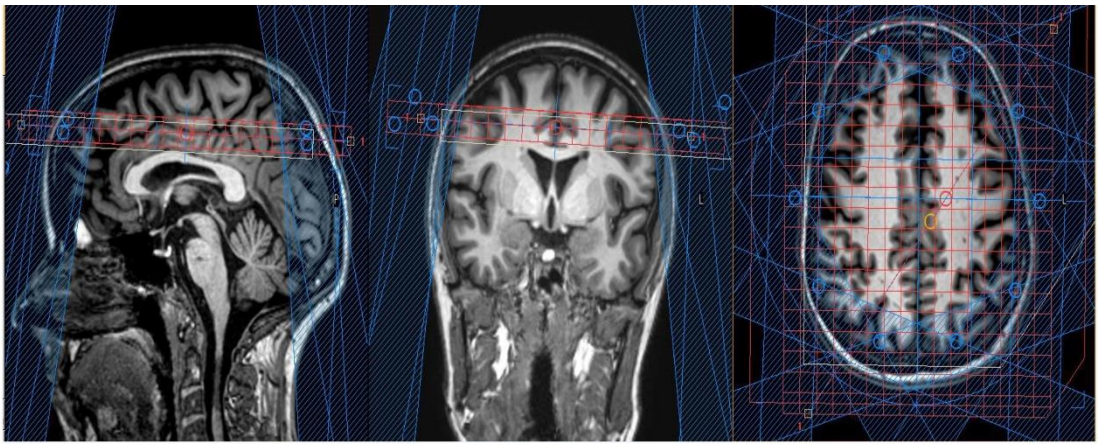

The red band shows the slice that was selected. The outer blue bands demonstrate the outer volume suppression.

Figure 3-2: Placement of volume of interest grid for chemical shift imaging acquisition in sagittal, coronal and axial planes

Structural MR imaging: Scans for structural information and lesion assessment were collected prior to CSI as detailed below and were used also for planning purposes of the VOI selected for CSI. A sagittal 3D-T1WI with matrix 256 x 256, field of view (FOV) 256 x 256mm^2, 180 sagittal slices 1mm thick, flip angle 8°, TR/TI/TE = 7/840/3.2 ms (turbo factor 230) was acquired for structural information. An axial PD-T2 (TR/TE1/TE2) = 3500/19/85 ms, turbo factor 10) and FLAIR (TR/TI/TE = 8000/2400/125 ms, turbo factor 24) with matrix 240 x 180, FOV 240 x 180 mm^2, 50 slices 3mm thick were acquired for lesion assessment.

Cervical cord imaging was acquired using a T1-weighted 3D-phase sensitive inversion recovery (PSIR) sequence. Images were acquired in the axial plane without parallel imaging containing 16 contiguous slices, FOV=256×256mm^2, matrix = 512×256, TR=8 ms, TE = 3.7ms, dual RF transmit, TI = 843.6ms and number of averaged signals = 3. The voxel dimensions were 0.5×0.5×3 mm^3 and the acquisition time was 14:00 min. The cervical cord was imaged in the axial-oblique plane from C2-C4 with the centre of the imaging volume positioned at the level of C2-3 intervertebral disc plane.

Magnetisation transfer ratio: The acquisition parameters for MTR are shown in Table 3-2.

Table 3-2. Acquisition parameters for chemical shift imaging and magnetisation transfer ratio

	MTR	**CSI**
Slice orientation	Sagittal	Axial
First echo time	2.7ms	35ms
Second echo time	4.3ms	N/A
Repetition time	6.45ms	2000ms
Number of slices	180	1
Echo train length	4	N/A
Field of view	25cms x 100%	24cms x 75%
Image matrix acquisition	256 x 256	240 x 240
Reconstructed pixel size	1 x 1mm	1 x 1mm
Frequency encoding	Anterior-posterior	Anterior-posterior

Phase encoding	Right/left	Right/left
Number of averages	1	1
Flip angle	9^0	90^0

ms = milliseconds, N/A = not applicable

3.2.9 **MRI analysis**

CSI:

The following CSI-derived metabolites were measured:

i) Total NAA (tNAA) = N-acetyl aspartate + N-acetyl aspartyl glutamate
ii) Glx = Glutamine + glutamate
iii) Total choline (tCho) = phosphocholine + glycerophosphocholine
iv) Total creatine (tCr) = creatine + phosphocreatine
v) Myo-inositol (mIns)

I also reported metabolite ratios to creatine. Although there is some evidence that tCr is not a stable metabolite in MS (Vrenken *et al.*, 2005), tCr has been used as a stable reference metabolite extensively in previous MS ^{1}H-MRS studies and so is useful for comparison.

CSI Spectra & image post-processing:

Following the acquisition, post-processing of spectra was completed using Linear Combination of Model Spectra (LCModel© version 6.3-1A) – a program used to fit MRS data to a basis set, which together with the water reference scan, enabled estimated quantification of metabolites as well as providing a set of parameters to perform quality assurance for each voxel (Provencher, 1993). The LCModel basis set was provided by S. Provencher (personal communication).

The water reference scan was used to find a scaling factor for the basis set, as detailed in the LCModel manual (Provencher, 1993). This carries with it the assumption that the concentration of water in the spectrum is equivalent to

healthy white matter (35880mM), which, in the absence of a specific measure per patient is often used as the default (Ernst, Kreis and Ross, 1993; Provencher, 1993). In addition to this to correct for T2 relaxation the default water attenuation was set to 0.7, based on TE=30 and on Ernst et al. who found the major water compartment in brain has T2 ≈ 80 ms. (exp(−TE/T2) = exp (−30/80) ≈ 0.7) (Ernst, Kreis and Ross, 1993; Provencher, 1993). If substituted for TE=35ms this reduces to 0.65, however in the absence of an accurate T2 in pathology, the default was again kept (Sec 11.2 LCModel manual). As I employed long TR and water scaling was used, no correction for T1 was made.

Spectra from individual voxels were automatically rejected if any metabolite Cramer-Rao lower bounds were > 20%, full width half-maximum of the tNAA spectral peak was >15Hz or SNR < 9. All voxels that passed the automated step were visually inspected by an experienced assessor (Dr. Bhavana Solanky) to look for baseline artefacts, non-random residuals or outer volume contamination that may prevent the accurate measurement of metabolites. The resulting set of voxels made up a “clean data” set which all passed the automated and visual quality assurance.

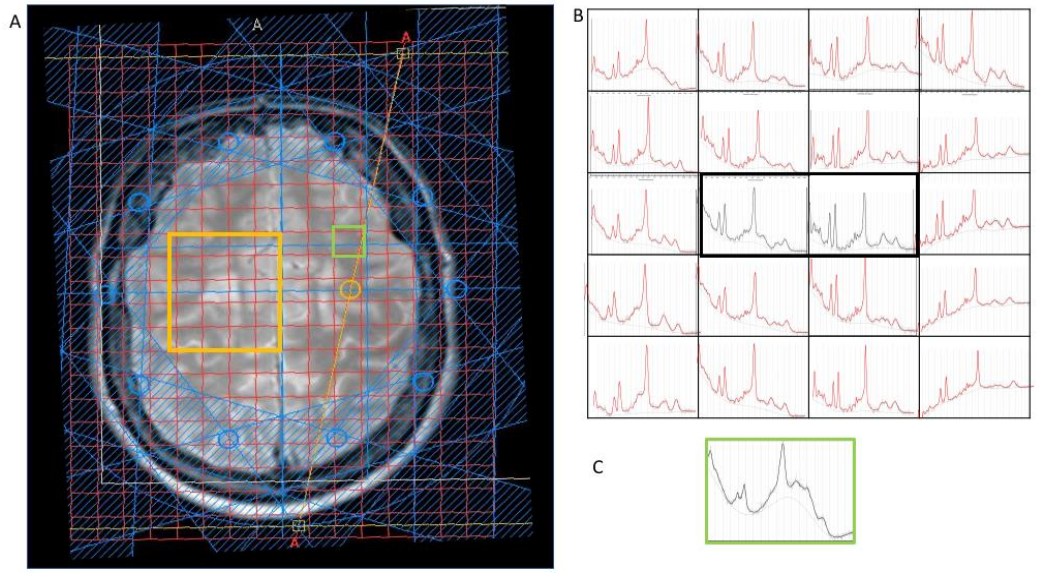

Figure 3-3. Example spectra and chemical shift grid

Figure 3-3 shows A) Position where representative spectra come from including a lesion, B) accepted spectra in red and lesion in black, C) spectra from rejected voxel, position shown in green in A **(Solanky *et al.*, 2020)**

Metabolite analysis:

Metabolites were analysed in the following two ways:

1 **Estimated metabolite concentrations:** The mean metabolite concentrations (tNAA, mIns, Glx, tCho, tCr) of all voxels which passed the automatic and visual quality assurance (clean data) were averaged for each participant to calculate per patient estimated metabolite concentration, reported in institutional units (IU).
2 **Metabolite ratios**: Mean metabolite ratios (tNAA, mIns, Glx, tCho) to total creatine (tCr) were calculated from the clean data for each participant.

Metabolite concentrations and ratios were then calculated in the following two tissue types:

i. Normal appearing white matter (NAWM)
ii. Grey matter (GM)

To eliminate contamination by WML and CSF, I firstly removed any voxels containing > 1% WML and > 15% CSF. Linear regression models were used to explore the association between the concentration of each metabolite and white or GM fraction on a voxel-by-voxel basis. These models were then extrapolated to find the value for each metabolite where GM or WM fraction was 100% to find the metabolite concentration for each tissue type. Metabolite outliers were removed from the regression models leaving us with per patient metabolite values. Major outliers were removed that were outside the upper outer [3rd quartile + (3 x interquartile range)] or lower outer fences [1st quartile - (3 x interquartile range)]. This method has been previously described (Baranzini *et al.*, 2010; Srinivasan *et al.*, 2010; Llufriu *et al.*, 2014; Solana *et al.*, 2018). Owing to the small lesion load in the acquired slice (average WML

fraction in SPMS cohort was 0.01), calculation of metabolite values in WML was unable to be completed.

Brain and WM lesion segmentation

A NIFTI image was created in the same space as the axial PD-T2 to represent the positioning of the CSI matrix in this space, and to act as a mask for the MRS volume (see Figure 3-4). The CSI mask contained identification numbers at each position that could be related back to rows and columns (voxel number) in the CSI matrix. This was completed by Jon Stutters and Dr Torben Schneider.

The T2 image corresponding to the position of the CSI mask was registered and resampled to the 3D T1 image using NiftyReg (Modat *et. al.*, 2014) and an identical transform applied to the CSI mask to get the matrix in the desired space for segmentation. This was completed by Mr. Jon Stutters.

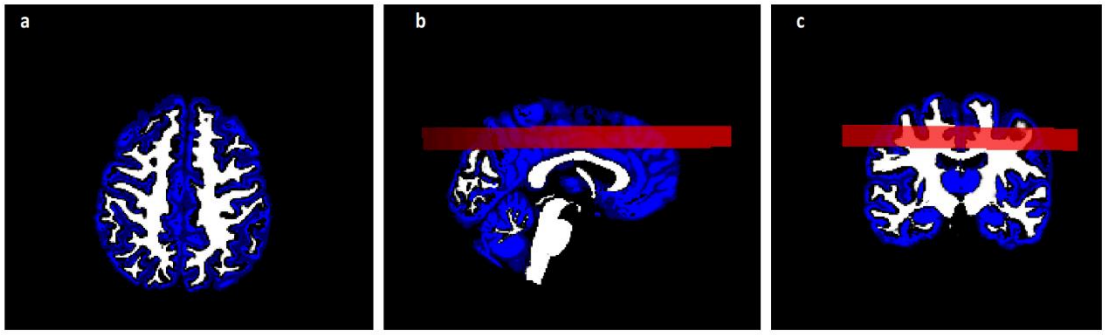

Figure 3-4: Masks for a) grey matter (blue) and white matter (white) segmentation, b) CSI mask in sagittal plane (red) and in c) coronal plane

Brain and white matter lesion segmentation

The 3DT1 image was segmented using Geodesic information flows (Cardoso *et. al.*, 2015) enabling us to calculate fractions of WM, GM and CSF. Geodesic information flows is an "algorithm where information is propagated along the geodesic path of the local data embeddings" enabling a more accurate method of tissue segmentation (Cardoso *et al.*, 2015). WML were semi-manually delineated using Jim 7 (Xinapse Systems) on the T2 image using the FLAIR image as a reference. Following WML segmentation, fractions of NAWM and

GM were calculated. As lesions were not segmented in GM, the GM segmentation likely contains both lesional and normal GM tissue.

Brain volume measures

Normalised brain volume (NBV) was calculated using the SIENAX method from the segmented 3D-T1WI (Smith *et al.*, 2002). SIENAX rescales each subject head to the Montreal Neurological Institute atlas size, hence correcting each individual brain volume. Thus, the NBV is the volume of the rescaled brain and it allows us to correct brain volume for variations in head size, effectively resulting in a measure of cross-sectional atrophy (Smith *et al.*, 2002). The MRI analysis pipeline for the calculation of NBV using SIENAX is demonstrated in Figure 3-5.

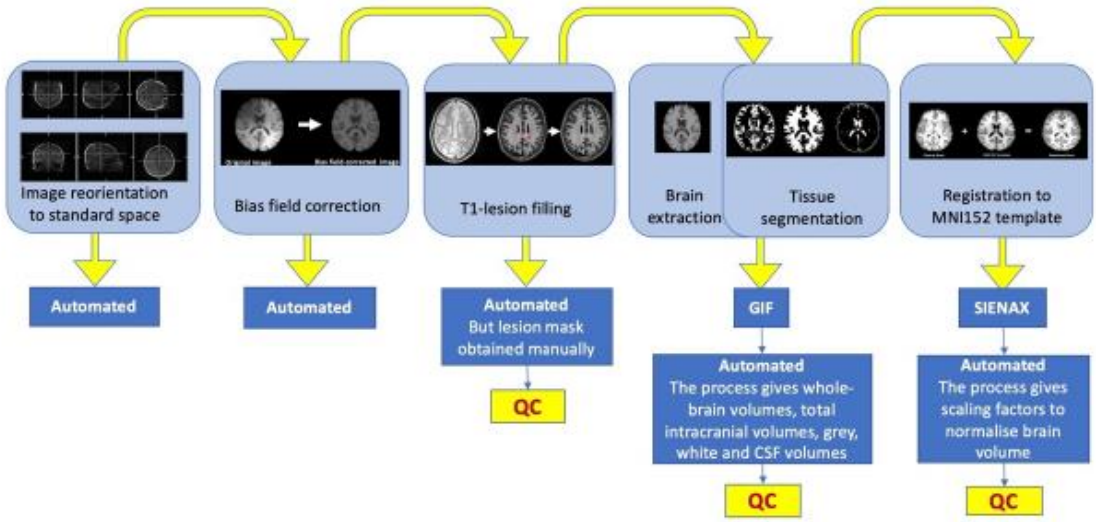

Diagram demonstrating processes involved in SIENAX analysis pipeline to calculate normalised brain volume

Used with permission from Dr. Floriana De Angelis

Figure 3-5. SIENAX MRI analysis pipeline

SIENA:

The SIENA technique was used to measure percentage brain volume change using 3D-T1 scans from baseline and 96-weeks. This technique was employed as previously described (Smith et al., 2002). For each timepoint, 3D-T1 sequences were acquired and underwent bias-field correction and lesion

filling. Segmentation of WM, GM, CSF was completed using Geodesical information flows (Cardoso et al., 2012). Co-registration of the 96-week scan to the baseline scan was completed before the SIENA algorithm was applied to calculate percentage brain volume change. This is summarised in Figure 3-6.

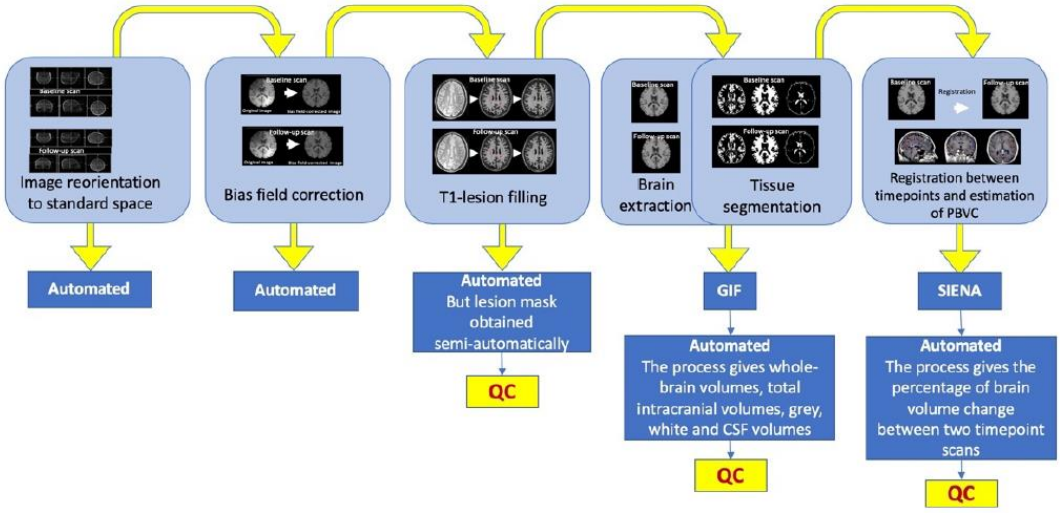

CSF= cerebrospinal fluid; GIF= Geodesical Information Flows; PBVC= percentage brain volume change; QC= quality check; SIENA= Structural Image Evaluation, using Normalisation, of Atrophy

Used with permission from Dr. Floriana De Angelis

Figure 3-6. SIENA MRI analysis pipeline

Mean upper cervical cord area:

Mean upper cervical cord area (MUCCA) was calculated using the active surface model on Jim software (version 7.0, Xinapse Systems, UK) from the 3D-PSIR image using the method as previously described by Kearney et al (Hugh Kearney *et al.*, 2014). This was completed by firstly placing a manual mark (centred at C2-C3) at the centre of the five intermediate 3-mm thick slices of the 3D-PSIR scan. Jim software was then used to automatically detect the cord edge and provide a marked cord area contour for each of the five selected slices. The results were then visually inspected and errors in cord segmentation were edited manually or the central marker was re-positioned (completed by Dr Floriana De Angelis). The software analysis was then re-run if necessary. The five resulting cord area measures were obtained from Jim

software and then averaged to calculate the final MUCCA (Figure 3-7). This process was completed for each participant. This semi-automated method of cord area detection has been demonstrated to show good inter-rater and intra-rater reproducibility (Hugh Kearney *et al.*, 2014).

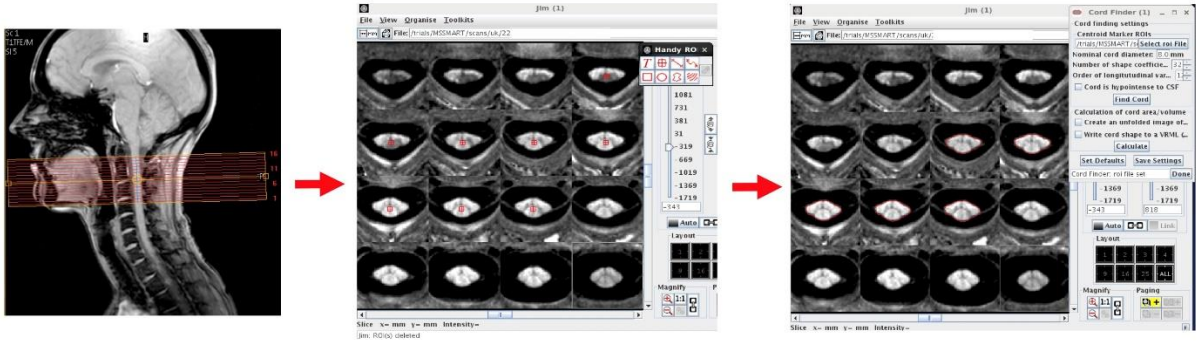

The left panel shows the positioning of the acquired volume scan (made of 16 slices) at the C2-C3 level. The middle panel shows the red cord markers that were manually positioned in the centre of the five cross-sectional slices acquired between C2-C3 (i.e. slices 7-11). JIM7 software was then used to run an automated cord edge detection tool, which found the cord area of the cross-sectional from the 5 slices marked. MUCCA was then calculated from the average of the 5 cross-sectional areas.

Taken with permission from Dr Floriana De Angelis

Figure 3-7. Cross-sectional cervical cord area measurement

Magnetisation transfer ratio:

The MTon and MToff images were co-registered to a halfway point using NiftyReg (Modat *et al.*, 2010). MTR maps (in percentage units) were calculated as [(MToff – MTon)/MToff) × 100]. The T1-weighted volume (in addition to lesion masks, and tissue segmentations for GM and NAWM) were co-registered to this same halfway point for further analysis and whole-brain, GM, NAWM and T2 lesion masks were measured (De Angelis *et al.*, 2020). Magnetisation transfer ratio maps underwent quality assurance by Dr. Floriana De Angelis and additional input from Dr Rebecca Samson and Mr Jon Stutters.

3.3 Clinically isolated syndromes study design

This section outlines the study design for the CIS cohort with a focus on initial recruitment, MRI/^{1}H-MRS acquisition protocols, clinical assessments completed at baseline, 3 month and 15-year follow-up visits.

3.3.1 **Recruitment, inclusion and exclusion criteria**

CIS patients seen at the National Hospital for Neurology and Neurosurgery and Moorfields Eye Hospital between 1995-2004 were initially invited to participate in a prospective, long term follow up study. Participants were included if they met the following criteria: i) age 16-50 years ii) a neuroinflammatory syndrome typical of CIS e.g., unilateral optic neuritis, partial transverse myelitis or brainstem syndromes iii) absence of previous symptoms suggesting an earlier demyelinating episode. Adjunctive investigations such as lumbar puncture, visual evoked potentials and blood tests were undertaken where indicated.

Participants underwent baseline scanning (MRI brain and spine) and clinical assessments within 3 months of CIS onset (P. A. Brex *et al.*, 1999; Dalton *et al.*, 2004). Following "baseline" assessment, participants were invited to participate in a ^{1}H-MRS substudy. 96 participants provided consent and underwent ^{1}H-MRS SVS and structural MR brain imaging at the first scheduled 3 month follow up visit with 90% having their ^{1}H-MRS scan within 6 months of CIS onset (Fernando *et al.*, 2004).

3.3.2 **Ethical approval and consent**

The study was approved by the National Hospital for Neurology and Neurosurgery ethics committee, and informed consent was obtained from all subjects before study entry.

3.3.3 **Follow-up**

After the initial "baseline assessment" and 3-month visit where ^{1}H-MRS was undertaken, patients were then invited for further visits at 1, 3 and 5 years (range 4.0 – 11.8 years). They were then invited for a 15 year follow up visit (range 10.9 – 19.7 years).

3.3.4 **Clinical assessments**

At the baseline visit, participants were assessed by the clinical fellow assigned to the study. At the 15-year time point, participants were re-recruited, consented and assessed by Dr. Wallace Brownlee.

At the initial baseline and 3 month visits participants were assessed using the EDSS (Kurtzke, 1983).

At the 15 year follow-up visit, participants underwent assessments of physical disability including EDSS, 9HPT and T25FW (Kurtzke, 1983; Feys *et al.*, 2017; Motl *et al.*, 2017). Cognitive testing included measures of IPS – PASAT3 and the SDMT (Gronwall, 1977; Benedict *et al.*, 2017). Additional cognitive testing was completed including two tests of executive function, the Brixton and Hayling tests (Burgess P and T, 1997); and tests of visual and verbal memory from the adult memory and information processing battery (Coughlan and Hollows, 1985).

Participants that were unable to attend in person for the 15 year visit were assessed using telephone-EDSS (Lechner-Scott *et al.*, 2003). Telephone EDSS has been shown to be highly correlated with EDSS completed by physical examination, particularly when EDSS > 4.5 (Lechner-Scott *et al.*, 2003).

Diagnosis of multiple sclerosis was made using the McDonald 2010 criteria and disease course (CIS, relapsing remitting MS, secondary progressive MS) was defined using Reinhold and Lublin 1996 criteria (Lublin and Reingold, 1996; Polman *et al.*, 2011).

3.3.5 **MRI acquisition**

Conventional MR:

MR scanning was undertaken on the 1.5T Tesla GE Signa Echospeed scanner (General Electric Medical Systems, Milwaukee, WI, USA). At baseline, brain T2/PD, brain pre and post-gadolinium (0.1mmol/kg) T1 and spinal cord (T2/PD and fast spoiled gradient echo sequences) were acquired. At the 3-month visit, the same brain imaging was acquired but spinal cord sequences were not completed. The sequence parameters are summarised in Table 3-3:

Table 3-3. MRI acquisition parameters: baseline and month 3 visits

	Plane	Slice thickness (mm)	TR (ms)	TE (ms)	Matrix
Brain					
T2/PD weighted	Axial	46 x 3	3200	15/90	256x256
Post-contrast T1-weighted	Axial	46 x 3	600	17	256x256
Spinal cord					
T2/PD-weighted (whole cord)	Sagittal	9 x 3	2500	56/92	512x512
FSPGR (cervical cord)	Sagittal	60 x 1	15.6	4.2	256x256

FSPGR = Fast spoiled gradient echo, PD = proton density, TR = repetition time, TE = echo time

Structural MR imaging of the brain using the same acquisition parameters was repeated at the 3-month visit (mean 13.1 weeks, SD 2.3, range 8±20 weeks after baseline scan, and mean 18.9 weeks, SD 3.5, range 12±28 weeks after the initial CIS).

^{1}H-MRS protocol:

SVS was undertaken 3 months (Month 3 visit) after initial baseline assessment which was within 6 months of CIS onset for 89 out of 96 participants. SVS (PRESS) with TR 3000 ms, TE 30 ms and 192 averages was acquired from the NAWM, with the volume of interest being manually placed in the posterior parietal area and semi-centrum ovale (Figure 3-8). *In vivo* metabolites values using the linear combination model (LCModel® version 1.3L) program were calculated for total NAA (tNAA = N-acetyl aspartate + N-acetyl aspartyl glutamate), myoinositol (mIns), Glx (glutamate + glutamine), total choline (tCho = phosphocholine + glycerophosphocholine) and total creatine (tCr = creatine + phosphocreatine). Spectral calibration was completed using an external phantom (Provencher, 1993; Fernando *et al.*, 2004). An example

spectrum is shown in Figure 3-9. Initial sequence, external calibration and LCModel set up were conducted by the original fellows on the study including Prof. M.A McLean, Dr. C.M. Dalton, Dr. K.T.M Fernando and Dr. Declan Chard.

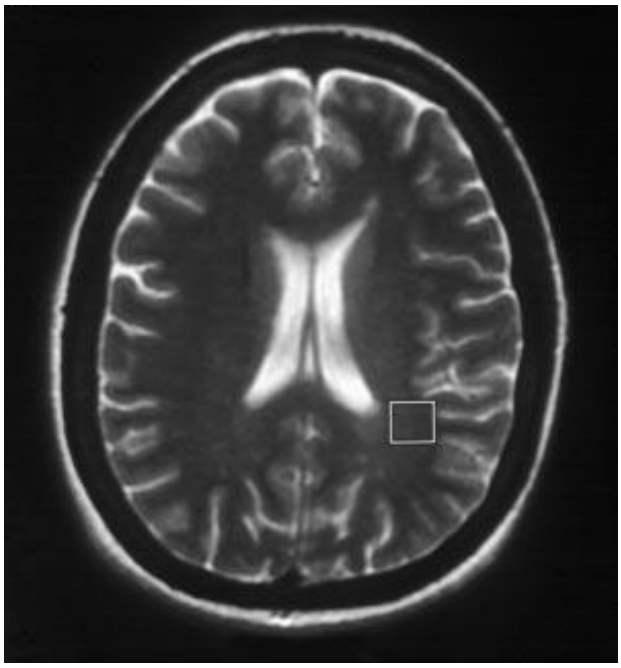

Figure 3-8. Axial MRI image showing voxel placement in normal appearing white matter

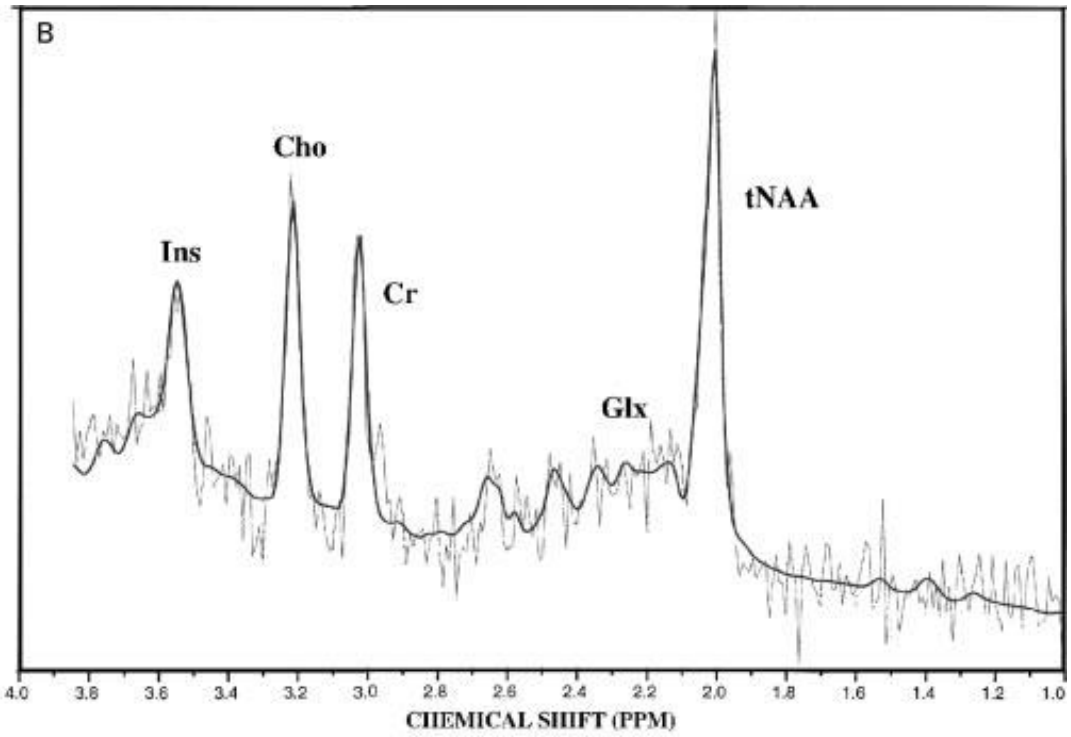

Figure 3-9. Example spectrum from a participant with clinically isolated syndrome

3.3.6 **MRI analysis**

Lesion volume

At the baseline and 3-month time points, lesions were marked on the PD-T2 image (using the FLAIR as a reference). This was completed with semi-automated edge finding software JIM6.0 (JIM6.0, Xinapse Systems, Aldwincle, UK). T2LV was then calculated by multiplying T2 lesions area by slice thickness.

This was completed by Dr. Wallace J Brownlee.

Normalised brain volume

Using the 2D T1-weighed fast-spin echo scans, the SIENAX method was employed to calculate normalised brain volume (Smith *et al.*, 2002). This is as previously described in section 3.2.9.

Dr. Wallace J Brownlee. Dr. Arman Eshaghi, Dr Ferran Prados and Mr John Stutters completed the SIENAX analysis.

Chapter 4. Proton magnetic resonance spectroscopy imaging in secondary progressive multiple sclerosis: a cross-sectional analysis of the association between metabolites and clinical disability measures

4.1 Introduction

Sections of this chapter have been published as outlined earlier in the thesis:

Bhavana S Solanky*, Nevin A John*, Floriana De Angelis *et al.* (2020) 'NAA is a Marker of Disability in Secondary-Progressive MS: A Proton MR Spectroscopic Imaging Study', *American Journal of Neuroradiology*. American Journal of Neuroradiology. doi: 10.3174/ajnr.A6809.

Biomarkers of brain injury are valuable in improving our understanding of the pathophysiology driving clinical disability in PMS. Imaging biomarkers such as MRI-based lesional and atrophy metrics can identify existing inflammatory injury and axonal loss and provide adjunctive prognostic information. Yet existing imaging based-measures are relatively limited in their ability to demonstrate metabolic or microstructural changes and show only a modest association with clinical disability outcomes in PMS (Brown and Chard, 2016). This is where advanced non-structural MRI techniques such as ^{1}H-MRS are attractive to further understand this neuropathology and its association with clinical disability in PMS.

Using ^{1}H-MRS, there are several metabolites of interest in MS (summarised in 2.3.2) including N-acetyl aspartate plus N-acetyl aspartyl glutamate (total NAA = tNAA), Glx – the sum of the excitatory neurotransmitter glutamate and its precursor glutamine; myo-inositol (mIns) and total Choline (tCho = glycerophosphocholine and phosphocholine). Many studies have demonstrated decreases in tNAA and tNAA/tCr; and increases in total creatine (tCr = creatine and phosphocreatine) and mIns in normal appearing white matter (NAWM) and GM in SPMS (Swanberg *et al.*, 2019). In a recent meta-analysis of ^{1}H-MRS studies, effect sizes for a reduction in NAA and NAA/tCr were larger in PMS compared to RRMS (Swanberg *et al.*, 2019). There have

been conflicting results from studies examining disability associations in PMS: several studies showed no association between metabolites (NAA, Glx, mIns, tCho) and the EDSS (Narayana *et al.*, 2004; Marco Rovaris *et al.*, 2005; Vrenken *et al.*, 2005; Geurts *et al.*, 2006); whilst others showed moderate associations with EDSS, 9HPT, T25FW in CGM and NAWM (Sastre-Garriga *et al.*, 2005; Hannoun *et al.*, 2012; Obert *et al.*, 2016). Of the studies examining cognitive performance (including IPS) in PMS, no associations were found in sample sizes ranging from 14-31, with only two of these studies containing pure SPMS cohorts (Foong *et al.*, 1999; Cox *et al.*, 2004; Sastre-Garriga *et al.*, 2005; Geurts *et al.*, 2006; Obert *et al.*, 2016).

The rationale for this cross-sectional study was to further define metabolite levels, and their associations with disability, in a much larger sample of people with SPMS than has been achieved before.

4.2 Methods

The methods including participant recruitment, clinical assessments, MRI acquisition and image post-processing are outlined in sections 3.2.2, 3.2.6, 3.2.7, 3.2.8 and 3.2.9.

4.2.1 Metabolite analysis

Metabolites were analysed in the following two ways:

i. Estimated metabolite concentrations: The mean metabolite concentrations (tNAA, mIns, Glx, tCho) of all voxels which passed the automatic and visual quality assurance (clean data) were averaged for each participant to calculate per patient estimated metabolite concentration reported in institutional units (IU).

ii. Metabolite ratios: Mean metabolite ratios (tNAA, mIns, Glx, tCho) to total creatine (tCr) were calculated from the clean data for each participant.

Metabolite concentrations and ratios were then calculated in the following two tissue types: NAWM and GM

The method of calculating tissue specific brain metabolites in NAWM and GM is described in 3.2.9.

4.2.2 Statistical analyses

Neurometabolic data and distribution over the cohort was summarised descriptively. Statistical analysis was completed using R statistical software (version 3.5.1) (R Core Team, 2017). All p values were two tailed and reported using a 0.05 significance level.

Metabolite correlations with clinical disability measures:

Given the non-normal distribution of the clinical disability measures, Spearman rank correlation coefficients were used to examine the association between tissue specific metabolites and clinical disability measures (EDSS, T25FW, 9HPT, PASAT3, SDMT). The scope of the analysis was to analyse the association between our key metabolites in NAWM and GM (tNAA, mIns, Glx, tCho and their ratios to tCr) and the disability measures listed above. These are reported in Table 4-3. In reporting multiple analyses, I was guided by considerations outlined in Patel & Ioannidis et al.: multiplicity adjustment is not required when a list of hypotheses of primary importance are pre-specified; emphasis is placed on being explicit and transparent about the extent of multiplicity; and the magnitude of observed associations is interpreted in the context of the background literature (Patel and Ioannidis, 2014). Furthermore, many of the associations are exploratory in nature as they have either not been tested before or not been tested in a sample size as large as this.

Where statistically significant correlations were found in the correlation analysis, a subsequent multivariable linear regression analysis was performed, with the following covariates: age, sex, disease-duration from onset, occurrence of relapses in the preceding two years, T2 lesion volume and normalised brain volume. Model diagnostics undertaken to assess the regression model included: plots of studentised residuals against adjusted predicted values to check residual homoscedasticity, Cook's distance to determine effect of leveraged data points; and calculation of variance inflation factors to determine multi-collinearity

4.3 Results

154 participants gave consent for the Advanced MRI sub-study from January 2015 to June 2016. Of these 154 participants, six failed the CSI quality assurance leaving 148 participants in the CSI arm of the Advanced MRI sub-study at baseline.

In total, 8361 CSI voxels passed both automatic and visual quality assurance. 3035 voxels remained after excluding voxels that contained > 1% WML and > 15% CSF (mean 20.5 voxels per patient, standard deviation 9.2). After calculating metabolite values and removing metabolic outliers, 119 SPMS participants remained for analysis. Cohort demographics are provided for the cohort of 119 participants that underwent correlation testing and regression analysis. 81/119 (68%) were female and 108/119 (91%) had not experienced a relapse in the two years prior to randomisation. Further details of the cohort are shown in Table 4-1.

Table 4-1. Baseline demographics and characteristics (n=119)

Clinical Variable	***Mean (standard deviation)***
Age (years)	54.2 (6.7)
EDSS^{+}	6.0 (4.0-6.5)
Normalised brain volume (mL)	1418 (87.3)
Nine-hole peg test (sec^{-1})*	0.035 (0.01)
SPMS duration (years)	22.3 (9.2)
PASAT3 Score (out of 60)	43.0 (11.5)
SDMT Score (out of 110)	46.9 (11.0)
T2 lesion volume^{+} (mL)	9.7 (0.3-34.6)
T25FW (sec)	10.6 (4.3-180.0)

[+] = median (range), EDSS = Expanded disability status scale, PASAT3 = Paced auditory serial addition test, SDMT = symbol digit modalities test, SPMS = Secondary progressive multiple sclerosis, T25FW = Timed 25-foot walk test

*Nine-hole peg test calculated by taking the reciprocal of the average of two trials for each arm and taking the mean

Estimated metabolite concentrations (in IU) and metabolite ratios to tCr for NAWM and GM can be found in Table 4-2.

Table 4-2: Summary statistics for metabolite estimated concentrations (in institutional units) and ratios to total creatine (n = 119)

Metabolite	Mean	SD	Median	Max	Min
NAWM tNAA	8.09	1.04	8.05	10.56	5.62
NAWM tNAA/tCr	1.34	0.14	1.34	1.82	1.08
NAWM mIns	4.72	0.91	4.68	7.03	2.75
NAWM mIns/tCr	0.79	0.13	0.78	1.14	0.52
NAWM Glx	10.01	1.62	9.96	14.23	6.28
NAWM Glx/tCr	1.68	0.23	1.69	2.75	1.07
NAWM tCho	1.46	0.26	1.44	2.19	0.70
NAWM tCho/tCr	0.24	0.03	0.24	0.32	0.17
GM tNAA	9.49	1.96	9.73	13.85	4.21
GM tNAA/tCr	1.36	0.23	1.35	1.88	0.75
GM mIns	5.11	1.41	5.05	8.68	1.60

GM mIns/tCr	0.73	0.21	0.72	1.43	0.19
GM Glx	12.22	3.44	11.91	20.02	5.54
GM Glx/tCr	1.75	0.45	1.77	3.05	0.79
GM tCho	1.60	0.39	1.63	2.34	0.37
GM tCho/tCr	0.23	0.06	0.23	0.39	0.02

Glx = glutamate and glutamine, GM = grey matter, mIns = myoinositol, NAWM = normal appearing white matter, SD = standard deviation, tCho = glycerophosphocholine and phosphocholine, tCr = creatine and phosphocreatine, tNAA = N-acetyl aspartate and N-acetyl aspartyl glutamate

Metabolite concentrations/ratios which showed statistically significant correlations to disability measures in NAWM and GM are shown in Table 4-3.

Table 4-3. Spearman Rank correlations between metabolites (Estimated concentrations and ratios) and disability measures (n = 119)

	EDSS			Timed 25-foot walk			Nine-hole peg test			PASAT3 scores			SDMT Scores		
	Rho	95% CI		Rho	95% CI		Rho	95% CI		Rho	95% CI		Rho	95% CI	
NAWM tNAA	0.10	-0.08	0.28	0.07	-0.11	0.25	**0.22***	**0.05**	**0.39**	**0.21***	**0.03**	**0.38**	**0.20***	**0.02**	**0.37**
NAWM tNAA/tCr	0.02	-0.17	0.19	-0.05	-0.23	0.13	**0.23***	**0.06**	**0.40**	**0.19***	**0.01**	**0.36**	0.14	-0.05	0.31
NAWM mIns	-0.11	-0.29	0.07	-0.06	-0.24	0.12	-0.01	-0.19	0.17	-0.15	-0.32	0.03	0.00	-0.18	0.18
NAWM mIns/tCr	**-0.26****	**-0.42**	**-0.09**	**-0.20***	**-0.37**	**-0.03**	-0.03	-0.21	0.15	**-0.23***	**-0.39**	**-0.05**	-0.08	-0.26	0.10
NAWM Glx	0.08	-0.10	0.26	0.10	-0.08	0.28	0.00	-0.18	0.18	0.00	-0.18	0.18	**0.19***	**0.01**	**0.36**
NAWM Glx/tCr	0.03	-0.15	0.21	0.07	-0.11	0.25	-0.12	-0.29	0.07	-0.12	-0.30	0.06	0.04	-0.15	0.22
NAWM tCho	-0.10	-0.27	0.08	0.00	-0.18	0.18	0.09	-0.09	0.26	0.17	-0.01	0.34	0.17	-0.01	0.34
NAWM tCho/tCr	-0.22	-0.39	-0.04	-0.12	-0.30	0.06	0.05	-0.14	0.22	0.12	-0.06	0.29	0.07	-0.12	0.24
GM tNAA	-0.16	-0.33	0.02	-0.14	-0.31	0.04	0.05	-0.13	0.22	0.02	-0.16	0.20	0.08	-0.10	0.26

GM tNAA/tCr	-0.05	-0.23	0.13	-0.01	-0.19	0.17	0.08	-0.11	0.25	0.05	-0.13	0.23	0.06	-0.12	0.24
GM mIns	0.10	-0.08	0.28	0.18	0.00	0.34	-0.14	-0.32	0.04	**-0.20***	**-0.37**	**-0.02**	-0.10	-0.27	0.09
GM mIns/tCr	0.18	0.00	0.35	**0.28****	**0.10**	**0.44**	-0.15	-0.32	0.03	-0.14	-0.32	0.04	**-0.18***	**-0.35**	**0.00**
GM Glx	**-0.28****	**-0.44**	**-0.10**	**-0.30*****	**-0.45**	**-0.13**	0.04	-0.14	0.22	0.14	-0.04	0.31	0.03	-0.15	0.21
GM Glx/tCr	**-0.22***	**-0.39**	**-0.04**	**-0.26*****	**-0.42**	**-0.08**	0.06	-0.12	0.24	0.19	0.01	0.36	-0.02	-0.20	0.17
GM tCho	0.11	-0.07	0.28	0.11	-0.07	0.29	-0.05	-0.23	0.13	**-0.24****	**-0.40**	**-0.06**	-0.08	-0.25	0.11
GM tCho/tCr	0.16	-0.02	0.33	0.19	0.01	0.36	0.00	-0.18	0.18	**-0.21***	**-0.37**	**-0.03**	-0.09	-0.27	0.09

Statistically significant correlation coefficients are highlighted in bold text. $p < .001$ ***, $p < .01$ **, $p < .05$ *

EDSS = Expanded disability status scale, GM = grey matter, Glx = glutamate and glutamine, mIns = myoinositol, NAWM = normal appearing white matter, PASAT3 = Paced auditory serial addition test, SDMT = symbol digit modalities test, tCho = glycerophosphocholine and phosphocholine, tCr = creatine and phosphocreatine, tNAA = N-acetyl aspartate and N-acetyl aspartyl glutamate

Table 4-4 shows the results of the regression analysis for metabolites that were significantly associated with clinical disability measures after adjusting for covariates. Metabolites that showed a statistically significant association on the Spearman rank correlation but lost statistical significance after regression analysis are not shown in Table 4-4. In NAWM, associations were seen between tNAA/tCr and 9HPT (β = 0.23, p = 0.04); tNAA and tNAA/tCr and PASAT3 (β = 0.17, p = 0.04), (β = 0.19, p = 0.02) respectively; and mIns/tCr and PASAT3 (β = -0.22, p = 0.007). In GM, tCho was associated with PASAT3 (β = -0.27, p = 0.04).

Table 4-4. Results from multiple regression analysis examining associations between metabolites and clinical disability measures

Nine-hole peg test* (n = 118)**			
Predictors	*std. Beta*	*std 95% CI*	*p*
NAWM tNAA/tCr	0.19	0.01 – 0.36	0.04
Paced auditory serial addition test (n = 119)			
Predictors	*std. Beta*	*std 95% CI*	*p*
NAWM tNAA	0.17	0.01 – 0.34	0.04
Gender*	-0.23	-0.42 to -0.05	0.01
T2 lesion volume	-0.47	-0.64 to -0.30	<0.001
Paced auditory serial addition test (n = 118)**			
Predictors	*std. Beta*	*std 95% CI*	*p*
NAWM tNAA/tCr	0.19	0.03 – 0.35	0.02

Gender*	-0.26	-0.44 to -0.08	0.006
T2 lesion volume	-0.46	-0.63 to -0.29	<0.001
Paced auditory serial addition test (n = 119)			
Predictors	*std. Beta*	*std 95% CI*	*p*
NAWM mIns/tCr	-0.22	-0.39 to -0.06	0.007
Gender*	-0.25	-0.43 to -0.07	0.008
T2 lesion volume	-0.47	-0.64 to -0.30	<0.001
Paced auditory serial addition test (n = 119)			
Predictors	*std. Beta*	*std 95% CI*	*p*
GM tCho	-0.17	-0.33 – -0.01	0.04
T2 lesion volume	-0.48	-0.65 – -0.31	<0.001

*Male is reference category. ** 118 participants in this cohort as 1 case removed due to a highly leveraged point ***Nine-hole peg test calculated by taking the reciprocal of the average of two trials for each arm and taking the mean

CI = confidence interval, GM = grey matter, mIns = myoinositol, NAWM = normal appearing white matter, SE = standard error, std = standardised, tCho = glycerophosphocholine and phosphocholine, tCr = creatine and phosphocreatine, tNAA = N-acetyl aspartate and N-acetyl aspartyl glutamate.

Covariates in model include: age, gender, duration from onset, occurrence of relapse in 2 years preceding randomisation, T2 lesion volume and normalised brain volume. Table highlights only the predictor variables that were significant from the multiple regression models.

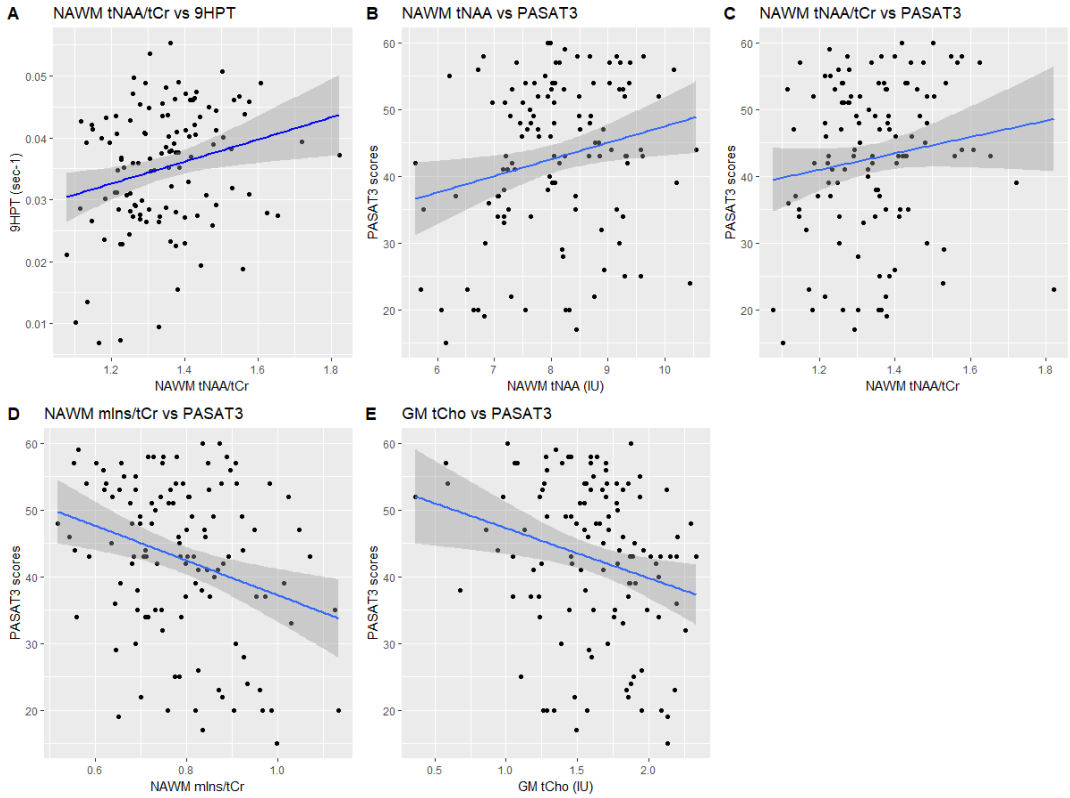

Figure 4-1. Associations between metabolites and clinical disability measures

4.4 Discussion

This is the largest reported cohort of people with SPMS undergoing ^{1}H-MRS. Table 3 shows all of the correlations with those in bold as statistically significant. They were then explored in a multiple regression analysis (Table 4-4). The results suggest a relationship in NAWM between tNAA (tNAA/tCr) and mIns/tCr and IPS performance (PASAT3); and between tNAA/tCr and upper limb function (9HPT). In GM, tCho was associated with IPS performance. Whilst a number of other correlations were identified in the correlation analysis, no associations with EDSS or T25FW were found in GM or NAWM after multiple regression analysis (Solanky *et al.*, 2020).

4.4.1 Relationships between metabolites and clinical disability

Upper limb function (Solanky *et al.*, 2020)

Previous smaller studies examining tNAA or tNAA/tCr in NAWM in PMS have not demonstrated statistically significant associations between neuroaxonal integrity and upper limb function (Sastre-Garriga *et al.*, 2005; Obert *et al.*, 2016). Our study suggests that as neuroaxonal integrity (and mitochondrial function) decreases, upper limb function, as reflected by 9HPT, also decreases. The association found between tNAA/tCr and 9HPT during the correlation analysis (see Table 4-3) and multiple linear regression head in the expected direction with decreased tNAA/tCr associated with decreased upper limb function (as reflected by 9HPT). It remains of interest as to whether this is reflective of regional changes in NAWM that affect specific tracts related to upper limb and hand function or if the changes are more reflective of generalised changes throughout the NAWM. It is possible that retrograde degeneration from the cervical cord may also affect tracts controlling upper limb function in NAWM. With the association being seen with 9HPT but not T25FW, it may suggest that changes in neuroaxonal integrity and mitochondrial function in the brain play a more significant role in upper limb dysfunction in the progressive stage of the disease. This could be further explained by the hypothesis that PMS is a length dependent central axonopathy whereby legs are affected earlier due to greater susceptibility of spinal cord motor neurons; and the greater reserve capacity of shorter neuronal pathways such as the upper limb earlier in progressive disease (Giovannoni *et al.*, 2017). Sastre-Garriga et al found an association between tNAA and 9HPT in CGM ($r = -0.48$, $p = 0.03$) and in this context the correlation in this study of 0.22 (see

table 3) is lower – although our association was in NAWM rather than CGM (Sastre-Garriga *et al.*, 2005). Our result contrasts with previous studies but this could be explained by the differences in cohort characteristics whereby Sastre-Garriga et al examined 43 predominantly male participants with early PPMS with a lower median EDSS of 4.5 and Obert et al analysed 15 SPMS with a median EDSS 4.5 (Sastre-Garriga *et al.*, 2005; Obert *et al.*, 2016).

Information processing speed (Solanky *et al.*, 2020)***:***

A previous much smaller study examining measures of IPS (PASAT3) and its relationship to in vivo metabolites in NAWM in SPMS (n = 15) did not show any associations (Obert *et al.*, 2016). Several other studies reported results in the form of standardised scores such as MS Functional composite or the Brief Repeatable battery, making it difficult to discern the true relationship between IPS and metabolites in PMS (Cox *et al.*, 2004; Sastre-Garriga *et al.*, 2005; Geurts *et al.*, 2006). Firstly, our findings of an association between NAWM tNAA and tNAA/tCr with PASAT3 scores (see Table 4-3 and Table 4-4) are in the expected direction, with decreased neuroaxonal integrity in NAWM, associated with decreased performance on the PASAT3. I was unable to determine whether there was a predilection to a specific region of NAWM or whether it was possibly associated with altered functional or structural connectivity. Solana et al examined this in a mixed cohort of relapsing remitting MS and SPMS, demonstrating that NAA/tCr and mIns/tCr in WM were associated with abnormal efficiency in the front-parietal network with abnormalities in this network associated with impaired attention and processing speed (compared to HC) (Solana *et al.*, 2018). Our findings differed from Obert et al who employed a similar ^{1}H-MRS acquisition to calculate NAA/tCr, but their SPMS cohort of 14 undergoing ^{1}H-MRS may not have had sufficient power to detect an association. Gender is also associated with IPS with females being associated with decreased PASAT3 scores compared to males adjusting for the other covariates (see Table 4-4). Neurometabolic differences between males and females in SPMS was examined by De Stefano et al. who did not find differences in NAA/tCr in NAWM (De Stefano *et al.*, 2001). There was also no difference in tNAA or tNAA/tCr in NAWM between males and females in our SPMS cohort (welch t test: p = 0.3, p = 0.7 respectively). Penny et al examined the longitudinal association between NAA and IPS in PMS and did not identify gender as being associated with 5-year measures of

IPS. Their results however may differ as they studied a cohort of PPMS that had a predominance of males and a lower baseline median EDSS of 4.5 (Penny *et al.*, 2010). T2 lesion volume reflecting the inflammatory lesion burden was also associated with IPS and cognitive performance– findings that have been demonstrated before confirming the strong association between inflammatory lesion burden and clinical disability in PMS (Cox *et al.*, 2004; Penny *et al.*, 2010).

I also found that mIns/tCr in NAWM had a negative association with PASAT3 scores (see Table 4-3 and Table 4-4). This relationship is in the expected direction with increased astrogliosis (as reflected by higher mIns/tCr) associated with decreased performance on PASAT3. mIns values were not associated with tests of IPS but the ratio between the two showed a weak negative association which suggests that as mIns/tCr ratio increases, PASAT3 scores decrease (see Figure 4-1). This finding could be driven by either an increased mIns or decreased tCr (tCr is more commonly used a reference metabolite) and reflective of increased astrogliosis in SPMS, causing IPS dysfunction.

There was a correlation between tNAA in NAWM and SDMT. However, this association was not significant after adjusting for covariates (age, gender, duration from onset, occurrence of relapse in 2 years preceding randomisation, T2 lesion volume and normalised brain volume) in the regression analysis. Whilst both PASAT3 and SDMT measure IPS, PASAT3 involves verbal work memory compared to SDMT which involves visuo-spatial memory and this may explain the association between neuroaxonal integrity in NAWM and PASAT3 but not SDMT (Sonder *et al.*, 2014). A separate study comparing PASAT3 to SDMT using fMRI found that PASAT3 activated more frontal areas and the left inferior parietal lobe, suggesting that PASAT3 required more working memory capacity and executive function to execute compared to SDMT (Forn *et al.*, 2011). However, studies in RRMS suggest strong correlation between PASAT3 and SDMT and with similar sensitivity and specificity between the two tests, so our lack of association with SDMT should be interpreted with caution (López-Góngora, Querol and Escartín, 2015).

A previous study of choline levels in CGM did not show any difference between primary progressive MS and HC; nor was there any association with clinical disability measures (Sastre-Garriga *et al.*, 2005). Our results suggest an association between

GM tCho (a measure of membrane turnover) and IPS - as GM tCho levels increase, IPS performance (reflected by PASAT3 scores) decreases (see Table 4-3, Table 4-4 and Figure 4-1). Phosphatidylcholine is one of the major choline containing compounds contained within cell membranes and there is evidence that this along with its precursor molecule phosphocholine and breakdown product glycerophosphocholine are measured by the tCho peak in ^{1}H-MRS (Miller, 1991). Along with this, the consistent finding of increased tCho (tCho/tCr) in active MS lesions suggests that tCho is a marker of membrane turnover (Swanberg *et al.*, 2019). Recent findings have demonstrated that meningeal lymphoid follicles release pro-inflammatory molecules that can lead to CGM inflammation in SPMS and our findings may support this with a metabolic measure of increased membrane turnover in CGM being associated with IPS (Magliozzi *et al.*, 2007; James *et al.*, 2020). However, this should be interpreted with caution because tCho was not associated with other measures of clinical disability. Our findings may have differed from the previous study as Sastre-Garriga et al examined a cohort of 41 participants with early PPMS and lower disability (median EDSS 4.5, mean disease duration 3.31 years) (Sastre-Garriga *et al.*, 2005).

Previous studies exploring the relationship between brain metabolites and measures of IPS in PMS did not report the correlation coefficients making it difficult to place our results in the context of previously reported results (Cox *et al.*, 2004; Sastre-Garriga *et al.*, 2005; MacMillan *et al.*, 2016; Obert *et al.*, 2016). Though, examining the associations in these studies between metabolites and other clinical disability measures e.g. EDSS would suggest that the size of our correlations (see Table 4-3) are not out of keeping with previously reported work (Sastre-Garriga *et al.*, 2005; Obert *et al.*, 2016).

Although there were statistically significant correlations in GM between mIns and PASAT3 scores, mIns/tCr and SDMT scores and mIns/tCr and T25FW (see Table 4-3), these were not significant in the regression analysis adjusting for other covariates and is generally in keeping with previous studies that have examined associations between CGM metabolites and clinical disability measures such as EDSS and the Brief repeatable battery in SPMS cohorts (Sarchielli *et al.*, 2002; Adalsteinsson *et al.*, 2003; Geurts *et al.*, 2006; Caramanos *et al.*, 2009). A single study found tNAA was

decreased in CGM compared to controls and tNAA in CGM showed a moderate association with EDSS and 9HPT but this was in early PPMS (Sastre-Garriga *et al.*, 2005). When calculating GM metabolites, several studies used careful placement of the VOI using single voxel spectroscopy (Sarchielli *et al.*, 2002; Geurts *et al.*, 2006); whilst the remaining studies used CSI followed by automated or manual tissue segmentation (Adalsteinsson *et al.*, 2003; Caramanos *et al.*, 2009). These differing techniques reflect the technical challenges in GM metabolite calculation where the partial volume effect can result in contamination of the VOI or leaving insufficient pure GM voxels. The other issue is that previous studies have reported clinical measures that reflect general disability or composite scores e.g. EDSS and Brief repeatable battery, making it difficult to determine associations with specific functional measures such as upper limb function or ambulation. I attempted to address these issues using CSI followed by segmentation; then using a regression method to calculate GM metabolite values, and then examining these associations with specific functional measures of clinical disability.

4.4.2 **Measures of ambulation and general disability**

Whilst there were several associations seen between metabolites and T25W and EDSS (see Table 4-3), after multiple regression analysis I did not find any significant associations between the T25FW performance or the EDSS and any metabolite levels. Previous studies examining SPMS cohorts have shown relationships between total choline and EDSS in NAWM; and tNAA/tCr in CGM and EDSS in a cohort of PPMS (n=15) (Obert *et al.*, 2016). The lack of association between metabolites and EDSS could be due to the limited distribution of scores in the cohort where 106/148 had an EDSS score of 6.0-6.5; compounded by the ceiling effect and non-linear characteristics of the EDSS.(Giovannoni *et al.*, 2017) EDSS particularly between 4.0-6.5 is defined by ambulatory distance and there is a moderate to strong correlation between the T25FW and EDSS (Motl *et al.*, 2017). Or there is no relationship to be found.

There were statistically significant correlations between GM Glx (Glx/tCr) and EDSS; and with T25TW (see Table 4-3) but after multiple regression analysis, I did not find any significant relationships between Glx or Glx/tCr and measures of clinical disability. Glutamatergic excitotoxicity has been shown to be involved in the pathogenesis of

PMS (Macrez *et al.*, 2016). When glutamate values were measured separately to glutamine using a TE averaged technique, glutamate was associated with a decline in neuroaxonal integrity in a mixed cohort of MS (number of PMS = 31/343) (Azevedo *et al.*, 2014). I measured Glx (glutamine + glutamate) due to the difficulty in resolving glutamate from its precursor glutamine at 3T. It also seems unlikely that I can measure glutamatergic excitotoxicity directly as the majority of Glx signal arises from the intracellular compartment and thereby is more likely to reflect neuro-axonal integrity.

4.4.3 **Methodological and analytical considerations**

The demographics and characteristics (n=119) of the cohort analysed in this study were consistent with those reported from the main MS-SMART study (n=445) (Chataway *et al.*, 2020). The placement of the CSI grid above the ventricles was designed to limit the effect of ventricles from which there is no metabolite signal, decrease partial volume effect and ensure consistency of shimming across the CSI slice. The predilection of WML to periventricular regions led to voxels containing predominantly WM and GM and meant I was unable to obtain metabolite values from WML. When determining metabolite values for NAWM and GM, I attempted to limit contamination by WML and CSF by excluding voxels that contained 1% WML and 15% CSF. These parameters kept the best balance between the loss of CSI voxels whilst minimising WML and CSF contamination of voxels used in NAWM and GM calculations. During the calculation of metabolite values in NAWM and GM, 29 participants were excluded as metabolite outliers. No formal statistical comparison was undertaken but the characteristics of these 29 participants were generally similar to those in the cohort that underwent analysis (n=119), except to note the median T2 lesion volume was higher in the excluded group (15.6mL v 9.7mL). While I outline a rationale for dealing with multiple comparisons, some caution is advised during interpretation of the associations due to the multiple comparisons being undertaken. Owing to technical difficulties in GM lesions detection, GM lesions were not segmented and this should be acknowledged when interpreting metabolite values and results pertaining to GM.

The metabolite ratios to tCr need careful interpretation as tCr is also affected by neuropathology (Vrenken *et al.*, 2005). There are however benefits to using tCr as a stable reference as it removes the need to adjust for head coil loading, T1 and T2

effects (Swanberg *et al.*, 2019). Estimated concentrations are reported using water reference for scaling which can be used to produce absolute concentrations; this in turn carries assumptions within LCModel about the water content of tissue, which is based on reports from normal healthy volunteers (Ernst, Kreis and Ross, 1993), given this assumption and the fact that at TR=2000ms T1 effects may still be present, I chose to present an estimated (rather than absolute) concentration in institutional units. The use of estimated concentrations allows for the fact that errors between the LCModel "absolute" concentrations and the true metabolite concentrations may be present.

4.5 Conclusion

In summary, after multiple regression analysis tNAA, tNAA/tCr and mIns/tCr in NAWM and tCho in GM are associated with clinical disability in upper limb function and information processing speed. These metabolites are therefore of interest as biomarkers of brain injury in SPMS.

Chapter 5. A proton magnetic resonance spectroscopic imaging study of three potential neuroprotective agents in secondary progressive multiple sclerosis

5.1 Introduction

The Multiple Sclerosis- Secondary Progressive Multi-Arm Randomisation Trial (MS-SMART NCT01910259) was designed to test the neuroprotective potential of three interventions (amiloride, fluoxetine and riluzole) in SPMS and included a CSI sub-study to explore the proposed target engagement of these drugs (Connick *et al.*, 2018).

I firstly examined the control (placebo) arm to investigate the natural history of brain metabolite changes in SPMS over 96-weeks. I postulate that progressive neuro-axonal degeneration and astrogliosis would result in a decrease in tNAA and increases in mIns respectively. With tCho being a marker of membrane turnover, I also hypothesise that it would also increase over the time period.

In terms of the candidate drugs, fluoxetine can stimulate astrocytic glycogenesis and has been shown to increase tNAA in cerebral white matter in MS (Mostert *et al.*, 2006, 2013; Sijens *et al.*, 2008; Cambron *et al.*, 2014). Furthermore, fluoxetine has a potential anti-inflammatory effect that could be confirmed by a decrease in mIns levels (Mostert *et al.*, 2008). Last, in a mixed cohort treated with fluoxetine for two weeks, tCho levels in CGM decreased by 5% per week (Sijens, Irwan, *et al.*, 2006). I would therefore hypothesise that fluoxetine would increase tNAA, reduce mIns and decrease tCho (in CGM), compared to the control arm.

Riluzole was assessed in MS-SMART due to its ability to reduce glutamatergic transmission and its effects of sodium channel blockade. Evidence for glutamatergic excitotoxicity has been demonstrated in experimental MS models (Werner, Pitt and Raine, 2001; Geurts *et al.*, 2003; Pitt *et al.*, 2003; Sarchielli *et al.*, 2003; Matute, Domercq and Sánchez-Gómez, 2006). In animal studies, glutamatergic ionotropic receptor antagonism ameliorates various aspects of disease activity but translational studies using glutamatergic receptor antagonists in MS participants have been mixed (Waubant *et al.*, 2014; Macrez *et al.*, 2016). Riluzole decreases glutamatergic

transmission in the central nervous system and I would therefore expect riluzole to reduce the Glx concentration compared to placebo (Bellingham, 2011).

Amiloride was assessed due to evidence from preclinical studies suggesting that the acid sensing ion channel-1 (ASIC-1) receptor is involved in sodium and calcium influxes that ultimately lead to axonal and oligodendrocyte injury. ASIC-1 is predominantly expressed on axons and oligodendrocytes and blockage of this receptor by amiloride ameliorates disease activity in the experimental mouse models of MS and also has a neuroprotective effect on axons and oligodendrocytes (Vergo *et al.*, 2011). Based on this mechanism of action, I would hypothesise that amiloride would lead to a relative increase in tNAA levels.

In Chapter 4, I demonstrated in a cross-sectional analysis of 119 participants with SPMS a number of significant associations, which were then confirmed by multiple linear regression. First, in the normal appearing white matter (NAWM): decreased tNAA correlated with a decreased performance in upper limb function (as measured by the 9HPT) and information processing speed (as measured by the PASAT3). Second, PASAT3 performance was found to inversely related to the mIns/tCr level in NAWM. Last, in grey matter (GM) a negative association was seen with tCho levels and PASAT3 scores. I now present the 96-week follow-up of this cohort to confirm these associations.

My hypotheses are therefore summarised as follows:

1 Natural history of metabolite changes
    a. tNAA levels will decrease in the placebo arm over 96 weeks
    b. mIns levels will increase in the placebo arm over 96 weeks
    c. tCho levels will increase in the placebo arm over 96 weeks
2 Effect of drug pathways on metabolites
    a. tNAA levels will be higher in the fluoxetine arm compared to placebo over 96 weeks
    b. mIns levels will be lower in the fluoxetine arm compared to placebo over 96 weeks
    c. tCho levels in cGM will be lower in the fluoxetine arm compared to placebo over 96 weeks

d. Glx levels will be lower in the riluzole arm compared to placebo over 96 weeks
e. tNAA levels will be higher in the amiloride arm compared to placebo over 96 weeks

3 Associations between MRI measures and clinical disability
   a. Baseline tNAA and tNAA/tCr in NAWM will be associated with 9HPT scores at 96 weeks
   b. Baseline tNAA, tNAA/tCr, mIns/tCr in NAWM will be associated with PASAT3 scores at 96 weeks
   c. Baseline tCho in cGM will be associated with PASAT3 scores at 96-weeks

5.2 Methods

Study design, drug interventions, participant recruitment, MRI acquisition and image post-processing including metabolite analysis are outlined in 3.2.1-3.2.4 and 3.2.6-3.2.9. Total N-acetyl aspartate (tNAA), myo-inositol (mIns) glutamate and its precursor glutamine (Glx), total choline (tCho) and their ratios to tCr were determined for NAWM and GM at baseline and week 96.

5.2.1 Statistical methodology

Statistical analysis was completed using R statistical software version 3.5.1 (R Core Team, 2017). All statistical tests and confidence intervals were two-sided. 95% confidence intervals were calculated with the significance of raw p-values assessed based on a 5% significance level. I used a complete-case analysis following removal of metabolite outlying observations based on the intention-to-treat population.

For the specific hypotheses examining change in the placebo group and drug specific changes in active treatment arms, the metabolite being considered was analysed using absolute concentration, ratio to tCr and their respective levels in GM and NAWM. As such, during the analysis, 48 comparisons were undertaken and each comparison was based on a specific hypothesis that was pre-specified *a priori* and therefore no adjustment for multiplicity was made. In reporting multiple analyses, I was again guided by the considerations outlined by Patel et al.: multiplicity adjustment is not required when a list of hypotheses of primary importance are pre-specified; there is a

focus on being explicit and transparent about the extent of multiplicity; and the magnitude of observed associations are interpreted in the context of the background literature (Patel and Ioannidis, 2014; Parker and Weir, 2020). For this study, 48 comparisons were completed out of a possible total of 144.

1) For hypotheses 1 (a-c) examining natural history of metabolites (in the placebo arm), a paired t test was used to analyse metabolite changes in the placebo arm over 96-weeks (Wilcoxon signed ranks test was used where data were not normally distributed).
2) For hypotheses 2 (a-e) examining the effect of drug pathways on metabolites, metabolite differences between each treatment group and placebo, a multiple linear regression method was used to calculate adjusted mean differences and 95% confidence intervals. Each metabolite was assessed in a separate model, where the week-96 metabolite concentration was the dependent variable. Independent variables included trial arm (with placebo as the reference category), the baseline metabolite level (corresponding to the outcome variable), and the minimisation variables: age, sex and EDSS score at randomisation.
3) For hypotheses 3 (a-c) analysing the associations between baseline metabolites and week 96 clinical disability measures (9HPT and PASAT3 scores), separate linear regression models were fitted for each relevant baseline metabolite predictor with 9HPT and PASAT3 at 96-weeks as the dependent variable. Trial arm was again included as an explanatory factor variable in each model. Where metabolites were associated with 96-week upper limb function or 9HPT in this preliminary model, this relationship between baseline metabolites and 96-week clinical disability measures was further analysed in a multiple linear regression model including the following covariates: age, sex, occurrence of a relapse in two years preceding randomisation, baseline T2 lesion volume, baseline normalised brain volume and trial arm. Age and sex were chosen as key demographic variables, whilst the occurrence of relapses in the 2 years preceding study entry was added to assess the impact of potential inflammatory activity. T2 lesion volume was also added as it has shown a strong association with longitudinal IPS and clinical disability whilst normalised brain volume was added to adjust for the potential

confounding effect of differing brain volumes at baseline (L. K. Fisniku *et al.*, 2008; Penny *et al.*, 2010). If the metabolite was significant in this model, then I examined the relationship between the baseline metabolite and the change in clinical disability outcome measure over 96 weeks by adding the baseline clinical disability measure (corresponding to the 96-week clinical disability measure) as a covariate into the model. Results are reported as standardised coefficients (β) with the respective standardised 95% confidence intervals.

In a post-hoc exploratory analysis, I also examined “non-linear” approaches to regression. This may be useful when the relationship between the explanatory variable (metabolite) and outcome/dependent variable (96-week clinical disability measure) is non-linear and therefore may demonstrate an improved fit for the data; and where the possibility of a threshold or plateau effect exists. This was explored only in the aforementioned hypotheses, which includes the relationship between NAWM tNAA, tNAA/tCr and 9HPT; and between NAWM tNAA, NAWM mIns/tCr, GM tCho and PASAT3 scores. A scatter plot was used to first visualise the relationship. In the regression models, the metabolite was included using a polynomial or log function. The dependent variable remained the 96-week clinical outcome measure of interest (9HPT or PASAT3) and the baseline covariates included age, sex, disease duration, trial arm, T2LV and NBV. The regression equation still took the form of: dependent variable = constant + coefficient (independent variable) + coefficient (independent variable 2), however the independent variable of interest (in this case the metabolite) could be raised by a polynomial function or take the logarithm. Combinations of these, for example combining various polynomial and log functions within the same regression equations, was not done as p values (or R^2) cannot be calculated for the independent variables. Furthermore, as the purpose of the regression analysis was to understand the relationship between the metabolite of interest and the respective outcome measure at 96-weeks rather than find an equation that would best predict the outcome measure at 96-weeks, this form on non-linear regression was not felt to be appropriate.

Distributional assumptions underlying the regression analyses were assessed by visual inspection of residual plots. Normality was examined by normal probability plots. Highly leveraged data observations were identified using Cook's distance.

5.3 Results

148 participants were initially randomised to receive: amiloride (n= 39), fluoxetine (n= 35), riluzole (n= 38) or placebo (n= 36). CSI data at the 96-week time point consisted of 122/148 (82%) where 26 participants (18%) were lost to follow up or failed quality assurance (see Figure 5-1).

The 122 participants provided 7402 CSI voxels and after removing voxels containing > 15% CSF, 3639 voxels remained. Removing voxels containing > 1% WML left 2655 voxels from the 96-week time point for analysis [median 20 (range 1-53) per patient]. After calculating metabolite values and removing metabolite outliers (as previously described in 3.2.9), 108 participants were left for analysis and the baseline characteristics of this cohort (n=108) are shown in Figure 5-1.

The demographics and characteristics of the analysed cohort were similar to those reported from the main MS-SMART study except for the median T2 lesion volume which was lower in the placebo arm of our cohort (see Table 5-1) (Chataway *et al.*, 2020). The baseline characteristics of the cohort that either did not have 96-week scan or were excluded as a metabolic outlier (n = 40) were generally similar to the analysed cohort (n=108).

5.3.1 **Natural history of metabolite changes**

In the placebo group (n = 28), the hypothesised decrease in tNAA or increase in mIns was not seen in either the NAWM or GM. There was an increase in GM tCho (and tCho/Cr) with mean differences of -0.32 IU, and -0.04 IU, respectively. Whilst NAWM tCho decreased (mean difference = 0.13 IU) (see Table 5-2).

There were no statistically significant changes in the remaining metabolites over 96-weeks in NAWM or GM (Table 5-2). All metabolite values and ratios at baseline and 96-weeks are shown in **Error! Reference source not found.**.

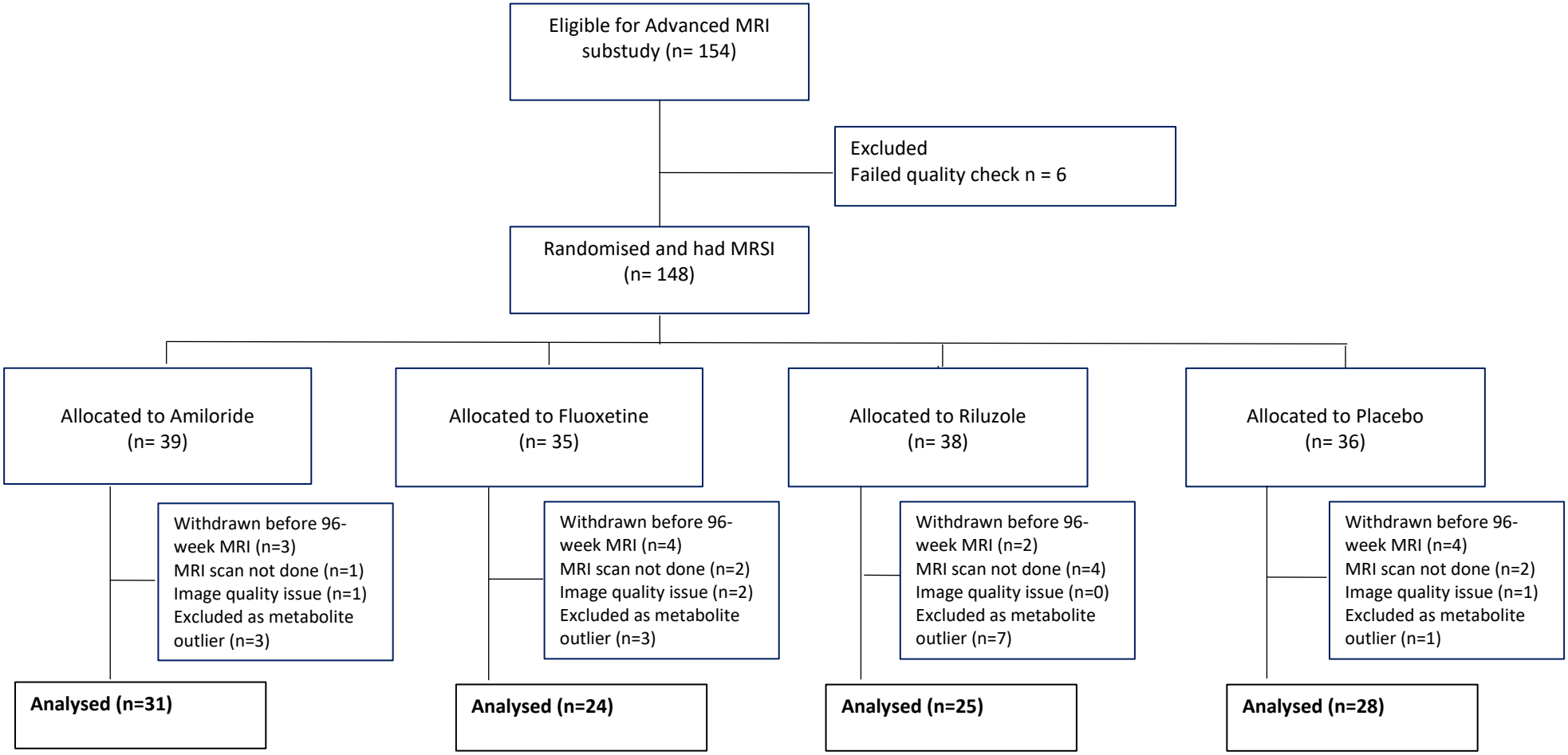

At week 96**,** 26 participants were either lost to follow up or failed MR quality assurance. Of the remaining 122 participants a further 14 were removed as metabolite outliers: 3 from the amiloride arm, 3 from the fluoxetine arm, 7 from the riluzole arm and 1 from the placebo arm leaving for 108 for study analysis.

Figure 5-1: Patient disposition through MR spectroscopy study

Table 5-1. Baseline characteristics of study participants stratified by trial arm

	Amiloride (N=31)	Fluoxetine (N=24)	Riluzole (N=25)	Placebo (N=28)	Total (N=108)
Age	57.4 (49.0-60.5)	56.7 (51.4-59.3)	54.9 (50.0-59.1)	58.3 (51.1-61.3)	56.6 (50.4-60.4)
Male	12 (38.7%)	7 (29.2%)	8 (32.0%)	9 (32.1%)	36 (33.3%)
Female	19 (61.3%)	17 (70.8%)	17 (68.0%)	19 (67.9%)	72 (66.7%)
EDSS	6.0 (5.5-6.5)	6.0 (5.5-6.1)	6.0 (5.5-6.0)	6.0 (5.2-6.0)	6.0 (5.5-6.5)
Time since MS onset (yrs)	24.7 (10.7)	23.0 (8.9)	22.4 (8.4)	19.4 (9.6)	22.4 (9.6)
PASAT3 scores (out of 60)	44.8 (10.0)	42.0 (12.3)	37.3 (15.9)	46.2 (9.8)	42.8 (12.4)
Timed 25 Foot Walk	9.2 (6.9-14.3)	12.0 (7.2-16.3)	9.9 (7.9-13.1)	8.3 (6.8-11.3)	9.3 (7.0-14.9)
9-Hole peg test (sec^{-1})	0.04 (0.01)	0.03 (0.01)	0.03 (0.01)	0.04 (0.01)	0.04 (0.01)
T2 Lesion volume (mL)	7.5 (4.2-15.90)	11.0 (5.3-17.4)	10.2 (3.1-22.9)	6.9 (3.0-13.8)	9.0 (3.7-17.2)
Baseline NBV (mL)	1405.5 (88.0)	1421.9 (73.9)	1410.6 (71.8)	1443.7 (91.737)	1420.2 (82.8)

Data presented are n (%), mean (SD), or median (IQR).

EDSS = Expanded disability status scale, NBV = normalised brain volume, PASAT3 = Paced auditory serial addition test,
Nine-hole peg test calculated by taking as reciprocal of each trial per hand, taking average of two trials and then taking average.

Table 5-2. Mean change between baseline and 96-weeks in the placebo arm (n = 28)

Metabolite	Mean difference	95% CI lower	95% CI higher	p value
NAWM tNAA	0.26	-0.29	0.80	0.34
NAWM tNAA/tCr	-0.02	-0.07	0.02	0.34
NAWM mIns	0.18	-0.22	0.58	0.37
NAWM mIns/tCr	-0.01	-0.05	0.03	0.62
NAWM Glx	0.37	-0.54	1.28	0.41
NAWM Glx/tCr	0.01	-0.11	0.13	0.91
NAWM tCho	**0.13**	**0.01**	**0.25**	**0.03**
NAWM tCho/tCr	0.01	-0.00	0.02	0.18
GM tNAA	0.54	-0.55	1.63	0.32
GM tNAA/tCr	0.10	-0.02	0.23	0.10
GM mIns	-0.19	-1.03	0.65	0.65
GM mIns/tCr	0.00	-0.11	0.10	0.93
GM Glx/tcr	0.14	-0.15	0.44	0.33
GM Glx	1.09	-0.91	3.08	0.28
GM tCho	**-0.32**	**-0.57**	**-0.07**	**0.02**
GM tCho/tCr	**-0.04**	**-0.07**	**-0.01**	**0.01**

Statistically significant results highlighted in bold. Mean difference measures using paired sample t test. CI = confidence interval, Glx = glutamate + glutamine, GM = grey matter, mIns = myoinositol, NAWM = normal appearing white matter, tCho = glycerophosphocholine and phosphocholine, tCr = creatine and phosphocreatine, tNAA = total N-acetyl aspartate and N-acetyl aspartyl glutamate

Table 5-3. Estimated metabolite concentrations (IU) and ratios to total creatine in grey matter and normal appearing white matter

	Amiloride	Fluoxetine	Riluzole	Placebo
Baseline NAWM tNAA	8.16 (1.26)	8.21 (1.22)	7.95 (1.07)	7.58 (1.22)
96-week NAWM tNAA	7.58 (1.28)	7.90 (1.54)	7.18 (1.20)	7.33 (1.07)
Baseline NAWM mIns	4.64 (0.98)	4.68 (0.99)	4.76 (0.72)	4.66 (1.02)
96-week NAWM mIns	4.24 (0.95)	4.12 (1.36)	4.25 (0.71)	4.48 (0.81)
Baseline NAWM Glx	9.87 (1.99)	10.19 (2.39)	9.69 (1.35)	9.49 (1.78)
96-week NAWM Glx	9.03 (1.93)	9.94 (1.72)	9.57 (1.29)	9.11 (1.68)
Baseline NAWM tCho	1.46 (0.25)	1.41 (0.28)	1.48 (0.22)	1.50 (0.28)
96-week NAWM tCho	1.33 (0.29)	1.34 (0.30)	1.31 (0.21)	1.36 (0.20)
Baseline NAWM tNAA/tCr	1.35 (0.12)	1.34 (0.13)	1.32 (0.15)	1.31 (0.11)
96-week NAWM tNAA/tCr	1.36 (0.12)	1.39 (0.15)	1.32 (0.15)	1.33 (0.13)

	Amiloride	Fluoxetine	Riluzole	Placebo
Baseline NAWM mIns/tCr	0.77 (0.15)	0.77 (0.14)	0.80 (0.14)	0.80 (0.10)
96-week NAWM mIns/tCr	0.77 (0.12)	0.72 (0.18)	0.79 (0.12)	0.81 (0.11)
Baseline NAWM Glx/tCr	1.64 (0.22)	1.67 (0.29)	1.63 (0.22)	1.66 (0.23)
96-week NAWM Glx/tCr	1.64 (0.30)	1.76 (0.26)	1.77 (0.21)	1.65 (0.24)
Baseline NAWM tCho/tCr	0.24 (0.04)	0.23 (0.04)	0.25 (0.04)	0.26 (0.02)
96-week NAWM tCho/tCr	0.24 (0.04)	0.24 (0.04)	0.24 (0.03)	0.25 (0.03)
Baseline GM tNAA	9.37 (2.01)	9.94 (2.53)	9.65 (1.78)	9.99 (2.69)
96-week GM tNAA	9.41 (2.10)	9.55 (1.75)	9.46 (1.68)	9.45 (2.05)
Baseline GM mIns	5.16 (1.37)	5.65 (1.55)	5.02 (1.52)	5.30 (2.07)
96-week GM mIns	5.06 (1.80)	5.02 (1.35)	5.45 (1.66)	5.48 (1.92)
Baseline GM Glx	12.79 (4.50)	12.40 (4.88)	12.46 (3.75)	13.61 (4.11)

	Amiloride	Fluoxetine	Riluzole	Placebo
96-week GM Glx	12.86 (4.37)	10.48 (3.14)	10.13 (3.47)	12.52 (3.60)
Baseline GM tCho	1.58 (0.38)	1.77 (0.31)	1.50 (0.32)	1.43 (0.51)
96-week GM tCho	1.60 (0.44)	1.65 (0.31)	1.69 (0.41)	1.76 (0.44)
Baseline GM tNAA/tCr	1.35 (0.23)	1.35 (0.26)	1.42 (0.18)	1.40 (0.25)
96-week GM tNAA/tCr	1.32 (0.25)	1.30 (0.24)	1.35 (0.18)	1.30 (0.24)
Baseline GM mIns/tCr	0.74 (0.21)	0.77 (0.21)	0.74 (0.25)	0.75 (0.26)
96-week GM mIns/tCr	0.70 (0.28)	0.69 (0.19)	0.76 (0.22)	0.75 (0.20)
Baseline GM Glx/tCr	1.87 (0.60)	1.66 (0.59)	1.82 (0.49)	1.90 (0.63)
96-week GM Glx/tCr	1.81 (0.66)	1.36 (0.45)	1.36 (0.41)	1.75 (0.51)
Baseline GM tCho/tCr	0.22 (0.06)	0.24 (0.06)	0.22 (0.05)	0.20 (0.07)
96-week GM tCho/tCr	0.23 (0.07)	0.23 (0.06)	0.24 (0.06)	0.24 (0.04)

Values reported as mean (standard deviation). Glx = sum of glutamate and glutamine, GM = grey matter, mIns = myoinositol, NAWM = normal appearing white matter, tCho = glycerophosphocholine and phosphocholine, tCr = creatine and phosphocreatine, tNAA = N-acetyl aspartate and N-acetyl aspartyl glutamate

5.3.2 **Effect of drug pathways on metabolites**

These are shown in Figure 5-2 - Figure 5-5 and Table 5-4. Compared to placebo, mIns/tCr levels in NAWM was lower in the fluoxetine arm at 96-weeks (β = -0.21, 95% CI [-0.40 to -0.02], p = 0.03). I did not identify any difference in NAWM tNAA (tNAA/tCr) or GM tCho (tCho/tCr) in the fluoxetine treatment arm compared to placebo. In the riluzole arm, there was no change in NAWM Glx; however, riluzole did decrease GM Glx (β = -0.25, 95% CI [-0.47 to -0.04], p = 0.02) and Glx/tCr (β = -0.29, 95% CI [-0.50 to -0.08], p = 0.007). There was no change in tNAA or tNAA/tCr levels compared to placebo in the amiloride arm in NAWM or GM.

Table 5-4. Drug specific effects on metabolites over 96-weeks

Metabolite	Amiloride vs placebo			Fluoxetine vs placebo			Riluzole vs placebo		
	Std beta	95% CI	p value	Std beta	95% CI	p value	Std beta	95% CI	p value
NAWM tNAA	0.04	-0.19 – 0.26	0.76	0.13	-0.09 – 0.35	0.24	-0.08	-0.30 – 0.13	0.45
NAWM tNAA/tCr	0.06	-0.16 – 0.27	0.61	0.14	-0.07 – 0.35	0.19	-0.05	-0.26 – 0.16	0.67
NAWM mIns	-0.09	-0.29 – 0.10	0.35	-0.16	-0.35 – 0.04	0.11	-0.13	-0.32 – 0.07	0.20
NAWM mIns/tCr	-0.08	-0.27 – 0.12	0.44	-0.21	**-0.40 to -0.02**	**0.03**	-0.07	-0.26 – 0.12	0.50
NAWM Glx	-0.03	-0.25 – 0.20	0.82	0.18	-0.04 – 0.40	0.11	0.10	-0.12 – 0.32	0.38
NAWM Glx/tCr	0.00	-0.23 – 0.24	0.97	0.17	-0.05 – 0.40	0.14	0.20	-0.03 – 0.42	0.09
NAWM tCho	-0.03	**-0.24 – 0.18**	**0.78**	**0.02**	-0.19 – 0.23	0.84	-0.09	-0.30 – 0.11	0.38
NAWM tCho/tCr	-0.02	**-0.22 – 0.17**	**0.83**	**0.00**	-0.20 – 0.19	0.96	-0.05	-0.23 – 0.14	0.64
GM tNAA	0.04	-0.20 – 0.27	0.76	0.03	-0.20 – 0.26	0.79	0.03	-0.20 – 0.25	0.81

Metabolite	Amiloride vs placebo			Fluoxetine vs placebo			Riluzole vs placebo		
	Std beta	95% CI	p value	Std beta	95% CI	p value	Std beta	95% CI	p value
GM tNAA/tCr	0.08	-0.14 – 0.31	0.47	0.04	-0.19 – 0.26	0.75	0.08	-0.14 – 0.31	0.46
GM mIns	-0.08	-0.30 – 0.14	0.48	-0.12	-0.33 – 0.09	0.25	0.02	-0.19 – 0.23	0.84
GM mIns/tCr	-0.09	-0.32 – 0.13	0.42	-0.11	-0.33 – 0.11	0.32	0.03	-0.19 – 0.25	0.80
GM Glx	0.05	-0.17 – 0.27	0.67	-0.20	-0.41 – 0.01	0.07	**-0.25**	**-0.47 to -0.04**	**0.02**
GM Glx/tCr	0.03	-0.18 – 0.25	0.77	**-0.28**	**-0.49 to -0.06**	**0.01**	**-0.29**	**-0.50 to -0.08**	**0.007**
GM tCho	-0.19	-0.42 – 0.05	0.12	-0.16	-0.40 – 0.07	0.17	-0.07	-0.30 – 0.15	0.51
GM tCho/tCr	-0.18	-0.41 – 0.06	0.14	-0.18	-0.41 – 0.05	0.14	-0.05	-0.28 – 0.17	0.65

CI = confidence interval, Glx = glutamate + glutamine, GM = grey matter, mIns = myoinositol, NAWM = normal appearing white matter, std = standardised, tCho = glycerophosphocholine and phosphocholine, tCr = creatine and phosphocreatine, tNAA = N-acetyl aspartate + N-acetyl aspartyl glutamate

To analyse drug specific effects on metabolites, multiple regression models for each 96-week metabolite included randomised treatment as an explanatory factor variable (with placebo as the reference category), the corresponding baseline metabolite of interest, and minimisation variables (age, sex, treatment centre, and Expanded Disability Status Scale score at baseline). Significant p values are highlighted in bold.

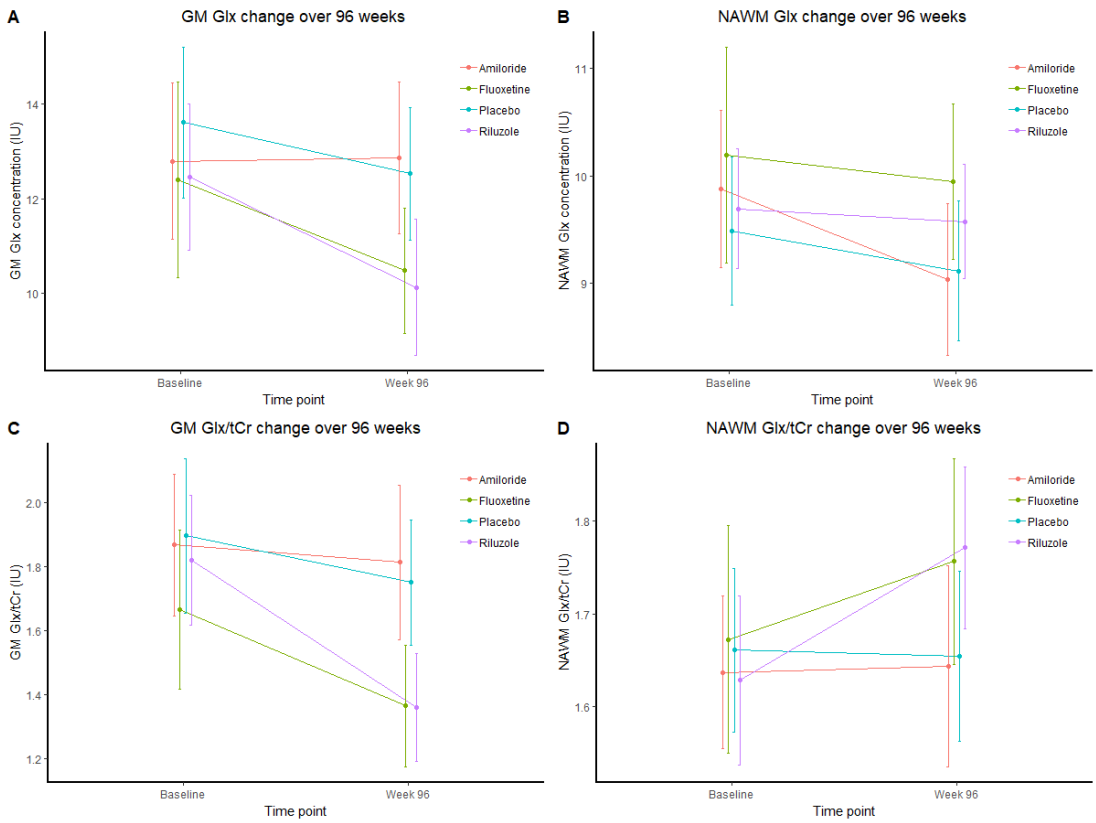

Figure 5-2. Glx and Glx/tCr mean change from baseline to 96-weeks

Glx = glutamate + glutamine, GM = grey matter, IU = institutional units, NAWM = normal appearing white matter, tCr = creatine and phosphocreatine

The left-sided panels A & C show the change in grey matter Glx (sum of glutamate and glutamine) and Glx/tCr over 96-weeks stratified by treatment allocation whilst the right-sided panels B & D show the change in Glx and Glx/tCr over 96-weeks in normal appearing white matter with 95% confidence intervals.

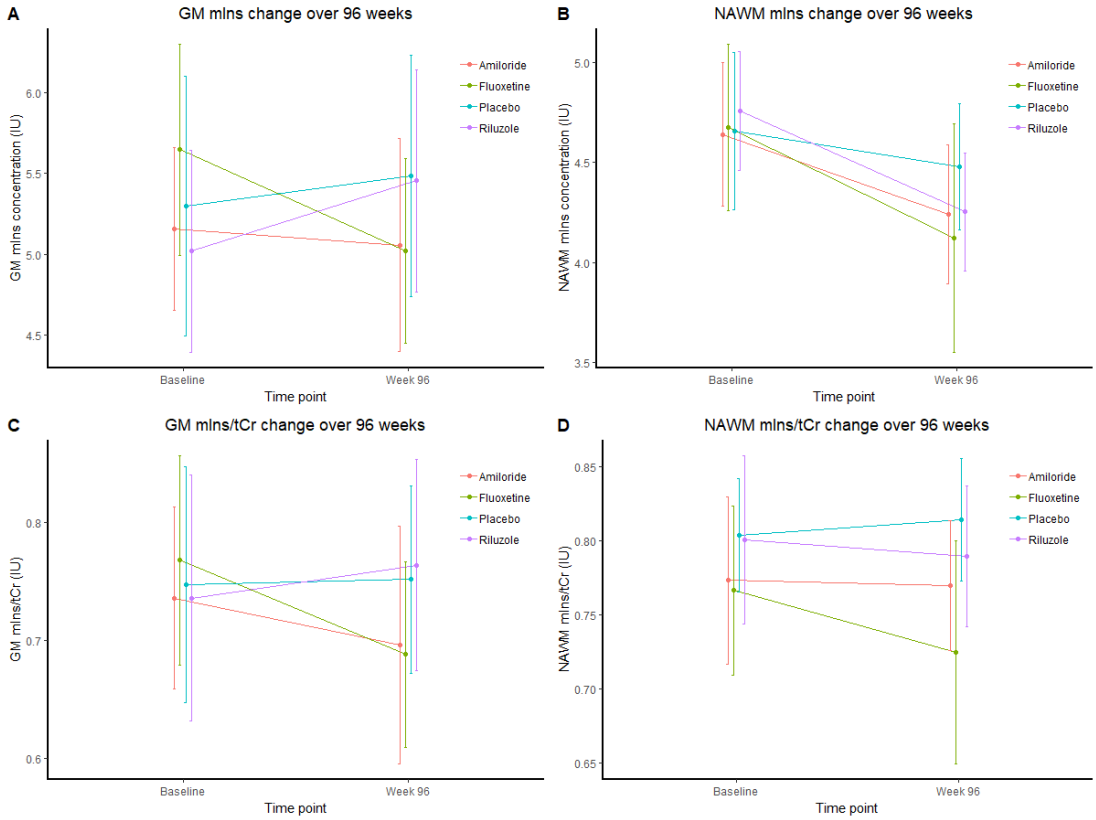

Figure 5-3. Myoinositol and myoinositol/tCr mean change from baseline to 96-weeks

GM = grey matter, IU = institutional units, mIns = myoinositol, NAWM = normal appearing white matter, tCr = creatine and phosphocreatine

The left-sided panels A & C show the change in grey matter myo-inositol and myoinositol/tCr over 96-weeks stratified by treatment allocation whilst the right-sided panels B & D show the change in myoinositol and myoinositol/tCr over 96-weeks in normal appearing white matter with 95% confidence intervals.

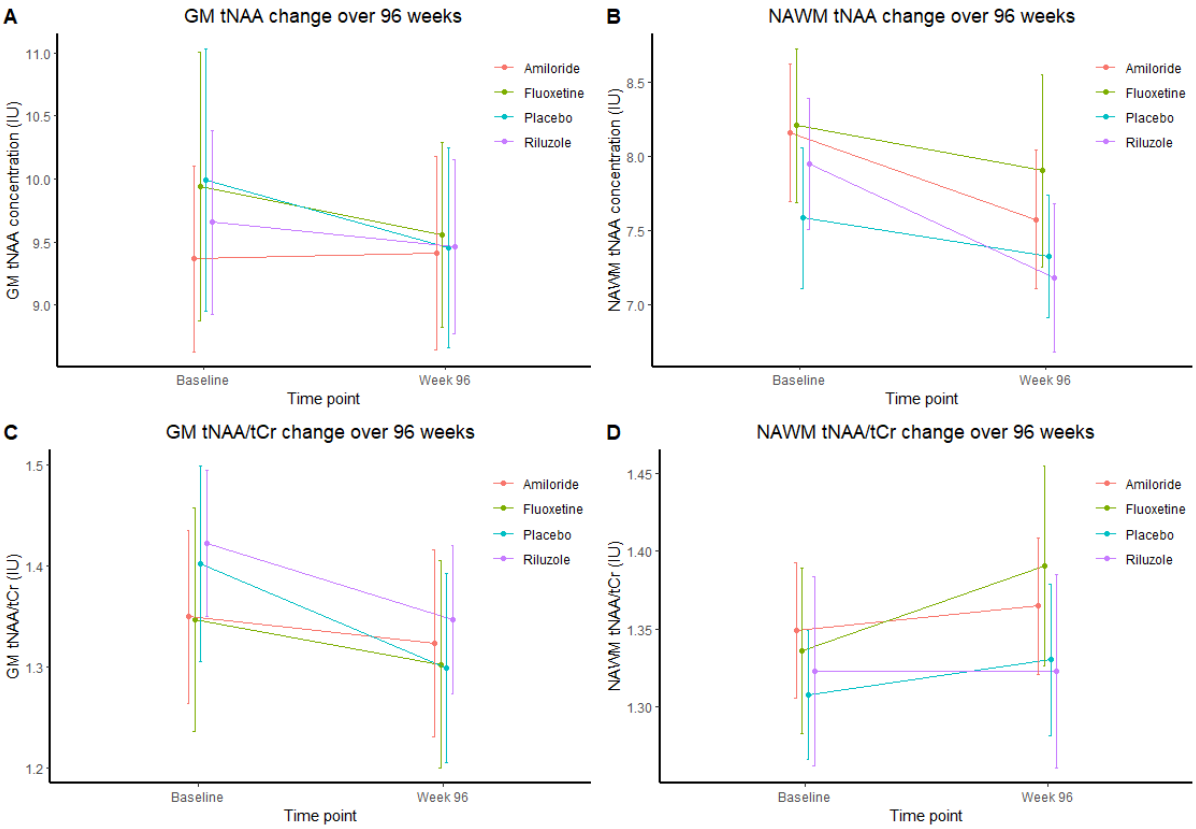

Figure 5-4. tNAA and tNAA/tCr mean change from baseline to 96-weeks

GM = grey matter, IU = institutional units, NAWM = normal appearing white matter, tCr = creatine and phosphocreatine, tNAA = total N-acetyl aspartate + N-acetyl aspartyl glutamate,

The left-sided panels A & C show the change in grey matter total N-acetyl aspartate (tNAA) and tNAA/tCr over 96-weeks stratified by treatment allocation whilst the right-sided panels B & D show the change in tNAA and tNAA/tCr over 96-weeks in normal appearing white matter with 95% confidence intervals.

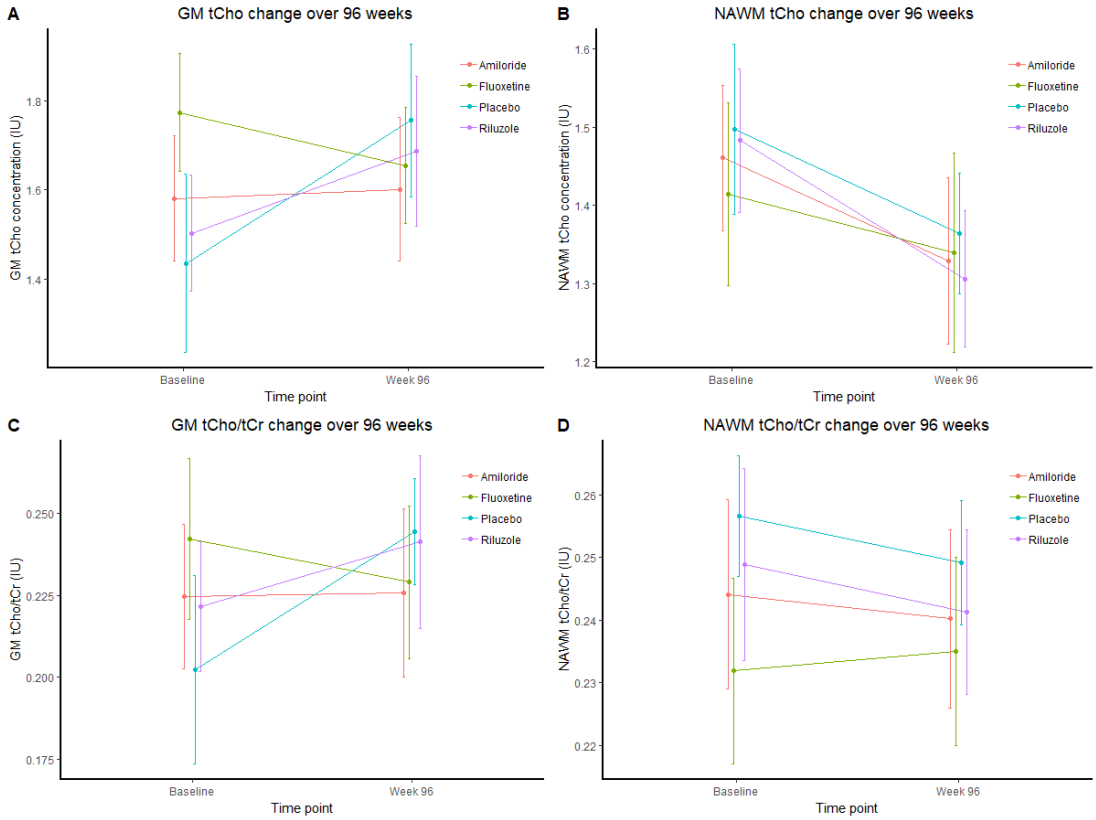

Figure 5-5. tCho and tCho/tCr mean change from baseline to 96-weeks

GM = grey matter, IU = institutional units, NAWM = normal appearing white matter, tCho = glycerophosphocholine and phosphocholine, tCr = creatine and phosphocreatine

The left-sided panels A & C show the change in grey matter total choline (tCho) and tCho/tCr over 96-weeks stratified by treatment allocation whilst the right-sided panels B & D show the change in tCho and tCho/tCr over 96-weeks in normal appearing white matter with 95% confidence intervals.

5.3.3 Associations between metabolites and clinical measures

In NAWM, baseline tNAA (β = 0.22, 95% CI [0.02-0.41], p = 0.03) and tNAA/tCr (β = 0.23, 95% CI [0.5-0.42], p = 0.02) were associated with week-96 9HPT scores after adjusting for model covariates (see

Table 5-5. Association between baseline tNAA in NAWM and week-96 nine-hole per test (preliminary model)

Predictors	*Standardised Beta*	*95% CI*	*p*
Baseline NAWM tNAA	0.25	0.06 – 0.44	**0.01**
Fluoxetine	-0.14	-0.37 – 0.09	0.24
Riluzole	-0.10	-0.32 – 0.13	0.41
Amiloride	-0.00	-0.24 – 0.23	0.97

Predictors	*Standardised Beta*	*95% CI*	*p*
Observations = 107[+]			

NAWM = normal appearing white matter, tNAA = N-acetyl aspartate and N-acetyl aspartyl glutamate

Model covariates = trial arm

[+]One participant missing as they did not complete the nine-hole peg test at 96-weeks

Table 5-6. Association between baseline tNAA/tCr in NAWM and week-96 nine-hole peg test (preliminary model)

Predictors	*Standardised Beta*	*95% CI*	*p*
Baseline NAWM tNAA/tcr	0.26	0.07 – 0.45	**0.008**
Fluoxetine	-0.10	-0.33 – 0.12	0.37
Riluzole	-0.07	-0.30 – 0.15	0.54
Amiloride	0.02	-0.21 – 0.25	0.89
Observations = 107[+]			

NAWM = normal appearing white matter, tCr = total creatine, tNAA = N-acetyl aspartate and N-acetyl aspartyl glutamate

Model covariates = trial arm

[+]One participant missing as they did not complete the nine-hole peg test at 96-weeks

and [+]One participant missing as they did not complete the nine-hole peg test at 96-weeks

; also

Table 5-9. Association between baseline tNAA in NAWM and change in nine-hole peg test over 96 weeks

Predictors	*Standardised Beta*	*95% CI*	*p*
Baseline tNAA	-0.01	-0.11 – 0.09	0.86
Baseline 9HPT score	0.88	0.79 – 0.98	**<0.001**
N = 107			
R^2 = 0.79			

9HPT = 9-hole peg test, CI = confidence interval, NAWM = normal appearing white matter, tNAA = N-acetyl aspartate and N-acetyl aspartyl glutamate

*Other non-significant covariates not shown in table.

**+One participant missing as they did not complete the nine-hole peg test at 96 week

Table 5-10. Association between baseline tNAA/tCr in NAWM and change in nine-hole peg test over 96 weeks

Predictors	*Standardised Beta*	*95% CI*	*p*
Baseline tNAA	-0.00	-0.10 – 0.09	0.93
Baseline 9HPT score	0.00	-0.26 – 0.27	0.97
N = 107			
R^2 = 0.79			

9HPT = 9-hole peg test, CI = confidence interval, NAWM = normal appearing white matter, tNAA = N-acetyl aspartate and N-acetyl aspartyl glutamate, tCr = creatine and phosphocreatine

*Other non-significant covariates not shown in table

**+One participant missing as they did not complete the nine-hole peg test at 96 week

and **Error! Reference source not found.**). Neither baseline tNAA nor tNAA/tCr in NAWM were associated with the change in 9HPT scores over 96-weeks (Table 5-9 & Table 5-10). There was no significant association between PASAT3 scores at 96-weeks and tNAA, tNAA/tCr or mIns/tCr in NAWM (

Table 5-9. Association between baseline tNAA in NAWM and change in nine-hole peg test over 96 weeks

Predictors	*Standardised Beta*	*95% CI*	*p*
Baseline tNAA	-0.01	-0.11 – 0.09	0.86
Baseline 9HPT score	0.88	0.79 – 0.98	**<0.001**
N = 107			
R^2 = 0.79			

9HPT = 9-hole peg test, CI = confidence interval, NAWM = normal appearing white matter, tNAA = N-acetyl aspartate and N-acetyl aspartyl glutamate

*Other non-significant covariates not shown in table.

**+One participant missing as they did not complete the nine-hole peg test at 96 week

Table 5-10. Association between baseline tNAA/tCr in NAWM and change in nine-hole peg test over 96 weeks

Predictors	*Standardised Beta*	*95% CI*	*p*
Baseline tNAA	-0.00	-0.10 – 0.09	0.93
Baseline 9HPT score	0.00	-0.26 – 0.27	0.97
N = 107			
R^2 = 0.79			

9HPT = 9-hole peg test, CI = confidence interval, NAWM = normal appearing white matter, tNAA = N-acetyl aspartate and N-acetyl aspartyl glutamate, tCr = creatine and phosphocreatine

*Other non-significant covariates not shown in table

**+One participant missing as they did not complete the nine-hole peg test at 96 week

-

Table 5-13).

In the GM, there was no association between baseline tCho and PASAT3 scores (Table 5-14).

In the post-hoc exploratory analysis using non-linear approaches to regression, when the metabolite was included using a polynomial (quadratic function), none of the metabolites had an association with the 96-clinical outcome measure suggesting that polynomial functions were not a good fit for these relationships. The metabolite associations between tNAA, tNAA/tCr and 96-week 9HPT remained when adding the metabolite as a log function. However, no additional variation was explained by doing this as the model R^2, adjusted R^2 and standard error were very similar when using a log function or using the linear regression. These results are shown in Table 5-15 to Table 5-18. Results for the quadratic and log functions are shown as scatter plots suggested that these functions may result in a better fit. Higher polynomial e.g. cubic functions were checked with none being significant; nor explaining any additional variation.

Table 5-5. Association between baseline tNAA in NAWM and week-96 nine-hole per test (preliminary model)

Predictors	***Standardised Beta***	***95% CI***	***p***
Baseline NAWM tNAA	0.25	0.06 – 0.44	**0.01**
Fluoxetine	-0.14	-0.37 – 0.09	0.24
Riluzole	-0.10	-0.32 – 0.13	0.41
Amiloride	-0.00	-0.24 – 0.23	0.97
Observations = 107[+]			

NAWM = normal appearing white matter, tNAA = N-acetyl aspartate and N-acetyl aspartyl glutamate

Model covariates = trial arm

[+]One participant missing as they did not complete the nine-hole peg test at 96-weeks

Table 5-6. Association between baseline tNAA/tCr in NAWM and week-96 nine-hole peg test (preliminary model)

Predictors	*Standardised Beta*	*95% CI*	*p*
Baseline NAWM tNAA/tcr	0.26	0.07 – 0.45	**0.008**
Fluoxetine	-0.10	-0.33 – 0.12	0.37
Riluzole	-0.07	-0.30 – 0.15	0.54
Amiloride	0.02	-0.21 – 0.25	0.89
Observations = 107[+]			

NAWM = normal appearing white matter, tCr = total creatine, tNAA = N-acetyl aspartate and N-acetyl aspartyl glutamate

Model covariates = trial arm

[+]One participant missing as they did not complete the nine-hole peg test at 96-weeks

Table 5-7. Regression analysis examining the association between baseline tNAA in normal appearing white matter and week-96 nine-hole peg test (full model)

Predictors	*Standardised Beta*	*95% CI*	*p*
Baseline tNAA	0.22	0.02 – 0.41	**0.03**
Age	0.15	-0.05 – 0.35	0.14
Gender	0.07	-0.14 – 0.29	0.51
Previous relapses	-0.08	-0.27 – 0.10	0.38
Duration from MS onset	-0.06	-0.27 – 0.15	0.56
Baseline T2 lesion volume	-0.02	-0.22 – 0.18	0.84
Baseline NBV	0.24	0.01 – 0.47	**0.04**
N = 107[+]			
R^2 = 0.18			

CI = confidence interval, NAWM = normal appearing white matter, NBV = normalised brain volume, tCr = creatine and phosphocreatine, tNAA = N-acetyl aspartate and N-acetyl aspartyl glutamate

Model covariates: Age, gender, T2 lesion volume, trial arm, occurrence of relapse in two years preceding randomisation. Trial arm was not found to be a significant variable in this multiple regression model and so is not shown.

[+]One participant missing as they did not complete the nine-hole peg test at 96-weeks

Table 5-8. Regression analysis examining the association between baseline tNAA/tCr in normal appearing white matter and week-96 nine-hole peg test (full model)

Predictors	*Standardised Beta*	*95% CI*	*p*
Baseline tNAA/tCr	0.23	0.05 – 0.42	**0.02**
Age	0.16	-0.04 – 0.35	0.13
Gender	0.08	-0.14 – 0.29	0.50
Previous relapses	-0.08	-0.27 – 0.10	0.39
Duration from MS onset	-0.05	-0.25 – 0.16	0.66
Baseline T2LV	-0.02	-0.22 – 0.18	0.83
Baseline NBV	0.24	0.01 – 0.47	**0.04**
N = 107[+]			
R^2 = 0.19			

CI = confidence interval, NAWM = normal appearing white matter, NBV = normalised brain volume, tCr = creatine and phosphocreatine, tNAA = N-acetyl aspartate and N-acetyl aspartyl glutamate, T2LV = T2 lesion volume

Model covariates: Age, gender, T2 lesion volume, trial arm, occurrence of relapse in two years preceding randomisation. Trial arm was not found to be a significant variable in this multiple regression model and so is not shown.

[+]One participant missing as they did not complete the nine-hole peg test at 96 week

Table 5-9. Association between baseline tNAA in NAWM and change in nine-hole peg test over 96 weeks

Predictors	*Standardised Beta*	*95% CI*	*p*
Baseline tNAA	-0.01	-0.11 – 0.09	0.86
Baseline 9HPT score	0.88	0.79 – 0.98	**<0.001**
N = 107			
R^2 = 0.79			

9HPT = 9-hole peg test, CI = confidence interval, NAWM = normal appearing white matter, tNAA = N-acetyl aspartate and N-acetyl aspartyl glutamate

*Other non-significant covariates not shown in table.

**+One participant missing as they did not complete the nine-hole peg test at 96 week

Table 5-10. Association between baseline tNAA/tCr in NAWM and change in nine-hole peg test over 96 weeks

Predictors	*Standardised Beta*	*95% CI*	*p*
Baseline tNAA	-0.00	-0.10 – 0.09	0.93
Baseline 9HPT score	0.00	-0.26 – 0.27	0.97
N = 107			
R^2 = 0.79			

9HPT = 9-hole peg test, CI = confidence interval, NAWM = normal appearing white matter, tNAA = N-acetyl aspartate and N-acetyl aspartyl glutamate, tCr = creatine and phosphocreatine

*Other non-significant covariates not shown in table

**+One participant missing as they did not complete the nine-hole peg test at 96 week

Table 5-11. Association between baseline tNAA in NAWM and week-96 PASAT3 scores

Predictors	*Standardised Beta*	*95% CI*	*p*
Baseline tNAA	0.14	-0.05 – 0.33	0.16
Fluoxetine	-0.33	-0.56 – -0.10	**0.005**
Riluzole	-0.28	-0.51 – -0.06	**0.02**
Amiloride	-0.10	-0.33 – 0.13	0.39
Observations = 106*			

NAWM = normal appearing white matter, PASAT3 = Paced auditory serial addition test, tNAA = N-acetyl aspartate and N-acetyl aspartyl glutamate

Model covariates = trial arm

* Two participants missing as they did not complete the PASAT3 at 96-weeks

Table 5-12. Association between baseline tNAA/tCr in NAWM and week-96 PASAT3 scores

Predictors	*Standardised Beta*	*95% CI*	*p*
Baseline tNAA/tCr	0.07	-0.11 – 0.26	0.45
Fluoxetine	-0.30	-0.53 – -0.08	**0.009**
Riluzole	-0.26	-0.49 – -0.04	**0.02**
Amiloride	-0.08	-0.31 – 0.15	0.50
Observations = 106*			

NAWM = normal appearing white matter, PASAT3 = Paced auditory serial addition test, tCr = total creatine, tNAA = N-acetyl aspartate and N-acetyl aspartyl glutamate

Model covariates = trial arm

* Two participants missing as they did not complete the PASAT3 at 96-weeks

Table 5-13. Association between baseline mIns/tCr in NAWM and week-96 PASAT3 scores

Predictors	*Standardised Beta*	*95% CI*	*p*
Baseline mIns/tCr	-0.09	-0.28 – 0.10	0.35
Fluoxetine	-0.31	-0.54 – -0.08	**0.008**
Riluzole	-0.26	-0.49 – -0.04	**0.02**
Amiloride	-0.08	-0.31 – 0.15	0.50
Observations = 106*			

mIns = myoinositol, NAWM = normal appearing white matter, PASAT3 = Paced auditory serial addition test, tCr = creatine and phosphocreatine

Model covariates = trial arm

* Two participants missing as they did not complete the PASAT3 at 96-weeks

Table 5-14. Association between baseline tCho in GM and week-96 PASAT3 scores

Predictors	*Standardised Beta*	*95% CI*	*p*
Baseline GM tCho	-0.13	-0.32 – 0.07	0.21
Fluoxetine	-0.62	-1.18 – -0.06	**0.03**
Riluzole	-0.54	-1.08 – 0.01	0.05
Amiloride	-0.11	-0.62 – 0.40	0.66
Observations = 106*			

GM = grey matter, PASAT3 = Paced auditory serial addition test, tCho = total choline

* Two participants missing as they did not complete the PASAT3 at 96-weeks

Table 5-15. Quadratic regression between baseline tNAA in NAWM and nine-hole peg test at 96 weeks

Predictors	**Standardised Beta**	**95 % CI**	**p**
Baseline tNAA	0.21	0.01 – 0.41	0.73

(Baseline tNAA)^2	-0.00	-0.10 – 0.10	0.98
Baseline NBV	0.24	0.00 – 0.47	**0.05**
Observations	107		
R^2	0.171		

NBV = normalised brain volume, tNAA = N-acetyl aspartate and N-acetyl aspartyl glutamate

*Non significant covariates not shown in table.

Table 5-16. Regression between logarithm of baseline tNAA in NAWM and nine-hole peg test at 96 weeks

Predictors	Standardised Beta	95% CI	p
Log (Baseline tNAA)	0.80	-0.02 – 1.63	**0.04**
Observations	107		
R^2	0.169		

tNAA = N-acetyl aspartate and N-acetyl aspartyl glutamate

*Non significant covariates not shown in table.

Table 5-17. Quadratic regression between baseline tNAA/tCr in NAWM and nine-hole peg test at 96 weeks

Predictors	Standardised Beta	95% CI	p
Baseline tNAA/tCr	0.25	0.06 – 0.44	0.19
(Baseline tNAA/tCr)^2	-0.09	-0.24 – 0.06	0.24
Baseline NBV	0.26	0.02 – 0.49	**0.03**
Observations	107		
R^2	0.195		

NBV = normalised brain volume, tNAA = N-acetyl aspartate and N-acetyl aspartyl glutamate, tCr = creatine and phosphocreatine

*Non significant covariates not shown in table.

Table 5-18. Regression between logarithm baseline tNAA/tCr in NAWM and nine-hole peg test at 96 weeks

Predictors	Standardised Beta	95% CI	p
log(Baseline tNAA/tCr)	0.75	0.20 – 1.29	**0.01**
Baseline NBV	0.25	0.02 – 0.48	**0.04**
Observations	107		
R^2	0.186		

NBV = normalised brain volume, tNAA = N-acetyl aspartate and N-acetyl aspartyl glutamate, tCr = creatine and phosphocreatine

*Non significant covariates not shown in table.

5.4 Discussion

Highlighting the natural history of metabolite changes in SPMS, I have shown an increase in GM tCho and a decrease in NAWM tCho over 96-weeks. Fluoxetine was shown to only reduce mIns/tCr levels, riluzole indeed reduced the Glx level, whilst amiloride had no effect on tNAA. Baseline tNAA and tNAA/tCr levels in NAWM are associated with decreased performance in upper limb function at 96-weeks.

5.4.1 Natural history of metabolite changes

Previous longitudinal studies of cohorts with PMS have demonstrated mixed findings for individual metabolites acquired from NAWM: some not detecting changes in metabolites (tNAA, Glx, mIns, tCho) over periods ranging 24-30 months (n= 17-18) (De Stefano *et al.*, 1998; Fu *et al.*, 1998), whilst others showed changes in NAA and Glx over 2 years (n= 15-47) (MacMillan *et al.*, 2016; Obert *et al.*, 2016). Accounting for the differing methods used in previous studies, the relative stability of tNAA, mIns and Glx (and their respective ratios to tCr) over 96-weeks could be due to several reasons. First, the presence of a matched control arm may have enabled a more accurate comparison. Second, acute axonal damage may decrease with disease duration of 10 years or more (Kuhlmann *et al.*, 2002). Therefore, changes in neuroaxonal integrity in non-active SPMS may occur over a longer duration than was measured in this study. Third, it is possible that the rate of change within the 96-week study period could be

better characterised by acquiring metabolite levels at additional time points. Last, longitudinal changes in tNAA in SPMS may encompass reductions in axonal density but also compensatory mechanisms to preserve neuro-axonal function. This can lead to partially reversible reductions in tNAA (NAA/tCr) that may explain why tNAA did not decrease in our cohort (Narayana, 2005).

Previous longitudinal studies of NAWM tCho in PMS have shown mixed results with one study showing no change (n=47, median EDSS=6.0) (MacMillan *et al.*, 2016), and another being inconclusive as to whether changes occurred in the RRMS or SPMS subgroup (SPMS=15, median EDSS=4.0) (Obert *et al.*, 2016). The tCho peak comprises free choline, phosphocholine, phosphatidylcholine (a major constituent of cell membranes) and glycerophosphocholine (Miller, 1991). Studies in animal MS models and those correlating in-vivo ^{1}H-MRS with histopathology have demonstrated increased tCho (and tCho/tCr) in acute WML (Nathoo, Yong and Dunn, 2014); with levels greatest in lesions with fibrillary gliosis (Richards *et al.*, 1995; Bitsch *et al.*, 1999). We therefore postulate that the increased tCho level in GM could be due to a combination of increased membrane turnover, fibrillary gliosis, increased cell membranes from glial cell proliferation and remyelination. This may also reflect the role of cortical GM damage mediated by meningeal inflammation in SPMS (Lassmann, 2019). The reduction in NAWM tCho may reflect a reduction in membrane turnover or in cell membranes/myelin. The difficulty in interpretation stems from the fact that the tCho peak contains differing proportions of choline-containing compounds. These compounds are involved in membrane formation, membrane break-down but also reflect membrane levels and therefore disentangling these contributions to the underlying pathology remains an ongoing challenge when using ^{1}H-MRS in MS.

5.4.2 **Effect of drug pathways on metabolites**

Fluoxetine

There was no significant change in tNAA or tNAA/tCr in the fluoxetine treatment arm compared to placebo. This analysed cohort contained 109 participants with SPMS, compared to the previous two pilot studies that demonstrated an increase in NAA/tCr in cerebral white matter (n = 11, RRMS 7/11, SPMS 4/11) (Mostert *et al.*, 2006); and an increase in WML after 2 weeks (n = 15, RRMS 8/15, PMS 8/15) (Sijens *et al.*, 2008). It underscores the combined results of 596 participants from MS-SMART and FLUOX-

PMS that fluoxetine has no therapeutic effect as a neuroprotective agent in non-inflammatory PMS (Cambron *et al.*, 2019; Chataway *et al.*, 2020).

I note that NAWM mIns/tCr levels were reduced by fluoxetine (Table 5-4). Results from the main cohort in MS-SMART showed that fluoxetine reduced new/enlarging lesions and thus there may be some value for examining mIns/tCr in NAWM as a marker of decreased astrogliosis and inflammatory activity in clinical trials of agents examining fluoxetine in inflammatory non-progressive forms of MS (Chataway *et al.*, 2020).

I did not identify any reduction in NAWM or GM tCho (or tCho/tCr) in the fluoxetine arm compared to placebo. Our cohort contained only SPMS whilst the previously suggestive study cohort that demonstrated a reduction in CGM tCho contained 8 with relapsing MS and 7 with PMS. They were treated with fluoxetine for 2 weeks whilst our cohort was treated for 96-weeks.

Glutamate, glutamine and riluzole

GM Glx in the riluzole treatment arm was significantly lower at 96-weeks when compared to placebo (refer Table 5-4), confirming the action of riluzole on glutamate. Evidence for glutamatergic excitotoxicity has been demonstrated in experimental models showing increased release of glutamate into the extracellular space by inflammatory cells, increased glutaminase activity around active WML in progressive forms of MS only, increased glutamatergic transmission in GM and intra-axonal sodium accumulation resulting in reverse operation of the Na^+ dependent glutamate transporters (Werner, Pitt and Raine, 2001; Geurts *et al.*, 2003; Pitt *et al.*, 2003; Sarchielli *et al.*, 2003; Matute, Domercq and Sánchez-Gómez, 2006). Riluzole has been shown to decrease pre-synaptic release of excitatory neurotransmitters including glutamate, increase glutamate uptake by synapses, inactivate voltage-dependent sodium channels; but direct effects of riluzole on glutamatergic NMDA receptors are limited and likely mediated by G-protein dependent processes (Bellingham, 2011).

Previous animal studies that used both acute and chronic PMS models demonstrated that glutamatergic ionotropic receptor antagonism can ameliorate various aspects of disease activity. However, translational studies using glutamatergic receptor antagonists in MS participants have largely been negative and specific studies using

riluzole include a phase II study in early MS that was negative for its primary endpoint in decreasing rates of brain atrophy (Waubant *et al.*, 2014; Macrez *et al.*, 2016). None of these animal or human studies used CSI to measure changes in glutamate concentration.

In this work, riluzole decreased GM Glx by -0.25 standard deviations compared to placebo (Table 5-4) but it did not translate into an effect on decreasing percentage brain volume change. Whilst there is evidence that riluzole reached its target and decreased Glx levels in GM, the failure to translate this into a significant reduction in whole brain atrophy suggests that glutamatergic excitotoxicity may not be a rate-limiting step for disease progression in SPMS. Riluzole also inhibits sodium channels, an effect that leads to a reduction in pre-synaptic glutamate release, therefore the measurement of Glx is an indirect method to assess the effect of sodium channel inhibition by riluzole (Bellingham, 2011). Our data is in keeping with previous clinical trials that did not demonstrate sodium channel blockade to be an effective neuroprotective strategy in PMS (Yang *et al.*, 2015). The additional use of sodium imaging to determine engagement of riluzole with sodium channels in progressive forms of MS would also be of interest.

I found an effect of riluzole on Glx in GM, but not NAWM and this could be due to riluzole having significant impact on GM, a finding indirectly supported by experimental studies that predominantly demonstrated effects of riluzole on ion channels in cortical neurons (Bellingham, 2011). It may also reflect the differing causes of glutamatergic excitotoxicity in GM and NAWM – where riluzole (via its action of decreasing presynaptic neuronal release of glutamate) is unlikely to impact white matter predominant mechanisms such as excess release by macrophages/microglia and dendritic cells (Pampliega *et al.*, 2011; Evonuk *et al.*, 2015; Macrez *et al.*, 2016), increased glutaminase activity in WML and altered expression of glutamatergic receptors on dystrophic axons and oligodendrocytes (Werner, Pitt and Raine, 2001; Geurts *et al.*, 2003; Pitt *et al.*, 2003); whilst riluzole may be more likely to have an effect in GM where excess presynaptic release is the purported mechanism (Macrez *et al.*, 2016).

Amiloride and tNAA

There was no significant difference seen in tNAA or tNAA/tCr (or indeed any other metabolite) between the amiloride and placebo treatment groups (Table 5-4). There are several explanations for why I did not identify a preservation of neuroaxonal integrity compared to placebo. Amiloride and its action on ASIC-1 was previously studied in the acute and chronic-relapsing experimental autoimmune encephalomyelitis models of MS (Vergo *et al.*, 2011). In these models, amiloride exerted its neuroprotective effect on axons when given at disease onset or at the onset of relapse but this is perhaps different from our cohort of non-active progressive SPMS in whom disease progression was driven by various mechanisms leading to neurodegeneration, rather than focal inflammation alone (Vergo *et al.*, 2011). ASIC-1 expression and co-localisation with damaged axons was greatest at the borders of active lesions but its expression in NAWM or CGM was not explored as extensively (Friese *et al.*, 2007; Vergo *et al.*, 2011). It is therefore possible that amiloride may have had a neuroprotective effect on neuroaxonal integrity in lesions. This was not captured in this study as I was unable to examine metabolite values in WML. Future work should aim to study tNAA in WML, using single voxel spectroscopy, higher field strengths or longer acquisitions to allow for the spatial resolution needed to reduce partial volume in lesional voxels.

5.4.3 Associations between metabolites and clinical disability

I therefore confirm our findings from the cross-sectional analysis, that baseline NAWM tNAA/tCr and tNAA is associated with a reduction in arm function 2 years later. The models explain approximately 20% of the variation in 9HPT scores (

Table 5-5. Association between baseline tNAA in NAWM and week-96 nine-hole per test (preliminary model)

Predictors	***Standardised Beta***	***95% CI***	***p***
Baseline NAWM tNAA	0.25	0.06 – 0.44	**0.01**
Fluoxetine	-0.14	-0.37 – 0.09	0.24
Riluzole	-0.10	-0.32 – 0.13	0.41
Amiloride	-0.00	-0.24 – 0.23	0.97
Observations = 107[+]			

NAWM = normal appearing white matter, tNAA = N-acetyl aspartate and N-acetyl aspartyl glutamate

Model covariates = trial arm

[+]One participant missing as they did not complete the nine-hole peg test at 96-weeks

Table 5-6. Association between baseline tNAA/tCr in NAWM and week-96 nine-hole peg test (preliminary model)

Predictors	*Standardised Beta*	*95% CI*	*p*
Baseline NAWM tNAA/tcr	0.26	0.07 – 0.45	**0.008**
Fluoxetine	-0.10	-0.33 – 0.12	0.37
Riluzole	-0.07	-0.30 – 0.15	0.54
Amiloride	0.02	-0.21 – 0.25	0.89
Observations = 107[+]			

NAWM = normal appearing white matter, tCr = total creatine, tNAA = N-acetyl aspartate and N-acetyl aspartyl glutamate

Model covariates = trial arm

[+]One participant missing as they did not complete the nine-hole peg test at 96-weeks

and **Error! Reference source not found.**). I did not examine whether the baseline neuroaxonal integrity was associated with change in 9HPT over 96-weeks.

When holding all other independent variables constant, for every 1-unit increase in tNAA and tNAA/tCr levels, the 9HPT increases (standardised beta 0.22 and 0.23 respectively). With 9HPT being expressed as a reciprocal, the regression output shows that decreased baseline neuroaxonal integrity in NAWM (as reflected by tNAA and tNAA/tCr) results in decreased upper limb function at 96-weeks.

There is only one small (n=15) previous study that has examined the relationship between baseline tNAA and longitudinal upper limb function in a cohort containing only progressive forms of MS, though it did not find a relationship (Obert *et al.*, 2016). Baseline normalised brain volume was also found to have an association with 96-week 9HPT. This was in the expected direction with decreased baseline normalised brain volume associated with decreased upper limb function at 96-weeks. Taken together, baseline measures of neuroaxonal integrity and brain volume are important determinants of upper limb function at 96-weeks.

Baseline neuroaxonal integrity (as reflected by tNAA), was not associated with a change in upper limb function over 96 weeks. This suggests that decreased neuroaxonal integrity and mitochondrial function in NAWM at baseline is associated with existing upper limb dysfunction that has occurred, but not with ongoing deterioration in the secondary progressive phase of MS.

None of the proposed PASAT3/IPS associations remained. This could be for several reasons: first, in the cross-sectional analysis, T2LV demonstrated the strongest association with IPS and the 96-week results further emphasised this, with the metabolites losing significance. Second, the relationship between tNAA, mIns/tCr and tCho may have a region-specific effect that was not analysed in this study. Our findings however, are in keeping with the only previous study that examined this relationship between metabolites, lesion load in NAWM and long-term performance on IPS in progressive forms of MS.

The examination of cognitive outcomes at 5 years in a cohort with primary progressive MS (n = 31, median EDSS = 4.5), showed that baseline T2 lesion load was the only significant predictor of cognitive impairment at 5 years; and that there was no relationship between any of the measured baseline metabolites (Penny *et al.*, 2010).

Non-linear regression did not fit the data better than linear methods. Using complex mathematical functions in non-linear regression can be helpful to model complex relationships and this can be beneficial when the goal is to make accurate predictions of the outcome variable. However, this approach is less useful as p values often cannot be calculated for each covariate and the interpretation of the relationship between each covariate and the outcome/dependent variable can be challenging or not possible depending on the equation used to fit the data.

5.4.4 Study strengths and study limitations

When calculating tissue specific metabolites, 14 participants were removed from the analysis as metabolite outliers and this along with the 26 participants who did not have a 96-week CSI scan will have reduced our power for certain comparisons. Despite this, this study cohort that underwent analysis (n=109) was more than two fold (previous ^{1}H-MRS studies of PMS patients ranged from 15-47) greater in size than other longitudinal studies examining PMS subjects (De Stefano *et al.*, 1998; Fu *et al.*, 1998; Sajja, Narayana and Wolinsky, 2008; MacMillan *et al.*, 2016; Obert *et al.*, 2016).

There are however several caveats – first, Glx measured using CSI cannot differentiate between signal arising from intra- or extracellular Glx. Second, there are technical difficulties in resolving glutamate from glutamine and whilst I demonstrated a reduction in Glx, the magnitude of the specific reduction in glutamate levels could be have been more accurately identified by other ^{1}H-MRS techniques that were not feasible, due to scan time limitations, in this study (Srinivasan *et al.*, 2005).

I used internal water as the internal reference for quantification but there are assumptions made about the water concentration of brain tissue in multiple

sclerosis. No adjustment for T2 relaxation was made beyond that applied by LCModel. For these reasons, I have reported estimated not absolute concentrations.

5.5 Conclusion

Here I report on the largest SPMS cohort to date undergoing longitudinal CSI. Over this 2-year period, there are changes in a marker of membrane turnover in both NAWM (reduced) and GM (increased), but not signatures of a reduction in neuroaxonal integrity or increase in astrogliosis. I confirm the known mechanism of action of riluzole (reducing Glx) but this is insufficient to reduce brain atrophy. No other postulated target mechanisms are confirmed. Lastly, I confirm that baseline NAWM tNAA (and tNAA/tCr) are durable markers of upper limb at 96-weeks, but not IPS. Ultimately, ^{1}H-MRS can provide a valuable tool to examine *in vivo* target engagement in drug trials where there is a clear mechanism of action

Chapter 6. MRI measures of disability progression in secondary progressive multiple sclerosis

6.1 Introduction

Candidate mechanisms that contribute to disease progression in SPMS include neuroinflammation mediated via chronic active lesions and meningeal lymphoid follicles, GM atrophy, axonal and mitochondrial dysfunction, gliosis in NAWM; and chronic demyelination (Kutzelnigg *et al.*, 2005; Mahad, Trapp and Lassmann, 2015; Correale *et al.*, 2017; Lassmann, 2019; Absinta, Lassmann and Trapp, 2020). There is a relative paucity of disease modifying and neuroprotective treatments in this phase of the disease reflecting our incomplete understanding of the pathophysiology.

Conventional structural MRI has greatly increased our understanding of MS, but in clinical practice is largely limited to detecting the development of WML (on T2 or FLAIR sequences). However, T2 lesions are not pathologically specific reflecting various degrees of inflammation, remyelination, gliosis and axonal loss and demonstrate only a modest correlation with clinical disability in PMS (Mostert *et al.*, 2010; Brown and Chard, 2016; Ammitzbøll *et al.*, 2018).

Advanced MRI techniques can be used to measure brain injury thereby providing valuable information on the *in vivo* pathological changes occurring in SPMS. For example, MTR is a marker of myelin with possible contributions from axonal density (Barkhof *et al.*, 2003; Schmierer *et al.*, 2004, 2007; Moccia *et al.*, 2020). Total N-acetyl-aspartate (tNAA) measured using ^{1}H-MRS is a marker of neuroaxonal integrity and mitochondrial function (Bjartmar *et al.*, 2000; Cifelli *et al.*, 2002; Davies *et al.*, 2002; Ciccarelli *et al.*, 2010).

Studies employing these techniques have shown that MTR and tNAA are abnormal in SPMS; and are associated with measures of clinical disability (S. M. Leary *et al.*, 1999; Dehmeshki *et al.*, 2003; Ramió-Torrentà *et al.*, 2006; Khaleeli, Cercignani, *et al.*, 2007; Khaleeli, Sastre-Garriga, *et al.*, 2007; Rovaris *et al.*, 2008; Hayton *et al.*, 2009, 2012; Tur, Khaleeli, *et al.*, 2011; Brown *et al.*, 2020). Regional atrophy occurs at all stages of MS with GM and

SCA being recognised as key drivers of neurodegeneration and disability progression in PMS (Fisniku *et al.*, no date; Stevenson *et al.*, 1998; Rovaris *et al.*, 2006; Fisher *et al.*, 2008; Stankiewicz *et al.*, 2009; Valsasina *et al.*, 2013; Daams *et al.*, 2015; Hugh Kearney *et al.*, 2015; Lukas *et al.*, 2015; Schlaeger *et al.*, 2015; Azevedo *et al.*, 2018; Tsagkas *et al.*, 2018; Eshaghi, Marinescu, *et al.*, 2018; Eshaghi, Prados, *et al.*, 2018). These advanced MRI measures are crucial to improving our understanding of the *in vivo* pathological changes driving disability in SPMS which can then aid in the development of more targeted therapeutic interventions.

As part of the MS-SMART advanced MRI substudy, MRI techniques were employed to measure biomarkers of brain injury at baseline and 96-weeks. These included MRI measures of myelin (MTR), neuroaxonal integrity and mitochondrial function (tNAA), WML load (WM T2LV), regional brain volumes (cortical and deep GM, WM) and cervical cord area (MUCCA).

Whilst there is a clear pathological basis for changes in myelin, axonal integrity, inflammation and regional atrophy in driving disease progression in SPMS, here I investigate which MRI measures of brain and spinal cord injury are most closely associated with physical and cognitive disability measures over 96-weeks in a cohort with non-active progressive SPMS.

The specific research questions are which baseline MRI measures are associated with:

1 Physical disability measures of upper limb (9HPT) and ambulatory function (as reflected by T25FW, EDSS) at 96 weeks
2 Change in physical disability measures (9HPT, T25FW, EDSS) over 96 weeks.
3 Performance on tests of information processing speed (PASAT3, SDMT) at 96-weeks
4 Change in performance on tests of information processing speed (PASAT3, SDMT) over 96-weeks

6.2 Methods

These have been described before in 3.2. Participants underwent a series of clinical assessments at baseline and 96-weeks including EDSS, T25FW, 9HPT and two standard measures of IPS: PASAT3 and SDMT (Kurtzke, 1983; Cutter *et al.*, 1999; Benedict *et al.*, 2017). 9HPT and T25FW were not normally distributed and were expressed as reciprocals, therefore lower values reflect decreased performance on these tests.

Consent was obtained for all participants according to the Declaration of Helsinki and ethical approval for the study was provided by the Scotland A Research Ethics Committee [13/SS/0007].

6.2.1 MRI acquisition and analysis

Acquisition parameters for the CSI and structural MR sequences; and details of MR analysis including brain volume, lesion segmentation, PBVC, spectra post-processing and calculation of tissue specific metabolite levels have been described previously in 3.2.

Magnetisation transfer imaging was acquired using sagittal slice orientation, TE1/TE2/TR 2.7/4.3/6.45 (all in milliseconds), slice thickness 1mm, matrix 256 x 256 and flip angle 9^0. Details of MTR and cervical cord imaging and MUCCA calculation are described in 3.2.

The following baseline MRI measures were obtained for analysis:

1) Mean MTR in brain NAWM, GM and WML
2) tNAA in brain NAWM and GM (institutional units)
3) Brain WM T2 lesion volume (mL)
4) Brain CGM volume, deep GM volume, WM volume (all expressed in mL)
5) Mean upper cervical cord area (mm^2)

6.2.2 **Statistical methodology**

Statistical analysis was completed using R statistical software version 3.5.1.(R Core Team, 2017). All statistical tests and confidence intervals were two-sided. 95% confidence intervals were calculated with the significance of raw p-values assessed based on a 5% significance level. We used a complete-case analysis (after removal of metabolite outliers for tNAA) based on the intention-to-treat population.

There were three steps in the analysis:

A. I examined the univariable relationships between clinical disability measures (EDSS, 9HPT, T25FW, SDMT, PASAT) and MRI measures; also between MRI measures themselves, using Spearman rank correlations.

B. Research questions 1 & 3 were examined using multiple linear regression to investigate the associations between baseline MRI markers and 96-week clinical disability measures. The dependent variable was the clinical disability measure at 96-weeks. The aforementioned baseline MRI measures were included as independent variables.

MUCCA was not included as an independent variable in the models for cognitive performance measures – PASAT3 and SDMT as I postulated that there would no association between a measure of cervical cord area and performance measures of processing speed in SPMS (Furby *et al.*, 2008; Hugh Kearney *et al.*, 2015). Due to multi-collinearity between mean MTR values in GM and NAWM, MTR-NAWM was omitted from the models as MTR in GM has shown stronger associations with physical disability measures such as T25FW in PMS (Khaleeli, Sastre-Garriga, *et al.*, 2007; Tur, Khaleeli, *et al.*, 2011). Furthermore, I postulate that GM MTR may demonstrate a stronger association with cognitive performance measures (Khaleeli, Cercignani, *et al.*, 2007).

Age, sex, disease duration from symptom onset and trial arm allocation were included as covariates. I used a backward stepwise approach to build the regression models using a p value threshold of 0.05. This analysis was competed using the OLSSR package in R (R Core Team, 2017).

C. Research questions 2 & 4 examined the association between baseline MRI measures and change in clinical disability over 96-weeks. The corresponding baseline clinical disability measure was included as an independent variable (covariate) in the model (Cronbach and Furby, 1970). Only those variables that were statistically significant from the initial multiple linear regression models were included. All results are presented as standardised beta coefficients and standardised 95% confidence intervals.

Model diagnostics undertaken to assess the regression model included: calculation of variance inflation factors to determine multi-collinearity; Cook's distance to determine effect of leveraged data points; plots of studentised residuals against adjusted predicted values to residual homoscedasticity and Q-Q plots to assess the normality of residuals.

No correction for multiplicity was made. The correlation coefficients were calculated to visualise cross-sectional relationships between MRI measures. The five multiple linear regression models were based on *a priori* hypotheses and the subsequent regression models examining change in clinical disability measures over 96-weeks were only undertaken if there were significant MRI predictors from the initial models.

6.3 Results

Baseline cohort demographics and characteristics are compatible with those seen in the main MS-SMART study (Table 6-1) (Chataway *et al.*, 2020). 96-week clinical outcome measures were available for 139/154 (90%) of study participants. 15 participants were lost to follow-up and did not undergo EDSS assessment at 96-weeks (Figure 1). Baseline MTR, tNAA levels and MUCCA

values were missing for 18/154 (33%),15/154 (10%) and 12/154 (8%) respectively. Reasons for this were acquisition failure, failing quality assurance or being excluded due to being metabolic outliers during the calculation of tissue specific tNAA levels. There was no missing data for any of the other baseline MRI variables.

Table 6-1. Baseline demographics and characteristics by trial arm

Characteristic	Amiloride, N = 41[1]	Fluoxetine, N = 37[1]	Riluzole, N = 38[1]	Placebo, N = 38[1]	Overall, N = 154[1]
Age (years)	54.44 (7.49)	55.31 (6.99)	54.37 (6.71)	54.00 (7.50)	54.52 (7.14)
Sex					
female	28 / 41 (68%)	26 / 37 (70%)	23 / 38 (61%)	28 / 38 (74%)	105 / 154 (68%)
Disease duration (years)	23.46 (10.06)	22.57 (8.13)	23.97 (9.91)	20.21 (9.30)	22.57 (9.42)
Baseline EDSS[2]	6.0 (4.0 - 6.5)	6.0 (4.0 - 6.5)	6.0 (4.0 - 6.5)	6.0 (4.0 - 6.5)	6.0 (4.0 - 6.5)
9-hole peg test (sec^{-1})	0.03 (0.01)	0.03 (0.01)	0.03 (0.01)	0.03 (0.01)	0.03 (0.01)
Timed 25ft walk (sec^{-1})	23.59 (33.35)	16.88 (15.02)	23.50 (38.92)	21.86 (36.05)	21.53 (32.12)
Baseline PASAT3	42.56 (12.31)	39.42 (13.64)	38.55 (14.99)	44.00 (10.81)	41.18 (13.07)
Baseline SDMT	46.68 (12.52)	45.35 (10.71)	44.68 (11.42)	45.47 (13.40)	45.58 (11.98)
Baseline deep GM volume (mL)	45.13 (4.31)	44.64 (4.21)	44.89 (4.41)	46.18 (4.92)	45.21 (4.46)

Characteristic	Amiloride, N = 41[1]	Fluoxetine, N = 37[1]	Riluzole, N = 38[1]	Placebo, N = 38[1]	Overall, N = 154[1]
Baseline CGM volume (mL)	791.40 (45.56)	787.22 (46.49)	784.64 (40.41)	798.12 (48.94)	790.39 (45.29)
Baseline WM volume (mL)	571.50 (44.61)	572.32 (39.04)	574.88 (46.68)	588.02 (48.70)	576.61 (44.99)
Baseline cord area (mm^2)	67.78 (7.60)	70.39 (9.59)	68.53 (9.94)	67.53 (9.98)	68.53 (9.28)
Baseline T2LV (mL)	11.89 (9.33)	13.78 (8.74)	14.19 (10.57)	10.95 (9.85)	12.68 (9.64)
Baseline WML MTR	24.77 (4.84)	23.57 (4.97)	24.60 (4.91)	24.50 (3.85)	24.38 (4.64)
Baseline NAWM MTR	36.48 (3.59)	35.97 (3.25)	36.38 (2.71)	36.27 (2.71)	36.28 (3.05)
Baseline GM MTR	29.81 (3.84)	29.03 (3.54)	29.50 (2.88)	29.55 (2.81)	29.48 (3.26)
Baseline NAWM tNAA (IU)	8.27 (1.25)	8.23 (1.30)	8.11 (1.01)	7.45 (1.22)	8.01 (1.23)

Characteristic	Amiloride, N = 41[1]	Fluoxetine, N = 37[1]	Riluzole, N = 38[1]	Placebo, N = 38[1]	Overall, N = 154[1]
Baseline GM tNAA (IU)	9.21 (1.99)	9.59 (2.53)	9.47 (1.93)	10.12 (2.78)	9.59 (2.32)

[1] Statistics presented: Mean (SD); n / N (%) *[2]EDSS presented as median (range). Overall (n = 154) represents total number of participants involved in MS-SMART UCL MRI substudy*

CGM = cortical grey matter, EDSS = expanded disability status scale, GM = grey matter, IU = instutitional units, MTR = magnetisation transfer ratio PASAT3 = paced auditory serial addition test, SDMT = symbol digit modalities test, WM = white matter, WML = white matter lesion

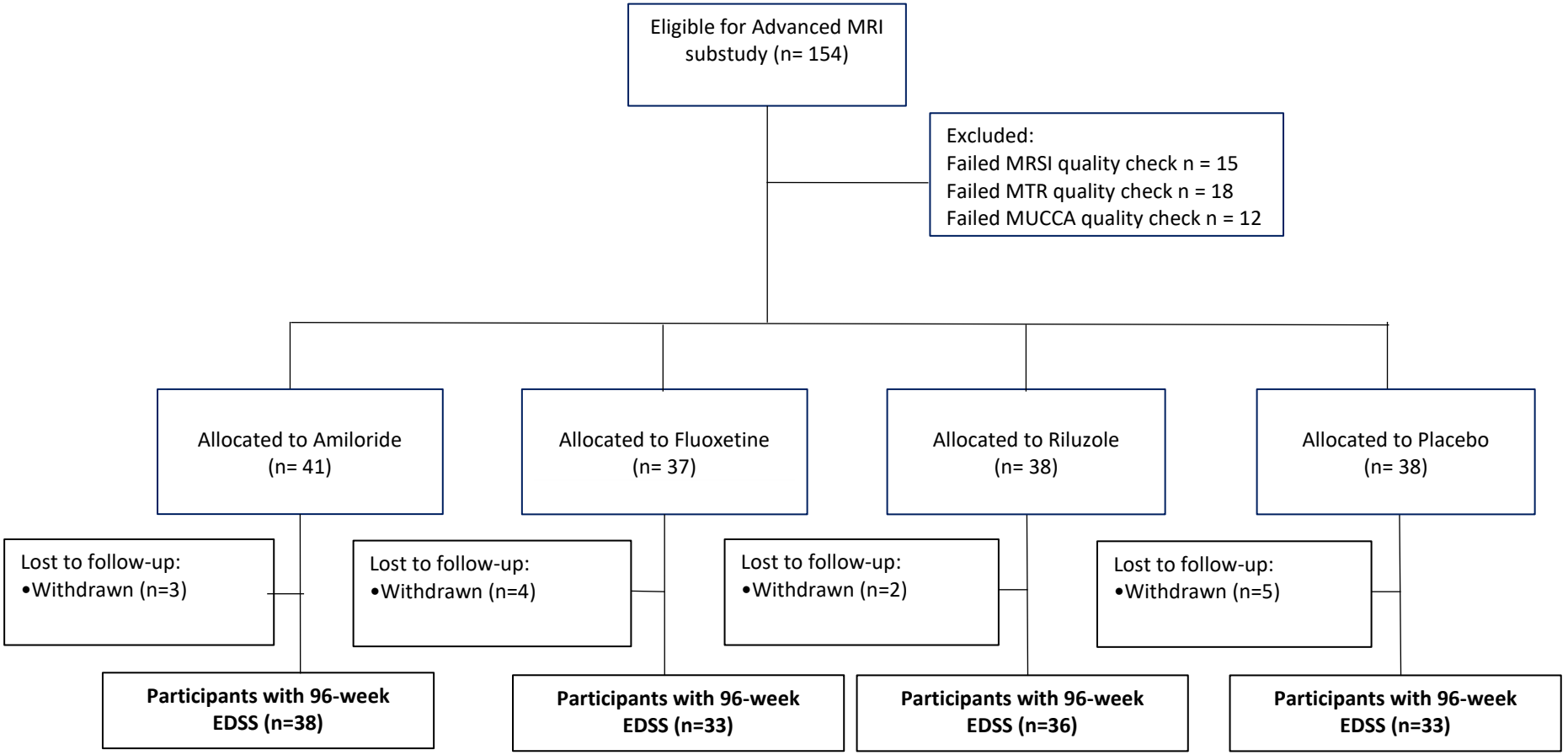

Figure 6-1. Study flow

Table 6-2. Spearman rank correlation coefficients for associations between baseline MRI measures and clinical disability measures at 96-weeks

	EDSS 96wks	T25FW 96wks	9HPT 96wks	PASAT3 96wks	SDMT 96wks	Baseline DGM vol	Baseline CGM vol	Baseline WM vol	Baseline T2LV	Baseline MUCCA	Baseline NAWM MTR	Baseline GM MTR	Baseline WML MTR	Baseline GM tNAA	Baseline NAWM tNAA
EDSS 96wks	1.00														
T25FW 96wks	**-0.81**	1.00													
9HPT 96wks	**-0.49**	**0.47**	1.00												
PASAT3 96wks	**-0.25**	**0.27**	**0.26**	1.00											
SDMT 96wks	**-0.34**	**0.29**	**0.51**	**0.59**	1.00										
Baseline DGM vol	-0.13	0.13	**0.34**	**0.29**	**0.44**	1.00									
Baseline CGM vol	-0.14	0.13	**0.26**	0.06	**0.24**	**0.62**	1.00								
Baseline WM vol	-0.16	**0.17**	**0.33**	**0.23**	**0.40**	**0.79**	**0.72**	1.00							
Baseline T2LV	**0.29**	**-0.27**	**-0.30**	**-0.46**	**-0.61**	**-0.54**	**-0.32**	**-0.45**	1.00						
Baseline MUCCA	**-0.38**	**0.28**	**0.47**	0.11	**0.23**	0.15	0.06	0.16	**-0.21**	1.00					
Baseline NAWM MTR	0.06	-0.13	0.02	0.14	0.07	-0.12	**-0.30**	-0.11	0.03	0.01	1.00				
Baseline GM MTR	0.03	-0.09	0.06	**0.18**	0.10	-0.07	**-0.25**	-0.04	-0.02	0.03	0.98	1.00			
Baseline WML MTR	-0.05	-0.02	**0.19**	**0.30**	**0.40**	0.23	-0.05	**0.21**	**-0.37**	0.05	**0.58**	**0.61**	1.00		
Baseline GM tNAA	-0.10	0.06	0.00	-0.04	-0.04	0.10	0.06	0.05	**-0.17**	0.05	0.00	0.00	0.06	1.00	
Baseline NAWM tNAA	0.01	-0.05	**0.23**	0.17	**0.20**	0.07	0.13	0.10	-0.07	0.09	-0.04	-0.05	0.04	**-0.34**	1.00

*Statistically significant correlation coefficients highlighted in bold

9HPT = 9-hole peg test, CGM = cortical grey matter, DGM = deep grey matter, EDSS = Expanded disability status scale, MTR = magnetisation transfer ratio, MUCCA = mean upper cervical cord area, NAWM = normal appearing white matter, PASAT3 = paced auditory serial addition test, SDMT = symbol digit modalities test, tNAA = total N-acetyl aspartate, T2LV = T2 lesion volume, T25FW = Timed 25 ft walk, Wks = weeks, WM = white matter

6.3.1 Univariable correlations

Statistically significant correlations between MRI features and clinical disability measures; and between MRI measures are shown above in Table 6-2.

6.3.2 Associations between baseline MRI measures and physical disability at 96 weeks (research question 1)

Baseline NAWM tNAA (β = 0.16, 95% CI [0.01 – 0.31], p = 0.04), CGM volume (β = 0.33, 95% CI [0.17 – 0.48], p < 0.001), and MUCCA (β = 0.39, 95% CI [0.24 – 0.54], p < 0.001) were associated with 9HPT at 96-weeks (**Error! Reference source not found.**).

Table 6-3. Association between baseline MRI measures and week-96 nine-hole peg test

Predictors	Standardised beta	standardized CI	p
Baseline NAWM tNAA (IU)	0.16	0.01 – 0.31	**0.04**
Baseline CGM volume (mL)	0.33	0.17 – 0.48	**<0.001**
Baseline MUCCA (mm^2)	0.39	0.24 – 0.54	**<0.001**
Observations	122		
R^2 / R^2 adjusted	0.32 / 0.30		

CGM = cortical grey matter, IU = institutional units, MUCCA = mean upper cervical cord area, NAWM = normal appearing white matter, tNAA = total N-acetyl aspartate + N-acetyl aspartyl glutamate

Baseline CGM (β = 0.25, 95% CI [0.06 – 0.44], p = 0.01), T2LV (β = -0.17, 95% CI [-0.17 – 0.00], p = 0.05) and MUCCA (β = 0.24, 95% CI [0.08 – 0.40], p < 0.01) were the MRI measures associated with T25FW at 96-weeks (Table 6-4).

Table 6-4. The association between baseline MRI measures and timed 25ft walk test at 96-weeks

Predictors	Standardised beta	Standardized CI	p
Baseline CGM volume (mL)	0.25	0.06 – 0.44	**0.01**
Baseline T2LV (mL)	-0.17	-0.34 – -0.00	**0.05**

Sex: female		-0.48	-0.85 – -0.10	**0.01**
Baseline MUCCA (mm^2)		0.24	0.08 – 0.40	**0.004**
Age		-0.17	-0.32 – -0.01	**0.04**
Observations	130			
R^2 / R^2 adjusted	0.23 / 0.19			

CGM = cortical grey matter, MUCCA = mean upper cervical cord area, T2LV = T2 lesion volume

Baseline MUCCA (β = -0.33, 95% CI [-0.49 to -0.17], p < 0.001) and CGM volume (β = -0.31, 95% CI [-0.49 to -0.12], p < 0.01) were the MR measures associated with EDSS scores at 96-weeks (

Table 6-5).

Table 6-5. The association between baseline MRI measures and week-96 Expanded Disability Status Scale

Predictors	Standardised beta	Standardized CI	p
Baseline MUCCA (mm^2)	-0.33	-0.49 – -0.17	**<0.001**
Baseline CGM volume (mL)	-0.31	-0.49 – -0.12	**0.001**
Sex: female	0.44	0.06 – 0.82	**0.02**
Observations	131		
R^2 / R^2 adjusted	0.20 / 0.19		

CGM = cortical grey matter, MUCCA = mean upper cervical cord area

6.3.3 Associations between baseline MRI measures and change in physical disability measures over 96 weeks (research question 2)

Baseline MUCCA (β = 0.12, 95% CI [0.04 – 0.21], p < 0.01) remained the only MRI variable associated with the change in 9HPT over 96-weeks (Table 6-6).

Table 6-6. The association between baseline MRI measures and change in 9-hole peg test over 96-weeks

Predictors	Standardised beta	standardized CI	p
9-hole peg test (sec-1)	0.83	0.74 – 0.92	**<0.001**
Baseline NAWM tNAA (IU)	-0.02	-0.10 – 0.06	0.63
MUCCA (mm^2)	0.12	0.04 – 0.21	**0.004**
Baseline CGM volume (mL)	0.07	-0.01 – 0.15	0.11
Observations	122		

R^2 / R^2 adjusted	0.82 / 0.81

CGM = cortical grey matter, IU = institutional units, MUCCA = mean upper cervical cord area, NAWM = normal appearing white matter, tNAA = total N-acetyl aspartate + N-acetyl aspartyl glutamate

Baseline MUCCA (β = 0.16, 95% CI [0.06 – 0.26], p < 0.001) being the only MRI variable associated with change in T25FW over 96-weeks (

).

Table 6-7. The association between baseline MRI measures and change in timed 25ft walk test over 96-weeks

Predictors	Standardised beta	Standardized CI	p
Baseline T2LV (mL)	-0.06	-0.16 – 0.04	0.26
Baseline CGM volume (mL)	-0.03	-0.15 – 0.09	0.66
Baseline MUCCA (mm^2)	0.16	0.06 – 0.26	**0.002**
Age (years)	-0.02	-0.12 – 0.08	0.63
Sex: female	0.12	-0.13 – 0.37	0.34
Baseline T25FW (sec^{-1})	0.79	0.68 – 0.90	**<0.001**
Observations	130		
R^2 / R^2 adjusted	0.71 / 0.69		

CGM = cortical grey matter, MUCCA = mean upper cervical cord area, T2LV = T2 lesion volume

Baseline MUCCA (β = -0.15, 95% CI [-0.27 to -0.04], p = 0.01) was the only independent MRI variable associated with change in EDSS scores over 96-weeks (Table 6-8).

Table 6-8. The association between baseline MRI measures and change in Expanded Disability Status Scale over 96-weeks

Predictors	Standardised beta	Standardized CI	p
Baseline EDSS	0.72	0.60 – 0.85	**<0.001**
Baseline MUCCA (mm^2)	-0.15	-0.27 – -0.04	**0.01**
Baseline CGM volume (mL)	-0.07	-0.20 – 0.06	0.31
Sex: female	-0.14	-0.42 – 0.14	0.32
Observations	131		
R^2 / R^2 adjusted	0.62 / 0.60		

CGM = cortical grey matter, EDSS = Expanded Disability Status Scale, MUCCA = mean upper cervical cord area

6.3.4 Associations between baseline MRI measures and performance measures of information processing speed at 96 weeks (research question 3)

Baseline NAWM tNAA (β = 0.24, 95% CI [0.10 – 0.38], p < 0.01), T2LV (β = -0.45, 95% CI [-0.62 to -0.29], p < 0.001), mean MTR in WML (β = 0.20, 95% CI [0.05 – 0.35], p = 0.01) and deep GM volume (β = 0.17, 95% CI [0.01 – 0.32], p = 0.03) were associated with SDMT scores at 96-weeks.

Table 6-9. The association between baseline MRI measures and symbol digit modalities test scores at 96-weeks

Predictors	Standardised beta	standardized CI	p
Baseline NAWM tNAA (IU)	0.24	0.10 – 0.38	**0.001**
Baseline T2LV (mL)	-0.45	-0.62 – -0.29	**<0.001**
Baseline WML MTR	0.20	0.05 – 0.35	**0.01**
Baseline deep GM volume (mL)	0.17	0.01 – 0.32	**0.03**
Observations	111		
R^2 / R^2 adjusted	0.49 / 0.48		

GM = grey matter, MTR = magnetisation transfer ratio, NAWM = normal appearing white matter, tNAA = total N-acetyl aspartate + N-acetyl aspartyl glutamate, T2LV = T2 lesion volume, WML = white matter lesion

6.3.5 96-week PASAT3 scores underwent cubic transformation to address residual heteroscedasticity. Baseline NAWM tNAA (β = 0.23, 95% CI [0.07 – 0.39], p < 0.01), T2LV (β = -0.26, 95% CI [-0.44 to –0.07], p < 0.01) and deep GM volume (β = 0.22, 95% CI [0.03 – 0.41], p = 0.41) were the MRI measures associated with PASAT3 scores at 96-weeks (Associations between baseline MRI measures and change in performance on measures of information processing speed over 96 weeks (research question 4)

Baseline NAWM tNAA (β = 0.13, 95% CI [0.04 – 0.22], p = < 0.01) and T2LV (β = -0.23, 95% CI [-0.35 to -0.11], p < 0.001) were the only MRI

measures that showed significant associations with change in SDMT scores over 96-weeks (Table 6-9 and

).

Table 6-11. The association between baseline MRI measures and change in symbol digit modalities test scores over 96-weeks

Predictors	Standardised beta	standardized CI	p
Baseline SDMT	0.65	0.54 – 0.77	**<0.001**
Baseline NAWM tNAA (IU)	0.13	0.04 – 0.22	**0.007**
Baseline WML MTR	0.07	-0.03 – 0.17	0.17
Baseline T2LV (mL)	-0.23	-0.35 – -0.11	**<0.001**
Baseline deep GM volume (mL)	0.05	-0.06 – 0.15	0.37
Observations	111		
R^2 / R^2 adjusted	0.78 / 0.76		

GM = grey matter, MTR = magnetisation transfer ratio, NAWM = normal appearing white matter, tNAA = total N-acetyl aspartate + N-acetyl aspartyl glutamate, T2LV = T2 lesion volume, WML = white matter lesion

When assessing change in PASAT3 scores over 96-weeks, fluoxetine (β = -0.43, 95% CI [-0.073 to -0.13], $p < 0.01$) remained the only significant variable (Table 6-12).

).

Table 6-10. The association between baseline MRI measures and PASAT3 scores at 96-weeks

Predictors	Standardised beta	standardized CI	p
Baseline NAWM tNAA (IU)	0.23	0.07 – 0.39	**0.005**
Baseline T2LV (mL)	-0.26	-0.44 – -0.07	**0.007**
Sex: female	-0.53	-0.87 – -0.18	**0.003**
Trial arm: Amiloride	-0.23	-0.69 – 0.22	0.31
Trial arm: Fluoxetine	-0.66	-1.13 – -0.20	**0.006**
Trial arm: Riluzole	-0.48	-0.94 – -0.02	**0.04**
Baseline deep GM volume (mL)	0.22	0.03 – 0.41	**0.03**
Observations	126		
R^2 / R^2 adjusted	0.29 / 0.24		

GM = grey matter, NAWM = normal appearing white matter, PASAT3 = Paced auditory serial addition test, tNAA = total N-acetyl aspartate + N-acetyl aspartyl glutamate, T2LV = T2 lesion volume

6.3.6 Associations between baseline MRI measures and change in performance on measures of information processing speed over 96 weeks (research question 4)

Baseline NAWM tNAA (β = 0.13, 95% CI [0.04 – 0.22], p = < 0.01) and T2LV (β = -0.23, 95% CI [-0.35 to -0.11], p < 0.001) were the only MRI measures that showed significant associations with change in SDMT scores over 96-weeks (Table 6-9 and

).

Table 6-11. The association between baseline MRI measures and change in symbol digit modalities test scores over 96-weeks

Predictors	Standardised beta	standardized CI	p
Baseline SDMT	0.65	0.54 – 0.77	**<0.001**

Baseline NAWM tNAA (IU)	0.13	0.04 – 0.22	**0.007**
Baseline WML MTR	0.07	-0.03 – 0.17	0.17
Baseline T2LV (mL)	-0.23	-0.35 – -0.11	**<0.001**
Baseline deep GM volume (mL)	0.05	-0.06 – 0.15	0.37
Observations	111		
R^2 / R^2 adjusted	0.78 / 0.76		

GM = grey matter, MTR = magnetisation transfer ratio, NAWM = normal appearing white matter, tNAA = total N-acetyl aspartate + N-acetyl aspartyl glutamate, T2LV = T2 lesion volume, WML = white matter lesion

When assessing change in PASAT3 scores over 96-weeks, fluoxetine (β = -0.43, 95% CI [-0.073 to -0.13], $p < 0.01$) remained the only significant variable (Table 6-12).

Table 6-12. The association between baseline MRI measures and change in PASAT3 scores over 96-weeks

Predictors	**Standardised beta**	**standardized CI**	**p**
Baseline PASAT3	0.76	0.64 – 0.88	**<0.001**
Baseline NAWM tNAA (IU)	0.00	-0.10 – 0.11	0.96
Baseline T2LV (mL)	-0.04	-0.17 – 0.08	0.51
Sex: female	-0.06	-0.29 – 0.17	0.61
Trial arm: Amiloride	-0.02	-0.30 – 0.27	0.91
Trial arm: Fluoxetine	-0.43	-0.73 – -0.13	**0.005**
Trial arm: Riluzole	-0.04	-0.34 – 0.26	0.81
Baseline deep GM volume (mL)	0.06	-0.06 – 0.19	0.31
Observations	126		
R^2 / R^2 adjusted	0.71 / 0.69		

GM = grey matter, NAWM = normal appearing white matter, PASAT3 = Paced auditory serial addition test, tNAA = total N-acetyl aspartate + N-acetyl aspartyl glutamate, T2LV = T2 lesion volume

6.4 Discussion

In a large cohort with SPMS, I examined markers of myelin and neuroaxonal injury, regional atrophy and WML load to investigate which pathological substrates in the brain and spinal cord were most closely associated with clinical disability over 96-weeks. I firstly demonstrate that decreased neuroaxonal integrity, CGM volume and cervical cord area are associated with decreased upper limb function at 96-weeks with decreased baseline MUCCA showing the strongest association with deterioration in upper limb function.

We also showed that decreased baseline cervical cord area is the best predictor of a decrease in ambulatory function as measured using the T25FW over 96-weeks.

Decreased white matter neuroaxonal integrity and increased lesion load were the strongest predictors of reduction in performance on tests of processing speed.

6.4.1 Correlations between baseline MRI features

There was a strong correlation between GM-MTR and NAWM-MTR (r = 0.99, 95% CI 0.98-0.99) and this was the cause of multi-collinearity between these variables in the multiple linear regression models (Table 6-2). The relationship between WML MTR and WM T2LV was in the expected direction with decreased WML myelin associated with increased WM T2LV. GM-MTR was negatively correlated with CGM volume which is unexpected. This could be explained by the presence of unsegmented cortical lesions. As expected, tNAA reflecting neuroaxonal integrity in NAWM and GM was not associated with MTR. WM T2LV showed weak negative associations with GM MRI features (CGM, dGM and GM NAWM) and MUCCA. This may represent Wallerian degeneration in WML affecting GM volumes and neuroaxonal integrity respectively (Henry *et al.*, 2009; Jehna *et al.*, 2013; Steenwijk *et al.*, 2015). GM and NAWM tNAA showed a weak negative correlation and is likely a reflection

of the regression method used to calculate metabolites in these tissue volumes (Solanky *et al.*, 2020).

6.4.2 Association between baseline MRI measures and physical disability at 96 weeks

Decreased baseline CGM volume, NAWM neuroaxonal integrity and MUCCA were associated with decreased upper limb function (as reflected by 9HPT scores) at 96-weeks. The associations were in the right direction: for every unit decrease in baseline CGM volume, NAWM tNAA and MUCCA, upper limb function at 96-weeks decreased by 0.31, 0.19 and 0.39 standard deviations respectively (Table 6-3).

In the previous analysis of this cohort in chapters 4 and 5, decreased baseline neuroaxonal integrity in NAWM showed a cross-sectional and longitudinal association with decreased upper limb function after adjusting for demographic covariates, disease duration, lesion load and brain volume (Solanky *et al.*, 2020). There has only been one previous study of an SPMS cohort that examined the longitudinal association between baseline tNAA and 9HPT – no association was found in a relatively small sample (n=15) (Obert *et al.*, 2016). Our analysis further supports the potential connection between baseline neuroaxonal damage and mitochondrial dysfunction in NAWM and upper limb function. A regional analysis would be of interest to investigate a predilection of neuroaxonal and mitochondrial dysfunction to corticospinal tracts traversing the NAWM.

In terms of GM atrophy, a 2 year study of SPMS (n = 56, median EDSS 6.0) showed that GM atrophy was moderately correlated with change in 9HPT z-score (r = 0.31) (Furby *et al.*, 2010); whilst two cross-sectional studies (n= 45-46) with early PPMS showed regional areas of CGM atrophy and GM fraction were correlated to 9HPT z-scores (r = 0.33-0.56) (Sastre-Garriga *et al.*, 2004; Khaleeli, Cercignani, *et al.*, 2007). We measured CGM volumes as a whole rather than specific regional GM regions of interest but it is possible that the changes seen in our cohort are driven changes in areas that control motor output e.g. pre-central gyrus – a finding shown in in early PPMS (Khaleeli, Cercignani, *et al.*, 2007). This regional predilection is also supported by a study

showing cortical thickness of the cortical area connected to corticospinal tracts was a significant predictor of 9HPT (n=195, PMS 71/195) (Daams *et al.*, 2015). CGM atrophy is likely mediated by several processes including inflammation mediated by meningeal lymphoid follicles (Magliozzi *et al.*, 2010, 2019; Howell *et al.*, 2011). However decreased myelin in GM was not associated with decreased upper limb function suggesting there are other more prominent mechanisms connecting CGM to upper limb dysfunction.

Studies have shown cross-sectional correlations between MUCCA and 9HPT [(r = -0.219, PMS 71/195), (r = 0.35, SPMS = 117/117); and MUCCA as an independent predictor of 9HPT (Furby *et al.*, 2008; Daams *et al.*, 2015; Hugh Kearney *et al.*, 2015). However, a longitudinal study of 56 SPMS outlined above did not demonstrate a correlation between SCA and change in 9HPT z-scores over 2 years (Furby *et al.*, 2010). We are unable to further postulate on the causes of SCA as spinal cord lesions and other advanced MR cord metrics were not available in this study. However, there have been mixed results when investigating cord lesions as the primary cause of SCA (Bergers *et al.*, 2002; Evangelou *et al.*, 2005; Stankiewicz *et al.*, 2009; Petrova *et al.*, 2018). Axonal loss occurring independent of lesions, metabolic changes and GM pathology demonstrated using diffusion tensor imaging are also important in cervical cord pathology in PMS (Kendi *et al.*, 2004; Abdel-Aziz *et al.*, 2015; H. Kearney *et al.*, 2015). It therefore may be of benefit to incorporate additional metrics to better understand the microstructural causes of cervical cord atrophy when analysing future SPMS cohorts.

Decreased baseline CGM, MUCCA and increased T2LV were associated with decreased ambulatory function at 96-weeks (as measured using T25FW). These associations head in the expected direction with a unit decrease in baseline CGM volume, MUCCA resulting in a decrease in T25FW by 0.25 and 0.24 standard deviations respectively (Table 6-4). The association between decreased CGM volumes and decreased ambulatory function at 96-weeks may be mediated by regional changes affecting the post-central gyrus caused by local meningeal based inflammation (Magliozzi *et al.*, 2007, 2010, 2019; Howell *et al.*, 2011). Increased WML load likely affects corticospinal tracts that

affect walking; although this association was of borderline significance (p = 0.045).

6.4.3 Association between baseline MRI measures and change in physical disability over 96 weeks

When examining change in upper limb function over 96-weeks, baseline MUCCA remained the only significant MRI measure (Table 6-6). This suggests that cervical cord pathology resulting in decreased cervical cord area is most closely associated with a deterioration in upper limb dysfunction; and of greater significance than the changes seen with markers of brain injury.

Decreased MUCCA remained associated with change in ambulatory function over 96-weeks where a unit decrease in baseline MUCCA results in a decrease of 0.16 standard deviations in T25FW over 96-weeks (

). This suggests that SCA has a greater impact on ambulatory function than markers of brain injury in SPMS. This finding is supported by several studies in cohorts with PMS that demonstrated spinal cord dysfunction and atrophy to be the associated with progressive worsening in ambulatory function (Daams *et al.*, 2015; Hugh Kearney *et al.*, 2015). However, a cross-sectional study of 117 SPMS patients did not identify an association between spinal cord area (or other MRI measures) and T25FW (Furby *et al.*, 2008).

Decreased baseline MUCCA was also associated with an increase in disability as measured using EDSS over 96-weeks. Whilst decreased CGM volume was associated, it was no longer significant when examining change in EDSS. The findings head in the expected direction where a unit decrease in baseline MUCCA is associated with an increase of 0.15 standard deviations reflecting an increase in disability with decreasing cervical cord area. Our findings are in keeping with numerous studies that have shown cervical cord area to be strongly associated with EDSS (Stevenson *et al.*, 1998; Lin, Blumhardt and Constantinescu, 2003; Valsasina *et al.*, 2013; H. Kearney, M. A. Rocca, *et al.*, 2014; Daams *et al.*, 2015; Hugh Kearney *et al.*, 2015; Lukas *et al.*, 2015; Schlaeger *et al.*, 2015; Tsagkas *et al.*, 2018). The median EDSS of the cohort was 6.0 (range 4.0 – 6.5) and EDSS scores at these levels are determined by ambulatory distance (with or without aid). Our findings are therefore concordant with our T25FW results which are also reflected in the strong correlation between baseline EDSS and T25FW (r = -0.81) in this cohort (Kurtzke, 1983). Decreased baseline CGM volume was associated with increased disability at 96-weeks but this lost significance once baseline EDSS was added to the model to examine change. Whilst there is an association between CGM damage and increased disability, cervical cord pathology demonstrated the strongest association with a deterioration in ambulatory function in SPMS.

6.4.4 Associations between baseline MRI measures and performance measures of information processing speed at 96-weeks and change over 96-weeks

Decreased baseline neuroaxonal integrity in NAWM, mean myelin levels in WML, deep GM volume and increased lesion load were all associated with SDMT scores at 96-weeks. The model coefficients were in the expected direction with a 1 unit decrease in tNAA, mean WML MTR and deep GM volume, resulting in decreases of 0.24, 0.20 and 0.17 standard deviations in SDMT scores at 96-weeks respectively. A 1 unit increase in T2LV was associated with a decrease of 0.45 standard deviations in 96-week SDMT scores (Table 6-9). Only NAWM tNAA and T2LV remained significant when examining the association with the change in SDMT scores over 96-weeks (

). First, this suggests that baseline decreased neuroaxonal integrity and mitochondrial function in NAWM is important in the development of decreased processing speed performance at 96-weeks. There are no previous studies that have examined this relationship with SDMT in SPMS. Second, WML load (as reflected by T2LV) is a stronger predictor than tNAA; a finding that has been demonstrated previously (Cox *et al.*, 2004; Penny *et al.*, 2010; Solanky *et al.*, 2020). Whilst this may suggest that NAWM tNAA is a reflection of WM T2LV, there was no correlation between WM T2LV and tNAA suggesting that both processes contribute IPS performance to albeit varying degrees. Taken together, it would suggest that alterations in subcortical white matter are more significant in the deterioration of processing speed than cortical structures. However, T2LV is not pathologically specific and represents a combination of chronic inflammation, remyelination, axonal loss and astrogliosis. This somewhat affects the ability to understand the underlying pathological substrates to target when developing therapies to address cognitive performance in SPMS. This could be addressed by the detection of chronic active lesions (slowly evolving lesions), the use of advanced MRI measures e.g., diffusion imaging and network analysis (functional MRI) to disentangle this issue.

Deep GM was associated in the model using SDMT scores at 96-weeks rather than change. Deep GM atrophy and decreased deep GM volumes are thought to be a driver of disability progression in MS and previous work has shown a modest relationship between various deep GM regions and SDMT scores in relapsing (n = 50) and mixed MS (SPMS 27/86, median EDSS 3.5) cohorts (Batista *et al.*, 2012; Eshaghi, Prados, *et al.*, 2018; Lorefice *et al.*, 2020). We may not have identified an association between decreased deep GM volume and change in SDMT as I analysed an SPMS cohort that may have different characteristics. It may also be of interest to analyse specific regions of interest within deep GM such as the thalamus.

6.4.5 We found similar results for baseline MRI measures and their association with PASAT3 at 96-weeks (Associations between baseline MRI measures and change in performance on measures of information processing speed over 96 weeks (research question 4)

Baseline NAWM tNAA (β = 0.13, 95% CI [0.04 – 0.22], p = < 0.01) and T2LV (β = -0.23, 95% CI [-0.35 to -0.11], p < 0.001) were the only MRI measures that showed significant associations with change in SDMT scores over 96-weeks (Table 6-9 and

).

Table 6-11. The association between baseline MRI measures and change in symbol digit modalities test scores over 96-weeks

Predictors	Standardised beta	standardized CI	p
Baseline SDMT	0.65	0.54 – 0.77	**<0.001**
Baseline NAWM tNAA (IU)	0.13	0.04 – 0.22	**0.007**
Baseline WML MTR	0.07	-0.03 – 0.17	0.17
Baseline T2LV (mL)	-0.23	-0.35 – -0.11	**<0.001**
Baseline deep GM volume (mL)	0.05	-0.06 – 0.15	0.37
Observations	111		

R^2 / R^2 adjusted	0.78 / 0.76

GM = grey matter, MTR = magnetisation transfer ratio, NAWM = normal appearing white matter, tNAA = total N-acetyl aspartate + N-acetyl aspartyl glutamate, T2LV = T2 lesion volume, WML = white matter lesion

When assessing change in PASAT3 scores over 96-weeks, fluoxetine (β = -0.43, 95% CI [-0.073 to -0.13], $p < 0.01$) remained the only significant variable (Table 6-12).

). However, none of the MRI predictors remained significant when examining change in PASAT3 over 96-weeks (Table 6-12). The difference in results between change in SDMT and PASAT3 may be due to several reasons. First, PASAT3 is known to exhibit a practice effect and is perhaps less efficient as longitudinal biomarker of processing speed compared to SDMT (Barkercollo, 2005; López-Góngora, Querol and Escartín, 2015; Benedict *et al.*, 2017). Second, SDMT and PASAT may assess differing cognitive domains – SDMT uses more visual-spatial memory compared to PASAT3 which involves verbal working memory (Sonder *et al.*, 2014). Functional MRI has also demonstrated differences in the networks involved in each of these tests (Forn *et al.*, 2011).

Previous studies in PMS examining MRI predictors of processing speed have demonstrated significant involvement of GM with CGM atrophy, decreased GM MTR being associated with long-term performance on information processing speed (Furby *et al.*, 2010; Tur, Khaleeli, *et al.*, 2011; Tur, Penny, *et al.*, 2011; Eijlers *et al.*, 2018). Our findings may have differed for several reasons. First, Furby et al demonstrated GM atrophy was associated with change in PASAT scores over 2 years in SPMS (n = 56, median EDSS 6.0) but GM was not segmented into cortical or deep volumes; SDMT was also not captured (Furby *et al.*, 2010). Second, studies by Tur et al were in early PPMS (n = 27-47) and examined only MTR and T2LV associations with PASAT (Tur, Khaleeli, *et al.*, 2011; Tur, Penny, *et al.*, 2011). Third, Eijlers et al demonstrated CGM volumes were a significant predictor of cognitive impairment in PMS (PMS = 52/234, EDSS not specified for PMS group) but their studies differed slightly in that they predicted cognitive impairment at follow up (mean 4.8 years for combined

MS group) and utilised different measures of WM and GM integrity (Eijlers *et al.*, 2018).

6.4.6 Strengths and limitations

The strengths of the study are the recruitment of a large cohort of non-active progressive SPMS that enabled us to focus on disability progression and neurodegeneration occurring independently of active inflammation. There were several limitations of the study. First, in examining the UCL cohort of 154 participants, missing 96-week data due to withdrawals, failed quality assurance for certain MR sequences and failure of MR analysis pipelines may have decreased our power to identify statistically significant associations. Second, internal water was used as the internal reference for CSI which makes assumptions about the water content in people with MS and thus tNAA levels are estimated ratios expressed in institutional units. Third, GM lesions were not segmented in deep and CGM. Fourth, there was no control group for cross-sectional or longitudinal comparisons. Last, WM T2LV may not be the most suitable marker of chronic inflammation in SPMS. Slowly expanding or chronic active lesions may be a better marker in PMS and recent developments in this field increase the likelihood of their use in the near future. The detection of CGM inflammation mediated via meningeal lymphoid follicles is another area of focus and ongoing developments in MRI analysis pipelines may increase our sensitivity in measuring this.

6.5 Conclusion

We investigated measures of brain and cervical cord injury in a large cohort with SPMS demonstrating that cervical cord pathology was most closely associated with deterioration in upper limb and ambulatory function over 96-weeks. Decreases in brain white matter neuroaxonal integrity and mitochondrial function; and increased lesion load were the pathological substrates most important in reducing processing speed. Multimodal MRI datasets may be important when understanding factors causing disability progression in SPMS. Therapeutic interventions in SPMS targeting preservation of upper limb function and processing speed may benefit from

increased focus on SCA, neuroaxonal integrity and mitochondrial dysfunction respectively.

Chapter 7. Decreased neuroaxonal integrity and mitochondrial function in early relapse onset MS is associated with long-term moderate-severe disability: A 15-year CIS follow up study

7.1 Introduction

The long-term course of relapse onset MS is highly variable and MRI markers are important to better understand the mechanisms driving the risk of long-term physical and cognitive disability. Established MRI metrics associated with long-term disability and SPMS disease course in early relapsing MS patients include lesional (brain T2 lesion load, infratentorial and spinal cord lesions, gadolinium-enhancing lesions) and non-lesional measures (GM fraction, upper cervical cord area (Filippi *et al.*, 1994; O'Riordan *et al.*, 1998; Sailer *et al.*, 1999; Eriksson, Andersen and Runmarker, 2003; Summers *et al.*, 2008; Leonora K. Fisniku *et al.*, 2008; Swanton *et al.*, 2009; Di Filippo *et al.*, 2010; Dalton *et al.*, 2012; Uher *et al.*, 2014; H. Kearney, M. Rocca, *et al.*, 2014; Brownlee *et al.*, 2017, 2019; Vidal-Jordana *et al.*, 2018; Chung *et al.*, 2020). These markers however, are not pathologically specific, do not completely explain the variance seen when predicting long term disability, the development of SPMS, and/or are challenging to translate into routine clinical settings.

^{1}H-MRS measures the concentration of brain metabolites *in vivo* providing adjunctive metabolic information on disease processes relevant to MS including tNAA, tCho, Glx and tCr (Bitsch *et al.*, 1999; Bjartmar *et al.*, 2000; Swanberg *et al.*, 2019). SVS can be acquired in clinical settings in acceptable scanning times, and can be used for the diagnosis and differential diagnosis of neoplastic brain lesions and some metabolic disorders (Faghihi *et al.*, 2017; Wilson *et al.*, 2019). ^{1}H-MRS may provide important information on disease processes relevant to MS. These changes include decreased tNAA in WML, NAWM and GM; increased mIns in WML and NAWM and increased tCho in acute WML (Swanberg *et al.*, 2019).

Metabolic changes may also be present from the earliest stages of MS. Studies of NAWM in CIS cohorts have shown reductions in tNAA (or tNAA/tCr) and increases in mIns levels (Rocca *et al.*, 2003; Fernando *et al.*, 2004; Wattjes *et al.*, 2007; M. P. Wattjes *et al.*, 2008; Mike P. Wattjes *et al.*, 2008).

Here I present the 15 year follow up of a CIS cohort to determine whether baseline metabolites in NAWM reflecting neuroaxonal integrity (tNAA), astrogliosis (mIns), membrane turnover (tCho); energy buffering systems (tCr) and glutamatergic activity (Glx) are associated with:

a) Long -term disability at 15 years defined as EDSS $\geq$ 3.0 and EDSS $\geq$ 6.0
b) Development of SPMS at 15 years
c) Clinical disability measures at 15 years including T25FW, 9HPT, SDMT and PASAT3.

I propose the following hypotheses:

1) Decreased tNAA and increased mIns levels are associated with moderate-severe disability at 15 years defined as EDSS $\geq$ 3.0, EDSS $\geq$ 6.0, at 15 years. Exploratory analyses between tCho, Glx and EDSS outcomes at 15 years are also investigated.
2) Decreased tNAA and increased mIns levels are associated with an increased risk of developing SPMS at 15 years. Exploratory analyses between tCho, Glx and risk of SPMS at 15 years are also completed.
3) Decreased tNAA and mIns levels are associated with decreased upper limb function (reflected by 9HPT), decreased ambulatory function (reflected by T25FW) and decreased performance on tests of IPS (reflected by PASAT3, SDMT) at 15 years. Exploratory associations between tCho, Glx and 9HPT, T25FW, PASAT3 and SDMT are also analysed with no *a priori* hypothesis.

7.2 Methods

The methods including participant recruitment, follow up, clinical assessments, MRI acquisition and analysis have been outlined in 3.3.

This study utilises data from the baseline, 3-month and year 15 visits (Figure 7-1).

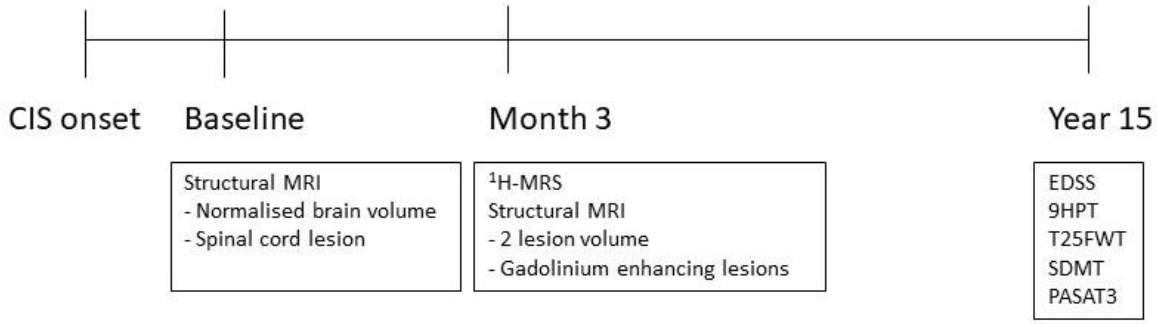

Figure 7-1. Time points used in this study.

7.2.1 Statistical analysis

Statistical analysis was completed using R statistical software version 3.5.1 (R Core Team, 2017). All p values were 2-sided and reported at the 0.05 significance level. I examined the association between metabolites acquired at the 3-month visit and the following outcomes at 15 years: development of SPMS, EDSS $\geq$ 3.0, EDSS $\geq$ 6.0, association with physical disability measures: 9HPT and T25FW; and measures of information processing speed: SDMT and PASAT3.

The analysis was completed in two main steps based on the type of 15-year variable being analysed:

1) Binary or categorical outcome variables at 15 years (research questions 1 & 2)
    a. A one-way ANOVA and Tukey's honestly significant difference post-hoc test was used to determine if there was a difference in metabolite levels at CIS onset between those diagnosed with SPMS, RRMS or CIS at 15 years.
    b. For binary 15-year clinical outcomes (conversion to SPMS, EDSS $\geq$ 6.0, EDSS $\geq$ 3.0), I undertook a bivariate analysis to determine if there was a statistically significant difference between different groups for a given metabolite. An F test was used to check if there was a difference in variance between the

two groups. If there was no difference between the variances, a two-sample t-test was then applied.

c. Where a statistically significant metabolite difference between groups was found, the following multiple logistic regression analysis was undertaken: The dependent variable was the binary 15-year outcome measure. The following MRI variables were included as explanatory variables in each multiple regression model: 3-month metabolite level (millimolar (mM) units), 3-month T2 lesion volume (in mL), number of gadolinium-enhancing lesions at 3 months, baseline NBV (in mL) and number of spinal cord lesions at baseline. NBV and the number of cord lesions were not measured at the 3-month visit and were therefore taken from the baseline visit. The confounding demographic variables and characteristics – age at onset, sex, duration of follow-up (disease duration), CIS presentation and baseline EDSS (for conversion to SPMS only) were added using a manual forward stepwise method, with the confounding variable being kept in the model if it caused a significant change in the coefficient or p value of the predictor variable; or was significant itself. In the multiple logistic regression models, none of the confounder variables were significant and were not included.

   Odds ratios with 95% confidence intervals were calculated, goodness of fit was checked using the Hosmer-Lemeshow method and the C-statistic calculated to determine the ability of the model to classify the binary outcome.

2) Continuous clinical outcome variables at 15 years (research question 3)

   a. Spearman rank correlation coefficients were calculated to explore the association between the 3-month metabolites and 15-year continuous clinical outcome measures (T25FW, 9HPT, EDSS, SDMT, PASAT3).

   b. 3-month metabolites that demonstrated a statistically significant correlation were then further examined in a multiple linear

regression analysis. The dependent variable was the respective 15-year continuous clinical outcome measure. I used the method described above to build the models. Follow-up (disease duration) was included in the model for EDSS (continuous variable). T25FW was transformed to its reciprocal and therefore, lower values reflect decreased performance. Distributional assumptions were assessed by visual inspection of residual plots, normal probability plots and highly leveraged data observations were identified using Cook's distance. As EDSS and T25FW violated normality assumptions, inference from these models is based on non-parametric bias-corrected and accelerated 95% confidence intervals calculated from 10,000 bootstrap replications (using case resampling).

Two post-hoc analyses were also undertaken:

1) Pearson correlation coefficients (Spearman rank when variable is non-parametric; Kendall tau-b in the event of tied ranks) were calculated to examine the association between specific metabolite levels at CIS onset and MRI abnormalities at 15 years as a measure of brain tissue damage not detected by clinical disability measures. This was calculated for:

i) mIns and brain T2LV
ii) tNAA and brain GM and WM volumes
iii) tCho and brain T2LV

2) Receiver operating curves (ROC) were generated to identify the optimal cut-off point (maximising accuracy) for 3-month metabolite levels that could best discriminate between participants that would develop the respective outcome at 15 years. Using this metabolite cut-off point, I stratified participants into two groups in the same cohort and then analysed their association with the respective 15-year outcome using the aforementioned multiple logistic regression model.

7.3 Results

The baseline MRI and demographics are shown in Table 7-5. Of the 91/96 CIS participants enrolled in the study who had follow up data at 15 years, 15 (20%) developed SPMS, 48 (53%) had RRMS, 28 (31%) remained CIS and 5 (5%) were lost to follow up. 71/96 (74%) remained untreated with DMT during the follow up period.

15-year EDSS data was available for 89/96 participants and comprised 26 participants that underwent telephone EDSS. The most common reasons for telephone follow up were patient choice (n = 18), living abroad (n = 4) and disability levels precluding travel to our site (n = 4). The median EDSS at 15 years across all participants was 1.5 (range 0-10). The median EDSS in those remaining CIS was 0 (range 0 - 1.0), relapsing remitting MS 2.0 (0 - 7.5) and SPMS 6.5 (3.5 – 10.0). PASAT3 and SDMT data were available for 59/96 and 57/96 respectively as they were added as outcome measures only after a proportion of participants had completed their 15-year visit.

7.3.1 The association between metabolite levels and EDSS at 15 years

3-month tNAA in NAWM was lower in the those with EDSS $\geq$ 3.0 (mean difference 0.64, p = 0.002, 95% CI 0.24-1.04) and EDSS $\geq$ 6.0 (mean difference 0.55, p = 0.031, 95% CI 0.05-1.05) (Table 7-1)

Table 7-1. Brain metabolite differences at clinical isolated syndrome onset in those with EDSS ≥ 3.0 and EDSS ≥ 6.0 at 15 years

	Expanded disability status scale ≥ 3.0		
	Mean difference	95% CI	p value
tNAA	**0.64**	**0.24 – 1.04**	**0.002**
Myo-inositol	-0.16	-0.67 - 0.35	0.53
Glx	-0.38	-1.02 – 0.25	0.23
Total choline	-0.02	-0.11 – 0.06	0.55
Total creatine	0.13	-0.09 – 0.35	0.24
	Expanded disability status scale ≥ 6.0		
	Mean difference	95% CI	p value
tNAA	**0.55**	**0.05 – 1.05**	**0.03**
Myo-inositol	-0.42	-1.04 – 0.20	0.18
Glx	-0.35	-1.13 – 0.42	0.37
Total choline	0.01	-0.09 – 0.12	0.77
Total creatine	-0.05	-0.31 – 0.22	0.74

Statistically significant differences highlighted in bold. Mean difference calculated in reference to mean from group that was Expanded disability status scale < 3.0, Expanded disability status scale < 6.0 and did not convert to secondary progressive multiple sclerosis respectively.

Glx = glutamate + glutamine, tNAA = total N-acetyl aspartate + N-acetyl aspartyl glutamate

In the multiple logistic regression models, 3-month tNAA was associated with increased odds of developing EDSS ≥ 3.0 at 15 years (OR 0.32, 95% CI 0.12 - 0.73). 3-month T2LV (OR 1.51, 95% CI 1.04 – 2.26) and the number of

baseline spinal cord lesions (OR 3.96, 95% CI 1.95 – 9.84) were also associated with increased odds of EDSS ≥ 3.0 at 15 years (Table 7-2). The model c-statistic was 0.90.

Table 7-2. Multiple logistic regression model examining 3-month tNAA in normal appearing white matter and EDSS > 3.0 at 15 years

Characteristic	OR[1]	95% CI[1]	p-value
3-month tNAA	0.32	0.12, 0.73	0.011
3-month T2LV	1.51	1.04, 2.26	0.029
Baseline NBV	1.00	0.99, 1.01	0.8
Number of GdE at 3-months	0.90	0.73, 1.20	0.3
Number of baseline cord lesions	3.96	1.95, 9.84	<0.001

[1] OR = Odds Ratio, CI = Confidence Interval

GdE = number of gadolinium enhancing lesions, NBV = normalised brain volume, tNAA = total NAA, T2LV = T2 lesion volume

The number of cord lesions at baseline (OR 3.61, 95% CI 1.84 - 8.26) was the only variable significantly associated with EDSS ≥ 6.0 at 15 years (model c-statistic 0.91) (Table 7-3).

Table 7-3. Multiple logistic regression model examining 3-month tNAA in normal appearing white matter and EDSS > 6.0 at 15 years

Characteristic	OR[1]	95% CI[1]	p-value
3-month tNAA	0.54	0.19, 1.36	0.2
3-month T2LV	1.40	0.91, 2.11	0.10
Baseline NBV	1.00	0.99, 1.01	>0.9
Number of GdE at 3-months	0.91	0.73, 1.15	0.4
Number of baseline cord lesions	3.61	1.84, 8.26	<0.001

[1] OR = Odds Ratio, CI = Confidence Interval

GdE = number of gadolinium enhancing lesions, NBV = normalised brain volume, tNAA = total NAA, T2LV = T2 lesion volume

When examining EDSS as a continuous variable, 3-month tNAA in NAWM had a negative association (Rho = -0.36, 95% CI -0.53 to -0.16). In the subsequent multiple linear regression model, 3-month tNAA (β = 0.01, p = 0.005), T2LV (β = 0.34, p = 0.01) and the number of spinal cord lesions (β = 1.5, p < 0.001) were associated with EDSS at 15 years (Table 7-4).

Table 7-4. Multiple linear regression model examining 3-month tNAA and EDSS at 15 years

Association between tNAA in NAWM and EDSS at 15-year visit (n = 83)				
Predictors	**Estimates**	**Standard error**	**95% CI**	**p**
3-month tNAA	-0.61	0.21	-1.03 - 0.19	**0.005**
Follow up	-0.07	0.10	-0.27 - 0.12	0.45
3-month T2LV	0.34	0.13	0.08 - 0.60	**0.01**
Baseline NBV	0.58	2.80	-5.00 - 6.16	0.84
3-month number of GdE lesions	-0.14	0.10	-0.34 - 0.06	0.16
Baseline number of cord lesions	1.51	0.23	1.05 - 1.98	<0.001
R^2 0.491				
Association between tNAA in NAWM and EDSS at 15-year visit with bootstrapping				

Predictors	Median bootstrapped estimates	Standard error	95% CI	Number of bootstraps
3-month tNAA	-0.58	0.22	-1.10 to -0.22	10000
Follow up	-0.07	0.09	-0.25 - 0.11	
3-month T2LV	0.35	0.19	0.02 - 0.75	
Baseline NBV	0.00	0.00	-0.01 to 0.01	
3-month GdE lesion number	-0.15	0.20	-0.60 - 0.21	
Baseline number of cord lesions	1.49	0.31	0.95 - 2.2	

GdE = gadolinium enhancing lesions, NBV = normalised brain volume, Std = standard, tNAA = total N-acetyl aspartate, T2LV = T2 lesion volume

No other metabolites showed an association with EDSS, EDSS $\geq$ 3.0 or EDSS $\geq$ 6.0 at 15 years (Table 7-1 and Table 7-6).

Table 7-5. Cohort demographic and characteristics

	CIS (N=28)	RRMS (N=48)	SPMS (N=15)	Total (N=91)
Age at onset (years)	32.3 (7.8)	33.1 (6.9)	34.4 (7.5)	33.1 (7.2)
Female (n, %)	15 (53.6%)	38 (79.2%)	7 (46.7%)	60 (65.9%)
CIS presentation (n, %)				
Optic neuritis	24 (85.7%)	47 (97.9%)	11 (73.3%)	82 (90.1%)
Spinal cord syndrome	1 (3.6%)	0 (0.0%)	2 (13.3%)	3 (3.3%)
Brainstem syndrome	3 (10.7%)	1 (2.1%)	2 (13.3%)	6 (6.6%)
Hemispheric syndrome	0 (0.0%)	0 (0.0%)	0 (0.0%)	0 (0.0%)
Follow up duration (years)	14.5 (4.0)	14.2 (1.7)	15.2 (2.4)	14.4 (2.7)
Baseline EDSS^{+}	1.0 (0.0, 2.0)	1.0 (1.0, 1.5)	1.0 (1.0, 2.8)	1.0 (1.0, 2.0)
3-month T2LV^{+} (mL)	0.0 (0.0, 0.1)	0.6 (0.2, 2.0)	2.1 (0.5, 5.3)	0.3 (0.0, 1.8)
Baseline NBV (mL)	1584.4 (80.5)	1582.4 (63.2)	1549.1 (84.4)	1577.5 (72.8)
3-month GdE (number of lesions)	0.0 (0.0)	0.9 (1.8)	5.7 (13.6)	1.4 (5.9)

Total Choline	1.2 (0.2)	1.2 (0.2)	1.2 (0.1)	1.2 (0.2)
Myo-inositol	3.6 (1.0)	3.9 (1.1)	4.0 (1.0)	3.9 (1.1)
tNAA	8.7 (0.7)	8.1 (0.9)	7.8 (0.8)	8.3 (0.9)
Glx	7.2 (1.6)	7.2 (1.4)	7.4 (1.1)	7.2 (1.4)

+ = data presented as median (interquartile range)

CIS = clinically isolated syndrome, EDSS = Expanded disability status scale, tNAA = total N-acetyl aspartate + N-acetyl aspartyl glutamate, T2LV = T2 lesion volume, NBV = normalised brain volume

GdE = number of gadolinium enhancing lesions, Glx = glutamine + glutamate

Table 7-6. Correlation coefficients between brain metabolites measured at CIS onset and clinical outcome measures at 15 years

	EDSS			Timed 25-foot walk test			Nine-hole peg test			PASAT3 scores			SDMT Scores		
	ρ	95% CI		ρ	95% CI		ρ	95% CI		ρ	95% CI		ρ	95% CI	
tNAA	**-0.36**	**-0.53**	**-0.16**	**0.28**	**0.03**	**0.49**	-0.20	-0.43	0.05	0.12	-0.14	0.37	0.04	-0.22	0.30
Myoinositol	0.12	-0.09	0.32	0.09	-0.16	0.36	0.03	-0.22	0.28	0.00	-0.25	0.26	0.01	-0.25	0.27
Glx	0.07	-0.15	0.27	0.17	-0.08	0.40	0.22	-0.03	0.45	-0.08	-0.33	0.18	-0.04	-0.30	0.22
Total choline	-0.03	-0.24	0.18	0.15	-0.10	0.38	0.03	-0.22	0.28	0.05	-0.21	0.31	-0.01	-0.27	0.25
Total creatine	-0.11	-0.31	0.10	-0.05	-0.29	0.20	-0.00	-0.25	0.25	0.01	-0.25	0.26	-0.07	-0.33	0.19

Statistically significant correlations highlighted in bold. Timed 25 foot walk test is taken as the reciprocal.

CIS = Clinically isolated syndrome, EDSS = expanded disability status scale, Glx = glutamate + glutamine, mIns = myoinositol, PASAT3 = paced auditory serial addition test, SDMT = symbol digit modalities test, tCho = total choline, tNAA = total N-acetyl aspartate + N-acetyl aspartyl glutamate

7.3.2 The association between metabolite levels and the development of secondary progressive multiple sclerosis at 15 years

There was a statistically significant difference in tNAA levels at CIS onset between those that developed SPMS, RRMS or remained CIS at 15 years ($F(2,88) = 7.35$, $p = 0.001$). A post hoc Tukey test showed that tNAA levels in those who developed SPMS or RRMS at 15 years differed significantly from those with CIS at $p < 0.05$ (**Error! Reference source not found.**). There was no difference in tNAA levels between SPMS and RRMS. There were no other statistically significant metabolite differences between CIS, RRMS or SPMS at 15 years.

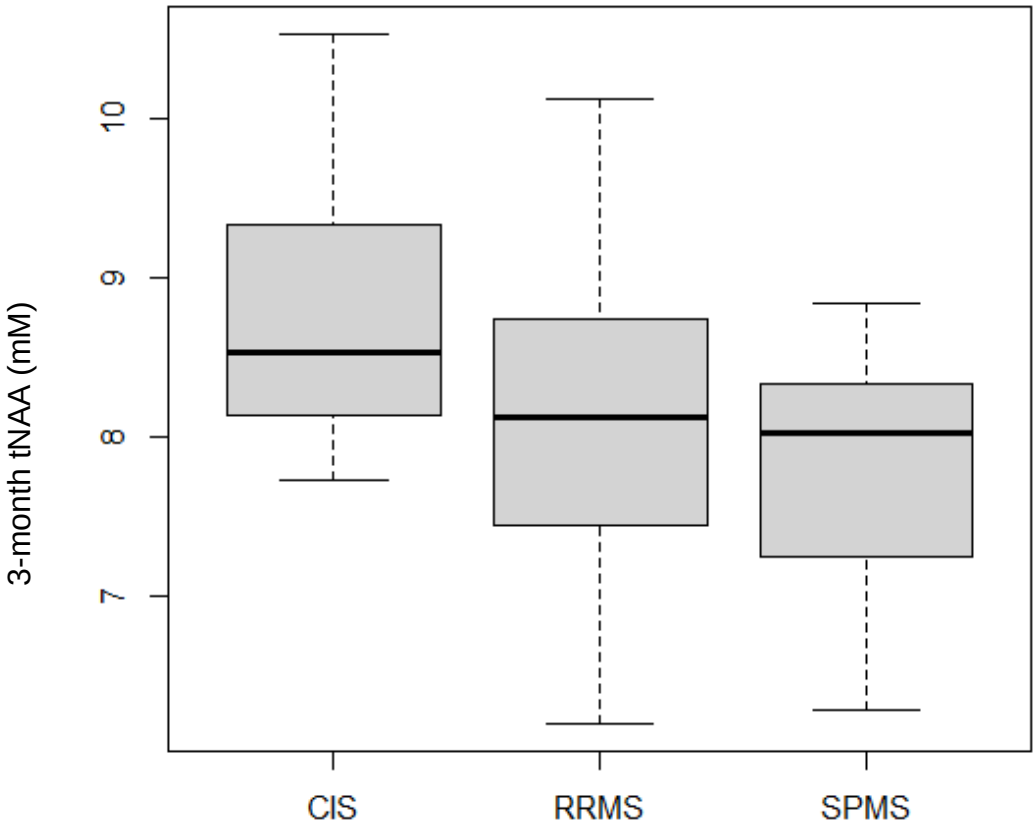

Figure 7-2. Difference in tNAA levels between groups at 15 years

3-month tNAA in NAWM at CIS was lower in those who developed to SPMS at 15 years (mean difference 0.57, $p = 0.02$, 95% CI 0.08-1.06). However, in the multiple logistic regression model, only the number of baseline spinal cord lesions was significantly associated with an increased risk of SPMS (OR 3.61, 95% CI 1.84 – 8.30, model c-statistic 0.91) (Table 7-8).

Table 7-7. Differences in metabolites based on development of SPMS at 15 years

	Development of secondary progressive multiple sclerosis		
	Mean difference	95% CI	p value
tNAA	**0.57**	**0.08 – 1.06**	**0.02**
Myo-inositol	-0.20	-0.81 – 0.40	0.51
Glx	-0.26	-1.06 – 0.54	0.52
Total choline	0.04	-0.05 – 0.14	0.35
Total creatine	0.20	-0.06 – 0.45	0.13

Table 7-8. Multiple logistic regression model examining 3-month tNAA and development of secondary progressive multiple sclerosis at 15 years

Characteristic	OR[1]	95% CI[1]	p-value
3-month tNAA	0.45	0.15, 1.18	0.12
3-month T2LV	1.43	0.93, 2.17	0.082
Baseline NBV	1.00	0.98, 1.01	0.5
Number of GdE at 3-months	0.94	0.75, 1.24	0.6
Number of baseline cord lesions	3.61	1.84, 8.30	<0.001

[1] OR = Odds Ratio, CI = Confidence Interval

GdE = number of gadolinium enhancing lesions, NBV = normalised brain volume, tNAA = total NAA, T2LV = T2 lesion volume

No other brain metabolites were associated with development of SPMS by 15 years (Table 7-1).

7.3.3 Association between metabolites with physical and cognitive performance measures at 15 years

3-month tNAA was correlated with T25FW (Rho = 0.28, 95% CI 0.03 - 0.49). In the model, only the number of cord lesions at baseline (β = -0.05, p < 0.001) was associated with T25FW performance at 15 years (

Table 7-9).

Table 7-9. Multiple linear regression model examining 3-month tNAA and timed 25-foot walk at 15 years

Association between tNAA in NAWM and Timed 25 ft walk test at 15-year visit (n = 61)				
Predictors	**Estimates**	**Standard error**	**95% CI**	**p**
3-month tNAA	0.01	0.01	-0.01 - 0.03	0.30
3-month T2LV	-0.01	0.01	-0.02 - 0.00	0.08
Baseline NBV	0.04	0.12	-0.20 - 0.28	0.76
3-month number of GdE lesions	0.00	0.00	-0.00 - 0.01	0.70
Baseline number of cord lesions	-0.05	0.01	-0.06 - 0.03	**<0.001**
R2 0.47				

Association between tNAA in NAWM and Timed 25 ft walk test at 15-year visit with bootstrapping				
Predictors	**Median bootstrapped estimates**	**Standard error**	**95% CI**	**Number of bootstraps**
3-month tNAA	0.09	0.27	-0.01 - 0.03	10000
3-month T2LV	0.01	0.01	-0.02 - 0.00	
Baseline NBV	0.01	0.01	-0.00 - 0.00	
3-month GdE lesion number	0.00	0.00	-0.01 - 0.01	
Baseline number of cord lesions	0.002	0.01	-0.07 to -0.02	

GdE = number of gadolinium enhancing lesions, NBV = normalised brain volume, tNAA = total NAA, T2LV = T2 lesion volume

None of the remaining 3-month metabolites were correlated with T25FW or 9HPT at 15 years. There was no association between any of the metabolites and performance measures of cognitive processing speed at 15 years (Table 7-6).

7.3.4 **Post hoc analyses**

Receiver operating curve analysis

For participants that developed an EDSS $\geq$ 3.0 at 15-years, the ROC analysis calculated an optimal 3-month tNAA cut-off point of 7.32 (Figure 7-3). This cut off had an accuracy of 0.74 and with a specificity of 0.91 was able to identify those who did not develop an EDSS $\geq$ 3.0 at 15 years; but suffered from low sensitivity (0.29). Using this tNAA cut-off of 7.32 to classify the participants into those above and below this level, tNAA < 7.32 (OR 6.22, 95% CI 1.35 – 31.5)

and the number of baseline spinal cord lesions (OR 4.08, 95% CI 2.07 – 9.68) were associated with an increased risk of EDSS ≥ 3.0 at 15 years (model c-statistic 0.90) (Table 7-10).

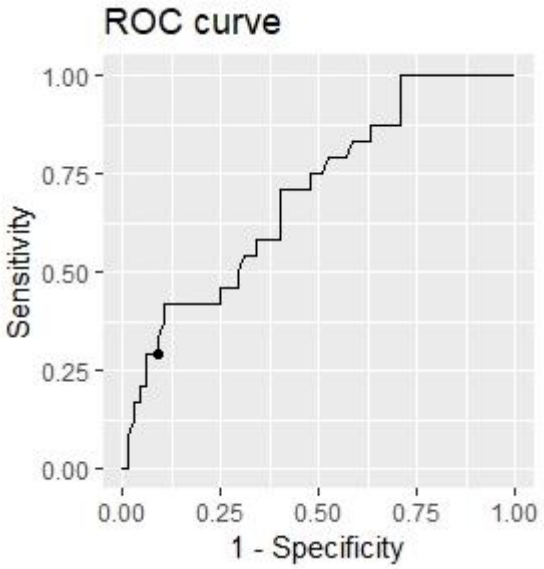

Figure 7-3. Receiver operating characteristic curve of 3-month tNAA and EDSS ≥ 3.0 at 15 years

Metabolite associations with specific MRI measures at 15 years

mIns (Kendall's tau-b = 0.08, p = 0.39) and tCho levels (Kendall's tau-b = 0.01, p = 0.93) at CIS onset were not associated with brain T2LV at 15 years. tNAA was not correlated with GM (r = -0.03, p = 0.82) or white matter volumes (r = 0.16, p = 0.23) at 15 years.

Table 7-10. Multiple logistic regression model examining 3-month tNAA cut-off of 7.32 and EDSS > 3.0 at 15 years

Characteristic	OR[1]	95% CI[1]	p-value
tNAA < 7.32			
No	—	—	
Yes	6.22	1.35, 31.5	0.021
Baseline NBV	1.00	0.99, 1.01	0.8
Number of GdE at 3-months	0.96	0.77, 1.31	0.7
3-month T2LV	1.32	0.92, 1.94	0.13
Number of baseline cord lesions	4.08	2.07, 9.68	<0.001

[1] OR = Odds Ratio, CI = Confidence Interval

GdE = number of gadolinium enhancing lesions, NBV = normalised brain volume, tNAA = total NAA, T2LV = T2 lesion volume

7.4 Discussion

In a 15-year follow-up study of a CIS cohort, I demonstrated that tNAA in NAWM measured in the early stages of MS, was associated with the development of moderate-severe disability at 15 years.

In keeping with previous studies of long-term follow-up cohorts with relapse onset MS, the number of spinal cord lesions was associated with development of SPMS and long-term moderate-severe physical disability.

In a post-hoc analyses, I identified a tNAA value of 7.32mM as the optimal cut-off for this dataset and stratifying our cohort I demonstrated that this cut-off was also associated with an increased odds of developing moderate-severe disability at 15 years.

7.4.1 The association between metabolite levels and EDSS outcomes at 15 years

tNAA as a marker of neuroaxonal integrity was associated with an increased risk of developing EDSS $\geq$ 3.0 at 15 years. Taking the reciprocal of the model odds ratio (1/0.392 = 2.55) suggests that holding all other covariates constant, a 1-unit decrease in tNAA levels results in a 2.5 increase in the odds of developing an EDSS $\geq$ 3.0 at 15 years after CIS. This would be in the expected

direction where decreased neuroaxonal integrity and mitochondrial function in NAWM at CIS onset is associated with an increased odds of developing moderate-severe disability over 15 years (Table 7-2). Similar results were seen when EDSS was used as a continuous variable with tNAA, T2LV and number of baseline cord lesions showing significant associations (

Table 7-9).

The majority of studies using ^{1}H-MRS in CIS have been cross-sectional with most showing that tNAA (or tNAA/tCr) is decreased in NAWM, CGM or WML when compared to HC (P A Brex *et al.*, 1999; Rocca *et al.*, 2003; Fernando *et al.*, 2004; M. Rovaris *et al.*, 2005; Audoin *et al.*, 2007; Wattjes *et al.*, 2007; M. P. Wattjes *et al.*, 2008). Several studies did not demonstrate any differences between CIS and controls (A Tourbah *et al.*, 1999; Sbardella *et al.*, 2011). In the previous longest follow up study that measured brain metabolites at CIS onset, 100 participants diagnosed with optic neuritis were followed up for 6 years. There was no association between tNAA in NAWM and the development of medium term disability (Swanton *et al.*, 2009). Despite using the same SVS acquisition and similarities in CIS presentation of both cohorts (optic neuritis 86/96 in our cohort), there may be several reasons for the differences between our results and those reported by Swanton J.K et al. First, our cohort underwent follow up at 15 years with 70% converting to MS compared to 48%. Second, of those EDSS scores at 15 years, 37% (24/89) had a score of $\geq$ 3.0 compared to just 12%. Last, our sample size that underwent ^{1}H-MRS was higher (n = 96 versus n = 74) thereby slightly increasing our statistical power (Swanton *et al.*, 2009).

To my knowledge, this 15 year follow up study is the longest follow up of a CIS cohort where brain metabolite values were measured at CIS onset. I demonstrated for the first time that decreased neuroaxonal integrity and mitochondrial function in NAWM in early relpase onset MS is associated with an increased risk of moderate-severe long-term disability. In the context of other established MRI predictors of long-term disability following CIS, tNAA in NAWM remained a significant predictor in the model that also included

measures of brain volume, lesion load, gadolonium-enhancing and spinal cord lesions.

T2LV was also associated with an increased risk of developing moderate-severe disability at 15 years. This is in keeping with multiple studies that have previously demonstrated the association between lesion load and long term disability (Filippi *et al.*, 1994; Sailer *et al.*, 1999; Brex *et al.*, 2002; L. K. Fisniku *et al.*, 2008; Swanton *et al.*, 2009).

There are however several considerations when interpreting our results. First, the cross-sectional analysis of this cohort did not identify a difference in NAWM tNAA between CIS and controls. However tNAA/tCr in NAWM was decreased compared to controls (Fernando *et al.*, 2004). The latter result in addition to several studies showing decreased tNAA in NAWM or whole brain suggest that neuroaxonal integrity is decreased in CIS compared to controls. The differences in ^{1}H-MRS acquisition and variations in CIS cohorts also need to be taken into account (M. Rovaris *et al.*, 2005; Audoin *et al.*, 2007; Wattjes *et al.*, 2007; M. P. Wattjes *et al.*, 2008).

7.4.2 The association between metabolite levels and risk of secondary progression multiple sclerosis at 15 years

When examining the cohort diagnosis at 15 years (CIS, RRMS or SPMS), tNAA levels at CIS onset were decreased in SPMS and RRMS compared to those who remained CIS.

3-month tNAA in NAWM was not associated with an increased risk of SPMS. This could be explained by the proportions of participants that developed each outcome – 15/91 (16%) for SPMS as opposed to 24/89 (27%) with EDSS $\geq$ 3.0. Whilst there is some overlap between the two groups, they may also reflect differing populations with SPMS likely representing a period of ongoing disability progression as opposed to those with an EDSS $\geq$ 3.0 who have developed this outcome following a relapse but may not go on to develop SPMS. Variability in definitions and classification of the secondary progressive phase of MS also need to be taken into account.

Previous studies have shown that gadolinium-enhancing lesions are associated with an increased odds of conversion to SPMS and the development of medium term disability. I did not identify this association which may be due to the smaller sample size of our cohort compared to that described by Brownlee et al (Brownlee *et al.*, 2019). The low proprotion of those with gadolinium enhancing lesions that developed SPMS (5/15) may have also affected our ability to find an association.

7.4.3 Associations with physical and cognitive performance measures at 15 years

Decreased 3-month tNAA levels was correlated with decreased T25FW performance at 15 years. However, this was not confirmed in the multiple regression model with baseline number of cord lesions being the only significant predictor of ambulation speed at 15 years. Spinal cord pathology has a significant impact on ambulation and may be in keeping with the central length dependent axonopathy hypothesis whereby ambulation is affected before upper limbs (Giovannoni *et al.*, 2017). The presence of spinal cord lesions early in relapse onset MS is established as a predictor of long term disability and reflects the significant impact of early spinal cord lesions and long term ambulatory disability (Brownlee *et al.*, 2017, 2019).

I did not find any other associations between 3-month metabolites (mIns, tCho, Glx, tCr, tNAA) and physical (9HPT, T25FW) and cognitive disability measures (PASAT3, SDMT) at 15 years. This could be for several reasons – firstly that there is no association between markers of astrogliosis, membrane turnover and glutamate/glutamine levels and measures of physical disability at 15-years. This may be supported by the lack of correlation between mIns, tCho and T2LV at 15 years. Second, each metabolite and its putative pathological correlate also needs consideration. For example, tCho is a marker of membrane turnover and cellularity and is increased in active demyelinating lesions (Brenner *et al.*, 1993; Roser *et al.*, 1995); and the shift the in pathology over 15 years from driven by focal inflammatory demyelination to one that is

predominantly neurodegenerative may make it less likely that baseline tCho in CIS is associated with long term disability in MS.

mIns and tCr were both increased in NAWM of the CIS cohort compared to HC in the cross-sectional analysis at the 3-month visit. I did not identify any metabolite differences in groups between those that developed disability at 15 years and those that did not (Fernando *et al.*, 2004). Furthermore, mIns was not associated with brain T2LV at 15 years and mIns was not significantly different between those that developed SPMS/RRMS or remained CIS.

No associations were found between tCr, mIns and physical and cognitive performance measures. This could be explained by the fact there were no cross-sectional correlations between tCr, mIns and EDSS – suggesting that these metabolite changes may be significant in understanding the pathology of CIS in NAWM, they are not long-term prognostic markers (Fernando *et al.*, 2004). Astrocytes promote neuroinflammation, glial scar formation but also facilite remyelination and neuroprotection and this duality may affect the ability of mIns to be used as a consistent long-term prognostic marker in CIS/MS (Correale and Farez, 2015; Ponath, Park and Pitt, 2018).

A significant proportion of participants did not undergo the SDMT or PASAT at 15-year follow-up (39/96 and 37/96 respectively) reducing our power to find a statistically significant association; or there is no association to be found. There are no previous studies reported for comparison.

7.4.4 **Post-hoc analyses**

I also identified a tNAA level of 7.32mM as the optimal cut-off in our dataset. Applying this cut-off in the multiple logistic regression model, having a tNAA value < 7.32 increased the odds of developing moderate-severe disability at 15 years by more than a factor of 6. The model had strong ability to discriminate between thoses who developed an EDSS $\geq$ 3.0 with a model c-statistic 0.90. The use of a cut-off can provide stratification of our cohort into two groups and adjunctive long-term prognostic information. The low sensitivity suggests that most practical use is to identify those more likely to take a benign course over 15 years. There are however, several key issues in

utilising tNAA as an individual prognostic marker in CIS or early relapse onset MS. These considerations include the fact that metabolite quantification is affected by scanner type and settings, sequence parameters, choice of internal reference, and metabolite fitting software. Our findings are therefore specific to this scanner and dataset only. There has been an attempt to generate consenus recommendations for the use of ^{1}H-MRS in clinical practice (Wilson *et al.*, 2019). However, further validation with different cohorts and scanner settings would be required before our findings can be generalised or utilised as a potential individual prognostic marker.

The number of spinal cord lesions at CIS onset was associated with long-term disability outcomes in each of the models. In each of the aforementioned models, for every unit increase in spinal cord lesions, the odds of developing SPMS or EDSS $\geq$ 3.0 is increased by 3.6-3.9. Furthermore, a higher baseline number of spinal cord lesions was associated with decreased performance on T25FW at 15 years.These findings are in keeping with previous long term CIS follow up studies that have shown spinal cord lesions to be a long-term prognostic marker following CIS (Swanton *et al.*, 2009; Tintore *et al.*, 2015; Brownlee *et al.*, 2017, 2019).

7.4.5 **Strengths and limitations**

The strengths of this study are the prospective design and duration of follow up of this largely untreated cohort from CIS to the 15-year visit. The rigorous data acquisition and willingness of participants to maintain participation in the study resulted in low rates of missing data. The SVS protocol and metabolite quantification technique used (LCModel®) could be generalised, with quality assurance and calibration requirements that appear to be feasible in clinical practice. I focused on metabolites measured in NAWM rather than WML to minimise contaimination of the volume of interest by different tissue types.

There are several limitations of the study – first, SVS was undertaken at 3 months after the baseline structural MRI which also resulted in the need to use normalised brain volume and spinal cord lesion measurements from the

baseline visit. However more than 90% of scans occurred within 6 months of CIS onset and the median time between baseline and 3-month MRI scans was 0.26 years. Second, the cohort contained a large proportion of participants that presented with optic neuritis (86/96) and combined with the low final EDSS (median 1.5) highlights the importance of validating our findings in cohorts containing a greater variety of CIS presentations and disability levels. Third, I did not include the use of DMT as a model covariate due the effect of reverse causality whereby those on therapy are more likely to have a favourable outcome which would distort the other model MRI varables. Fourth, tCr has been widely used in the literature as a stable reference metabolite in ^{1}H-MRS studies in CIS/MS. However, I did not calculate metabolite ratios to tCr due to initial concerns that tCr may not be stable reference metabolite in MS (Suhy *et al.*, 2000; Vrenken *et al.*, 2005). Changes to the McDonald MS diagnostic criteria over the 15 years, may have had an impact on disease classification with the recent inclusion of CSF oligoclonal bands potentially resulting in a greater proportion of participants with CIS being diagnosed with MS than was determined when this study was completed (Thompson *et al.*, 2018). Finally, telephone EDSS was used to capture EDSS data in 26/89 (29%) of participants. Whilst there is strong correlation between the two methods, especially at higher EDSS scores, the differences in EDSS capture between the examination and telephone methods needs to be taken into account (Lechner-Scott *et al.*, 2003).

7.4.6 **Conclusion**

Alterations in NAWM neuroxonal integrity and mitochondrial function in early relapse onset MS is associated with an increased risk of moderate-severe disability at 15 years. The use of tNAA as an individual prognostic marker is currently difficult due to an inability to validate and generalise metabolite results across difference scanners and acquisitions. Further validation and consenus guidelines on the generalisabilty of ^{1}H-MRS is required to support its role as a long-term prognostic marker in the early stages of MS. Early spinal cord pathology in relapse onset MS is a significant predictor of ambulatory dysfunction at 15 years.

Chapter 8. Conclusions and future directions

8.1 Introduction

I have used ^{1}H-MRS to examine metabolic markers of brain injury in SPMS and CIS with five main objectives: (1) improve our understanding of metabolic changes occurring over 96-weeks in SPMS; (2) explore the mechanism of action of three potential neuroprotective agents used in a phase 2b multi-arm placebo-controlled trial SPMS; (3) identify biomarkers of clinical disability in SPMS (4) use MRI measures of axonal injury, myelin loss, regional atrophy and lesion load to better understand disability progression in SPMS over 96-weeks; and (5) determine if metabolic markers measured during early relapse onset MS are associated with long-term disability.

8.2 Brain metabolite changes occurring over 96-weeks in secondary progressive multiple sclerosis

Examining the placebo trial arm from the study cohort to identify the change in brain metabolites over 96-weeks did not demonstrate any changes in tNAA, mIns or Glx in NAWM or CGM. Over 96-weeks, there was an increase in tCho (and tCho/tCr) in CGM; and a decrease in NAWM tCho. These findings are from a smaller sample size and several of the results are in keeping with previous longitudinal studies of brain metabolite changes in SPMS where no change in tNAA or mIns were found. The increase in tCho in GM may support the increasingly recognised role of cortical damage mediated by meningeal inflammation. However, when balanced against the reduction in tCho in NAWM, it underscores the challenges in interpreting tCho due to the various choline compounds contained within the tCho spectrum peak.

8.3 Mechanism of action of three potential neuroprotective agents used in a phase 2b multi-arm placebo-controlled trial in secondary progressive multiple sclerosis

I used ^{1}H-MRS to explore whether amiloride, fluoxetine and riluzole reached their purported mechanistic targets of action when used as neuroprotective agents in a phase 2b trial in SPMS. Exploring drug-specific *a priori* defined

hypotheses, I demonstrated that fluoxetine had no effect on tNAA or tCho, amiloride had no effect on tNAA and riluzole decreased Glx levels in CGM but not NAWM.

Fluoxetine has previously demonstrated effects on neuroaxonal integrity and inflammatory activity but in smaller cohorts in different MS subtypes. In this larger randomised control trial of SPMS, fluoxetine had no effect on metabolic markers of neuroaxonal integrity and membrane turnover. This was in keeping with the overall results of this and other clinical trials of fluoxetine in PMS which have not shown any benefit.

Amiloride has a neuroprotective effect on axons and oligodendrocytes in animal models of MS and therefore tNAA was the most appropriate candidate to measure the response of amiloride to engage axons as part of its therapeutic mechanism of action in PMS. I did not identify any effect of amiloride on tNAA suggesting that amiloride had minimal benefit on preserving neuroaxonal integrity.

Riluzole was thought to have neuroprotective potential in SPMS by decreasing glutamatergic excitotoxicity and sodium channel blockade. I found that riluzole decreased Glx levels in CGM but not NAWM. This was interesting on several levels. First, riluzole appeared to engage its mechanistic target and decreased Glx levels in CGM but this did translate into a decrease in the rate of brain atrophy. Second, riluzole had a compartmentalised effect in decreasing Glx levels in CGM but having no effect on NAWM. This of course was caveated by the limitations of the technique with uncertainty surrounding differentiation between measuring intracellular or extracellular Glx levels and the fact that I was unable to resolve glutamate and glutamine using this CSI technique.

My findings support the role of ^{1}H-MRS in analysing the mechanistic pathways of therapeutic agents used in phase I and phase II clinical trials. One can test biologically plausible *in vivo* targets in various forms of MS where ^{1}H-MRS can provide valuable information that extends beyond the metrics provided by more conventional structural MRI.

8.4 Brain metabolic markers of clinical disability in secondary progressive multiple sclerosis

In the MS-SMART advanced MRI substudy, decreased baseline NAWM tNAA was associated with upper limb function – measured using 9HPT. This was firstly demonstrated in a cross-sectional analysis, and then confirmed at 96-weeks after adjusting demographic variables, lesion load and brain volumes. This suggests a key role for neuroaxonal integrity and mitochondrial function in NAWM in the development of decreased upper limb function.

I further examined the question of which pathological substrates drive clinical disability in SPMS by using a multiple regression analysis to explore which baseline MRI markers of axonal loss/dysfunction, myelin damage, regional atrophy and inflammation (lesion volume) were best associated with clinical disability over 96-weeks. The findings further supported those seen in chapter 5 with decreased baseline CGM volume and NAWM tNAA associated with upper limb function at 96-weeks.

We then undertook a multi-modal analysis of different pathological substrates in SPMS in the brain and spine. SCA was the most significant predictor of both upper limb and ambulatory disability, exhibiting a stronger association than that seen with brain markers.

All of this is instructive. First, it is important to continue to develop our understanding of the microstructural changes that lead to SCA and CGM atrophy using advanced multi-modal MRI datasets. Second, it may be of benefit to address spinal cord as a key therapeutic target when developing agents that seek to stabilise or improve arm and walking disability in SPMS. Third, it supports the hypothesis that PMS is a central length dependent axonopathy affecting legs first before later affecting upper limb function, which relies on pathways predominantly residing in the brain and cervical cord.

Decreased baseline NAWM tNAA was associated with decreased IPS in a cross-sectional analysis. This was not confirmed at 96-weeks and it became clear that baseline brain T2 lesion load was most closely associated with a reduction in IPS performance. This builds on previous findings in other PMS

cohorts. T2LV (lesion load) is not pathologically specific and our finding emphasises the need to develop improved biomarkers of chronic inflammation in PMS.

8.5 Metabolic changes in clinically isolated syndrome and their association with long term disability

In a 15-year follow up study of CIS, NAWM tNAA is associated with the development of moderate-severe disability defined as an EDSS $\geq$ 3.0 at 15 years. Decreases in neuroaxonal integrity and mitochondrial function during the earliest stages of MS are associated with long term disability. This association was significant after accounting for various lesion metrics and NBV.

Multiple studies examining the long-term outcomes following CIS have demonstrated predominantly lesion based measures as predictors of long-term disability. However, these imaging measures do not completely explain the variance seen between CIS and long-term disability, and apart from enhancing lesions, are not pathologically specific. This finding improves our understanding of the metabolic changes in early relapse onset MS and its association with long term disability. Of particular interest is the concept of early changes in energy metabolism in non-lesional white matter that impact long term disability. Whilst requiring further validation, this presents a potential therapeutic target in early MS.

8.6 Future directions

The role of decreased NAWM neuroaxonal integrity, CGM and SCA in driving upper limb function in SPMS requires further examination and validation. A regional analysis is planned to determine if specific regions in CGM or NAWM are associated with long-term upper limb dysfunction. Further analysis in another cohort with PMS is required. This should include comparison with age and sex matched HC, examination of values in WM and GM lesions, and incorporation of a greater proportion of available brain tissue (if feasible given timing constraints).

The analysis used WM T2 lesion volume as the main measure of lesion load and inflammation. There is evidence that smouldering inflammation reflected by chronic active or slowly expanding lesions in WM are better markers of chronic neuroinflammation seen in PMS. These are being identified and segmented using an algorithm developed at Queen Square UCL Institute of Neurology. It would be of interest to incorporate them into the models as a potentially more sensitive marker of inflammation in SPMS.

Our finding that decreased NAWM tNAA in CIS a long-term prognostic marker requires further validation. This would take several forms: first, using a different CIS cohort with long term follow up. Second, testing the hypothesis in a CIS cohort with slightly different characteristics; such as one with a more balanced CIS phenotype that had a lower proportion of optic neuritis. Last, validation accounting for different scanner types, acquisition parameters and software analysis programs is required to determine generalisability with a view to its potential use in clinical practice. Furthermore, consensus guidelines to standardise ^{1}H-MRS acquisition and metabolite quantification across different settings is required before any consideration can be given to its use as an individual prognostic marker.

There is the additional availability of data on serum neurofilament light chains in the 15-year CIS follow up cohort. I plan to add this into the models and explore its association cross-sectional and longitudinal association between tNAA in NAWM and serum neurofilament light chain.

8.7 Conclusions

In an SPMS cohort studied using CSI, I identified alterations in a marker of membrane turnover over 96-weeks. Exploring drug target engagement suggests an ongoing role for ^{1}H-MRS in early phase trials of neuroprotective agents in SPMS; where the effect of agents on biologically plausible metabolic markers of brain injury informs the mechanisms of *in vivo* targets. Spinal cord pathology was the strongest predictor of upper limb and ambulatory dysfunction over 96-weeks in SPMS. Further understanding of the causes of SCA are needed to aid the development of neuroprotective strategies that

focus on the preservation of upper limb function and mobility in PMS. T2LV was best associated with deterioration in IPS but further study needed to understand the microstructural changes that underpin this. Finally, in a 15-year follow up study of people with CIS, early changes in NAWM neuroaxonal integrity and mitochondrial function are associated with moderate to severe disability 15 years later.

References

Abdel-Aziz, K. *et al.* (2015) ‘Evidence for early neurodegeneration in the cervical cord of patients with primary progressive multiple sclerosis.’, *Brain : a journal of neurology*. Oxford University Press, 138(Pt 6), pp. 1568–82. doi: 10.1093/brain/awv086.

Aboul-Enein, F. *et al.* (2010) ‘Reduced NAA-levels in the NAWM of patients with MS is a feature of progression. A study with quantitative magnetic resonance spectroscopy at 3 Tesla.’, *PloS one*. Public Library of Science, 5(7), p. e11625. doi: 10.1371/journal.pone.0011625.

Absinta, M., Lassmann, H. and Trapp, B. D. (2020) ‘Mechanisms underlying progression in multiple sclerosis.’, *Current opinion in neurology*. NLM (Medline), 33(3), pp. 277–285. doi: 10.1097/WCO.0000000000000818.

Adalsteinsson, E. *et al.* (2003) ‘Gray Matter n-Acetyl Aspartate Deficits in Secondary Progressive but Not Relapsing-Remitting Multiple Sclerosis’, *American Journal of Neuroradiology*, 24(10). Available at: http://www.ajnr.org/content/24/10/1941.long (Accessed: 7 September 2018).

Allen, C. M. *et al.* (2020) ‘Prognostication and contemporary management of clinically isolated syndrome’, *Journal of Neurology, Neurosurgery and Psychiatry*. BMJ Publishing Group, pp. 1–7. doi: 10.1136/jnnp-2020-323087.

Allen, I. V. and McKeown, S. R. (1979) ‘A histological, histochemical and biochemical study of the macroscopically normal white matter in multiple sclerosis’, *Journal of the Neurological Sciences*, 41(1), pp. 81–91. doi: 10.1016/0022-510X(79)90142-4.

Almeida, L. S. *et al.* (2006) ‘Exocytotic release of creatine in rat brain’, *Synapse*, 60(2), pp. 118–123. doi: 10.1002/syn.20280.

Alroughani, R. A. *et al.* (2015) ‘Clinical predictors of disease progression in multiple sclerosis patients with relapsing onset in a nation-wide cohort’, *International Journal of Neuroscience*, 125(11), pp. 831–837. doi: 10.3109/00207454.2014.976641.

Amann, M. *et al.* (2015) ‘Magnetization transfer ratio in lesions rather than normal-appearing brain relates to disability in patients with multiple sclerosis’, *Journal of Neurology*. Springer Berlin Heidelberg, 262(8), pp. 1909–1917. doi: 10.1007/s00415-015-7793-5.

Ammitzbøll, C. *et al.* (2018) ‘Disability in progressive MS is associated with T2 lesion changes’, *Multiple Sclerosis and Related Disorders*. Elsevier B.V., 20, pp. 73–77. doi: 10.1016/j.msard.2017.12.010.

De Angelis, F. *et al.* (2020) ‘Amiloride, fluoxetine or riluzole to reduce brain volume loss in secondary progressive multiple sclerosis: the MS-SMART four-arm RCT’, *Efficacy and Mechanism Evaluation*, 7(3), pp. 1–72. doi: 10.3310/eme07030.

Arnett, P. A. *et al.* (1994) ‘Relationship between frontal lobe lesions and Wisconsin card sorting test performance in patients with multiple sclerosis’, *Neurology*, 44(3), pp. 420–425. doi: 10.1212/wnl.44.3_part_1.420.

Arnold, D. L. *et al.* (1990) ‘Proton magnetic resonance spectroscopy of human brain in vivo in the evaluation of multiple sclerosis: assessment of the load of disease.’, *Magnetic resonance in medicine*, 14(1), pp. 154–9. Available at: http://www.ncbi.nlm.nih.gov/pubmed/2161982 (Accessed: 30 May 2019).

Arnold, D. L. *et al.* (1994) ‘Use of proton magnetic resonance spectroscopy for monitoring disease progression in multiple sclerosis’, *Annals of Neurology*, 36(1), pp. 76–82. doi: 10.1002/ana.410360115.

Ascherio, A. *et al.* (2014) ‘Vitamin D as an early predictor of multiple sclerosis activity and progression’, *JAMA Neurology*. American Medical Association, 71(3), pp. 306–314. doi: 10.1001/jamaneurol.2013.5993.

Audoin, B. *et al.* (2007) ‘Onset and underpinnings of white matter atrophy at the very early stage of multiple sclerosis - a two-year longitudinal MRI/MRSI study of corpus callosum’, *Multiple Sclerosis Journal*, 13(1), pp. 41–51. doi: 10.1177/1352458506071215.

Azevedo, C. J. *et al.* (2014) ‘In vivo evidence of glutamate toxicity in multiple

sclerosis', *Annals of Neurology*. John Wiley & Sons, Ltd, 76(2), pp. 269–278. doi: 10.1002/ana.24202.

Azevedo, C. J. *et al.* (2018) 'Thalamic atrophy in multiple sclerosis: A magnetic resonance imaging marker of neurodegeneration throughout disease', *Annals of Neurology*. John Wiley and Sons Inc., 83(2), pp. 223–234. doi: 10.1002/ana.25150.

Bagert, B. A. (2009) 'Epstein-Barr virus in multiple sclerosis', *Current Neurology and Neuroscience Reports*, pp. 405–410. doi: 10.1007/s11910-009-0059-9.

Bagory, M. *et al.* (2007) '"Absolute" quantification in magnetic resonance spectroscopy: validation of a clinical protocol in multiple sclerosis.', *Conference proceedings : ... Annual International Conference of the IEEE Engineering in Medicine and Biology Society. IEEE Engineering in Medicine and Biology Society. Annual Conference*. IEEE, 2007, pp. 3458–61. doi: 10.1109/IEMBS.2007.4353075.

Baranzini, S. E. *et al.* (2010) 'Genetic variation influences glutamate concentrations in brains of patients with multiple sclerosis', *Brain*. Oxford University Press, 133(9), pp. 2603–2611. doi: 10.1093/brain/awq192.

Barkercollo, S. (2005) 'Within session practice effects on the PASAT in clients with multiple sclerosis', *Archives of Clinical Neuropsychology*, 20(2), pp. 145–152. doi: 10.1016/j.acn.2004.03.007.

Barkhof, F. *et al.* (2003) 'Remyelinated lesions in multiple sclerosis: Magnetic resonance image appearance', *Archives of Neurology*. American Medical Association, 60(8), pp. 1073–1081. doi: 10.1001/archneur.60.8.1073.

Barkhof, F. *et al.* (2009) 'Imaging outcomes for neuroprotection and repair in multiple sclerosis trials', *Nature Reviews Neurology*, 5(5), pp. 256–266. doi: 10.1038/nrneurol.2009.41.

Batista, S. *et al.* (2012) 'Basal ganglia, thalamus and neocortical atrophy predicting slowed cognitive processing in multiple sclerosis', *Journal of*

Neurology, 259(1), pp. 139–146. doi: 10.1007/s00415-011-6147-1.

Béard, E. and Braissant, O. (2010) 'Synthesis and transport of creatine in the CNS: importance for cerebral functions', *Journal of Neurochemistry*, 115(2), pp. 297–313. doi: 10.1111/j.1471-4159.2010.06935.x.

Beecham, A. H. *et al.* (2013) 'Analysis of immune-related loci identifies 48 new susceptibility variants for multiple sclerosis', *Nature Genetics*. Nature Publishing Group, 45(11), pp. 1353–1362. doi: 10.1038/ng.2770.

Bellenberg, B. *et al.* (2013) '1H-Magnetic Resonance Spectroscopy in diffuse and focal cervical cord lesions in Multiple Sclerosis', *European Radiology*, 23(12), pp. 3379–3392. doi: 10.1007/s00330-013-2942-7.

Bellingham, M. C. (2011) 'A Review of the Neural Mechanisms of Action and Clinical Efficiency of Riluzole in Treating Amyotrophic Lateral Sclerosis: What have we Learned in the Last Decade?', *CNS Neuroscience & Therapeutics*. Wiley-Blackwell, 17(1), p. 4. doi: 10.1111/J.1755-5949.2009.00116.X.

Benedict, R. H. *et al.* (2017) 'Validity of the Symbol Digit Modalities Test as a cognition performance outcome measure for multiple sclerosis.', *Multiple sclerosis (Houndmills, Basingstoke, England)*. SAGE Publications, 23(5), pp. 721–733. doi: 10.1177/1352458517690821.

Benuck, M. and D'Adamo, A. F. (1968) 'Acetyl transport mechanisms Metabolism of acid in the non-nervous tissues of the rat', *Biochimica et Biophysica Acta (BBA) - Lipids and Lipid Metabolism*, 152(3), pp. 611–618. doi: 10.1016/0005-2760(68)90101-X.

Bergamaschi, R. *et al.* (2016) 'Immunomodulatory therapies delay disease progression in multiple sclerosis.', *Multiple sclerosis (Houndmills, Basingstoke, England)*, 22(13), pp. 1732–1740. doi: 10.1177/1352458512445941.

Bergers, E. *et al.* (2002) 'Axonal damage in the spinal cord of MS patients occurs largely independent of T2 MRI lesions', *Neurology*. Lippincott Williams and Wilkins, 59(11), pp. 1766–1771. doi: 10.1212/01.WNL.0000036566.00866.26.

Bhakoo, K. K. and Pearce, D. (2001) ‘In Vitro Expression of N-Acetyl Aspartate by Oligodendrocytes’, *Journal of Neurochemistry*, 74(1), pp. 254–262. doi: 10.1046/j.1471-4159.2000.0740254.x.

Bitsch, A. *et al.* (1999) ‘Inflammatory CNS demyelination: histopathologic correlation with in vivo quantitative proton MR spectroscopy.’, *AJNR. American journal of neuroradiology*. American Journal of Neuroradiology, 20(9), pp. 1619–27. Available at: http://www.ncbi.nlm.nih.gov/pubmed/10543631 (Accessed: 24 November 2017).

Bjartmar, C. *et al.* (2000) ‘Neurological disability correlates with spinal cord axonal loss and reduced N-acetyl aspartate in chronic multiple sclerosis patients.’, *Annals of neurology*, 48(6), pp. 893–901. Available at: http://www.ncbi.nlm.nih.gov/pubmed/11117546 (Accessed: 27 December 2018).

Bjartmar, C. *et al.* (2001) ‘Axonal loss in normal-appearing white matter in a patient with acute MS.’, *Neurology*, 57(7), pp. 1248–52. Available at: http://www.ncbi.nlm.nih.gov/pubmed/11591844 (Accessed: 30 April 2019).

Bjartmar, C. *et al.* (2002) ‘N-acetylaspartate is an axon-specific marker of mature white matter in vivo: a biochemical and immunohistochemical study on the rat optic nerve.’, *Annals of neurology*, 51(1), pp. 51–8. Available at: http://www.ncbi.nlm.nih.gov/pubmed/11782984 (Accessed: 11 July 2019).

Bjartmar, C., Wujek, J. R. and Trapp, B. D. (2003) ‘Axonal loss in the pathology of MS: consequences for understanding the progressive phase of the disease.’, *Journal of the neurological sciences*, 206(2), pp. 165–71.

Bloch, F. (1946) ‘Nuclear induction’, *Physical Review*. American Physical Society, 70(7–8), pp. 460–474. doi: 10.1103/PhysRev.70.460.

Bot, J. C. J. *et al.* (2004) ‘The Spinal Cord in Multiple Sclerosis: Relationship of High-Spatial-Resolution Quantitative MR Imaging Findings to Histopathologic Results’, *Radiology*. Radiological Society of North America, 233(2), pp. 531–540. doi: 10.1148/radiol.2332031572.

Bothwell, J. H. *et al.* (2001) ‘Hypo-osmotic swelling-activated release of organic osmolytes in brain slices: implications for brain oedema in vivo’, *Journal of Neurochemistry*, 77(6), pp. 1632–1640. doi: 10.1046/j.1471-4159.2001.00403.x.

Bothwell, J. H., Styles, P. and Bhakoo, K. K. (2002) ‘Swelling-activated Taurine and Creatine Effluxes from Rat Cortical Astrocytes are Pharmacologically Distinct’, *Journal of Membrane Biology*, 185(2), pp. 157–164. doi: 10.1007/s00232-001-0121-2.

Bottomley, P. A. and Park, C. (1982) *United States Patent - Selective Volume Method for Performing Localised NMR*.

Braissant, O. *et al.* (2001) ‘Endogenous synthesis and transport of creatine in the rat brain: an in situ hybridization study’, *Molecular Brain Research*, 86(1–2), pp. 193–201. doi: 10.1016/S0169-328X(00)00269-2.

Braissant, O. *et al.* (2010) ‘Dissociation of AGAT, GAMT and SLC6A8 in CNS: Relevance to creatine deficiency syndromes’, *Neurobiology of Disease*, 37(2), pp. 423–433. doi: 10.1016/j.nbd.2009.10.022.

Brand, A., Richter-Landsberg, C. and Leibfritz, D. (1993) ‘Multinuclear NMR Studies on the Energy Metabolism of Glial and Neuronal Cells’, *Developmental Neuroscience*. Karger Publishers, 15(3–5), pp. 289–298. doi: 10.1159/000111347.

Brass, S. D. *et al.* (2004) ‘Axonal Damage in Multiple Sclerosis Patients with High versus Low Expanded Disability Status Scale Score’, *The Canadian Journal of Neurological Sciences*. Cambridge University Press, 31(02), pp. 225–228. doi: 10.1017/S0317167100053877.

Brenner, R. E. *et al.* (1993) ‘The proton NMR spectrum in acute EAE: The significance of the change in the Cho:Cr ratio’, *Magnetic Resonance in Medicine*. Magn Reson Med, 29(6), pp. 737–745. doi: 10.1002/mrm.1910290605.

Brex, P. A. *et al.* (1999) ‘Multisequence MRI in clinically isolated syndromes

and the early development of MS', *Neurology*. Lippincott Williams and Wilkins, 53(6), pp. 1184–1190. doi: 10.1212/wnl.53.6.1184.

Brex, P A *et al.* (1999) 'Proton MR spectroscopy in clinically isolated syndromes suggestive of multiple sclerosis.', *Journal of the neurological sciences*, 166(1), pp. 16–22. doi: 10.1016/s0022-510x(99)00105-7.

Brex, P. A. *et al.* (2000) 'Lesion heterogeneity in multiple sclerosis: a study of the relations between appearances on T1 weighted images, T1 relaxation times, and metabolite concentrations.', *Journal of neurology, neurosurgery, and psychiatry*. BMJ Publishing Group Ltd, 68(5), pp. 627–32. doi: 10.1136/JNNP.68.5.627.

Brex, P. A. *et al.* (2002) 'A Longitudinal Study of Abnormalities on MRI and Disability from Multiple Sclerosis', *New England Journal of Medicine*. New England Journal of Medicine (NEJM/MMS), 346(3), pp. 158–164. doi: 10.1056/nejmoa011341.

Brink, H. F., Buschmann, M. D. and Rosen, B. R. (1989) 'NMR chemical shift imaging', *Computerized Medical Imaging and Graphics*. Pergamon, 13(1), pp. 93–104. doi: 10.1016/0895-6111(89)90081-5.

Brodsky, M. *et al.* (2008) 'Multiple sclerosis risk after optic neuritis: Final optic neuritis treatment trial follow-up', *Archives of Neurology*, 65(6), pp. 727–732. doi: 10.1001/archneur.65.6.727.

Brown, J. W. L. *et al.* (2019) 'Association of Initial Disease-Modifying Therapy with Later Conversion to Secondary Progressive Multiple Sclerosis', *JAMA - Journal of the American Medical Association*. American Medical Association, 321(2), pp. 175–187. doi: 10.1001/jama.2018.20588.

Brown, J. W. L. *et al.* (2020) 'Magnetisation transfer ratio abnormalities in primary and secondary progressive multiple sclerosis', *Multiple Sclerosis Journal*. SAGE Publications Ltd, 26(6), pp. 679–687. doi: 10.1177/1352458519841810.

Brown, J. W. L. and Chard, D. T. (2016) 'The role of MRI in the evaluation of

secondary progressive multiple sclerosis', *Expert Review of Neurotherapeutics*. Taylor and Francis Ltd, pp. 157–171. doi: 10.1586/14737175.2016.1134323.

Brown, T. R., Kincaid, B. M. and Ugurbil, K. (1982) 'NMR chemical shift imaging in three dimensions.', *Proceedings of the National Academy of Sciences*, 79(11), pp. 3523–3526. doi: 10.1073/pnas.79.11.3523.

Browne, P. *et al.* (2014) 'Atlas of multiple sclerosis 2013: A growing global problem with widespread inequity', *Neurology*. Lippincott Williams and Wilkins, pp. 1022–1024. doi: 10.1212/WNL.0000000000000768.

Brownlee, W. J. *et al.* (2017) 'Association of asymptomatic spinal cord lesions and atrophy with disability 5 years after a clinically isolated syndrome', *Multiple Sclerosis*. SAGE Publications Ltd, 23(5), pp. 665–674. doi: 10.1177/1352458516663034.

Brownlee, W. J. *et al.* (2019) 'Early imaging predictors of long-term outcomes in relapse-onset multiple sclerosis', *Brain : a journal of neurology*. NLM (Medline), 142(8), pp. 2276–2287. doi: 10.1093/brain/awz156.

Brownlee, W. J. and Miller, D. H. (2014) 'Clinically isolated syndromes and the relationship to multiple sclerosis', *Journal of Clinical Neuroscience*. Churchill Livingstone, pp. 2065–2071. doi: 10.1016/j.jocn.2014.02.026.

Burgess P and T, S. (1997) *The Hayling and Brixton Tests*. Bury St Edmunds: Thames Valley Test Company.

Calabrese, M. *et al.* (2009) 'Cortical lesions and atrophy associated with cognitive impairment in relapsing-remitting multiple sclerosis', *Archives of Neurology*, 66(9), pp. 1144–1150. doi: 10.1001/archneurol.2009.174.

Calvi, A. *et al.* (2020) 'In vivo imaging of chronic active lesions in multiple sclerosis', *Multiple Sclerosis Journal*. SAGE Publications Ltd, p. 135245852095858. doi: 10.1177/1352458520958589.

Cambron, M. *et al.* (2014) 'Fluoxetine in Progressive Multiple Sclerosis

(FLUOX-PMS): study protocol for a randomized controlled trial', *Trials*, 15(1), p. 37. doi: 10.1186/1745-6215-15-37.

Cambron, M. *et al.* (2019) 'Fluoxetine in progressive multiple sclerosis: The FLUOX-PMS trial.', *Multiple sclerosis (Houndmills, Basingstoke, England)*, 25(13), pp. 1728–1735. doi: 10.1177/1352458519843051.

Caramanos, Z. *et al.* (2009) '1H-MRSI evidence for cortical gray matter pathology that is independent of cerebral white matter lesion load in patients with secondary progressive multiple sclerosis', *Journal of the Neurological Sciences*. Elsevier, 282(1–2), pp. 72–79. doi: 10.1016/J.JNS.2009.01.015.

Caramanos, Z., Narayanan, S. and Arnold, D. L. (2005) '1H-MRS quantification of tNA and tCr in patients with multiple sclerosis: a meta-analytic review', *Brain*, 128(11), pp. 2483–2506. doi: 10.1093/brain/awh640.

Cardoso, M. J. *et al.* (2012) 'Geodesic information flows.', *Medical image computing and computer-assisted intervention : MICCAI ... International Conference on Medical Image Computing and Computer-Assisted Intervention*, 15(Pt 2), pp. 262–70. Available at: http://www.ncbi.nlm.nih.gov/pubmed/23286057 (Accessed: 25 May 2018).

Cardoso, M. J. *et al.* (2015) 'Geodesic Information Flows: Spatially-Variant Graphs and Their Application to Segmentation and Fusion', *IEEE Transactions on Medical Imaging*, 34(9), pp. 1976–1988. doi: 10.1109/TMI.2015.2418298.

Casserly, C. *et al.* (2018) 'Spinal Cord Atrophy in Multiple Sclerosis: A Systematic Review and Meta-Analysis', *Journal of Neuroimaging*. Blackwell Publishing Inc., 28(6), pp. 556–586. doi: 10.1111/jon.12553.

Cawley, N. *et al.* (2015) 'Reduced gamma-aminobutyric acid concentration is associated with physical disability in progressive multiple sclerosis.', *Brain : a journal of neurology*. Oxford University Press, 138(Pt 9), pp. 2584–95. doi: 10.1093/brain/awv209.

Charcot, J.-M. J.-M. (1885) 'Leçons sur les Maladies du Système Nerveux.', *Paris A. Delahaye.*, 26, p. 564.

Chataway, J. *et al.* (2001) ‘Multiple sclerosis in sibling pairs: an analysis of 250 families’, *Journal of Neurology, Neurosurgery & Psychiatry*, 71, pp. 757–761. doi: 10.1136/jnnp.71.6.757.

Chataway, J. *et al.* (2020) ‘Efficacy of three neuroprotective drugs in secondary progressive multiple sclerosis (MS-SMART): a phase 2b, multiarm, double-blind, randomised placebo-controlled trial’, *The Lancet Neurology*. Lancet Publishing Group, 19(3), pp. 214–225. doi: 10.1016/S1474-4422(19)30485-5.

Chiaravalloti, N. D. and DeLuca, J. (2008) ‘Cognitive impairment in multiple sclerosis’, *The Lancet Neurology*, 7(12), pp. 1139–1151. doi: 10.1016/S1474-4422(08)70259-X.

Choi, I.-Y. *et al.* (2011) ‘Lower levels of glutathione in the brains of secondary progressive multiple sclerosis patients measured by 1H magnetic resonance chemical shift imaging at 3 T.’, *Multiple sclerosis (Houndmills, Basingstoke, England)*. NIH Public Access, 17(3), pp. 289–96. doi: 10.1177/1352458510384010.

Choi, I.-Y. *et al.* (2017) ‘Longitudinal changes of cerebral glutathione (GSH) levels associated with the clinical course of disease progression in patients with secondary progressive multiple sclerosis.’, *Multiple sclerosis (Houndmills, Basingstoke, England)*. NIH Public Access, 23(7), pp. 956–962. doi: 10.1177/1352458516669441.

Chung, K. K. *et al.* (2020) ‘A 30-Year Clinical and Magnetic Resonance Imaging Observational Study of Multiple Sclerosis and Clinically Isolated Syndromes’, *Annals of Neurology*. John Wiley and Sons Inc., 87(1), pp. 63–74. doi: 10.1002/ana.25637.

Ciccarelli, O. *et al.* (2010) ‘Assessing neuronal metabolism in vivo by modeling imaging measures.’, *The Journal of neuroscience : the official journal of the Society for Neuroscience*, 30(45), pp. 15030–3. doi: 10.1523/JNEUROSCI.3330-10.2010.

Cifelli, A. *et al.* (2002) ‘Thalamic neurodegeneration in multiple sclerosis.’, *Annals of neurology*, 52(5), pp. 650–3. doi: 10.1002/ana.10326.

Clark, J. F. *et al.* (2006) ‘N-Acetylaspartate as a reservoir for glutamate’, *Medical Hypotheses*, 67(3), pp. 506–512. doi: 10.1016/j.mehy.2006.02.047.

Clements, R. S. and Diethelm, A. G. (1979) ‘The metabolism of myo-inositol by the human kidney.’, *The Journal of laboratory and clinical medicine*, 93(2), pp. 210–9. Available at: http://www.ncbi.nlm.nih.gov/pubmed/372466 (Accessed: 22 July 2019).

Connick, P. *et al.* (2018) ‘Multiple Sclerosis-Secondary Progressive Multi-Arm Randomisation Trial (MS-SMART): a multiarm phase IIb randomised, double-blind, placebo-controlled clinical trial comparing the efficacy of three neuroprotective drugs in secondary progressive multiple sclerosis’, *BMJ Open*. British Medical Journal Publishing Group, 8(8), p. e021944. doi: 10.1136/BMJOPEN-2018-021944.

Connick, P., Chandran, S. and Bak, T. H. . (2013) ‘Patterns of cognitive dysfunction in progressive MS’, *Behavioural Neurology*, 27(3), pp. 259–265. doi: 10.3233/BEN-120286.

Coret, F. *et al.* (2018) ‘Onset of secondary progressive multiple sclerosis is not influenced by current relapsing multiple sclerosis therapies’, *Multiple Sclerosis Journal - Experimental, Translational and Clinical*. SAGE Publications, 4(2), p. 205521731878334. doi: 10.1177/2055217318783347.

Correale, J. *et al.* (2017) ‘Progressive multiple sclerosis: from pathogenic mechanisms to treatment’, *Brain : a journal of neurology*, 140, pp. 527–546. doi: 10.1093/brain/aww258.

Correale, J. and Farez, M. F. (2015) ‘The role of astrocytes in multiple sclerosis progression’, *Frontiers in Neurology*. Frontiers Media S.A., p. 1. doi: 10.3389/fneur.2015.00180.

Cotsapas, C. and Mitrovic, M. (2018) ‘Genome-wide association studies of multiple sclerosis’, *Clinical and Translational Immunology*. John Wiley and Sons Inc. doi: 10.1002/cti2.1018.

Coughlan, A. K. and Hollows, S. E. (1985) *The adult memory and information*

processing battery (AMIPB) test manual. St James University Hospital, Leeds.

Cox, D. *et al.* (2004) 'The unique impact of changes in normal appearing brain tissue on cognitive dysfunction in secondary progressive multiple sclerosis patients', *Multiple Sclerosis Journal*. SAGE PublicationsSage CA: Thousand Oaks, CA, 10(6), pp. 626–629. doi: 10.1191/1352458504ms1095oa.

Cree, B. A. C. *et al.* (2016) 'Long-term evolution of multiple sclerosis disability in the treatment era', *Annals of Neurology*. John Wiley and Sons Inc., 80(4), pp. 499–510. doi: 10.1002/ana.24747.

Criste, G., Trapp, B. and Dutta, R. (2014) 'Axonal loss in multiple sclerosis: causes and mechanisms.', *Handbook of clinical neurology*, 122, pp. 101–13. doi: 10.1016/B978-0-444-52001-2.00005-4.

Cronbach, L. J. and Furby, L. (1970) 'How we should measure "change": Or should we?', *Psychological Bulletin*, 74(1), pp. 68–80. doi: 10.1037/h0029382.

Cucurella, M. G. *et al.* (2000) 'Proton magnetic resonance spectroscopy in primary and secondary progressive multiple sclerosis.', *NMR in biomedicine*, 13(2), pp. 57–63. Available at: http://www.ncbi.nlm.nih.gov/pubmed/10797633 (Accessed: 27 September 2018).

Cutter, G. R. *et al.* (1999) 'Development of a multiple sclerosis functional composite as a clinical trial outcome measure', *Brain*. Oxford University Press, 122(5), pp. 871–882. doi: 10.1093/brain/122.5.871.

Daams, M. *et al.* (2015) 'Unraveling the neuroimaging predictors for motor dysfunction in long-standing multiple sclerosis', *Neurology*. Lippincott Williams and Wilkins, 85(3), pp. 248–255. doi: 10.1212/WNL.0000000000001756.

Dale, B. M., Brown, M. A. and Semelka, R. C. (2015) *MRI Basic Principles and Applications*. 5th edn. Wiley Blackwell.

Dalton, C. M. *et al.* (2004) 'Early development of multiple sclerosis is associated with progressive grey matter atrophy in patients presenting with clinically isolated syndromes', *Brain*. Brain, pp. 1101–1107. doi:

10.1093/brain/awh126.

Dalton, C. M. *et al.* (2012) ‘Brain lesion location and clinical status 20 years after a diagnosis of clinically isolated syndrome suggestive of multiple sclerosis’, *Multiple Sclerosis Journal*. Mult Scler, 18(3), pp. 322–328. doi: 10.1177/1352458511420269.

Davie, C. A. *et al.* (1997) ‘1H magnetic resonance spectroscopy of chronic cerebral white matter lesions and normal appearing white matter in multiple sclerosis.’, *Journal of neurology, neurosurgery, and psychiatry*. BMJ Publishing Group, 63(6), pp. 736–42. Available at: http://www.ncbi.nlm.nih.gov/pubmed/9416807 (Accessed: 21 December 2018).

Davie, C. A. *et al.* (1999) ‘Does the extent of axonal loss and demyelination from chronic lesions in multiple sclerosis correlate with the clinical subgroup?’, *Journal of neurology, neurosurgery, and psychiatry*. BMJ Publishing Group, 67(6), pp. 710–5. Available at: http://www.ncbi.nlm.nih.gov/pubmed/10567484 (Accessed: 7 January 2019).

Davies, S. E. *et al.* (1995) ‘High resolution proton NMR spectroscopy of multiple sclerosis lesions.’, *Journal of neurochemistry*, 64(2), pp. 742–8. Available at: http://www.ncbi.nlm.nih.gov/pubmed/7830068 (Accessed: 28 December 2018).

Davies, S. E. C. *et al.* (2002) ‘High Resolution Proton NMR Spectroscopy of Multiple Sclerosis Lesions’, *Journal of Neurochemistry*. John Wiley & Sons, Ltd (10.1111), 64(2), pp. 742–748. doi: 10.1046/j.1471-4159.1995.64020742.x.

Debernard, L. *et al.* (2015) ‘Deep grey matter MRI abnormalities and cognitive function in relapsing-remitting multiple sclerosis’. doi: 10.1016/j.pscychresns.2015.10.004.

Degelman, M. L. and Herman, K. M. (2017) ‘Smoking and multiple sclerosis: A systematic review and meta-analysis using the Bradford Hill criteria for causation’, *Multiple Sclerosis and Related Disorders*. Elsevier B.V., pp. 207–

216. doi: 10.1016/j.msard.2017.07.020.

Degenhardt, A. *et al.* (2009) ‘Clinical prognostic factors in multiple sclerosis: A natural history review’, *Nature Reviews Neurology*, pp. 672–682. doi: 10.1038/nrneurol.2009.178.

Dehmeshki, J. *et al.* (2003) ‘The normal appearing grey matter in primary progressive multiple sclerosis: A magnetisation transfer imaging study’, *Journal of Neurology*. J Neurol, 250(1), pp. 67–74. doi: 10.1007/s00415-003-0955-x.

Deloire, M. S. *et al.* (2011) ‘MRI predictors of cognitive outcome in early multiple sclerosis.[Erratum appears in Neurology. 2012 Feb 21;78(8):608]’, *Neurology*, 76(13), pp. 1161–1167. Available at: http://ovidsp.ovid.com/ovidweb.cgi?T=JS&CSC=Y&NEWS=N&PAGE=fulltext&D=med7&AN=21444901%0Ahttp://man-fe.hosted.exlibrisgroup.com/openurl/44MAN/44MAN_services_page?sid=OVID:medline&id=pmid:21444901&id=doi:10.1212%2FWNL.0b013e318212a8be&issn=0028-3878&isbn=&v (Accessed: 7 January 2020).

Ebers, G. C. *et al.* (2010) ‘Analysis of clinical outcomes according to original treatment groups 16 years after the pivotal IFNB-1b trial’, *Journal of Neurology, Neurosurgery and Psychiatry*, 81(8), pp. 907–912. doi: 10.1136/jnnp.2009.204123.

Eijlers, A. J. C. *et al.* (2018) ‘Predicting cognitive decline in multiple sclerosis: A 5-year follow-up study’, *Brain*. Oxford University Press, 141(9), pp. 2605–2618. doi: 10.1093/brain/awy202.

Elliott, C., Belachew, S., *et al.* (2019) ‘Chronic white matter lesion activity predicts clinical progression in primary progressive multiple sclerosis’, *Brain*. Oxford University Press, 142(9), pp. 2787–2799. doi: 10.1093/brain/awz212.

Elliott, C., Wolinsky, J. S., *et al.* (2019) ‘Slowly expanding/evolving lesions as a magnetic resonance imaging marker of chronic active multiple sclerosis lesions’, *Multiple Sclerosis Journal*. SAGE Publications Ltd, 25(14), pp. 1915–1925. doi: 10.1177/1352458518814117.

Eriksson, M., Andersen, O. and Runmarker, B. (2003) ‘Long-term follow up of patients with clinically isolated syndromes, relapsing-remitting and secondary progressive multiple sclerosis’, *Multiple Sclerosis*. Mult Scler, 9(3), pp. 260–274. doi: 10.1191/1352458503ms914oa.

Ernst, T., Kreis, R. and Ross, B. D. (1993) ‘Absolute Quantitation of Water and Metabolites in the Human Brain. I. Compartments and Water’, *Journal of Magnetic Resonance, Series B*. Academic Press, 102(1), pp. 1–8. doi: 10.1006/JMRB.1993.1055.

Eshaghi, A., Prados, F., *et al.* (2018) ‘Deep gray matter volume loss drives disability worsening in multiple sclerosis.’, *Annals of neurology*, 83(2), pp. 210–222. doi: 10.1002/ana.25145.

Eshaghi, A., Marinescu, R. V, *et al.* (2018) ‘Progression of regional grey matter atrophy in multiple sclerosis.’, *Brain : a journal of neurology*, 141(6), pp. 1665–1677. doi: 10.1093/brain/awy088.

Evangelou, N. *et al.* (2000) ‘Quantitative pathological evidence for axonal loss in normal appearing white matter in multiple sclerosis’, *Annals of Neurology*. John Wiley & Sons, Ltd, 47(3), pp. 391–395. doi: 10.1002/1531-8249(200003)47:3<391::AID-ANA20>3.0.CO;2-J.

Evangelou, N. *et al.* (2005) ‘Pathological study of spinal cord atrophy in multiple sclerosis suggests limited role of local lesions’, *Brain*. Brain, 128(1), pp. 29–34. doi: 10.1093/brain/awh323.

Evonuk, K. S. *et al.* (2015) ‘ Inhibition of System Xc − Transporter Attenuates Autoimmune Inflammatory Demyelination ’, *The Journal of Immunology*. The American Association of Immunologists, 195(2), pp. 450–463. doi: 10.4049/jimmunol.1401108.

Faghihi, R. *et al.* (2017) ‘Magnetic Resonance Spectroscopy and its Clinical Applications: A Review’, *Journal of Medical Imaging and Radiation Sciences*. Elsevier Inc., pp. 233–253. doi: 10.1016/j.jmir.2017.06.004.

Falini, A. *et al.* (1998) ‘Benign versus secondary-progressive multiple

sclerosis: the potential role of proton MR spectroscopy in defining the nature of disability.', *AJNR. American journal of neuroradiology*. American Journal of Neuroradiology, 19(2), pp. 223–9. Available at: http://www.ncbi.nlm.nih.gov/pubmed/9504469 (Accessed: 31 December 2018).

Fambiatos, A. *et al.* (2019) 'Risk of secondary progressive multiple sclerosis: A longitudinal study', *Multiple Sclerosis Journal*. SAGE Publications Ltd. doi: 10.1177/1352458519868990.

Fazekas, F. *et al.* (1999) 'The contribution of magnetic resonance imaging to the diagnosis of multiple sclerosis', *Neurology*. Lippincott Williams and Wilkins, pp. 448–456. doi: 10.1212/wnl.53.3.448.

Fernando, K. T. M. *et al.* (2004) 'Elevated white matter myo-inositol in clinically isolated syndromes suggestive of multiple sclerosis', *Brain*. Oxford University Press, 127(6), pp. 1361–1369. doi: 10.1093/brain/awh153.

Feys, P. *et al.* (2017) 'The Nine-Hole Peg Test as a manual dexterity performance measure for multiple sclerosis', *Multiple Sclerosis*. SAGE Publications Ltd, pp. 711–720. doi: 10.1177/1352458517690824.

Filippi, M. *et al.* (1994) 'Quantitative brain MRI lesion load predicts the course of clinically isolated syndromes suggestive of multiple sclerosis', *Neurology*. Neurology, 44(4), pp. 635–641. doi: 10.1212/wnl.44.4.635.

Filippi, M. *et al.* (2000) 'Changes in the normal appearing brain tissue and cognitive impairment in multiple sclerosis', *Journal of Neurology Neurosurgery and Psychiatry*. BMJ Publishing Group, 68(2), pp. 157–161. doi: 10.1136/jnnp.68.2.157.

Filippi, M. *et al.* (2012) 'Association between pathological and MRI findings in multiple sclerosis', *The Lancet Neurology*. Lancet Neurol, pp. 349–360. doi: 10.1016/S1474-4422(12)70003-0.

Filippi, M. *et al.* (2019) 'Association between pathological and MRI findings in multiple sclerosis.', *The Lancet. Neurology*. Lancet Publishing Group, 18(2),

pp. 198–210. doi: 10.1016/S1474-4422(18)30451-4.

Filippi, M. and Rocca, M. A. (2010) ‘MRI and cognition in multiple sclerosis’, *Neurological Sciences*, 31(SUPPL. 2). doi: 10.1007/s10072-010-0367-5.

Di Filippo, M. *et al.* (2010) ‘Brain atrophy and lesion load measures over 1 year relate to clinical status after 6 years in patients with clinically isolated syndromes’, *Journal of Neurology, Neurosurgery and Psychiatry*. J Neurol Neurosurg Psychiatry, 81(2), pp. 204–208. doi: 10.1136/jnnp.2009.171769.

Fischer, M. *et al.* (2014) ‘How reliable is the classification of cognitive impairment across different criteria in early and late stages of multiple sclerosis?’, *Journal of the Neurological Sciences*. doi: 10.1016/j.jns.2014.05.042.

Fischer, M. T. *et al.* (2012) ‘NADPH oxidase expression in active multiple sclerosis lesions in relation to oxidative tissue damage and mitochondrial injury’, *Brain*. Oxford University Press, 135(3), pp. 886–899. doi: 10.1093/brain/aws012.

Fisher, E. *et al.* (2008) ‘Gray matter atrophy in multiple sclerosis: A longitudinal study’, *Annals of Neurology*. Ann Neurol, 64(3), pp. 255–265. doi: 10.1002/ana.21436.

Fisniku, L. K. *et al.* (2008) ‘Disability and T2 MRI lesions: a 20-year follow-up of patients with relapse onset of multiple sclerosis’, *Brain*, 131(3), pp. 808–817. doi: 10.1093/brain/awm329.

Fisniku, Leonora K. *et al.* (2008) ‘Gray matter atrophy is related to long-term disability in multiple sclerosis’, *Annals of Neurology*, 64(3), pp. 247–254. doi: 10.1002/ana.21423.

Fisniku, L. K. *et al.* (2009) ‘Magnetization transfer ratio abnormalities reflect clinically relevant grey matter damage in multiple sclerosis’, *Multiple Sclerosis*. Mult Scler, 15(6), pp. 668–677. doi: 10.1177/1352458509103715.

Fisniku, L. K. *et al.* (no date) ‘Gray matter atrophy is related to long-term

disability in multiple sclerosis.[Erratum appears in Ann Neurol. 2009 Feb;65(2):232]', *Annals of neurology*.

Foong, J. *et al.* (1999) 'Correlates of Executive Function in Multiple Sclerosis':, *The Journal of Neuropsychiatry and Clinical Neurosciences*, 11(1), pp. 45–50. doi: 10.1176/jnp.11.1.45.

Forn, C. *et al.* (2011) 'Anatomical and functional differences between the paced auditory serial addition test and the symbol digit modalities test', *Journal of Clinical and Experimental Neuropsychology*. Taylor & Francis Group , 33(1), pp. 42–50. doi: 10.1080/13803395.2010.481620.

Frahm, J. *et al.* (1989) 'Localized high-resolution proton NMR spectroscopy using stimulated echoes: Initial applications to human brainin vivo', *Magnetic Resonance in Medicine*, 9(1), pp. 79–93. doi: 10.1002/mrm.1910090110.

Friese, M. A. *et al.* (2007) 'Acid-sensing ion channel-1 contributes to axonal degeneration in autoimmune inflammation of the central nervous system', *Nature Medicine*, 13(12), pp. 1483–1489. doi: 10.1038/nm1668.

Fu, L. *et al.* (1996) 'Statistics for investigation of multimodal MR imaging data and an application to multiple sclerosis patients.', *NMR in biomedicine*, 9(8), pp. 339–46. doi: 10.1002/(SICI)1099-1492(199612)9:8<339::AID-NBM422>3.0.CO;2-X.

Fu, L. *et al.* (1998) 'Imaging axonal damage of normal-appearing white matter in multiple sclerosis.', *Brain : a journal of neurology*, 121 (Pt 1, pp. 103–13. Available at: http://www.ncbi.nlm.nih.gov/pubmed/9549491 (Accessed: 31 December 2018).

Furby, J. *et al.* (2008) 'Magnetic resonance imaging measures of brain and spinal cord atrophy correlate with clinical impairment in secondary progressive multiple sclerosis', *Multiple Sclerosis*. Mult Scler, 14(8), pp. 1068–1075. doi: 10.1177/1352458508093617.

Furby, J. *et al.* (2010) 'A longitudinal study of MRI-detected atrophy in secondary progressive multiple sclerosis', *Journal of Neurology*, 257(9), pp.

1508–1516. doi: 10.1007/s00415-010-5563-y.

Gass, A. *et al.* (1994) ‘Correlation of magnetization transfer ration with clinical disability in multiple sclerosis’, *Annals of Neurology*. Ann Neurol, 36(1), pp. 62–67. doi: 10.1002/ana.410360113.

Gass, A. *et al.* (2015) ‘MRI monitoring of pathological changes in the spinal cord in patients with multiple sclerosis’, *The Lancet Neurology*. Lancet Publishing Group, pp. 443–454. doi: 10.1016/S1474-4422(14)70294-7.

van Geest, Q. *et al.* (2018) ‘Cognition and multiple sclerosis: The role of magnetic resonance imaging.’, in *Cognition and behavior in multiple sclerosis.* American Psychological Association, pp. 33–65. doi: 10.1037/0000097-003.

Geurts, J. J. and Barkhof, F. (2008) ‘Grey matter pathology in multiple sclerosis’, *The Lancet Neurology*. Elsevier, pp. 841–851. doi: 10.1016/S1474-4422(08)70191-1.

Geurts, J. J. G. *et al.* (2003) ‘Altered expression patterns of group I and II metabotropic glutamate receptors in multiple sclerosis’, *Brain*. Brain, 126(8), pp. 1755–1766. doi: 10.1093/brain/awg179.

Geurts, J. J. G. *et al.* (2006) ‘MR spectroscopic evidence for thalamic and hippocampal, but not cortical, damage in multiple sclerosis’, *Magnetic Resonance in Medicine*. John Wiley & Sons, Ltd, 55(3), pp. 478–483. doi: 10.1002/mrm.20792.

Geurts, J. J. G. *et al.* (2012) ‘Measurement and clinical effect of grey matter pathology in multiple sclerosis’, *The Lancet Neurology*. Elsevier, pp. 1082–1092. doi: 10.1016/S1474-4422(12)70230-2.

Gh Popescu, B. F. and Lucchinetti, C. F. (2012) ‘Meningeal and cortical grey matter pathology in multiple sclerosis’, *BMC Neurology*. BioMed Central Ltd. doi: 10.1186/1471-2377-12-11.

Gilmore, C. P. *et al.* (2009) ‘Spinal cord grey matter lesions in multiple sclerosis detected by post-mortem high field MR imaging’, *Multiple Sclerosis*. SAGE

PublicationsSage UK: London, England, 15(2), pp. 180–188. doi: 10.1177/1352458508096876.

Giovannoni, G. *et al.* (2017) 'Is multiple sclerosis a length-dependent central axonopathy? The case for therapeutic lag and the asynchronous progressive MS hypotheses', *Multiple Sclerosis and Related Disorders*. Elsevier B.V., pp. 70–78. doi: 10.1016/j.msard.2017.01.007.

Glanville, N. T. *et al.* (1989) 'Differences in the metabolism of inositol and phosphoinositides by cultured cells of neuronal and glial origin', *Biochimica et Biophysica Acta (BBA) - Lipids and Lipid Metabolism*, 1004(2), pp. 169–179. doi: 10.1016/0005-2760(89)90265-8.

Goldstein, F. B. (1969) 'The enzymatic synthesis of N-acetyl-L-aspartic acid by subcellular preparations of rat brain.', *The Journal of biological chemistry*, 244(15), pp. 4257–60. Available at: http://www.ncbi.nlm.nih.gov/pubmed/5800445 (Accessed: 11 July 2019).

Goodkin, D. E., Hertsguard, D. and Seminary, J. (1988) 'Upper extremity function in multiple sclerosis: Improving assessment sensitivity with box-and-block and nine-hole peg tests', *Archives of Physical Medicine and Rehabilitation*, 69(10), pp. 850–854. doi: 10.5555/uri:pii:0003999388900093.

Govindaraju, V., Young, K. and Maudsley, A. A. (2000) 'Proton NMR chemical shifts and coupling constants for brain metabolites', *NMR in Biomedicine*, 13(3), pp. 129–153. doi: 10.1002/1099-1492(200005)13:3<129::AID-NBM619>3.0.CO;2-V.

Graveron-Demilly, D. (2014) 'Quantification in magnetic resonance spectroscopy based on semi-parametric approaches', *Magnetic Resonance Materials in Physics, Biology and Medicine*. Springer Verlag, pp. 113–130. doi: 10.1007/s10334-013-0393-4.

Gronwall, D. M. (1977) 'Paced auditory serial-addition task: a measure of recovery from concussion.', *Perceptual and motor skills*, 44(2), pp. 367–73. doi: 10.2466/pms.1977.44.2.367.

Guan, Y. *et al.* (2019) ‘The role of Epstein-Barr virus in multiple sclerosis: From molecular pathophysiology to in vivo imaging’, *Neural Regeneration Research*. Wolters Kluwer Medknow Publications, pp. 373–386. doi: 10.4103/1673-5374.245462.

Gustafsson, M. C. *et al.* (2007) ‘Low Choline Concentrations in Normal-Appearing White Matter of Patients with Multiple Sclerosis and Normal MR Imaging Brain Scans’, *American Journal of Neuroradiology*, 28(7), pp. 1306–1312. doi: 10.3174/ajnr.A0580.

Hametner, S. *et al.* (2013) ‘Iron and neurodegeneration in the multiple sclerosis brain’, *Annals of Neurology*, 74(6), pp. 848–861. doi: 10.1002/ana.23974.

Hannoun, S. *et al.* (2012) ‘Correlation of Diffusion and Metabolic Alterations in Different Clinical Forms of Multiple Sclerosis’, *PLoS ONE*. Edited by J. Najbauer. Public Library of Science, 7(3), p. e32525. doi: 10.1371/journal.pone.0032525.

Harirchian, M. H. *et al.* (2018) ‘Worldwide prevalence of familial multiple sclerosis: A systematic review and meta-analysis’, *Multiple Sclerosis and Related Disorders*. Elsevier B.V., pp. 43–47. doi: 10.1016/j.msard.2017.12.015.

Hauser, G. and Finelli, V. N. (1963) ‘The biosynthesis of free and phosphatide myo-inositol from glucose by mammalian tissue slices.’, *The Journal of biological chemistry*, 238, pp. 3224–8. Available at: http://www.ncbi.nlm.nih.gov/pubmed/14085365 (Accessed: 22 July 2019).

Hayton, T. *et al.* (2009) ‘Grey matter magnetization transfer ratio independently correlates with neurological deficit in secondary progressive multiple sclerosis’, *Journal of Neurology*. J Neurol, 256(3), pp. 427–435. doi: 10.1007/s00415-009-0110-4.

Hayton, T. *et al.* (2012) ‘Longitudinal changes in magnetisation transfer ratio in secondary progressive multiple sclerosis: Data from a randomised placebo controlled trial of lamotrigine’, *Journal of Neurology*. J Neurol, 259(3), pp. 505–514. doi: 10.1007/s00415-011-6212-9.

Van Hecke, P. *et al.* (1991) ‘Human brain proton localized NMR spectroscopy in multiple sclerosis.’, *Magnetic resonance in medicine*, 18(1), pp. 199–206. Available at: http://www.ncbi.nlm.nih.gov/pubmed/2062231 (Accessed: 31 December 2018).

Hedström, A. K., Olsson, T. and Alfredsson, L. (2012) ‘High body mass index before age 20 is associated with increased risk for multiple sclerosis in both men and women’, *Multiple Sclerosis Journal*, 18(9), pp. 1334–1336. doi: 10.1177/1352458512436596.

Henry, R. G. *et al.* (2009) ‘Connecting white matter injury and thalamic atrophy in clinically isolated syndromes’, *Journal of the Neurological Sciences*. J Neurol Sci, 282(1–2), pp. 61–66. doi: 10.1016/j.jns.2009.02.379.

Howell, O. W. *et al.* (2011) ‘Meningeal inflammation is widespread and linked to cortical pathology in multiple sclerosis’, *Brain*. Oxford University Press, 134(9), pp. 2755–2771. doi: 10.1093/brain/awr182.

Huijbregts, S. C. J. *et al.* (2004) ‘Differences in cognitive impairment of relapsing remitting, secondary, and primary progressive MS.’, *Neurology*, 63(2), pp. 335–339. doi: 10.1212/01.WNL.0000129828.03714.90.

Husted, C. A. *et al.* (1994) ‘Biochemical alterations in multiple sclerosis lesions and normal-appearing white matter detected by in vivo31P and1H spectroscopic imaging’, *Annals of Neurology*, 36(2), pp. 157–165. doi: 10.1002/ana.410360207.

Ion-Mărgineanu, A. *et al.* (2017) ‘Machine Learning Approach for Classifying Multiple Sclerosis Courses by Combining Clinical Data with Lesion Loads and Magnetic Resonance Metabolic Features’, *Frontiers in Neuroscience*. Frontiers, 11, p. 398. doi: 10.3389/fnins.2017.00398.

James, R. E. *et al.* (2020) ‘Persistent elevation of intrathecal pro-inflammatory cytokines leads to multiple sclerosis-like cortical demyelination and neurodegeneration’, *Acta Neuropathologica Communications*. BioMed Central Ltd., 8(1). doi: 10.1186/s40478-020-00938-1.

Jehna, M. *et al.* (2013) ‘An Exploratory Study on the Spatial Relationship Between Regional Cortical Volume Changes and White Matter Integrity in Multiple Sclerosis’, *Brain Connectivity*. Brain Connect, 3(3), pp. 255–264. doi: 10.1089/brain.2012.0108.

JH, van W. *et al.* (1999) ‘Axonal loss in multiple sclerosis lesions: magnetic resonance imaging insights into substrates of disability’, *Annals of neurology*. Ann Neurol, 46(5). doi: 10.1002/1531-8249(199911)46:5<747::AID-ANA10>3.3.CO;2-W.

Johnen, A. *et al.* (2017) ‘Distinct cognitive impairments in different disease courses of multiple sclerosis—A systematic review and meta-analysis’, *Neuroscience and Biobehavioral Reviews*, pp. 568–578. doi: 10.1016/j.neubiorev.2017.09.005.

Kalkers, N. F. *et al.* (2000) ‘MS Functional Composite’, *Neurology*, 54(6). Available at: http://n.neurology.org/content/54/6/1233.long (Accessed: 27 September 2018).

Kapeller, P. *et al.* (2002) ‘Quantitative 1H MRS imaging 14 years after presenting with a clinically isolated syndrome suggestive of multiple sclerosis’, *Multiple Sclerosis Journal*. Sage PublicationsSage CA: Thousand Oaks, CA, 8(3), pp. 207–210. doi: 10.1191/1352458502ms822oa.

Katz Sand, I. *et al.* (2014) ‘Diagnostic uncertainty during the transition to secondary progressive multiple sclerosis.’, *Multiple sclerosis (Houndmills, Basingstoke, England)*, 20(12), pp. 1654–7. doi: 10.1177/1352458514521517.

Kaunzner, U. W. and Gauthier, S. A. (2017) ‘MRI in the assessment and monitoring of multiple sclerosis: an update on best practice.’, *Therapeutic advances in neurological disorders*. SAGE Publications Ltd, 10(6), pp. 247–261. doi: 10.1177/1756285617708911.

Kearney, Hugh *et al.* (2014) ‘Improved MRI quantification of spinal cord atrophy in multiple sclerosis’, *Journal of Magnetic Resonance Imaging*. J Magn Reson Imaging, 39(3), pp. 617–623. doi: 10.1002/jmri.24194.

Kearney, H., Rocca, M. A., *et al.* (2014) 'Magnetic resonance imaging correlates of physical disability in relapse onset multiple sclerosis of long disease duration', *Multiple Sclerosis*, 20(1), pp. 72–80. doi: 10.1177/1352458513492245.

Kearney, H., Rocca, M., *et al.* (2014) 'Magnetic resonance imaging correlates of physical disability in relapse onset multiple sclerosis of long disease duration', *Multiple Sclerosis Journal*, 20(1), pp. 72–80. doi: 10.1177/1352458513492245.

Kearney, Hugh *et al.* (2015) 'Cervical cord lesion load is associated with disability independently from atrophy in MS', *Neurology*. Lippincott Williams and Wilkins, 84(4), pp. 367–373. doi: 10.1212/WNL.0000000000001186.

Kearney, H. *et al.* (2015) 'Spinal cord grey matter abnormalities are associated with secondary progression and Physical disability in multiple sclerosis', *Journal of Neurology, Neurosurgery and Psychiatry*. BMJ Publishing Group, 86(6), pp. 608–614. doi: 10.1136/jnnp-2014-308241.

Kearney, H., Miller, D. H. and Ciccarelli, O. (2015) 'Spinal cord MRI in multiple sclerosis-diagnostic, prognostic and clinical value', *Nature Reviews Neurology*. Nature Publishing Group, pp. 327–338. doi: 10.1038/nrneurol.2015.80.

Kendi, A. T. K. *et al.* (2004) 'MR spectroscopy of cervical spinal cord in patients with multiple sclerosis', *Neuroradiology*. Springer-Verlag, 46(9), pp. 764–769. doi: 10.1007/s00234-004-1231-1.

Khaleeli, Z., Cercignani, M., *et al.* (2007) 'Localized grey matter damage in early primary progressive multiple sclerosis contributes to disability', *NeuroImage*. Neuroimage, 37(1), pp. 253–261. doi: 10.1016/j.neuroimage.2007.04.056.

Khaleeli, Z., Sastre-Garriga, J., *et al.* (2007) 'Magnetisation transfer ratio in the normal appearing white matter predicts progression of disability over 1 year in early primary progressive multiple sclerosis', *Journal of Neurology, Neurosurgery and Psychiatry*. J Neurol Neurosurg Psychiatry, 78(10), pp.

1076–1082. doi: 10.1136/jnnp.2006.107565.

Kidd, D. *et al.* (1996) ‘MRI dynamics of brain and spinal cord in progressive multiple sclerosis’, *Journal of Neurology Neurosurgery and Psychiatry*. BMJ Publishing Group, 60(1), pp. 15–19. doi: 10.1136/jnnp.60.1.15.

Kidd, D. *et al.* (1999) ‘Cortical lesions in multiple sclerosis’, *Brain*. Brain, 122(1), pp. 17–26. doi: 10.1093/brain/122.1.17.

Kilsdonk, I. D. *et al.* (2016) ‘Increased cortical grey matter lesion detection in multiple sclerosis with 7 T MRI: a post-mortem verification study’, *Brain*. Oxford University Press, 139(5), pp. 1472–1481. doi: 10.1093/brain/aww037.

Kister, I. *et al.* (2013) ‘Natural history of multiple sclerosis symptoms’, *International Journal of MS Care*, 15(3), pp. 146–158. doi: 10.7224/1537-2073.2012-053.

Koch, M. *et al.* (2008) ‘Factors associated with the risk of secondary progression in multiple sclerosis.’, *Multiple sclerosis (Houndmills, Basingstoke, England)*, 14(6), pp. 799–803. doi: 10.1177/1352458508089361.

Koga, Y. *et al.* (2005) ‘Brain creatine functions to attenuate acute stress responses through GABAnergic system in chicks’, *Neuroscience*, 132(1), pp. 65–71. doi: 10.1016/j.neuroscience.2005.01.004.

Kreis, R., Ernst, T. and Ross, B. D. (1993) ‘Absolute Quantitation of Water and Metabolites in the Human Brain. II. Metabolite Concentrations’, *Journal of Magnetic Resonance, Series B*. Academic Press, 102(1), pp. 9–19. doi: 10.1006/JMRB.1993.1056.

Kuhlmann, T. *et al.* (2002) ‘Acute axonal damage in multiple sclerosis is most extensive in early disease stages and decreases over time’, *Brain*. Oxford University Press, 125(10), pp. 2202–2212. doi: 10.1093/brain/awf235.

Kurtzke, J. F. (1983) ‘Rating neurologic impairment in multiple sclerosis: an expanded disability status scale (EDSS).’, *Neurology*. Wolters Kluwer Health, Inc. on behalf of the American Academy of Neurology, 33(11), pp. 1444–52.

doi: 10.1212/WNL.33.11.1444.

Kutzelnigg, A. *et al.* (2005) ‘Cortical demyelination and diffuse white matter injury in multiple sclerosis’, *Brain*. Oxford University Press, 128(11), pp. 2705–2712. doi: 10.1093/brain/awh641.

Lassmann, H. (2017) ‘Targets of therapy in progressive MS.’, *Multiple sclerosis (Houndmills, Basingstoke, England)*. SAGE Publications Ltd, 23(12), pp. 1593–1599. doi: 10.1177/1352458517729455.

Lassmann, H. (2018) ‘Multiple sclerosis pathology’, *Cold Spring Harbor Perspectives in Medicine*. Cold Spring Harbor Laboratory Press. doi: 10.1101/cshperspect.a028936.

Lassmann, H. (2019) ‘Pathogenic mechanisms associated with different clinical courses of multiple sclerosis’, *Frontiers in Immunology*. Frontiers Media S.A. doi: 10.3389/fimmu.2018.03116.

Lassmann, H. and Lucchinetti, C. F. (2008) ‘Cortical demyelination in CNS inflammatory demyelinating diseases’, *Neurology*. Lippincott Williams and Wilkins, pp. 332–333. doi: 10.1212/01.wnl.0000298724.89870.d1.

Leary, S M *et al.* (1999) ‘1H magnetic resonance spectroscopy of normal appearing white matter in primary progressive multiple sclerosis.’, *Journal of neurology*, 246(11), pp. 1023–6. Available at: http://www.ncbi.nlm.nih.gov/pubmed/10631633 (Accessed: 7 January 2019).

Leary, S. M. *et al.* (1999) ‘Magnetisation transfer of normal appearing white matter in primary progressive multiple sclerosis’, *Multiple Sclerosis*. Nature Publishing Group, 5(5), pp. 313–316. doi: 10.1177/135245859900500502.

Lechner-Scott, L. *et al.* (2003) ‘Can the Expanded Disability Status Scale be assessed by telephone?’, *Multiple Sclerosis*. Mult Scler, 9(2), pp. 154–159. doi: 10.1191/1352458503ms884oa.

De Leener, B. *et al.* (2017) ‘SCT: Spinal Cord Toolbox, an open-source software for processing spinal cord MRI data’, *NeuroImage*. Academic Press

Inc., 145(Pt A), pp. 24–43. doi: 10.1016/j.neuroimage.2016.10.009.

Lin, X., Blumhardt, L. D. and Constantinescu, C. S. (2003) 'The relationship of brain and cervical cord volume to disability in clinical subtypes of multiple sclerosis: A three-dimensional MRI study', *Acta Neurologica Scandinavica*. Acta Neurol Scand, 108(6), pp. 401–406. doi: 10.1034/j.1600-0404.2003.00160.x.

Llufriu, S. *et al.* (2014) 'Magnetic Resonance Spectroscopy Markers of Disease Progression in Multiple Sclerosis', *JAMA Neurology*. Springer, New York, NY, 71(7), p. 840. doi: 10.1001/jamaneurol.2014.895.

Longo, R. and Vidimari, R. (1994) 'In vivo localized ^{1}H NMR spectroscopy: an experimental characterization of the PRESS technique', *Physics in Medicine and Biology*, 39(1), pp. 207–215. doi: 10.1088/0031-9155/39/1/013.

López-Góngora, M., Querol, L. and Escartín, A. (2015) 'A one-year follow-up study of the Symbol Digit Modalities Test (SDMT) and the Paced Auditory Serial Addition Test (PASAT) in relapsing-remitting multiple sclerosis: An appraisal of comparative longitudinal sensitivity', *BMC Neurology*. BioMed Central Ltd., 15(1), p. 40. doi: 10.1186/s12883-015-0296-2.

Lorefice, L. *et al.* (2020) 'The impact of deep grey matter volume on cognition in multiple sclerosis', *Multiple Sclerosis and Related Disorders*. Elsevier B.V., 45, p. 102351. doi: 10.1016/j.msard.2020.102351.

Lorscheider, J. *et al.* (2016) 'Defining secondary progressive multiple sclerosis', *Brain*. Narnia, 139(9), pp. 2395–2405. doi: 10.1093/brain/aww173.

Losseff, N. A. *et al.* (1996) 'Spinal cord atrophy and disability in multiple sclerosis', *Brain*. Oxford Academic, 119(3), pp. 701–708. doi: 10.1093/brain/119.3.701.

Lublin, F. D. *et al.* (2014) 'Defining the clinical course of multiple sclerosis: The 2013 revisions', *Neurology*. Lippincott Williams and Wilkins, pp. 278–286. doi: 10.1212/WNL.0000000000000560.

Lublin, F. D. and Reingold, S. C. (1996) ‘Defining the clinical course of multiple sclerosis: results of an international survey. National Multiple Sclerosis Society (USA) Advisory Committee on Clinical Trials of New Agents in Multiple Sclerosis.’, *Neurology*, 46(4), pp. 907–11. Available at: http://www.ncbi.nlm.nih.gov/pubmed/8780061 (Accessed: 27 December 2019).

Lukas, C. *et al.* (2004) ‘Sensitivity and reproducibility of a new fast 3D segmentation technique for clinical MR-based brain volumetry in multiple sclerosis’, *Neuroradiology*. Neuroradiology, 46(11), pp. 906–915. doi: 10.1007/s00234-004-1282-3.

Lukas, C. *et al.* (2015) ‘Cervical spinal cord volume loss is related to clinical disability progression in multiple sclerosis’, *Journal of Neurology, Neurosurgery and Psychiatry*. BMJ Publishing Group, 86(4), pp. 410–418. doi: 10.1136/jnnp-2014-308021.

Lunde, H. M. B. *et al.* (2017) ‘Survival and cause of death in multiple sclerosis: a 60-year longitudinal population study’, *Journal of Neurology, Neurosurgery & Psychiatry*. BMJ Publishing Group Ltd, 88(8), pp. 621–625. doi: 10.1136/JNNP-2016-315238.

Mackenzie, I. S. *et al.* (2014) ‘Incidence and prevalence of multiple sclerosis in the UK 1990-2010: a descriptive study in the General Practice Research Database.’, *Journal of neurology, neurosurgery, and psychiatry*, 85(1), pp. 76–84. doi: 10.1136/jnnp-2013-305450.

MacMillan, E. *et al.* (2016) ‘Progressive multiple sclerosis exhibits decreasing glutamate and glutamine over two years’, *Multiple Sclerosis Journal*. SAGE PublicationsSage UK: London, England, 22(1), pp. 112–116. doi: 10.1177/1352458515586086.

Macrez, R. *et al.* (2016) ‘Mechanisms of glutamate toxicity in multiple sclerosis: biomarker and therapeutic opportunities’, *The Lancet Neurology*. Elsevier, 15(10), pp. 1089–1102. doi: 10.1016/S1474-4422(16)30165-X.

Magliozzi, R. *et al.* (2007) ‘Meningeal B-cell follicles in secondary progressive

multiple sclerosis associate with early onset of disease and severe cortical pathology.', *Brain : a journal of neurology*, 130(Pt 4), pp. 1089–104. doi: 10.1093/brain/awm038.

Magliozzi, R. *et al.* (2010) 'A Gradient of neuronal loss and meningeal inflammation in multiple sclerosis', *Annals of Neurology*. Ann Neurol, 68(4), pp. 477–493. doi: 10.1002/ana.22230.

Magliozzi, R. *et al.* (2019) 'Meningeal inflammation changes the balance of TNF signalling in cortical grey matter in multiple sclerosis', *Journal of Neuroinflammation*. BioMed Central Ltd., 16(1). doi: 10.1186/s12974-019-1650-x.

Magyari, M. and Sorensen, P. S. (2020) 'Comorbidity in Multiple Sclerosis', *Frontiers in Neurology*. Frontiers Media S.A., p. 851. doi: 10.3389/fneur.2020.00851.

Mahad, D. H., Trapp, B. D. and Lassmann, H. (2015) 'Pathological mechanisms in progressive multiple sclerosis', *The Lancet Neurology*. Elsevier, 14(2), pp. 183–193. doi: 10.1016/S1474-4422(14)70256-X.

Manouchehrinia, A. *et al.* (2013) 'Tobacco smoking and disability progression in multiple sclerosis: United Kingdom cohort study', *Brain*. Oxford University Press, 136(7), pp. 2298–2304. doi: 10.1093/brain/awt139.

Marrie, R. A. *et al.* (2010) 'Vascular comorbidity is associated with more rapid disability progression in multiple sclerosis', *Neurology*. Lippincott Williams and Wilkins, 74(13), pp. 1041–1047. doi: 10.1212/WNL.0b013e3181d6b125.

Marrie, R. A., Cohen, J., *et al.* (2015) 'A systematic review of the incidence and prevalence of comorbidity in multiple sclerosis: Overview', *Multiple Sclerosis Journal*. SAGE Publications Ltd, pp. 263–281. doi: 10.1177/1352458514564491.

Marrie, R. A., Elliott, L., *et al.* (2015) 'Effect of comorbidity on mortality in multiple sclerosis', *Neurology*. Lippincott Williams and Wilkins, 85(3), pp. 240–247. doi: 10.1212/WNL.0000000000001718.

Marshall, I. *et al.* (2018) ‘Characterisation of tissue-type metabolic content in secondary progressive multiple sclerosis: a magnetic resonance spectroscopic imaging study.’, *Journal of neurology*, 265(8), pp. 1795–1802. doi: 10.1007/s00415-018-8903-y.

Matthews, P. M. *et al.* (1991) ‘Proton magnetic resonance spectroscopy for metabolic characterization of plaques in multiple sclerosis.’, *Neurology*, 41(8), pp. 1251–6. Available at: http://www.ncbi.nlm.nih.gov/pubmed/1650931 (Accessed: 28 December 2018).

Matthews, P. M. *et al.* (1996) ‘Assessment of lesion pathology in multiple sclerosis using quantitative MRI morphometry and magnetic resonance spectroscopy.’, *Brain : a journal of neurology*, 119 (Pt 3), pp. 715–22. Available at: http://www.ncbi.nlm.nih.gov/pubmed/8673485 (Accessed: 31 December 2018).

Matute, C., Domercq, M. and Sánchez-Gómez, M. V. (2006) ‘Glutamate-mediated glial injury: Mechanisms and clinical importance’, *GLIA*. Glia, pp. 212–224. doi: 10.1002/glia.20275.

McDonald, W. I. *et al.* (2001) ‘Recommended diagnostic criteria for multiple sclerosis: Guidelines from the International Panel on the Diagnosis of Multiple Sclerosis’, *Annals of Neurology*, 50(1), pp. 121–127. doi: 10.1002/ana.1032.

Michaelis, T. *et al.* (1993) ‘Absolute concentrations of metabolites in the adult human brain in vivo: quantification of localized proton MR spectra.’, *Radiology*, 187(1), pp. 219–227. doi: 10.1148/radiology.187.1.8451417.

Mierisová, Š. and Ala-Korpela, M. (2001) ‘MR spectroscopy quantitation: A review of frequency domain methods’, *NMR in Biomedicine*. John Wiley & Sons, Ltd, pp. 247–259. doi: 10.1002/nbm.697.

Miller, B. L. (1991) ‘A review of chemical issues in1H NMR spectroscopy:N-acetyl-l-aspartate, creatine and choline’, *NMR in Biomedicine*. John Wiley & Sons, Ltd, 4(2), pp. 47–52. doi: 10.1002/nbm.1940040203.

Miller, B. L. *et al.* (1996) ‘In vivo 1H MRS choline:Correlation with in vitro

chemistry/histology', *Life Sciences*. Elsevier Inc., 58(22), pp. 1929–1935. doi: 10.1016/0024-3205(96)00182-8.

Miller, D. H., Chard, D. T. and Ciccarelli, O. (2012) 'Clinically isolated syndromes', *The Lancet Neurology*. Lancet Neurol, pp. 157–169. doi: 10.1016/S1474-4422(11)70274-5.

Moccia, M. *et al.* (2019) 'Advances in spinal cord imaging in multiple sclerosis', *Therapeutic Advances in Neurological Disorders*. SAGE Publications Ltd. doi: 10.1177/1756286419840593.

Moccia, M. *et al.* (2020) 'Pathologic correlates of the magnetization transfer ratio in multiple sclerosis', *Neurology*. NLM (Medline), 95(22), pp. e2965–e2976. doi: 10.1212/WNL.0000000000010909.

Moccia, M., de Stefano, N. and Barkhof, F. (2017) 'Imaging outcome measures for progressive multiple sclerosis trials', *Multiple Sclerosis*. SAGE Publications Ltd, 23(12), pp. 1614–1626. doi: 10.1177/1352458517729456.

Modat, M. *et al.* (2010) 'Fast free-form deformation using graphics processing units', *Computer Methods and Programs in Biomedicine*. Elsevier, 98(3), pp. 278–284. doi: 10.1016/j.cmpb.2009.09.002.

Moffett, J. *et al.* (2006) *N-acetylaspartate: A unique neuronal molecule in the central nervous system*. Available at: https://link.springer.com/book/10.1007/0-387-30172-0 (Accessed: 11 July 2019).

Moffett, J. R. *et al.* (1991) 'Immunohistochemical localization of N-acetylaspartate in rat brain.', *Neuroreport*, 2(3), pp. 131–4. Available at: http://www.ncbi.nlm.nih.gov/pubmed/1768855 (Accessed: 11 July 2019).

Moffett, J. R. and Namboodiri, M. A. (1995) 'Differential distribution of N-acetylaspartylglutamate and N-acetylaspartate immunoreactivities in rat forebrain.', *Journal of neurocytology*, 24(6), pp. 409–33. Available at: http://www.ncbi.nlm.nih.gov/pubmed/7595659 (Accessed: 11 July 2019).

Mokry, L. E. *et al.* (2016) ‘Obesity and Multiple Sclerosis: A Mendelian Randomization Study’, *PLoS Medicine*. Public Library of Science, 13(6). doi: 10.1371/journal.pmed.1002053.

Moll, N. M. *et al.* (2008) ‘Cortical demyelination in PML and MS: Similarities and differences’, *Neurology*. Lippincott Williams and Wilkins, 70(5), pp. 336–343. doi: 10.1212/01.wnl.0000284601.54436.e4.

Moll, N. M. *et al.* (2011) ‘Multiple sclerosis normal-appearing white matter: pathology-imaging correlations.’, *Annals of neurology*. NIH Public Access, 70(5), pp. 764–73. doi: 10.1002/ana.22521.

Moonen, C. T. *et al.* (1989) ‘Comparison of single-shot localization methods (STEAM and PRESS) for in vivo proton NMR spectroscopy.’, *NMR in biomedicine*, 2(5–6), pp. 201–8. Available at: http://www.ncbi.nlm.nih.gov/pubmed/2641894 (Accessed: 16 October 2019).

Morrissey, S. P. *et al.* (1993) ‘The significance of brain magnetic resonance imaging abnormalities at presentation with clinically isolated syndromes suggestive of multiple sclerosis: A 5-year follow-up study’, *Brain*. Brain, 116(1), pp. 135–146. doi: 10.1093/brain/116.1.135.

Mostert, J. *et al.* (2013) ‘The Effect of Fluoxetine on Progression in Progressive Multiple Sclerosis: A Double-Blind, Randomized, Placebo-Controlled Trial’, *ISRN Neurology*, 2013, pp. 1–6. doi: 10.1155/2013/370943.

Mostert, J. P. *et al.* (2006) ‘Fluoxetine increases cerebral white matter NAA/Cr ratio in patients with multiple sclerosis.’, *Neuroscience letters*, 402(1–2), pp. 22–4. doi: 10.1016/j.neulet.2006.03.042.

Mostert, J. P. *et al.* (2008) ‘Effects of fluoxetine on disease activity in relapsing multiple sclerosis: A double-blind, placebo-controlled, exploratory study’, *Journal of Neurology, Neurosurgery and Psychiatry*. BMJ Publishing Group, 79(9), pp. 1027–1031. doi: 10.1136/jnnp.2007.139345.

Mostert, J. P. *et al.* (2010) ‘T2 lesions and rate of progression of disability in multiple sclerosis’, *European Journal of Neurology*. Eur J Neurol, 17(12), pp.

1471–1475. doi: 10.1111/j.1468-1331.2010.03093.x.

Motl, R. W. *et al.* (2017) ‘Validity of the timed 25-foot walk as an ambulatory performance outcome measure for multiple sclerosis’, *Multiple Sclerosis*. SAGE Publications Ltd, pp. 704–710. doi: 10.1177/1352458517690823.

Mottershead, J. P. *et al.* (2003) ‘High field MRI correlates of myelin content and axonal density in multiple sclerosis: A post-mortem study of the spinal cord’, *Journal of Neurology*. J Neurol, 250(11), pp. 1293–1301. doi: 10.1007/s00415-003-0192-3.

Mowry, E. M. *et al.* (2010) ‘Vitamin D status is associated with relapse rate in pediatric-onset multiple sclerosis’, *Annals of Neurology*, 67(5), pp. 618–624. doi: 10.1002/ana.21972.

Mumford, C. J. *et al.* (1994) ‘The british isles survey of multiple sclerosis in twins’, *Neurology*, 44(1), pp. 11–15. doi: 10.1212/wnl.44.1.11.

Munger, K. L. *et al.* (2013) ‘Childhood body mass index and multiple sclerosis risk: A long-term cohort study’, *Multiple Sclerosis Journal*, 19(10), pp. 1323–1329. doi: 10.1177/1352458513483889.

Munger, K. L., Chitnis, T. and Ascherio, A. (2009) ‘Body size and risk of MS in two cohorts of US women’, *Neurology*. Lippincott Williams and Wilkins, 73(19), pp. 1543–1550. doi: 10.1212/WNL.0b013e3181c0d6e0.

Nantes, J. C. *et al.* (2017) ‘GABA and glutamate levels correlate with MTR and clinical disability: Insights from multiple sclerosis’, *NeuroImage*. Academic Press, 157, pp. 705–715. doi: 10.1016/J.NEUROIMAGE.2017.01.033.

Narayana, P. A. *et al.* (2004) ‘Multicentre proton magnetic resonance spectroscopy imaging of primary progressive multiple sclerosis.’, *Multiple sclerosis (Houndmills, Basingstoke, England)*, 10 Suppl 1, pp. S73-8. Available at: http://www.ncbi.nlm.nih.gov/pubmed/15218814 (Accessed: 8 January 2019).

Narayana, P. A. (2005) ‘Magnetic resonance spectroscopy in the monitoring

of multiple sclerosis.', *Journal of neuroimaging : official journal of the American Society of Neuroimaging*. NIH Public Access, 15(4 Suppl), pp. 46S-57S. doi: 10.1177/1051228405284200.

Narayanan, S. *et al.* (1997) 'Imaging of axonal damage in multiple sclerosis: Spatial distribution of magnetic resonance imaging lesions', *Annals of Neurology*. John Wiley & Sons, Ltd, 41(3), pp. 385–391. doi: 10.1002/ana.410410314.

Nathoo, N., Yong, V. W. and Dunn, J. F. (2014) 'Understanding disease processes in multiple sclerosis through magnetic resonance imaging studies in animal models', *NeuroImage: Clinical*, 4, pp. 743–756. doi: 10.1016/j.nicl.2014.04.011.

Neu, A. *et al.* (2002) 'Activation of GABAA Receptors by Guanidinoacetate: A Novel Pathophysiological Mechanism', *Neurobiology of Disease*, 11(2), pp. 298–307. doi: 10.1006/nbdi.2002.0547.

Nicholas, J M *et al.* (2017) 'Effect of high-dose simvastatin on cognitive, neuropsychiatric, and health-related quality-of-life measures in secondary progressive multiple sclerosis: secondary analyses from the MS-STAT randomised, placebo-controlled trial', *The Lancet*. doi: 10.1016/S1474-4422(17)30113-8.

Nijeholt, G. J. L. à *et al.* (2001) 'Post-mortem high-resolution MRI of the spinal cord in multiple sclerosis', *Brain*. Oxford University Press, 124(1), pp. 154–166. doi: 10.1093/brain/124.1.154.

Noseworthy, J. H. *et al.* (1990) 'Interrater variability with the expanded disability status scale (EDSS) and functional systems (FS) in a multiple sclerosis clinical trial', *Neurology*, 40(6), pp. 971–975. doi: 10.1212/wnl.40.6.971.

O'Riordan, J. I. *et al.* (1998) 'The prognostic value of brain MRI in clinically isolated syndromes of the CNS. A 10-year follow-up', *Brain*. Brain, 121(3), pp. 495–503. doi: 10.1093/brain/121.3.495.

Obert, D. *et al.* (2016) ‘Brain Metabolite Changes in Patients with Relapsing-Remitting and Secondary Progressive Multiple Sclerosis: A Two-Year Follow-Up Study’, *PLOS ONE*. Edited by H. Sawada. Public Library of Science, 11(9), p. e0162583. doi: 10.1371/journal.pone.0162583.

Ogg, R. J., Kingsley, P. B. and Taylor, J. S. (1994) ‘WET, a T1- and B1-insensitive water-suppression method for in vivo localized 1H NMR spectroscopy.’, *Journal of magnetic resonance. Series B*, 104(1), pp. 1–10. Available at: http://www.ncbi.nlm.nih.gov/pubmed/8025810 (Accessed: 16 October 2019).

Oh, J. (2004) ‘Mechanisms of normal appearing corpus callosum injury related to pericallosal T1 lesions in multiple sclerosis using directional diffusion tensor and 1H MRS imaging’, *Journal of Neurology, Neurosurgery & Psychiatry*, 75(9), pp. 1281–1286. doi: 10.1136/jnnp.2004.039032.

Oh, J., Pelletier, D. and Nelson, S. J. (2004) ‘Corpus Callosum Axonal Injury in Multiple Sclerosis Measured by Proton Magnetic Resonance Spectroscopic Imaging’, *Archives of Neurology*. American Medical Association, 61(7), pp. 1081–1086. doi: 10.1001/archneur.61.7.1081.

Orton, S. M. *et al.* (2006) ‘Sex ratio of multiple sclerosis in Canada: a longitudinal study’, *Lancet Neurology*, 5(11), pp. 932–936. doi: 10.1016/S1474-4422(06)70581-6.

Pampliega, O. *et al.* (2011) ‘Increased expression of cystine/glutamate antiporter in multiple sclerosis’, *Journal of Neuroinflammation*. BioMed Central, 8(1), p. 63. doi: 10.1186/1742-2094-8-63.

Pan, J. W. *et al.* (2002) ‘Metabolic differences between multiple sclerosis subtypes measured by quantitative MR spectroscopy’. doi: 10.1191/1352458502ms802oa.

Parker, R. A. and Weir, C. J. (2020) ‘Non-adjustment for multiple testing in multi-arm trials of distinct treatments: rationale and justification’, *Clinical Trials*, ((In Press)).

Patel, C. J. and Ioannidis, J. P. A. (2014) ‘Placing epidemiological results in the context of multiplicity and typical correlations of exposures’, *J Epidemiol Community Health*, 68, pp. 1096–1100. doi: 10.1136/jech-2014-204195.

Patel, T. B. and Clark, J. B. (1979) ‘Synthesis of *N* -acetyl-l-aspartate by rat brain mitochondria and its involvement in mitochondrial/cytosolic carbon transport’, *Biochemical Journal*, 184(3), pp. 539–546. doi: 10.1042/bj1840539.

Patt, S. L. and Sykes, B. D. (1972) ‘Water eliminated fourier transform NMR spectroscopy’, *The Journal of Chemical Physics*. American Institute of PhysicsAIP, pp. 3182–3184. doi: 10.1063/1.1677669.

Pelletier, D. *et al.* (2002) ‘3-D echo planar (1)HMRS imaging in MS: metabolite comparison from supratentorial vs. central brain.’, *Magnetic resonance imaging*, 20(8), pp. 599–606. Available at: http://www.ncbi.nlm.nih.gov/pubmed/12467867 (Accessed: 27 June 2019).

Pelletier, D. *et al.* (2003) ‘MRI lesion volume heterogeneity in primary progressive MS in relation with axonal damage and brain atrophy’, *Journal of Neurology, Neurosurgery & Psychiatry*, 74(7), pp. 950–952. doi: 10.1136/jnnp.74.7.950.

Penny, S. *et al.* (2010) ‘Early imaging predicts later cognitive impairment in primary progressive multiple sclerosis’, *Neurology*, 74(7), pp. 545–552. doi: 10.1212/WNL.0b013e3181cff6a6.

Peral, M. J., Vázquez-Carretero, M. D. and Ilundain, A. A. (2010) ‘Na+/Cl−/creatine transporter activity and expression in rat brain synaptosomes’, *Neuroscience*, 165(1), pp. 53–60. doi: 10.1016/j.neuroscience.2009.10.001.

Peters, A. *et al.* (1995) ‘A study of multiple sclerosis patients with magnetic resonance spectroscopic imaging’, *Multiple Sclerosis Journal*. SAGE PublicationsSage UK: London, England, 1(1), pp. 25–31. doi: 10.1177/135245859500100105.

Petrova, N. *et al.* (2018) ‘Axonal loss in the multiple sclerosis spinal cord

revisited', *Brain Pathology*. Blackwell Publishing Ltd, 28(3), pp. 334–348. doi: 10.1111/bpa.12516.

Pfeuffer, J. *et al.* (1999) 'Toward an in Vivo Neurochemical Profile: Quantification of 18 Metabolites in Short-Echo-Time 1H NMR Spectra of the Rat Brain', *Journal of Magnetic Resonance*, 141(1), pp. 104–120. doi: 10.1006/jmre.1999.1895.

Pike, G. B. *et al.* (1999) 'Combined Magnetization Transfer and Proton Spectroscopic Imaging in the Assessment of Pathologic Brain Lesions in Multiple Sclerosis', *American Journal of Neuroradiology*, 20(5). Available at: http://www.ajnr.org/content/20/5/829.long (Accessed: 27 September 2018).

Pitt, D. *et al.* (2003) 'Glutamate uptake by oligodendrocytes: Implications for excitotoxicity in multiple sclerosis', *Neurology*. Lippincott Williams and Wilkins, 61(8), pp. 1113–1120. doi: 10.1212/01.WNL.0000090564.88719.37.

Polman, C. H. *et al.* (2005) 'Diagnostic criteria for multiple sclerosis: 2005 revisions to the "McDonald Criteria"', *Annals of Neurology*, 58(6), pp. 840–846. doi: 10.1002/ana.20703.

Polman, C. H. *et al.* (2011) 'Diagnostic criteria for multiple sclerosis: 2010 Revisions to the McDonald criteria', *Annals of Neurology*, 69(2), pp. 292–302. doi: 10.1002/ana.22366.

Ponath, G., Park, C. and Pitt, D. (2018) 'The role of astrocytes in multiple sclerosis', *Frontiers in Immunology*. Frontiers Media S.A., p. 1. doi: 10.3389/fimmu.2018.00217.

Poser, C. M. *et al.* (1983) 'New diagnostic criteria for multiple sclerosis: Guidelines for research protocols', *Annals of Neurology*, 13(3), pp. 227–231. doi: 10.1002/ana.410130302.

Poullet, J.-B., Sima, D. M. and Van Huffel, S. (2008) 'MRS signal quantitation: A review of time- and frequency-domain methods', *Journal of Magnetic Resonance*, 195, pp. 134–144. doi: 10.1016/j.jmr.2008.09.005.

Poullet, J. B. *et al.* (2007) ‘An automated quantification of short echo time MRS spectra in an open source software environment: AQSES’, *NMR in Biomedicine*. NMR Biomed, 20(5), pp. 493–504. doi: 10.1002/nbm.1112.

Pouwels, P. J. and Frahm, J. (1997) ‘Differential distribution of NAA and NAAG in human brain as determined by quantitative localized proton MRS.’, *NMR in biomedicine*, 10(2), pp. 73–8. Available at: http://www.ncbi.nlm.nih.gov/pubmed/9267864 (Accessed: 11 July 2019).

Provencher, S. W. (1993) ‘Estimation of metabolite concentrations from localized in vivo proton NMR spectra.’, *Magnetic resonance in medicine*, 30(6), pp. 672–9. Available at: http://www.ncbi.nlm.nih.gov/pubmed/8139448 (Accessed: 6 December 2018).

Pulizzi, A. *et al.* (2007) ‘Determinants of Disability in Multiple Sclerosis at Various Disease Stages’, *Archives of Neurology*. American Medical Association, 64(8), p. 1163. doi: 10.1001/archneur.64.8.1163.

R Core Team (2017) ‘R: A language and environment for statistical computing’. Vienna: R Foundation for Statistical Computing. Available at: https://www.r-project.org/.

Rackayova, V., Pouwels, P. J. W. and Braissant, O. (2017) ‘Creatine in the central nervous system: From magnetic resonance spectroscopy to creatine deficiencies’, *Analytical Biochemistry*. Academic Press, 529, pp. 144–157. doi: 10.1016/J.AB.2016.11.007.

Rahimian, N. *et al.* (2013) ‘Magnetic resonance spectroscopic findings of chronic lesions in two subtypes of multiple sclerosis: primary progressive versus relapsing remitting.’, *Iranian journal of radiology : a quarterly journal published by the Iranian Radiological Society*. Kowsar Medical Institute, 10(3), pp. 128–32. doi: 10.5812/iranjradiol.11336.

Rahn, A. C. *et al.* (2019) ‘Magnetic resonance imaging as a prognostic disability marker in clinically isolated syndrome: A systematic review’, *Acta Neurologica Scandinavica*. Blackwell Publishing Ltd, 139(1), pp. 18–32. doi: 10.1111/ane.13010.

Ramió-Torrentà, L. *et al.* (2006) ‘Abnormalities in normal appearing tissues in early primary progressive multiple sclerosis and their relation to disability: A tissue specific magnetisation transfer study’, *Journal of Neurology, Neurosurgery and Psychiatry*. BMJ Publishing Group, 77(1), pp. 40–45. doi: 10.1136/jnnp.2004.052316.

Ranjeva, J. P. *et al.* (2003) ‘MRI/MRS of corpus callosum in patients with clinically isolated syndrome suggestive of multiple sclerosis’, *Multiple Sclerosis Journal*, 9(6), pp. 554–565. doi: 10.1191/1352458503ms938oa.

Rao, S. M. *et al.* (1989) ‘Correlation of magnetic resonance imaging with neuropsychological testing in multiple sclerosis’, *Neurology*, 39(2), pp. 161–166. doi: 10.1212/wnl.39.2.161.

Rao, S. M. *et al.* (1991) ‘Cognitive dysfunction in multiple sclerosis.: I. Frequency, patterns, and prediction’, *Neurology*, 41(5), pp. 685–691. doi: 10.1212/WNL.41.5.685.

Ratiney, H. *et al.* (2005) ‘Time-domain semi-parametric estimation based on a metabolite basis set’, *NMR in Biomedicine*. NMR Biomed, 18(1), pp. 1–13. doi: 10.1002/nbm.895.

Reynolds, G. *et al.* (2006) ‘An algorithm for the automated quantitation of metabolites in in vitro NMR signals’, *Magnetic Resonance in Medicine*. John Wiley and Sons Inc., 56(6), pp. 1211–1219. doi: 10.1002/mrm.21081.

Richards, T. L. *et al.* (1995) ‘Experimental allergic encephalomyelitis in non-human primates: mri and mrs may predict the type of brain damage’, *NMR in Biomedicine*, 8(2), pp. 49–58. doi: 10.1002/nbm.1940080202.

Rocca, M. A. *et al.* (2003) ‘Evidence for axonal pathology and adaptive cortical reorganization in patients at presentation with clinically isolated syndromes suggestive of multiple sclerosis.’, *NeuroImage*, 18(4), pp. 847–55. doi: 10.1016/s1053-8119(03)00043-0.

Rocca, M. A. *et al.* (2015) ‘Clinical and imaging assessment of cognitive dysfunction in multiple sclerosis’, *The Lancet Neurology*. Elsevier Ltd, 14(3),

pp. 302–317. doi: 10.1016/S1474-4422(14)70250-9.

Rocca, M. A. *et al.* (2017) ‘Brain MRI atrophy quantification in MS’, *Neurology*. Lippincott Williams and Wilkins, 88(4), pp. 403–413. doi: 10.1212/WNL.0000000000003542.

Roser, W. *et al.* (1995) ‘Proton MRS of Gadolinium-enhancing MS Plaques and Metabolic Changes in Normal-Appearing White Matter’, *Magnetic Resonance in Medicine*. John Wiley & Sons, Ltd, 33(6), pp. 811–817. doi: 10.1002/mrm.1910330611.

Rovaris, Marco *et al.* (2005) ‘Axonal Injury and Overall Tissue Loss Are Not Related in Primary Progressive Multiple Sclerosis’, *Archives of Neurology*, 62(6), pp. 898–902. doi: 10.1001/archneur.62.6.898.

Rovaris, M. *et al.* (2005) ‘Axonal injury in early multiple sclerosis is irreversible and independent of the short-term disease evolution’, *Neurology*, 65(10), pp. 1626–1630. doi: 10.1212/01.wnl.0000184493.06254.a6.

Rovaris, M. *et al.* (2006) ‘Grey matter damage predicts the evolution of primary progressive multiple sclerosis at 5 years’, *Brain*. Brain, 129(10), pp. 2628–2634. doi: 10.1093/brain/awl222.

Rovaris, M. *et al.* (2008) ‘Large-scale, multicentre, quantitative MRI study of brain and cord damage in primary progressive multiple sclerosis’, *Multiple Sclerosis*. Mult Scler, 14(4), pp. 455–464. doi: 10.1177/1352458507085129.

Rudick, R. *et al.* (1997) ‘Recommendations from the national multiple sclerosis society clinical outcomes assessment task force’, *Annals of Neurology*. John Wiley and Sons Inc., 42(3), pp. 379–382. doi: 10.1002/ana.410420318.

Rudick, R. A. *et al.* (1999) ‘Use of the brain parenchymal fraction to measure whole brain atrophy in relapsing-remitting MS’, *Neurology*. Lippincott Williams and Wilkins, 53(8), pp. 1698–1704. doi: 10.1212/wnl.53.8.1698.

Runia, T. F. *et al.* (2012) ‘Lower serum vitamin D levels are associated with a higher relapse risk in multiple sclerosis’, *Neurology*. Lippincott Williams and

Wilkins, 79(3), pp. 261–266. doi: 10.1212/WNL.0b013e31825fdec7.

Saade, C. *et al.* (2018) ‘Gadolinium and multiple sclerosis: Vessels, barriers of the brain, and glymphatics’, *American Journal of Neuroradiology*. American Society of Neuroradiology, pp. 2168–2176. doi: 10.3174/ajnr.A5773.

Sadovnick, A. D. *et al.* (1993) ‘A population-based study of multiple sclerosis in twins: Update’, *Annals of Neurology*, 33(3), pp. 281–285. doi: 10.1002/ana.410330309.

Sailer, M. *et al.* (1999) ‘Quantitative MRI in patients with clinically isolated syndromes suggestive of demyelination’, *Neurology*. Lippincott Williams and Wilkins, 52(3), pp. 599–606. doi: 10.1212/wnl.52.3.599.

Sajja, B., Narayana, P. and Wolinsky, J. (2008) ‘Longitudinal magnetic resonance spectroscopic imaging of primary progressive multiple sclerosis patients treated with glatiramer acetate: multicenter study’, *Multiple Sclerosis*, 14, pp. 73–80. doi: 10.1177/1352458507079907.

Salibi, N. and Brown, M. A. (1997) *Clinical MR Spectroscopy: First Principles*. Wiley.

Sarchielli, P. *et al.* (1999) ‘Absolute quantification of brain metabolites by proton magnetic resonance spectroscopy in normal-appearing white matter of multiple sclerosis patients.’, *Brain : a journal of neurology*, 122 (Pt 3), pp. 513–21. Available at: http://www.ncbi.nlm.nih.gov/pubmed/10094259 (Accessed: 29 January 2018).

Sarchielli, P. *et al.* (2002) ‘Localized 1 H magnetic resonance spectroscopy in mainly cortical gray matter of patients with multiple sclerosis’, *Journal of Neurology*. Steinkopff-Verlag, 249(7), pp. 902–910. doi: 10.1007/s00415-002-0758-5.

Sarchielli, P. *et al.* (2003) ‘Excitatory amino acids and multiple sclerosis: Evidence from cerebrospinal fluid’, *Archives of Neurology*. Arch Neurol, 60(8), pp. 1082–1088. doi: 10.1001/archneur.60.8.1082.

Sastre-Garriga, J. *et al.* (2004) ‘Grey and white matter atrophy in early clinical stages of primary progressive multiple sclerosis’, *NeuroImage*. Neuroimage, 22(1), pp. 353–359. doi: 10.1016/j.neuroimage.2004.02.008.

Sastre-Garriga, J. *et al.* (2005) ‘Metabolite Changes in Normal-Appearing Gray and White Matter Are Linked With Disability in Early Primary Progressive Multiple Sclerosis’, *Archives of Neurology*, 62(4), p. 569. doi: 10.1001/archneur.62.4.569.

Sbardella, E. *et al.* (2011) ‘Pronounced focal and diffuse brain damage predicts short-term disease evolution in patients with clinically isolated syndrome suggestive of multiple sclerosis’, *Multiple Sclerosis Journal*, 17(12), pp. 1432–1440. doi: 10.1177/1352458511414602.

Scalfari, A. *et al.* (2011) ‘Age and disability accumulation in multiple sclerosis’, *Neurology*. Lippincott Williams and Wilkins, 77(13), pp. 1246–1252. doi: 10.1212/WNL.0b013e318230a17d.

Scalfari, A. *et al.* (2014) ‘Onset of secondary progressive phase and long-term evolution of multiple sclerosis’, *Journal of Neurology, Neurosurgery and Psychiatry*. BMJ Publishing Group, 85(1), pp. 67–75. doi: 10.1136/jnnp-2012-304333.

Schlaeger, R. *et al.* (2015) ‘Association between thoracic spinal cord gray matter atrophy and disability in multiple sclerosis’, *JAMA Neurology*. American Medical Association, 72(8), pp. 897–904. doi: 10.1001/jamaneurol.2015.0993.

Schmidt, A. (2004) ‘Severely altered guanidino compound levels, disturbed body weight homeostasis and impaired fertility in a mouse model of guanidinoacetate N-methyltransferase (GAMT) deficiency’, *Human Molecular Genetics*, 13(9), pp. 905–921. doi: 10.1093/hmg/ddh112.

Schmierer, K. *et al.* (2004) ‘Magnetization transfer ratio and myelin in postmortem multiple sclerosis brain’, *Annals of Neurology*. Ann Neurol, 56(3), pp. 407–415. doi: 10.1002/ana.20202.

Schmierer, K. *et al.* (2007) ‘Quantitative magnetization transfer imaging in

postmortem multiple sclerosis brain', *Journal of Magnetic Resonance Imaging*. Europe PMC Funders, 26(1), pp. 41–51. doi: 10.1002/jmri.20984.

Sedel, F. *et al.* (2015) 'High doses of biotin in chronic progressive multiple sclerosis: A pilot study', *Multiple Sclerosis and Related Disorders*. Elsevier, 4(2), pp. 159–169. doi: 10.1016/J.MSARD.2015.01.005.

Shen, J. *et al.* (1999) 'Linear projection method for automatic slice shimming.', *Magnetic resonance in medicine*, 42(6), pp. 1082–8. Available at: http://www.ncbi.nlm.nih.gov/pubmed/10571929 (Accessed: 3 April 2019).

Signori, A. *et al.* (2016) 'Long-term impact of interferon or Glatiramer acetate in multiple sclerosis: A systematic review and meta-analysis', *Multiple Sclerosis and Related Disorders*. Elsevier B.V., 6, pp. 57–63. doi: 10.1016/j.msard.2016.01.007.

Sijens, P. E. *et al.* (2005) 'Analysis of the human brain in primary progressive multiple sclerosis with mapping of the spatial distributions using 1H MR spectroscopy and diffusion tensor imaging', *European Radiology*, 15(8), pp. 1686–1693. doi: 10.1007/s00330-005-2775-0.

Sijens, P. E., Mostert, J. P., *et al.* (2006) '1H MR spectroscopy of the brain in multiple sclerosis subtypes with analysis of the metabolite concentrations in gray and white matter: initial findings', *European Radiology*. Springer-Verlag, 16(2), pp. 489–495. doi: 10.1007/s00330-005-2839-1.

Sijens, P. E., Irwan, R., *et al.* (2006) 'Relationships between brain water content and diffusion tensor imaging parameters (apparent diffusion coefficient and fractional anisotropy) in multiple sclerosis', *European Radiology*. Springer-Verlag, 16(4), pp. 898–904. doi: 10.1007/s00330-005-0033-0.

Sijens, P. E. *et al.* (2008) 'Impact of fluoxetine on the human brain in multiple sclerosis as quantified by proton magnetic resonance spectroscopy and diffusion tensor imaging', *Psychiatry Research: Neuroimaging*, 164(3), pp. 274–282. doi: 10.1016/j.pscychresns.2007.12.014.

Simone, I. L. *et al.* (2001) 'Axonal damage in multiple sclerosis plaques: a

combined magnetic resonance imaging and 1H-magnetic resonance spectroscopy study.', *Journal of the neurological sciences*, 182(2), pp. 143–50. Available at: http://www.ncbi.nlm.nih.gov/pubmed/11137520 (Accessed: 7 January 2019).

Simpson, S. *et al.* (2010) 'Higher 25-hydroxyvitamin D is associated with lower relapse risk in multiple sclerosis', *Annals of Neurology*. John Wiley and Sons Inc., 68(2), pp. 193–203. doi: 10.1002/ana.22043.

Sintzel, M. B., Rametta, M. and Reder, A. T. (2018) 'Vitamin D and Multiple Sclerosis: A Comprehensive Review', *Neurology and Therapy*. Springer Healthcare, pp. 59–85. doi: 10.1007/s40120-017-0086-4.

Smith, S. M. *et al.* (2002) 'Accurate, Robust, and Automated Longitudinal and Cross-Sectional Brain Change Analysis', *NeuroImage*. Academic Press, 17(1), pp. 479–489. doi: 10.1006/NIMG.2002.1040.

Smith, S. M. (2002) 'Fast robust automated brain extraction', *Human Brain Mapping*. Wiley-Blackwell, 17(3), pp. 143–155. doi: 10.1002/hbm.10062.

Smith, S. M. *et al.* (2007) 'Longitudinal and cross-sectional analysis of atrophy in Alzheimer's disease: Cross-validation of BSI, SIENA and SIENAX', *NeuroImage*. Academic Press, 36(4), pp. 1200–1206. doi: 10.1016/J.NEUROIMAGE.2007.04.035.

Smolders, J. *et al.* (2008) 'Association of vitamin D metabolite levels with relapse rate and disability in multiple sclerosis', *Multiple Sclerosis*, 14(9), pp. 1220–1224. doi: 10.1177/1352458508094399.

Solana, E. *et al.* (2018) 'Magnetic resonance markers of tissue damage related to connectivity disruption in multiple sclerosis.', *NeuroImage. Clinical*. Elsevier, 20, pp. 161–168. doi: 10.1016/j.nicl.2018.07.012.

Solanky, B. S. *et al.* (2020) 'NAA is a Marker of Disability in Secondary-Progressive MS: A Proton MR Spectroscopic Imaging Study', *American Journal of Neuroradiology*. American Journal of Neuroradiology. doi: 10.3174/ajnr.A6809.

Sonder, J. M. *et al.* (2014) ‘Comparing long-term results of PASAT and SDMT scores in relation to neuropsychological testing in multiple sclerosis’, *Multiple Sclerosis Journal*. SAGE PublicationsSage UK: London, England, 20(4), pp. 481–488. doi: 10.1177/1352458513501570.

Srinivasan, R. *et al.* (2005) ‘Evidence of elevated glutamate in multiple sclerosis using magnetic resonance spectroscopy at 3 T’, *Brain*. Oxford University Press, 128(5), pp. 1016–1025. doi: 10.1093/brain/awh467.

Srinivasan, R. *et al.* (2010) ‘MR spectroscopic imaging of glutathione in the white and gray matter at 7 T with an application to multiple sclerosis’, *Magnetic Resonance Imaging*. Elsevier, 28(2), pp. 163–170. doi: 10.1016/J.MRI.2009.06.008.

Stankiewicz, J. M. *et al.* (2009) ‘Spinal cord lesions and clinical status in multiple sclerosis: A 1.5 T and 3 T MRI study’, *Journal of the Neurological Sciences*. NIH Public Access, 279(1–2), pp. 99–105. doi: 10.1016/j.jns.2008.11.009.

Steen, C. *et al.* (2010) ‘Reduced Creatine Kinase B Activity in Multiple Sclerosis Normal Appearing White Matter’, *PLoS ONE*. Edited by C. Kleinschnitz, 5(5), p. e10811. doi: 10.1371/journal.pone.0010811.

Steenwijk, M. D. *et al.* (2015) ‘Unraveling the relationship between regional gray matter atrophy and pathology in connected white matter tracts in long-standing multiple sclerosis’, *Human Brain Mapping*. John Wiley and Sons Inc., 36(5), pp. 1796–1807. doi: 10.1002/hbm.22738.

De Stefano, N. *et al.* (1995) ‘Chemical pathology of acute demyelinating lesions and its correlation with disability’, *Annals of Neurology*. John Wiley & Sons, Ltd, 38(6), pp. 901–909. doi: 10.1002/ana.410380610.

De Stefano, N. *et al.* (1998) ‘Axonal damage correlates with disability in patients with relapsing-remitting multiple sclerosis. Results of a longitudinal magnetic resonance spectroscopy study.’, *Brain : a journal of neurology*, 121 (Pt 8, pp. 1469–77. Available at: http://www.ncbi.nlm.nih.gov/pubmed/9712009 (Accessed: 4 January 2019).

De Stefano, N. *et al.* (2001) ‘Evidence of Axonal Damage in the Early Stages of Multiple Sclerosis and Its Relevance to Disability’, *Archives of Neurology*. American Medical Association, 58(1), pp. 65–70. doi: 10.1001/archneur.58.1.65.

De Stefano, N. *et al.* (2010) ‘Assessing brain atrophy rates in a large population of untreated multiple sclerosis subtypes’, *Neurology*, 74(23), pp. 1868–1876. doi: 10.1212/WNL.0b013e3181e24136.

Stevenson, V. L. *et al.* (1998) ‘Spinal cord atrophy and disability in MS: A longitudinal study’, *Neurology*. Lippincott Williams and Wilkins, 51(1), pp. 234–238. doi: 10.1212/WNL.51.1.234.

Strasser-Fuchs, S. *et al.* (2008) ‘Clinically benign multiple sclerosis despite large T2 lesion load: Can we explain this paradox?’, *Multiple Sclerosis Journal*, 14(2), pp. 205–211. doi: 10.1177/1352458507082354.

Strober, L. *et al.* (2019) ‘Symbol Digit Modalities Test: A valid clinical trial endpoint for measuring cognition in multiple sclerosis’, *Multiple Sclerosis Journal*. SAGE PublicationsSage UK: London, England, 25(13), pp. 1781–1790. doi: 10.1177/1352458518808204.

Suhy, J. *et al.* (2000) ‘1H MRSI comparison of white matter and lesions in primary progressive and relapsing-remitting MS.’, *Multiple sclerosis (Houndmills, Basingstoke, England)*. NIH Public Access, 6(3), pp. 148–55. doi: 10.1177/135245850000600303.

Summers, M. *et al.* (2008) ‘Cognitive impairment in multiple sclerosis can be predicted by imaging early in the disease’, *Journal of Neurology, Neurosurgery and Psychiatry*. J Neurol Neurosurg Psychiatry, 79(8), pp. 955–958. doi: 10.1136/jnnp.2007.138685.

Sumowski, J. F. *et al.* (2018) ‘Cognition in multiple sclerosis: State of the field and priorities for the future’, *Neurology*. United States, 90(6), pp. 278–288. doi: 10.1212/WNL.0000000000004977.

Swanberg, K. M. *et al.* (2019) ‘Quantifying the Metabolic Signature of Multiple

Sclerosis by in vivo Proton Magnetic Resonance Spectroscopy: Current Challenges and Future Outlook in the Translation From Proton Signal to Diagnostic Biomarker', *Frontiers in Neurology*. Frontiers Media S.A. doi: 10.3389/fneur.2019.01173.

Swanton, J. K. *et al.* (2006) 'Is the frequency of abnormalities on magnetic resonance imaging in isolated optic neuritis related to the prevalence of multiple sclerosis? A global comparison', *Journal of Neurology, Neurosurgery and Psychiatry*, 77(9), pp. 1070–1072. doi: 10.1136/jnnp.2006.090910.

Swanton, J. K. *et al.* (2009) 'Early MRI in optic neuritis: The risk for disability', *Neurology*. Lippincott Williams and Wilkins, 72(6), pp. 542–550. doi: 10.1212/01.wnl.0000341935.41852.82.

Swirsky-Sacchetti, T. *et al.* (1992) 'Neuropsychological and structural brain lesions in multiple sclerosis: A regional analysis', *Neurology*, 42(7), pp. 1291–1295. doi: 10.1212/wnl.42.7.1291.

Tachikawa, M. *et al.* (2004) 'Distinct cellular expressions of creatine synthetic enzyme GAMT and creatine kinases uCK-Mi and CK-B suggest a novel neuron-glial relationship for brain energy homeostasis', *European Journal of Neuroscience*, 20(1), pp. 144–160. doi: 10.1111/j.1460-9568.2004.03478.x.

Tallan, H. H. (1957) 'Studies on the distribution of N-acetyl-L-aspartic acid in brain.', *The Journal of biological chemistry*, 224(1), pp. 41–5. Available at: http://www.ncbi.nlm.nih.gov/pubmed/13398385 (Accessed: 11 July 2019).

Tallan, H. H., Moore, S. and Stein, W. H. (1956) 'N-Acetyl-L-aspartic acid in brain.', *The Journal of biological chemistry*, 219(1), pp. 257–64. Available at: http://www.ncbi.nlm.nih.gov/pubmed/13295277 (Accessed: 11 July 2019).

Tartaglia, M. C. *et al.* (2002) 'Choline is increased in pre-lesional normal appearing white matter in multiple sclerosis', *Journal of Neurology*. Steinkopff Verlag, 249(10), pp. 1382–1390. doi: 10.1007/s00415-002-0846-6.

Tedeholm, H. *et al.* (2013) 'Time to secondary progression in patients with multiple sclerosis who were treated with first generation immunomodulating

drugs', *Multiple Sclerosis Journal*, 19(6), pp. 765–774. doi: 10.1177/1352458512463764.

Thompson, A. J. *et al.* (2018) 'Diagnosis of multiple sclerosis: 2017 revisions of the McDonald criteria', *The Lancet Neurology*, 17(2), pp. 162–173. doi: 10.1016/S1474-4422(17)30470-2.

Thompson, A. J. and Baneke, P. (2013) *Multiple Sclerosis International Federation (MSIF) Design and editorial support by Summers Editorial & Design Graphics by Nutmeg Productions Printed by Modern Colour Solutions*. Available at: www.msif.org (Accessed: 3 January 2020).

Tintore, M. *et al.* (2010) 'Brainstem lesions in clinically isolated syndromes', *Neurology*. Neurology, 75(21), pp. 1933–1938. doi: 10.1212/WNL.0b013e3181feb26f.

Tintore, M. *et al.* (2015) 'Defining high, medium and low impact prognostic factors for developing multiple sclerosis', *Brain*. Oxford University Press, 138(7), pp. 1863–1874. doi: 10.1093/brain/awv105.

Tintore, M. *et al.* (2019) 'The long-term outcomes of CIS patients in the Barcelona inception cohort: Looking back to recognize aggressive MS.', *Multiple sclerosis (Houndmills, Basingstoke, England)*, p. 1352458519877810. doi: 10.1177/1352458519877810.

Tintoré, M. *et al.* (2006) 'Baseline MRI predicts future attacks and disability in clinically isolated syndromes', *Neurology*. Neurology, 67(6), pp. 968–972. doi: 10.1212/01.wnl.0000237354.10144.ec.

Tofts, P., Steens, S. and van Buchem, M. (2003) 'MT: Magnetization transfer', in Tofts, P. (ed.) *Quantitative MRI of the brain*. Chichester: Wiley, pp. 257–298.

Tourbah, A *et al.* (1999) 'Localized proton magnetic resonance spectroscopy in relapsing remitting versus secondary progressive multiple sclerosis.', *Neurology*, 53(5), pp. 1091–7. doi: 10.1212/wnl.53.5.1091.

Tourbah, A. *et al.* (1999) 'Normal-appearing white matter in optic neuritis and

multiple sclerosis: a comparative proton spectroscopy study', *Neuroradiology*. Springer-Verlag, 41(10), pp. 738–743. doi: 10.1007/s002340050835.

Trapp, B. D. *et al.* (1998) 'Axonal Transection in the Lesions of Multiple Sclerosis', *New England Journal of Medicine*, 338(5), pp. 278–285. doi: 10.1056/NEJM199801293380502.

Trapp, B. D. and Stys, P. K. (2009) 'Virtual hypoxia and chronic necrosis of demyelinated axons in multiple sclerosis.', *The Lancet. Neurology*, 8(3), pp. 280–91. doi: 10.1016/S1474-4422(09)70043-2.

Tsagkas, C. *et al.* (2018) 'Spinal cord volume loss: A marker of disease progression in multiple sclerosis', *Neurology*. NLM (Medline), 91(4), pp. e349–e358. doi: 10.1212/WNL.0000000000005853.

Tur, C., Khaleeli, Z., *et al.* (2011) 'Complementary roles of grey matter MTR and T2 lesions in predicting progression in early PPMS', *Journal of Neurology, Neurosurgery and Psychiatry*. J Neurol Neurosurg Psychiatry, 82(4), pp. 423–428. doi: 10.1136/jnnp.2010.209890.

Tur, C., Penny, S., *et al.* (2011) 'Grey matter damage and overall cognitive impairment in primary progressive multiple sclerosis.', *Multiple sclerosis (Houndmills, Basingstoke, England)*. Mult Scler, 17(11), pp. 1324–32. doi: 10.1177/1352458511410341.

Tur, C. *et al.* (2018) 'Assessing treatment outcomes in multiple sclerosis trials and in the clinical setting', *Nature Reviews Neurology*. Nature Publishing Group, pp. 75–93. doi: 10.1038/nrneurol.2017.171.

Uher, T. *et al.* (2014) 'MRI correlates of disability progression in patients with CIS over 48 months', *NeuroImage: Clinical*. Elsevier Inc., 6, pp. 312–319. doi: 10.1016/j.nicl.2014.09.015.

Urenjak, J. *et al.* (1992) 'Specific Expression of N-Acetylaspartate in Neurons, Oligodendrocyte-Type-2 Astrocyte Progenitors, and Immature Oligodendrocytes In Vitro', *Journal of Neurochemistry*, 59(1), pp. 55–61. doi: 10.1111/j.1471-4159.1992.tb08875.x.

Valsasina, P. *et al.* (2013) ‘Regional cervical cord atrophy and disability in multiple sclerosis: A voxel-based analysis’, *Radiology*, 266(3), pp. 853–861. doi: 10.1148/radiol.12120813.

Vanhamme, L. *et al.* (2001) ‘MR spectroscopy quantitation: A review of time-domain methods’, *NMR in Biomedicine*. John Wiley & Sons, Ltd, pp. 233–246. doi: 10.1002/nbm.695.

Vanhamme, L., Van Den Boogaart, A. and Van Huffel, S. (1997) ‘Improved Method for Accurate and Efficient Quantification of MRS Data with Use of Prior Knowledge’, *Journal of Magnetic Resonance*. Academic Press Inc., 129(1), pp. 35–43. doi: 10.1006/jmre.1997.1244.

Vergo, S. *et al.* (2011) ‘Acid-sensing ion channel 1 is involved in both axonal injury and demyelination in multiple sclerosis and its animal model’, *Brain*. Narnia, 134(2), pp. 571–584. doi: 10.1093/brain/awq337.

Vesterinen, H. M. *et al.* (2015) ‘Drug Repurposing: A Systematic Approach to Evaluate Candidate Oral Neuroprotective Interventions for Secondary Progressive Multiple Sclerosis’, *PLOS ONE*. Edited by R. S. Fujinami. Public Library of Science, 10(4), p. e0117705. doi: 10.1371/journal.pone.0117705.

Vidal-Jordana, A. *et al.* (2018) ‘Brain atrophy 15 years after CIS: Baseline and follow-up clinico-radiological correlations.’, *Multiple sclerosis (Houndmills, Basingstoke, England)*. SAGE Publications Ltd, 24(6), pp. 721–727. doi: 10.1177/1352458517707070.

Vrenken, H. *et al.* (2005) ‘MR spectroscopic evidence for glial increase but not for neuro-axonal damage in MS normal-appearing white matter’, *Magnetic Resonance in Medicine*. John Wiley & Sons, Ltd, 53(2), pp. 256–266. doi: 10.1002/mrm.20366.

van der Vuurst de Vries, R. M. *et al.* (2018) ‘Smoking at time of CIS increases the risk of clinically definite multiple sclerosis’, *Journal of Neurology*. Dr. Dietrich Steinkopff Verlag GmbH and Co. KG, 265(5), pp. 1010–1015. doi: 10.1007/s00415-018-8780-4.

Van Walderveen, M. A. A. *et al.* (1999) 'Neuronal damage in T1-hypointense multiple sclerosis lesions demonstrated in vivo using proton magnetic resonance spectroscopy', *Annals of Neurology*. John Wiley & Sons, Ltd, 46(1), pp. 79–87. doi: 10.1002/1531-8249(199907)46:1<79::AID-ANA12>3.0.CO;2-9.

van Walderveen, M. A. *et al.* (1998) 'Histopathologic correlate of hypointense lesions on T1-weighted spin-echo MRI in multiple sclerosis.', *Neurology*, 50(5), pp. 1282–8. Available at: http://www.ncbi.nlm.nih.gov/pubmed/9595975 (Accessed: 7 January 2019).

Wallimann, T. *et al.* (1992) 'Intracellular compartmentation, structure and function of creatine kinase isoenzymes in tissues with high and fluctuating energy demands: the "phosphocreatine circuit" for cellular energy homeostasis', *Biochemical Journal*, 281(1), pp. 21–40. doi: 10.1042/bj2810021.

Wallimann, T., Tokarska-Schlattner, M. and Schlattner, U. (2011) 'The creatine kinase system and pleiotropic effects of creatine', *Amino Acids*, 40(5), pp. 1271–1296. doi: 10.1007/s00726-011-0877-3.

Wallin, M. T. *et al.* (2012) 'The Gulf War era multiple sclerosis cohort: Age and incidence rates by race, sex and service', *Brain*. Oxford University Press, 135(6), pp. 1778–1785. doi: 10.1093/brain/aws099.

Wallin, M. T. *et al.* (2019) 'Global, regional, and national burden of multiple sclerosis 1990–2016: a systematic analysis for the Global Burden of Disease Study 2016', *The Lancet Neurology*. Lancet Publishing Group, 18(3), pp. 269–285. doi: 10.1016/S1474-4422(18)30443-5.

Wattjes, M. P. *et al.* (2007) 'Axonal Damage But No Increased Glial Cell Activity in the Normal-Appearing White Matter of Patients with Clinically Isolated Syndromes Suggestive of Multiple Sclerosis Using High-Field Magnetic Resonance Spectroscopy', *American Journal of Neuroradiology*, 28(8), pp. 1517–1522. doi: 10.3174/ajnr.A0594.

Wattjes, M. P. *et al.* (2008) 'High field MR imaging and 1H-MR spectroscopy

in clinically isolated syndromes suggestive of multiple sclerosis', *Journal of Neurology*. Steinkopff-Verlag, 255(1), pp. 56–63. doi: 10.1007/s00415-007-0666-9.

Wattjes, Mike P. *et al.* (2008) 'Prognostic value of high-field proton magnetic resonance spectroscopy in patients presenting with clinically isolated syndromes suggestive of multiple sclerosis', *Neuroradiology*, 50(2), pp. 123–129. doi: 10.1007/s00234-007-0325-y.

Waubant, E. *et al.* (2014) 'A randomized controlled phase II trial of riluzole in early multiple sclerosis', *Annals of Clinical and Translational Neurology*, 1(5), pp. 340–347. doi: 10.1002/acn3.60.

Weinshenker, B. G. *et al.* (1989) 'The natural history of multiple sclerosis: A geographically based study: I. Clinical course and disability', *Brain*, 112(1), pp. 133–146. doi: 10.1093/brain/112.1.133.

Werner, P., Pitt, D. and Raine, C. S. (2001) 'Multiple sclerosis: Altered glutamate homeostasis in lesions correlates with oligodendrocyre and axonal damage', *Annals of Neurology*. Ann Neurol, 50(2), pp. 169–180. doi: 10.1002/ana.1077.

West, J. *et al.* (2014) 'Normal Appearing and Diffusely Abnormal White Matter in Patients with Multiple Sclerosis Assessed with Quantitative MR', *PLoS ONE*. Edited by P. Villoslada. Public Library of Science, 9(4), p. e95161. doi: 10.1371/journal.pone.0095161.

Westbrook, C. and Kaut, C. (1998) *MRI in practice*. 2nd edn. Blackwell Science.

Wilson, M. *et al.* (2011) 'A constrained least-squares approach to the automated quantitation of in vivo ^{1}H magnetic resonance spectroscopy data', *Magnetic Resonance in Medicine*, 65(1), pp. 1–12. doi: 10.1002/mrm.22579.

Wilson, M. *et al.* (2019) 'Methodological consensus on clinical proton MRS of the brain: Review and recommendations', *Magnetic Resonance in Medicine*. John Wiley and Sons Inc, pp. 527–550. doi: 10.1002/mrm.27742.

Wyss, M. and Kaddurah-Daouk, R. (2000) ‘Creatine and Creatinine Metabolism’, *Physiological Reviews*, 80(3), pp. 1107–1213. doi: 10.1152/physrev.2000.80.3.1107.

‘Xinapse. Cord finder – Introduction, http:// www.xinapse.com/Manual/ (2018, accessed 28 December 2018)’ (2018).

Yang, C. *et al.* (2015) ‘Sodium channel blockers for neuroprotection in multiple sclerosis’, *Cochrane Database of Systematic Reviews*. John Wiley and Sons Ltd. doi: 10.1002/14651858.CD010422.pub2.

Yiannakas, M. C. *et al.* (2016) ‘Fully automated segmentation of the cervical cord from T1-weighted MRI using PropSeg: Application to multiple sclerosis’, *NeuroImage: Clinical*. Elsevier Inc., 10, pp. 71–77. doi: 10.1016/j.nicl.2015.11.001.

Yildiz, M. *et al.* (2014) ‘Association of cognitive impairment and lesion volumes in multiple sclerosis - A MRI study’, *Clinical Neurology and Neurosurgery*. Elsevier, 127, pp. 54–58. doi: 10.1016/j.clineuro.2014.09.019.

Young, K., Soher, B. J. and Maudsley, A. A. (1998) ‘Automated spectral analysis II: Application of wavelet shrinkage for characterization of non-parameterized signals’, *Magnetic Resonance in Medicine*. Lippincott Williams and Wilkins, 40(6), pp. 816–821. doi: 10.1002/mrm.1910400606.

Zhang, T. *et al.* (2015) ‘Beta-interferon exposure and onset of secondary progressive multiple sclerosis’, *European Journal of Neurology*. Blackwell Publishing Ltd, 22(6), pp. 990–1000. doi: 10.1111/ene.12698.